

Enol Catalysis
—
**Enantioselective Transformations *via* Bifunctional Brønsted Acid
Promoted Enolization**

Dissertation

zur

Erlangung des Doktorgrades
der Mathematisch-Naturwissenschaftlichen Fakultät
der Universität zu Köln

vorgelegt von

Grigory André Shevchenko
aus Leningrad (Russland)

Köln 2018

Berichterstatter:

Prof. Dr. Benjamin List

Prof. Dr. Hans-Günther Schmalz

Tag der mündlichen Prüfung: 20.07.2018

Table of Contents

Abstract	III
Kurzzusammenfassung	IV
List of Abbreviations.....	V
1 Introduction	1
1.1 Asymmetric Organocatalysis	1
1.2 Asymmetric Brønsted Acid Catalysis	3
2 Background.....	7
2.1 Enols.....	7
2.2 Direct Asymmetric α -Functionalization of Ketones	11
2.2.1 Activation via Cooperative Lewis Acid/Brønsted Base Catalysis.....	11
2.2.2 Activation by Strong Brønsted Bases	12
2.2.3 Activation by Lewis Base Catalysis.....	13
2.2.4 Functionalization via Brønsted Acid Catalysis.....	14
2.3 Catalytic Asymmetric Robinson Annulations	19
2.4 Catalytic Asymmetric α -Aminations of Ketones	25
2.5 Direct α -Oxidations of Ketones.....	29
2.5.1 Direct α -Hydroxylations of Simple α -Branched Ketones.....	29
2.5.2 Catalytic Asymmetric Aminoxylation Reactions	30
2.5.3 Alternative Approaches	33
2.5.4 Oxidation of Enols.....	34
2.5.5 Properties of Enol Cation Radicals	34
2.5.6 Reactions of Enol Cation Radicals.....	35
2.5.7 Proton Coupled Electron Transfer.....	37
2.5.8 Recent Applications of PCET in Asymmetric Catalysis	40
3 Objectives	43
4 Results and Discussion	45
4.1 Brønsted Acid-Catalyzed Asymmetric Robinson Annulations.....	45
4.1.1 Initial Studies.....	45
4.1.2 Breakthrough and Fine-Tuning of Reaction Conditions.....	47
4.1.3 Preliminary Substrate Scope.....	50

4.1.4 Revisiting the Catalyst Structure.....	52
4.1.5 Conclusions	58
4.2 Catalytic Asymmetric α -Amination of α -Branched Ketones via Enol Catalysis ^[180]	59
4.2.1 Optimization Studies	59
4.2.2 Substrate Scope	62
4.2.3 Synthesis of Carbamate-Protected α -Amino Ketones	65
4.2.4 Conclusions	67
4.3 The Direct α -Hydroxylation of Cyclic α -Branched Ketones via Enol Catalysis	69
4.3.1 Oxidative Cleavage of α -Branched Ketones	69
4.3.2 Development of a Non-Enantioselective Direct α -Hydroxylation of α -Branched Cyclic Ketones	73
4.3.3 Development of a Direct Enantioselective α -Hydroxylation of α -Branched Cyclic Ketones	78
4.3.4 Conclusions	92
4.4 α -Oxidation of Cyclic Ketones with 1,4-Benzoquinones via Enol Catalysis ^[189]	93
4.4.1 Exploration of the Reactivity.....	94
4.4.2 Exploration of the Asymmetric Transformation.....	97
4.4.3 Study of the Reaction Mechanism	104
4.4.4 Conclusions	110
5 Summary	111
6 Outlook.....	115
7 Experimental Section	119
8 Bibliography	212
9 Appendix	222

Abstract

Enantiopure carbonyl compounds bearing tetrasubstituted α -stereogenic centers are versatile building blocks for the synthesis of pharmaceuticals, fragrances, and natural products. The direct synthesis of such motifs *via* asymmetric α -functionalization of the corresponding ketones is a major challenge in both metal- and organocatalysis. In this work we report on development of *enol catalysis*, a novel strategy allowing the direct enantioselective α -functionalization of carbonyl compounds *via* Brønsted acid promoted enolization. Within this thesis, we established the generality of this strategy in a variety of enantioselective C–C, C–N and C–O bond forming reactions using simple α -branched and unbranched ketones as substrates. Along the same line of research we developed a highly enantioselective Robinson annulation of 1,3-diketones that afforded derivatives of the synthetically valuable Wieland–Miescher ketone. Furthermore, this strategy was successfully applied to direct α -amination and α -hydroxylation reactions using either diazocarboxylates or nitrosobenzene as reagents. And finally, we discovered that *enol catalysis* enables serendipitously-discovered α -aryloxylation of ketones using 1,4-benzoquinones. Taken together, this work has established *enol catalysis* as a generic enantioselective and scalable methodology applicable to a broad scope of challenges of organic synthesis.

Kurzzusammenfassung

Enantiomerenreine Carbonylverbindungen mit tetrasubstituierten α -Stereozentren sind vielseitige Bausteine für die Synthese von Pharmazeutika, Duftstoffen und Naturstoffen. Die direkte Synthese solcher Motive durch asymmetrische α -Funktionalisierung der entsprechenden Ketone ist eine große Herausforderung in der Metall- sowie Organokatalyse. In dieser Arbeit berichten wir über die Entwicklung der *Enolkatalyse*, einer neuartigen Strategie, welche die direkte enantioselektive α -Funktionalisierung von Carbonylverbindungen durch Brønsted-Säure katalysierte Enolisierung ermöglicht. Im Rahmen dieser Arbeit haben wir die allgemeine Anwendbarkeit dieser Strategie in einer Vielzahl von enantioselektiven C–C, C–N und C–O bindungsknüpfenden Reaktionen unter Verwendung einfacher α -verzweigter und unverzweigter Ketone untersucht. Zunächst berichten wir über eine enantioselektive Robinson-Anellierung von 1,3-Diketonen. Darüber hinaus wurde diese Strategie erfolgreich auf direkte α -Aminierungs- und α -Hydroxylierungsreaktionen angewendet. Abschließend wird über die zufällige Entdeckung einer direkten α -Aryloxylierung von Ketonen berichtet. Zusammengefasst erweitert diese Arbeit Anwendungsbereich der *Enolkatalyse* und etabliert diese als allgemeingültiges Konzept, welches auf eine Vielzahl von Herausforderungen der organischen Synthese anwendbar ist.

List of Abbreviations

Ac	acetyl
AcO	acetate
Alk	alkyl
Ar	aryl, aromatic
aq.	aqueous
BDFE	bond dissociation free energy
BHT	dibutylhydroxytoluene
BINAM	2,2'-diamino-1,1'-binaphthalene
BINOL	1,1'-bi-2-naphthol
Bn	benzyl
Boc	<i>tert</i> -butoxycarbonyl
Bu	butyl
CAN	Cerium ammonium nitrate
cat.	catalyst/catalytic.
conv.	conversion
d	doublet
d	day(s)
DBAD	ditertbutyl azadicarboxylate
DEAD	diethyl azadicarboxylate
DIAD	diisopropyl azadicarboxylate
DKR	dynamic kinetic resolution
DMF	dimethylformamide
DMSO	dimethylsulfoxide
DPP	diphenyl phosphoric acid
dr	diastereomeric ratio
E	electrophile
EI	electron impact
equiv.	equivalent(s)
er	enantiomeric ratio
Et	ethyl
ESI	electrospray ionization
FCC	flash column chromatography
GC (GC-MS)	gas chromatography (gas chromatography coupled with mass detection)
h	hour(s)
HAT	H-atom transfer
HMDS	hexamethyldisilazene
HOESY	heteronuclear Overhauser effect spectroscopy
HOMO	highest occupied molecular orbital
HPLC	high performance liquid chromatography
HRMS	high resolution mass spectrometry
<i>i</i>	iso
iso	isocratic (temperature regime in GC)
LA	Lewis acid
LDA	lithium diisopropylamide
LHMDS	lithium hexamethyldisilazane

Lit.	literature
LUMO	lowest unoccupied molecular orbital
<i>m</i>	<i>meta</i>
m	multiplet
M	molar (Concentration)
Me	Methyl
MeCy	methyl cyclohexane
Mes	mesityl (2,4,6-trimethylphenyl)
MS	mass spectrometry, molecular sieves
Ms	methylsulfonyl
MTBE	methyl <i>tert</i> -butyl ether
<i>m/z</i>	atomic mass units per charge
n	normal
n.a.	not available
NaHMDS	sodium hexamethyldisilazane
NBS	N-bromosuccinimide
n.d.	not determined
NMR	nuclear magnetic resonance spectroscopy
Nu-H/Nu	nucleophile
<i>o</i>	<i>ortho</i>
<i>p</i>	<i>para</i>
PCET	proton coupled electron transfer
Ph	phenyl
Pr	propyl
<i>p</i> TsOH	<i>para</i> -toluenesulfonic acid
py	pyridine
quint	quintet
rac.	Racemic
rt	room temperature
sept	septet
sext	sextet
SOMO	singly occupied molecular orbital
SPINOL	1,1'-pirobiindane-7,7'-diol
t	tert, tertiary
t	triplet
Tf	trifluoromethylsulfonyl
TFA	trifluoroacetic acid
THF	tetrahydrofuran
TLC	thin layer chromatography
TMS	trimethylsilyl
TRIP	3,3'-bis(2,4,6-triisopropylphenyl)-1,1'-binaphthyl-2,2'-diyl hydrogen phosphate
Ts	<i>para</i> -toluenesulfonyl

Acknowledgments

I am grateful to Prof. Benjamin List for giving me the unique opportunity to become a member of his outstanding group and work in the fantastic scientific environment of the Max-Planck-Institut für Kohlenforschung. Professor List has been an inspiring teacher and I will always follow his advice to tackle the real (and rewarding) challenges. I am very thankful for his trust and the freedom he granted me during my studies and for the great and inspiring working atmosphere he created.

I would also like to thank Prof. Dr. Hans-Günther Schmalz for accepting to review this thesis and Prof. Dr. Mathias Wickleder and Dr. Monika Lindner for serving on my defense committee.

A special thank you goes out to Jenni Kennemur, Lucas Schreyer and Nobuya Tsuji for careful proofreading this thesis.

The results presented in this thesis would have not been possible to achieve without my outstanding collaborators: Gabriele Pupo, with whom we worked together on the enol catalysis project(s); Dr. Giovanni Bistoni, who performed calculations that provided mechanistic insight into *enol catalysis*; Barry Oppelaar, who helped me with the oxidation project; Stefanie Dehn, who helped me with the non-enantioselective hydroxylation and Dr. Desislava Petkova, who helped me with Robinson annulation studies. Furthermore, I want to thank Dr. M. Klussmann and Dr. Chandra Kanta De for the organization of the PhD seminars and the fruitful discussions.

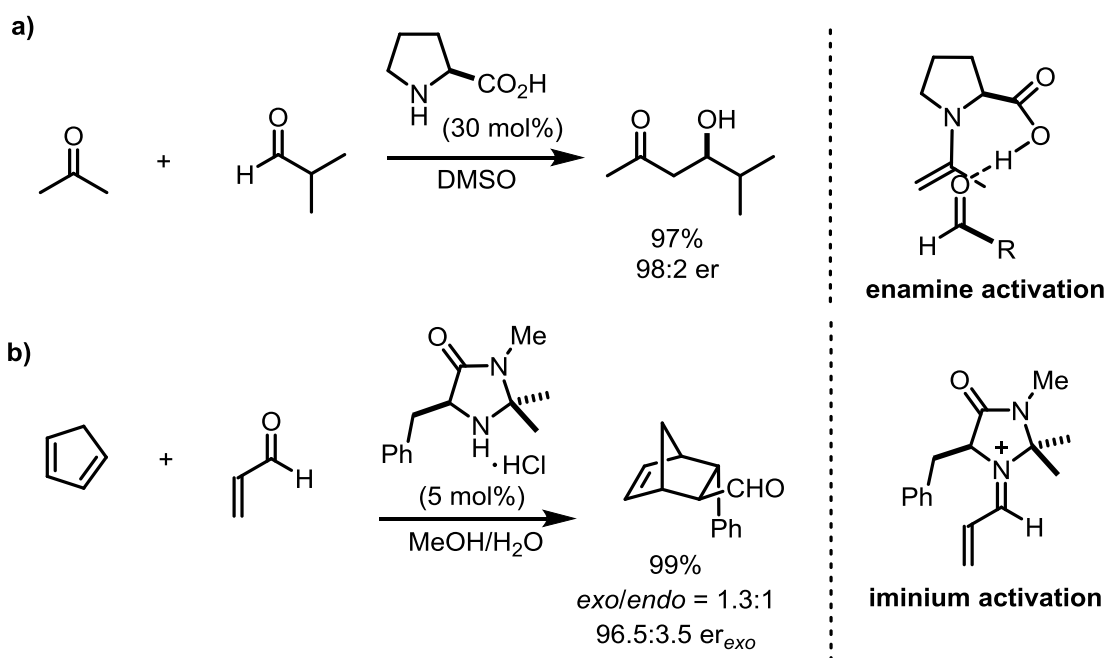
I would like to thank our administration and technician team for their valuable assistance and technical support, in particular Arno Döhring and Alexandra Kaltsidis for always finding a creative/unusual solution of whatever problem I might have had. Furthermore, I owe a sincere gratitude to the HPLC, mass spectrometry, NMR and X-Ray departments of the Max-Planck-Institut für Kohlenforschung for their outstanding experimental support.

I would like to thank all present and former members of the List, Klussmann and Morandi groups (Max-Planck-Institut für Kohlenforschung) for sharing ideas, chemicals and creating a fantastic and creative atmosphere outside and inside the lab. Nobuya Tsuji, Lucas Schreyer and Dr. Markus Leutzsch are thanked for the critical discussions.

1 Introduction

1.1 Asymmetric Organocatalysis

The increased demand of pharmaceutical, agrochemical or food industry for enantiomerically pure compounds has inspired generations of chemists to develop efficient and highly enantioselective synthetic methods. Due to obvious limitations of traditional approaches, such as resolution of racemic mixtures or use of chiral pool materials, modern strategies focus on asymmetric catalysis and these efforts have been acknowledged with the Nobel Prize awarded to William Knowles, Ryoji Noyori and K. Barry Sharpless in 2001.^[1]



Scheme 1.1: Pioneering work in a) enamine and b) iminium catalysis.

Until the beginning of the 21st century the field of asymmetric catalysis was dominated by bio- and transition metal catalysts and despite early examples the idea that small organic molecules could catalyze enantioselective reactions was regarded as highly exotic.^[2] However, in 2000 List^[3] and, independently MacMillan^[4] demonstrated the application of chiral secondary amines as catalysts for the activation of aldehydes and ketones (Scheme 1.1). List *et al.* reported direct aldol reactions of acetone and aldehydes catalyzed by L-proline. The reactions proceed *via in situ* generated enamine intermediates, which, due to their energetically increased highest occupied molecular orbitals (HOMO) are better nucleophiles compared to corresponding enols (Scheme 1.1 a). It was also suggested that the carboxylic acid moiety of proline additionally

activates the electrophile *via* Brønsted acid catalysis. MacMillan reported a chiral imidazolidinone-catalyzed Diels-Alder reaction of enals, proceeding *via* an *in situ* formed iminium intermediate. Electron density is removed from the enals double bond, decreasing the energy level of their lowest unoccupied molecular orbital (LUMO) and thus making it a better electrophile (Scheme 1.1 b). In the following two decades the field of organocatalysis has established itself, as the third pillar of homogeneous catalysis, complementing bio- and transition metal catalysis.^[5]

Interactions of functional groups with organic catalysts can be explained by Lewis and Brønsted acid-base theories. In line with this concept Seayad and List suggested a simple classification of organocatalysts.^[6] Accordingly, organocatalysts can be classified in four categories: Lewis bases (electron donors, e.g. enamine/iminium catalysis), Lewis acids (electron acceptors) and Brønsted acid (proton donors) or bases (proton acceptors). However, bifunctionality of catalysts is common and plays a key role in numerous transformations (Figure 1.1).^[7]

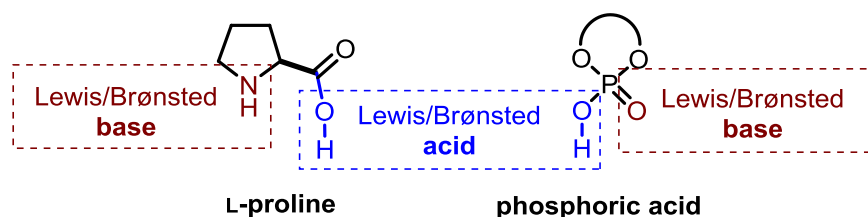


Figure 1.1: Examples of bifunctional organocatalysts.

1.2 Asymmetric Brønsted Acid Catalysis

By definition Brønsted acids are chemical species which can donate a proton to a corresponding Brønsted base, however it can also be considered as the smallest possible electron acceptor and therefore as a Lewis acid.^[8] Accordingly, a common strategy in Brønsted acid catalysis is LUMO lowering *via* protonation of an electrophile.^[9] Depending on the pK_a -differences between catalyst and substrate, acid catalysis is further divided into two classes (Figure 1.2). In general acid catalysis small pK_a difference results in partial protonation of the substrate through hydrogen-bonding. In specific acid catalysis the pK_a difference is sufficient to fully protonate the substrate and leads to the formation of ion pairs.^[10] However, both scenarios are borderline and often an accurate distinction can be challenging.^[11]

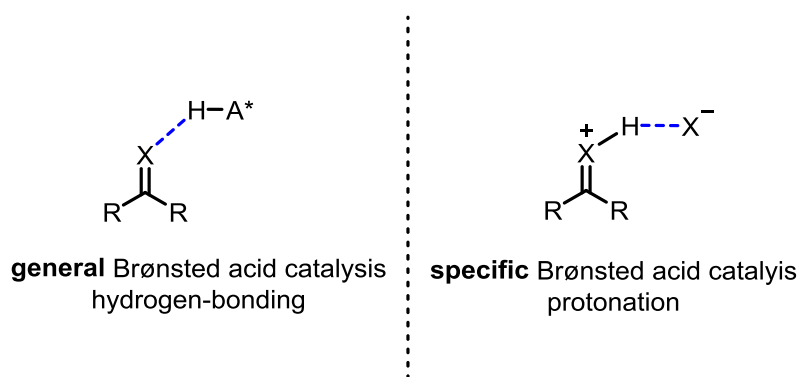


Figure 1.2: Activation modes in Brønsted acid catalysis.

Although hydrogen bonding is a fundamental activation mechanism in enzyme catalysis, examples utilizing this concept in asymmetric catalysis were only published relatively recently. A pioneering study is the asymmetric Strecker reaction catalyzed by a chiral thiourea as a dual hydrogen bond donor reported by Jacobsen *et al.* in 1998 (Figure 1.3).^[12] Five years later Rawal group reported the application of a chiral TADDOL in asymmetric hetero Diels–Alder reactions of aldehydes and activated dienes.^[13] Despite these early studies, it took several years to fully recognize the generality and true mechanistic nature of this approach.^[14]

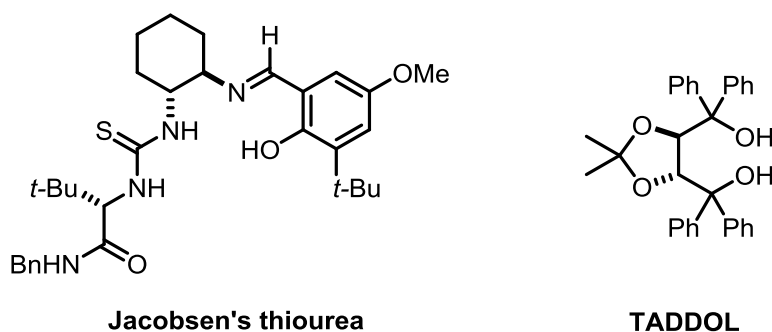


Figure 1.3: Hydrogen-bonding catalysts reported by Jacobsen and Rawal.^[12-13]

In 2004 Akiyama^[15] and subsequently Terada^[16] reported the development and application of BINOL-derived strong phosphoric acids in asymmetric catalysis (Figure 1.4). Although Ishihara group later showed that the catalytic species in Terada's report was not the free acid, but the corresponding calcium salt formed during purification,^[17] the last decade has proven that their early studies on Brønsted acid-catalyzed Mannich reactions with silyl ketene acetals and β -diketones have started a new era in asymmetric catalysis.

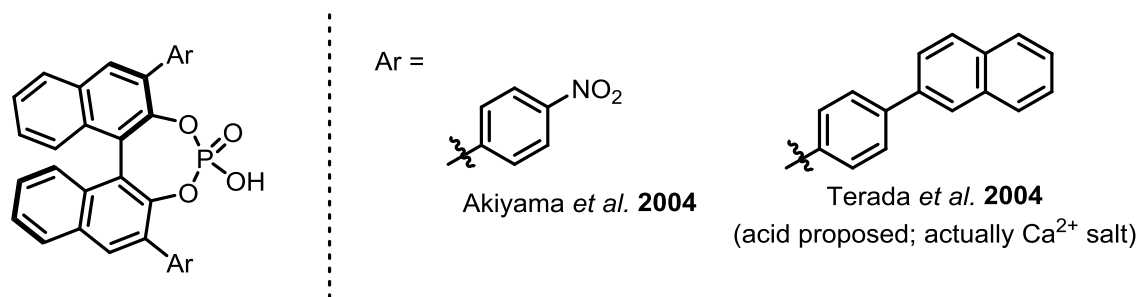


Figure 1.4: BINOL-derived phosphoric catalysts reported by Akiyama and Terada.

Because of their straight-forward synthesis, the field of asymmetric Brønsted-acid catalysis is dominated by BINOL-derived phosphoric acids, with TRIP (**1a**) being the most successfully applied catalyst.^[9, 18] However, various derivatives and modifications of phosphoric acids have been reported. A selection of common catalyst structures is outlined below.

A selection of backbone modifications is shown in Figure 1.5. TADDOL-derived phosphoric acids **2** were reported by Akiyama *et al.* in the context of enantioselective Mannich reactions using silyl enol ethers as nucleophiles.^[19] In 2006 Gong *et al.* reported the application of hydrogenated H_8 -BINOL derived phosphoric acids **3** in asymmetric Biginelli reactions.^[20] VAPOL-derived phosphoric acids **4** were applied to enantioselective additions of electron-poor amines to carbamate protected imines by the Antilla group.^[21] Recently, Akiyama reported the

development of biphenol-derived acids **5** as efficient catalysts for asymmetric tetrahydroquinoline synthesis.^[22] SPINOL derived catalysts **6**, which in contrast to previously reported structures are not axially chiral, were reported independently by List and Wang groups as highly efficient catalysts for enantioselective acetalizations and Friedel-Crafts reactions, respectively.^[23]

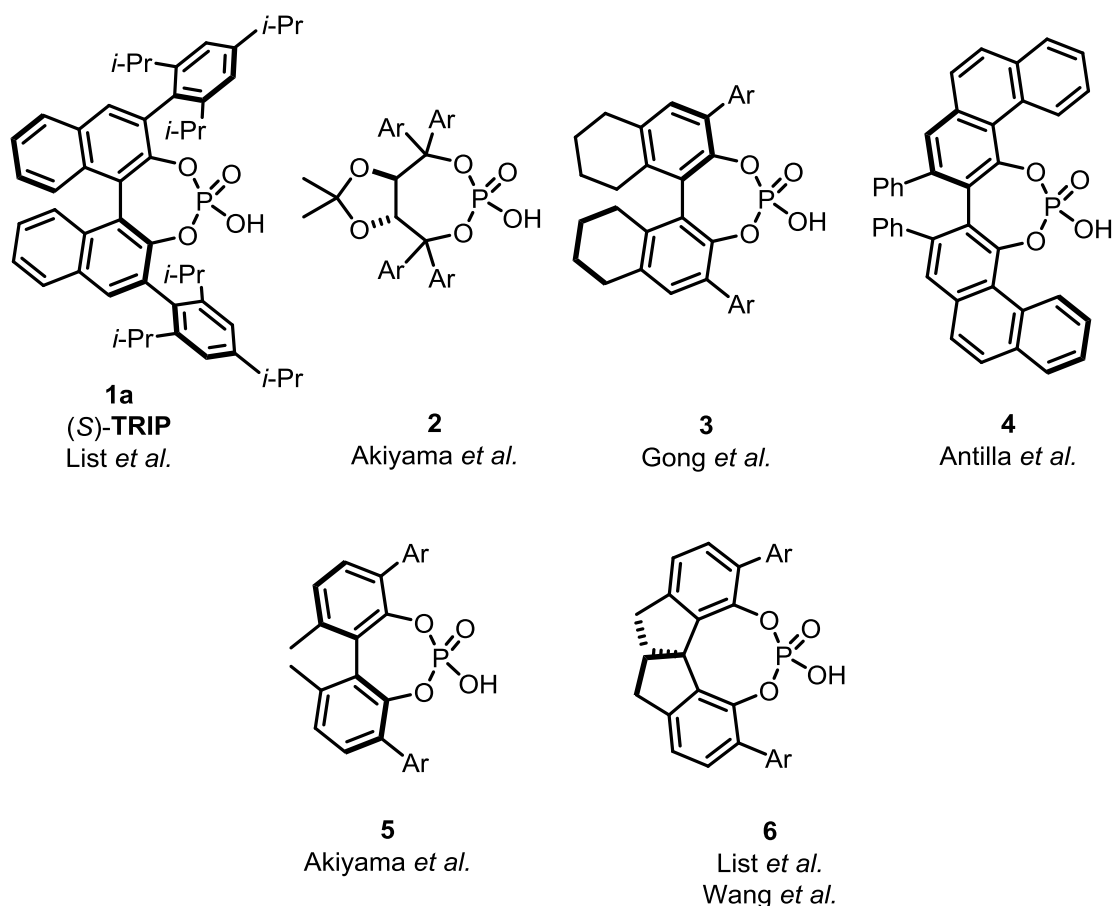


Figure 1.5: Chiral backbones for asymmetric phosphoric acids.

Modifications of the backbone do not necessary affect the catalysts acidity. Since it is however often correlated with the activity, modifications of the phosphoric acid moiety itself towards more acidic derivatives were developed (Figure 1.6). In 2006 Yamamoto reported *N*-triflyl phosphoramides **7** and their application in asymmetric Diels–Alder reactions.^[24] Compared to the corresponding phosphoric acids these compounds are significantly more acidic (pK_a (MeCN)^[25] ~13–14 vs 6–7, respectively) and have been widely applied.^[9] BINOL-derived dithiophosphoric acids **8** were developed by the Blanchet group and later applied to hydroamination reactions by Toste *et al.*^[26] The List group recently developed chiral

disulfonimids **9** (DSI), which are not only highly acidic Brønsted acids but could also be applied as precatalysts in Lewis acid organocatalysis.^[27]

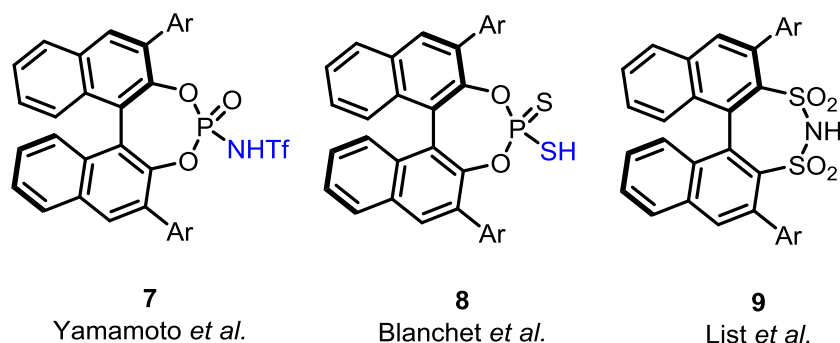


Figure 1.6: Selected examples of chiral BINOL-derived Brønsted acids with increased acidity.

To activate small and unbiased molecules, List group developed highly confined dimeric imidodiphosphates **10** (IDP) and used them in a variety of reactions, such as asymmetric acetalizations or sulfoxidations (Figure 1.7).^[28] Furthermore, List group demonstrated that the acidity of these confined catalysts could be increased by formal substitution of the phosphor-oxygen double bond to *N*-triflate groups, giving access to two new structural motifs: imino-imidodiphosphates **11** (*i*IDP)^[29] and highly acidic imidodiphosphorimidates **12** (IDPi).^[30] Recently, the latter found impressive applications in catalytic asymmetric hetero-Diels–Alder reactions and hydroalkoxylations of unactivated alkenes.^[31]

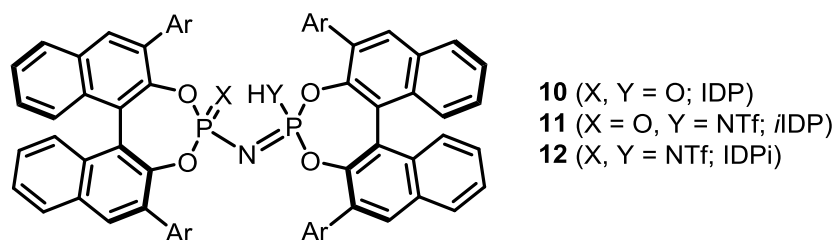


Figure 1.7: Recently developed highly confined Brønsted acids.

2 Background

2.1 Enols

Chemistry of the carbonyl group is the basis of organic synthesis. Due to the large difference in the electronegativity of carbon and oxygen, the $\pi_{\text{C=O}}$ and $\pi^*_{\text{C=O}}$ orbitals are not only lower in energy compared to the corresponding $\pi_{\text{C=C}}$ and $\pi^*_{\text{C=C}}$ orbitals, but also the anti-bonding $\pi^*_{\text{C=O}}$ orbital is distorted towards oxygen (Figure 2.1). This generates a partial positive charge on the carbon atom thus making carbonyl groups highly susceptible to nucleophilic attacks.^[32] Since the bond polarization is correlated to the (formal) charge, the electrophilicity can be further increased by the coordination of Lewis acids to the non-bonding n_{O} -orbitals.

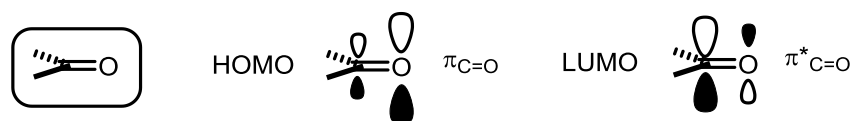


Figure 2.1: Molecular orbitals of C=O π bonds.^[32]

At the same time, carbonyls are also good nucleophiles. Already in 1904 Lapworth studied the kinetic of acetone halogenation. He reported that the apparent rates of first order kinetics were independent from the used halogen or its concentration. Whereas the rates were very low in neutral solutions the addition of mineral acids dramatically accelerated the reaction. Since these reactions were not affected by light and did not occur with “paraffins”, he concluded that the “enolic form” of the ketone must be involved in the reaction mechanism. He further argued that the formation of this compound was rate limiting.^[33]

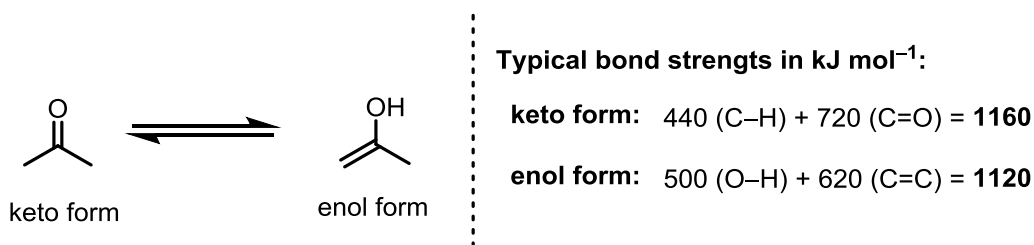


Figure 2.2: Thermodynamic data of keto-enol tautomers. Adapted from^[34]

A plausible explanation for the observed kinetics is that because of the highly polarized C=O double bond carbonyl compounds are rather C–H acidic. Their pK_{a} values vary within the range from 7.7 (α -nitro acetophenone, DMSO) up to 26.5 (acetone, DMSO).^[35] This means that

they could be deprotonated by many common bases, but also that they are present in chemical equilibrium with their corresponding enol-tautomers. Tautomers are interconverting isomers which differ by the placement of an atom or a group, most commonly a proton. Because of thermodynamic reasons the keto-tautomer is ca. 11–14 kcal mol⁻¹ more stable than the corresponding enol-tautomer (Figure 2.2).^[34] Dominance of the keto-form could be reversed by certain structural features, such as extended conjugation. Equilibrium constants of simple ketones suggest a typical enol concentration of 0.1 to 10 ppm (Figure 2.3 a).^[36] Nevertheless, if the corresponding protonation (ketonization) is kinetically blocked, the equilibrium can be completely shifted towards the enol-form. (Figure 2.3 b).^[37]

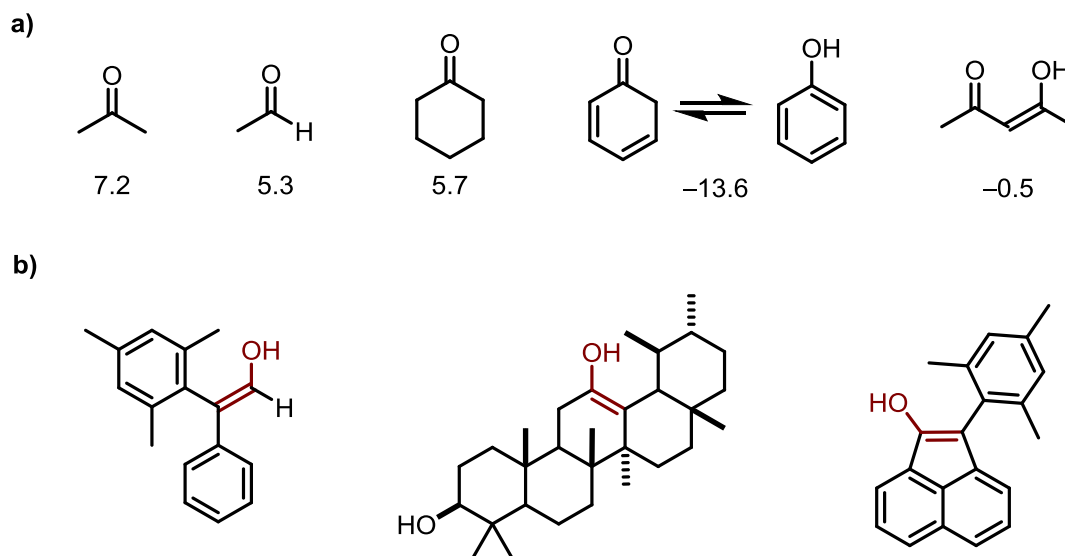


Figure 2.3: a) Equilibrium constants for keto-enol tautomerizations of selected carbonyl compounds (*pK*). The lower the number, the more the equilibrium is shifted towards the enol tautomer. b) Selected examples of stable simple enols.^[37]

The interconversion between both tautomers can be catalyzed by both acids (Brønsted and Lewis) and bases and is very slow in neutral solutions (Figure 2.4). In the base-catalyzed mechanism, initial deprotonation at the α -position yields the corresponding enolate, which is subsequently protonated and produces the enol-tautomer. Whereas C–H abstraction is slow and therefore rate-limiting, the last protonation step is very fast. In contrast, the acid-catalyzed enolization is initiated by fast and reversible protonation of the carbonyl oxygen followed by rate-determining deprotonation.^[34, 36a]

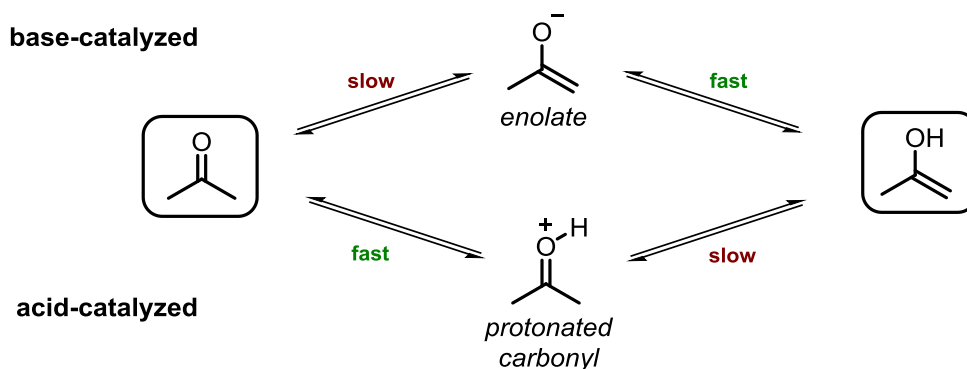


Figure 2.4: Mechanism of a) acid-catalyzed and b) base-catalyzed keto-enol tautomerization of acetone.

Unsymmetrically substituted ketones (*e.g.* ethyl methyl ketone) could yield a mixture of isomers. Under basic conditions the regioselectivity (kinetic *vs.* thermodynamic enolate) is influenced by the base and temperature: bulky bases and lower temperatures preferentially lead to the kinetic enolate, whereas high temperatures give the thermodynamic product (Figure 2.5 a). However, under acidic conditions the formation of more substituted enol is preferred (Figure 2.5 b). This could be explained by the Hammond postulate: Since bond energies of enols are higher than of the corresponding carbonyls, the tautomerization must proceed *via* a transition state which sterically resembles the products.^[38] Hyperconjugation, which preferentially stabilizes more substituted enols, is also stabilizing the corresponding transition states. Since this is also influenced by sterics, a bulky substituent could inverse the selectivity.^[39] An additional challenge is the control of *E/Z*-geometry of enol and enolates that requires empirical adjustments to for the impact of sterics, solvents, bases and additives (Figure 2.5 c).

By their reactivity enols are comparable to enolates. The reactive orbitals (HOMO) of enolates suggested that the net negative charge is unequally distributed between the three atoms and while the oxygen atom attracts more of the charge the carbon atom has more of the HOMO (Scheme 2.6). This explains why hard electrophiles (*e.g.* anhydrides) preferentially react at oxygen atoms, whereas soft electrophiles (*e.g.* vinyl ketones) react at carbon atoms (HSAB theory).^[34]

Enols and enolates are key intermediates in a wide range of synthetically useful α -functionalization reactions of carbonyls, such as α -halogenations, aldol reactions/condensations, Michael additions or Claisen condensations, to mention only a few.^[34] It is therefore not

surprising that their selective preparation is a key for direct and enantioselective α -functionalization. Considering the topics discussed in this thesis, the following sections will give a comprehensive overview of common enantioselective methods developed for the direct α -functionalization of ketones.

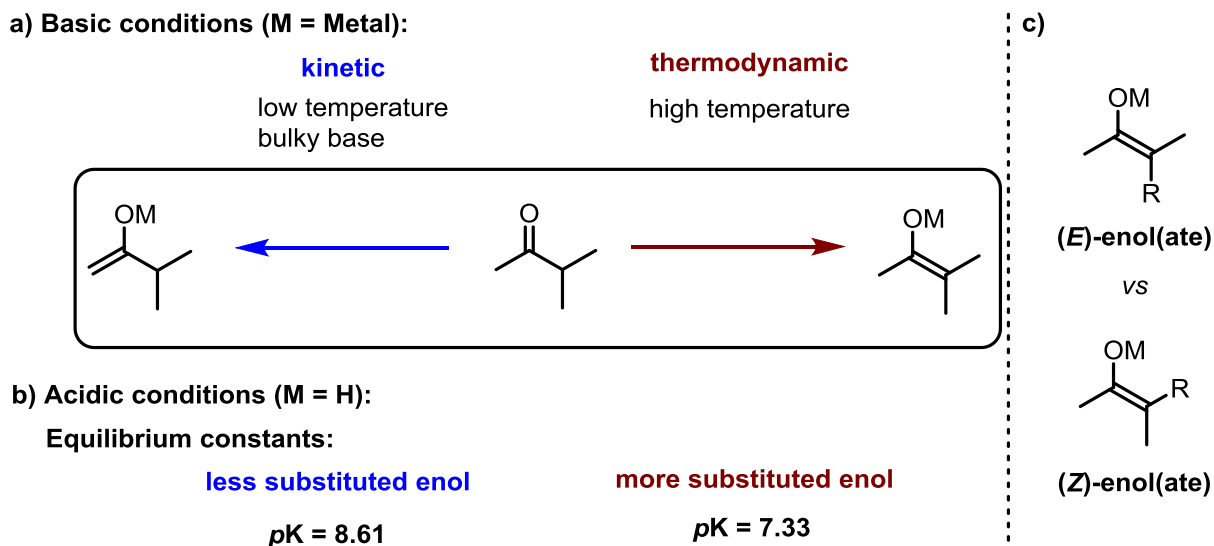


Figure 2.5: Regioselectivity of enol(ate) formation under a) basic and b) acidic conditions. c) (E)- vs (Z)-enol(ate). Equilibrium constants according to^[36b]

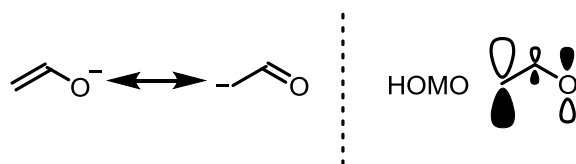


Figure 2.6: HOMO orbitals of enolates.

2.2 Direct Asymmetric α -Functionalization of Ketones

Because of its simplicity the direct α -functionalization of ketones is the most straightforward approach towards the synthesis of their α -mono- and α,α -disubstituted analogues. For long time most enantioselective approaches were taking advantage of either chiral pool materials or chiral auxiliaries and catalytic transformations were only realized by employing enol-surrogates, *e.g.* corresponding enol ethers or esters, or activated substrates equipped with additional activating electron-withdrawing groups. At the end of the 20th century, methods of direct functionalization of ketones by *in situ* generation of catalytic amounts of enol/enolate-equivalents were developed. Besides their great potential, only few of them enable the synthesis of tertiary/quaternary stereocenters starting from unactivated α -branched carbonyl compounds. The following section will give a brief overview over common synthetic catalytic strategies (excluding biocatalytic approaches) and their application in asymmetric aldol, Mannich or amination reactions. Some strategies, such as phase-transfer catalysis (PTC), are not considered here since they require (over)stoichiometric amounts of reagent for catalysts turnover (*e.g.* bases).

2.2.1 Activation *via* Cooperative Lewis Acid/Brønsted Base Catalysis

Its concept relies upon the cooperative interaction of a Lewis-acidic site of the catalyst lowering the LUMO of the acceptor by coordination and the Brønsted-basic site activating the donor through formation of the corresponding enolate. Close proximity of both reactive sites ensures both high reactivity and selectivity.

The first example of a catalytic system that relies on this activation mode was reported by Shibasaki in 1997 (Figure 2.7).^[40] They found that 20 mol% of the previously developed bifunctional complex **13**^[41] enabled the direct aldol reaction of simple ketones and aldehydes in good yields (up to 90%) and good to excellent enantioselectivities (er from 72:28 to 97:3). Branching at the α -position was required for both reactivity and selectivity: Reactions with unbranched aldehydes resulted in diminished yields and enantiomeric excess. Notable limitations, such as the requirement of high amount of donor and the overall low reactivity (3–11.5 d reaction time) were circumvented in later publications.^[42] Over the following two decades these catalytic systems were broadly used in the field, including industrial scale applications.^[43] Although attempts to use α -hydroxy ketones as the starting materials, the Shibasaki system is restricted to the activation of simple unbranched ketones.^[44]

The Trost group reported a catalytic system based on a similar concept: The binuclear complex (**14**) obtained upon treatment of the corresponding substituted phenol with 2 equivalents of Et_2Zn enabled direct dia- and enantioselective aldol reactions (Figure 2.7).^[45] The Zn-ProPhenol system has proven to be a highly successful tool for enantio- and diastereoselective aldol reactions, Mannich reactions, Henry reactions, conjugate additions and alkyne additions.^[46] More recently, it was successfully applied to direct Mannich and α -amination reactions of challenging α -alkyl ketones (Scheme 2.12 a).^[47] At the same time, enolate regioselectivity remained unclear, since only indanone and tetralone analogues were employed as starting materials.

Conceptionally similar, yet less popular systems for direct aldol reactions of ketones were developed by Nishiyama^[48] and Mahrwald.^[49] Feng *et al.* reported that an *in situ* generated chiral Scandium-based Lewis acid in combination with catalytic amounts of a Brønsted-base (Li_2CO_3) enabled direct enantioselective amination of cyclic ketones using α -diazoesters as electrophilic nitrogen reagents.^[50] The group of Wasa recently reported the application of chiral frustrated Lewis acid/Brønsted base complexes for direct amination and Mannich reactions of ketones.^[51] However, these systems did not functionalize α -substituted ketones.

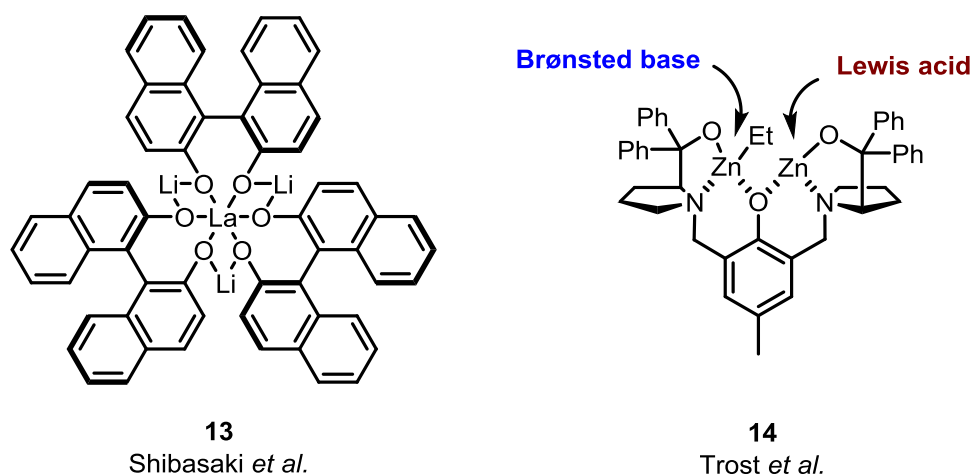


Figure 2.7: Selected examples of catalytic cooperative Lewis-acid/Brønsted-base systems disclosed for the activation of ketones.

2.2.2 Activation by Strong Brønsted Bases

Due to the low acidity of unactivated ketones (their pK_a values are within the range of 20 to 28) chiral Brønsted base catalysts were only applied to activated α -substituted ketones.^[52]

However, Terada *et al.* recently published a new class of chiral guanidine-derived organosuperbase precursors, which upon activation with Na/LHMDS enable direct electrophilic amination of α -alkyl substituted indanone and tetralone analogues (Figure 2.8 and Scheme 2.12b).^[53]

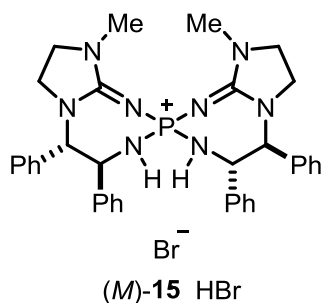


Figure 2.8: Chiral organosuperbase by Terada.^[53a]

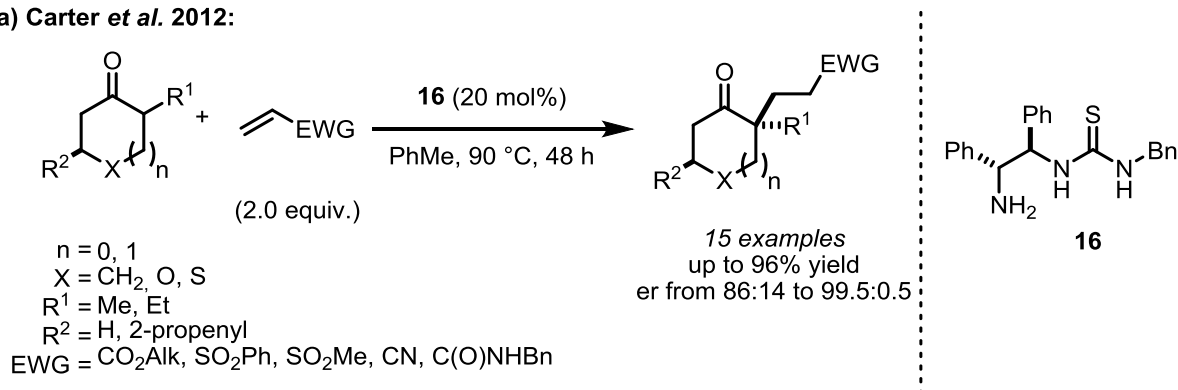
2.2.3 Activation by Lewis Base Catalysis

The major disadvantage shared by all previously reported systems is that they are highly air and water sensitive and should be handled under inert gas atmosphere. Although the proline-catalyzed Hajos–Parrish–Eder–Sauer–Wiechert reaction attracted a lot of attention, it remained largely undervalued by the scientific community because of its misinterpreted mechanism and a common notion that enantioselective reactions ultimately require transition metal catalysis. However, in 2000 List *et al.* reported proline-catalyzed enantioselective direct aldol reactions (Scheme 1.1 a).^[3] Later not only the generality of enamine catalysis, named after its reactive intermediate, was established and organocatalysis has become an important branch of homogeneous catalysis.^[54]

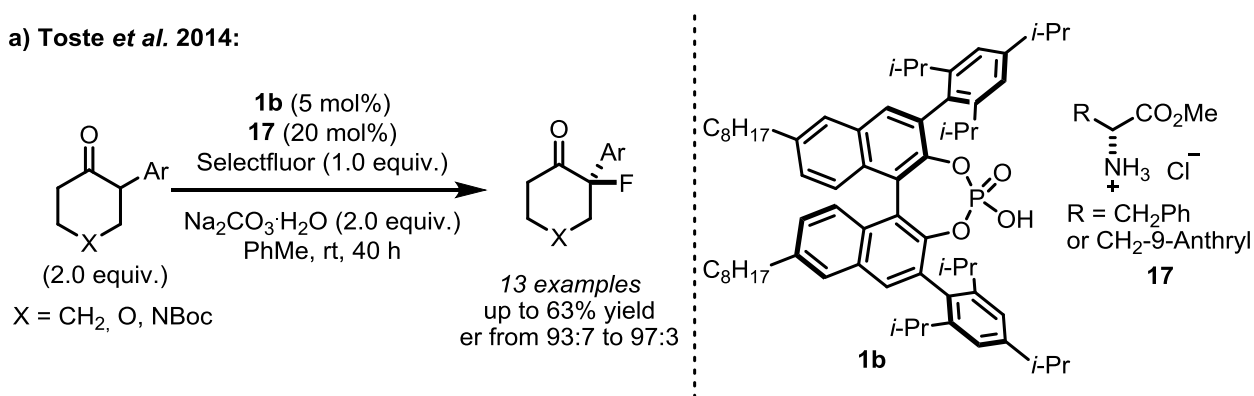
Nowadays, chiral secondary amines are the catalysts of choice for enantioselective α -functionalization of linear aldehydes and ketones.^[54a, 54b] Because of the strong steric hindrance in the enamine intermediate the use of disubstituted aldehydes was challenging, however it was subsequently achieved by using chiral primary amines.^[55] The use of simple α -branched ketones was not reported with the only exceptions of reports by Carter and Toste groups. In 2012, Carter group reported conjugate additions of α -branched cyclic ketones to unsaturated esters, sulfones, nitriles and carbamates catalyzed by thiourea-based primary amine **16**, proposing a cooperative enamine/Brønsted acid activation mode (Scheme 2.1 a).^[56] Toste *et al.* reported the direct α -

fluorination of α -branched ketones enabled by a combination of enamine catalysis and chiral anion phase-transfer catalysis (Scheme 2.1 b).^[57]

a) Carter *et al.* 2012:



a) Toste *et al.* 2014:



Scheme 2.1: Direct α -functionalization of branched ketones by a) Carter and b) Toste.

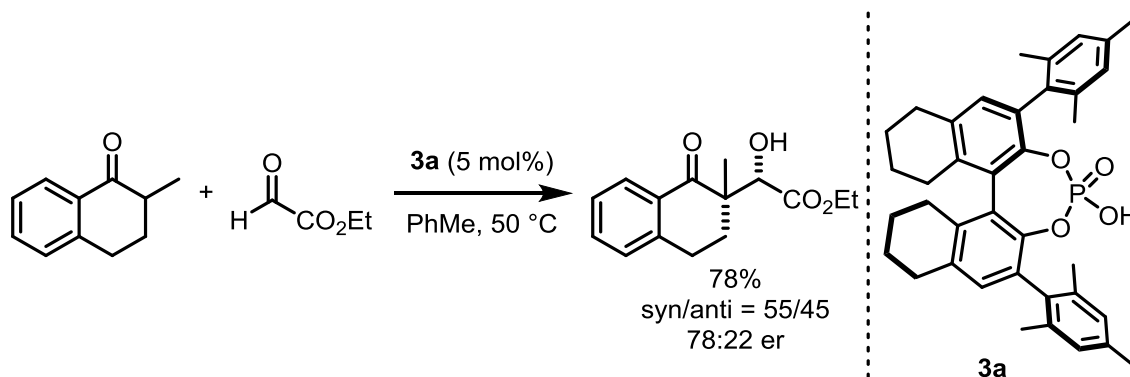
2.2.4 Functionalization *via* Brønsted Acid Catalysis

Although the tautomerization of carbonyl compounds can be catalyzed by Brønsted acids, only few examples of Brønsted acid-catalyzed enolizations were reported in the context of asymmetric α -functionalization of ketones. In 2006 Rueping and Gong independently reported enantioselective *aza*-Diels–Alder reactions of cyclic enones and imines.^[58] Whereas Rueping *et al.* used a combination of chiral phosphoric acid and acetic acid and proposed that the former activates the imine by protonation and the latter is responsible for ketone enolization, Gong *et al.* showed that just a catalytic amount of a chiral phosphoric acid suffices for the reaction. Shortly after, Gong *et al.* extended this catalytic system to a one-pot three-component Mannich reaction of unbranched cyclohexanone-derivatives, aromatic aldehydes and aniline.^[59] Although

mechanisms involving phosphoric acid-catalyzed enolizations have been proposed, these reactions could potentially also proceed *via* enamine intermediates.

Even more clear example was provided by Akiyama *et al.* who showed that methyl ketones can undergo phosphoric acid-catalyzed enolization in an enantioselective aldol reaction of *meso*-1,3-diones (Scheme 2.8).^[60] Acid-catalyzed α -alkylations of unbranched ketones was reported by Guo and Peng.^[61] According to the proposed mechanism, the phosphoric acids promoted enolization of the corresponding ketone and simultaneously activated the electrophile by protonation.

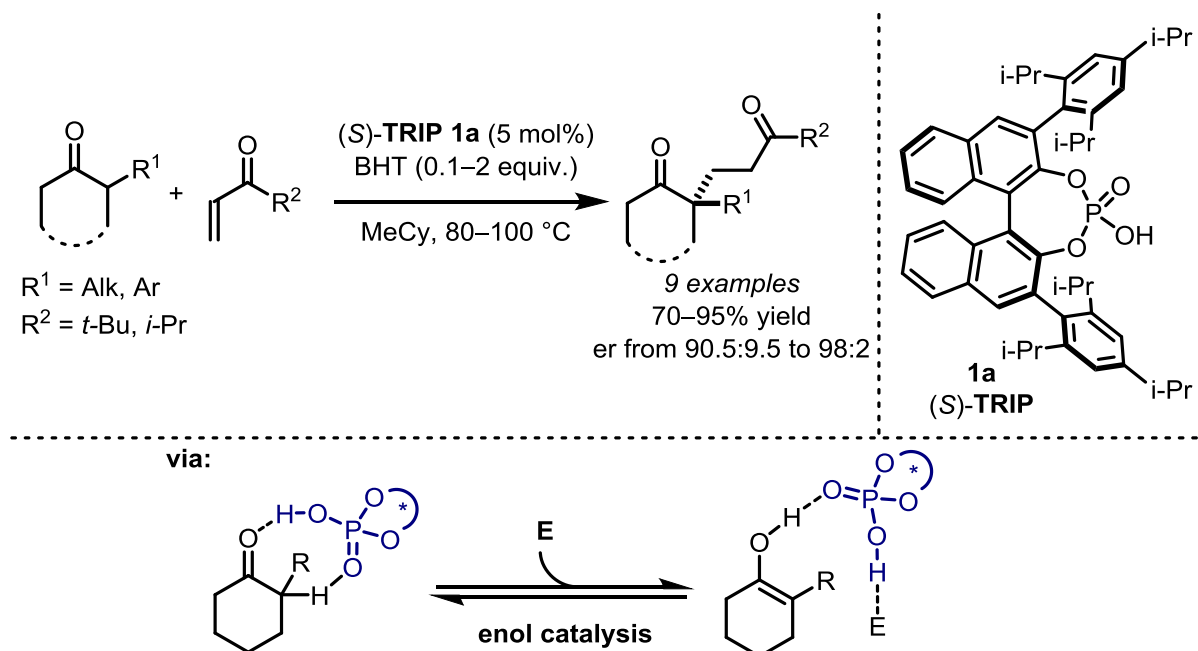
Acetophenones as well as indanone- and tetralone-derived ketones are challenging substrates for enamine catalysis, presumably because of a twisted and, conceivably, less reactive enamine intermediate. In an attempt to overcome these limitations, the Blanchet group reported chiral phosphoric acid-catalyzed *syn*-selective aldol reactions of glyoxylates and unbranched ketones.^[62] However, in just one example, 2-methyl tetralone was successfully used as the starting material, giving the corresponding quaternary α -carbonyl stereocenter in good yields (78%) and moderate dia- and enantioselectivity (*syn/anti* = 55/45; 78:22 *er*) (Scheme 2.2).



Scheme 2.2: Chiral phosphoric acid-catalyzed aldol reaction using 2-methyl tetralone.

Apart from this example, the functionalization of challenging α -branched ketones *via* Brønsted acid catalysis was not addressed until the List group introduced the concept of *enol catalysis* by reporting enantioselective conjugate additions of α -branched cyclic ketones to enones catalyzed by a chiral phosphoric acid (Scheme 2.3).^[63] Remarkably, in the presence of a chiral phosphoric acid only the higher substituted enol was formed giving access to the α,α -disubstituted ketones in excellent yields (up to 95%) and enantioselectivities (*er* from 90.5:9.5 to

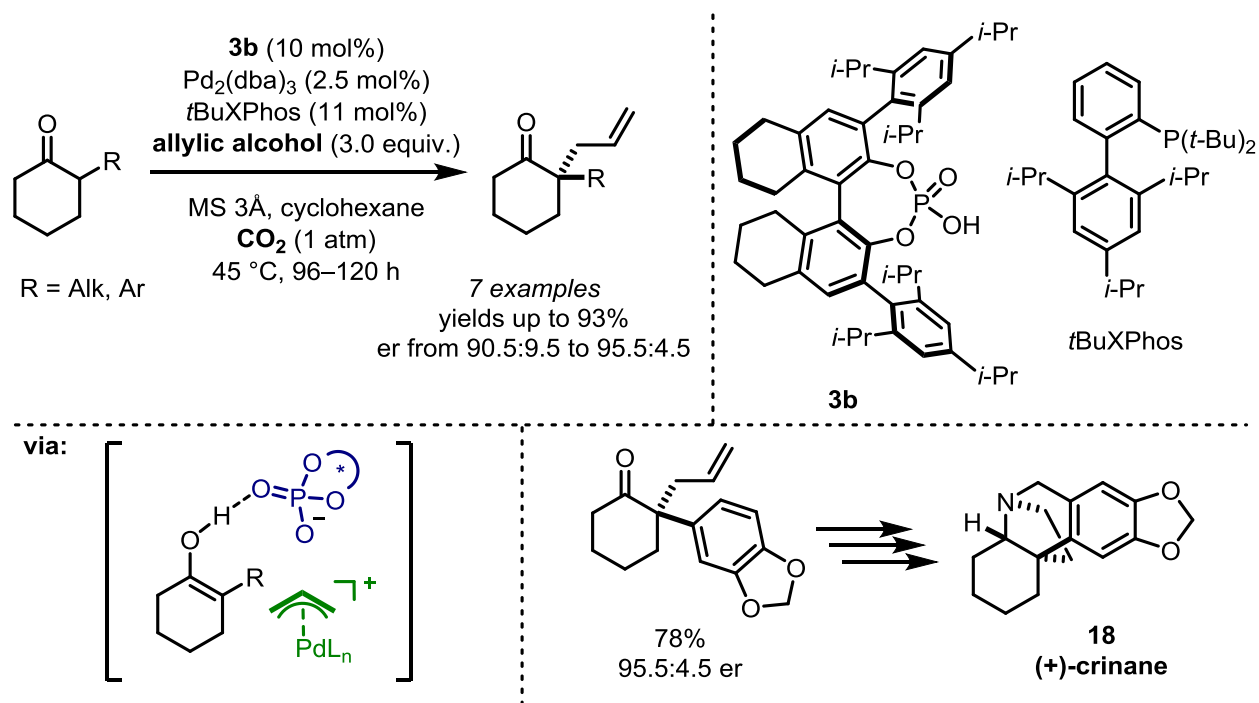
97.5:2.5). It was suggested, that the Brønsted-acidic P–OH and basic P=O moieties of the chiral phosphoric acid not only accelerated the enolization but also activated both reaction partners *via* hydrogen bonding. Shortly after, intramolecular versions of Brønsted acid-catalyzed Michael reactions were reported by Lam and Yao groups using unbranched ketones.^[64] Furthermore, Toste *et al.* reported on chiral phosphoric acid-catalyzed addition of α -branched ketones to allenamides.^[65]



Scheme 2.3: Phosphoric acid catalyzed addition of α -branched ketones to enones.

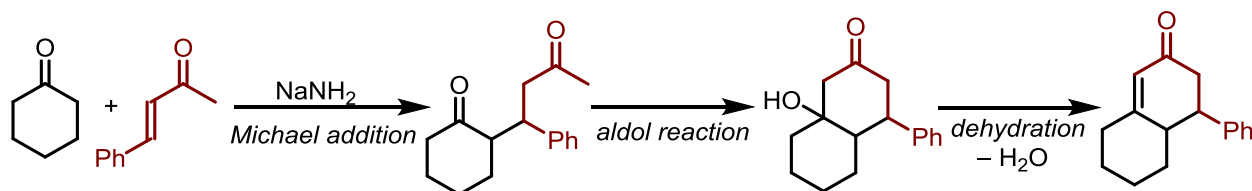
Recently, the List groups achieved the direct allylation of α -branched cyclic ketones *via* enol catalysis (Scheme 2.4).^[66] The combination of a palladium catalyst, chiral phosphoric acid **3b** and an atmosphere of CO₂ enabled an asymmetric Tsuji-Trost-type allylation using allylic alcohols as reagents. This reaction is highly atom-economic, as only one equivalent of water is produced as side product. The targeted ketones, bearing a quaternary stereocenter were obtained in excellent yields (up to 93%) and enantioselectivities (er from 90.5:9.5 to 95.5:4.5). This methodology was applied in a formal total synthesis of (+)-crinane (**18**).

The application of this strategy to C–X bond-forming reactions has not been reported prior to this thesis.

**Scheme 2.4:** Direct allylation of α -branched ketones by List *et al.*^[66]

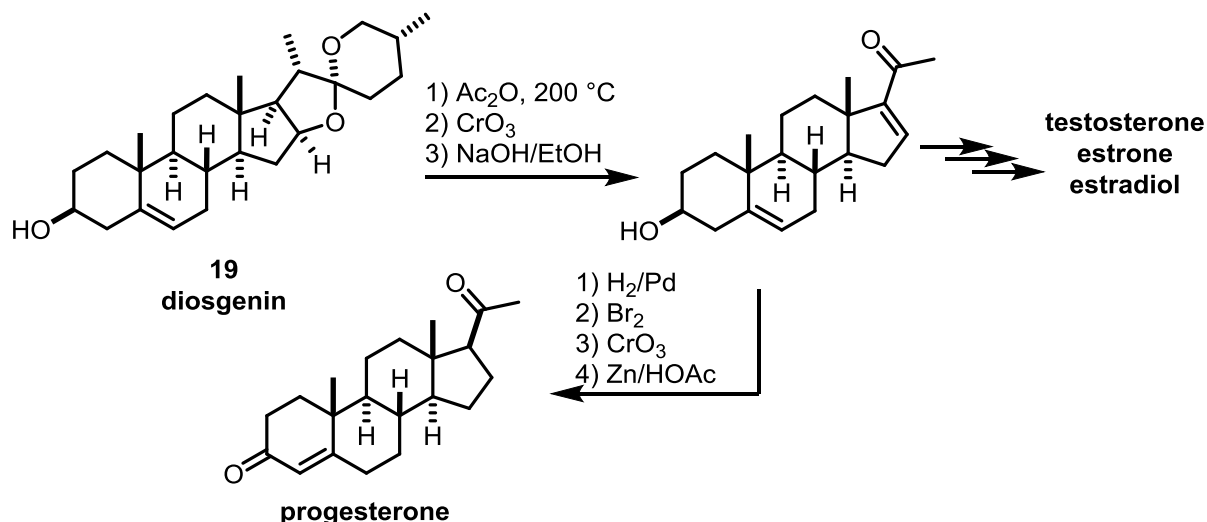
2.3 Catalytic Asymmetric Robinson Annulations

Discovered by Sir Robert Robinson in 1935, the reaction now termed *Robinson annulation* is one of the most powerful transformations for the synthesis of cyclohexanone derivatives.^[67] Being one of the first reported tandem reactions, it consists of three successive steps: (1) Michael-addition of a carbonyl compound to a vinyl ketone (*e.g.* methyl vinyl ketone), (2) intramolecular aldol reaction and (3) irreversible dehydration furnishing a bicyclic enone (Scheme 2.5). The reaction can be carried out under basic conditions that favored initial formation of the enolate; but also under acidic conditions favoring the final dehydration step.^[68] Interestingly, when unsymmetrically substituted ketones were used as starting materials, alkylation usually occurred at the more substituted α -carbon.^[67c, 68] Since this reaction enables simultaneous formation of two C–C bonds producing just one molecule of water as a side product, it was applied in numerous total synthesis, *e.g.* of hispidospermidin,^[69] (+)-codein^[70] or (\pm)-guanacastepene A.^[71]



Scheme 2.5: Base-mediated sequence of conjugate addition and aldol condensation initially reported by Robinson *et al.*

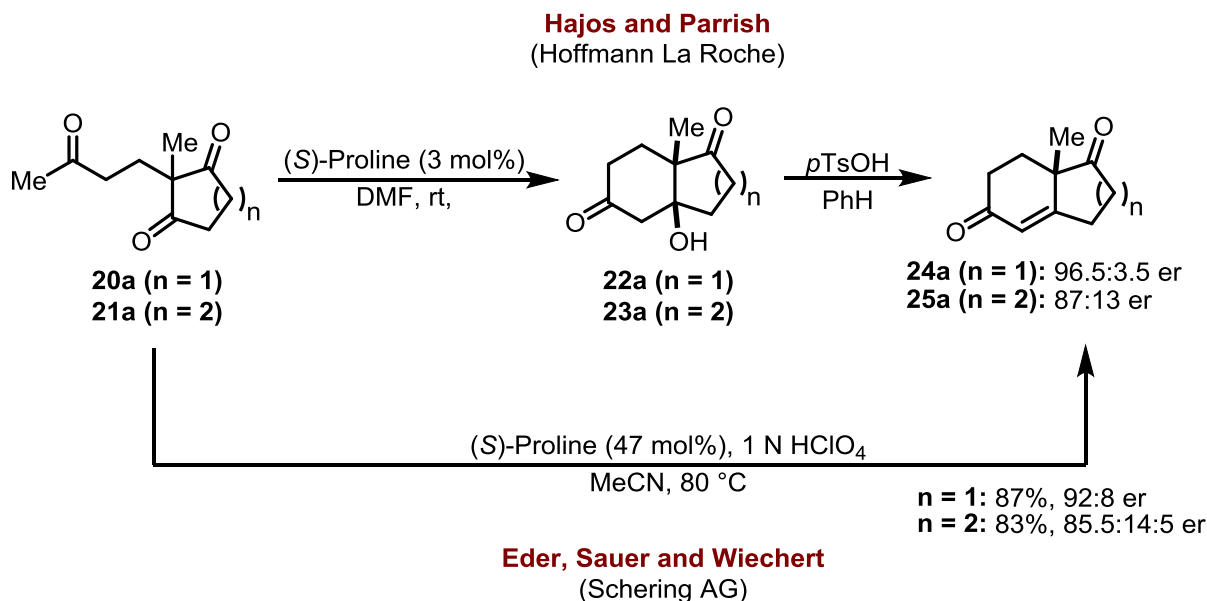
The discovery, structural elucidation and medical application of testosterone, estrone, estradiol and progesterone in the first half of the 20th century increased the demand for steroid-derived pharmaceuticals. The commercial success of steroid-based contraceptive agents fostered the design and development of novel synthetic methods. At this time, Marker degradation was the major semi-synthetic method for the synthesis of steroids from diosgenine (**19**) which can be isolated from a Mexcian wild yam (Scheme 2.6).^[72]



Scheme 2.6: Marker degradation starting from diosgenine (**19**).

Since only Mexico harvested the yams at the industrial magnitude, it rapidly became a world center for steroid production.^[73] Endiones of type **24a** and **25b**, which are reminiscent of the corresponding AB- or CD-ring systems in steroids, were recognized as an attractive alternative intermediates for the totals synthesis. Both can be easily accessed in racemic form *via* stepwise Robinson annulation starting from the corresponding 1,3-diketones catalyzed by pyrrolidine.^[74] However, enantiopure endiones could only be afforded *via* resolution or microbiological transformation of one antipode.^[75] Since these methods limit the yield of the targeted products to maximum 50%, an asymmetric synthesis was highly desired.

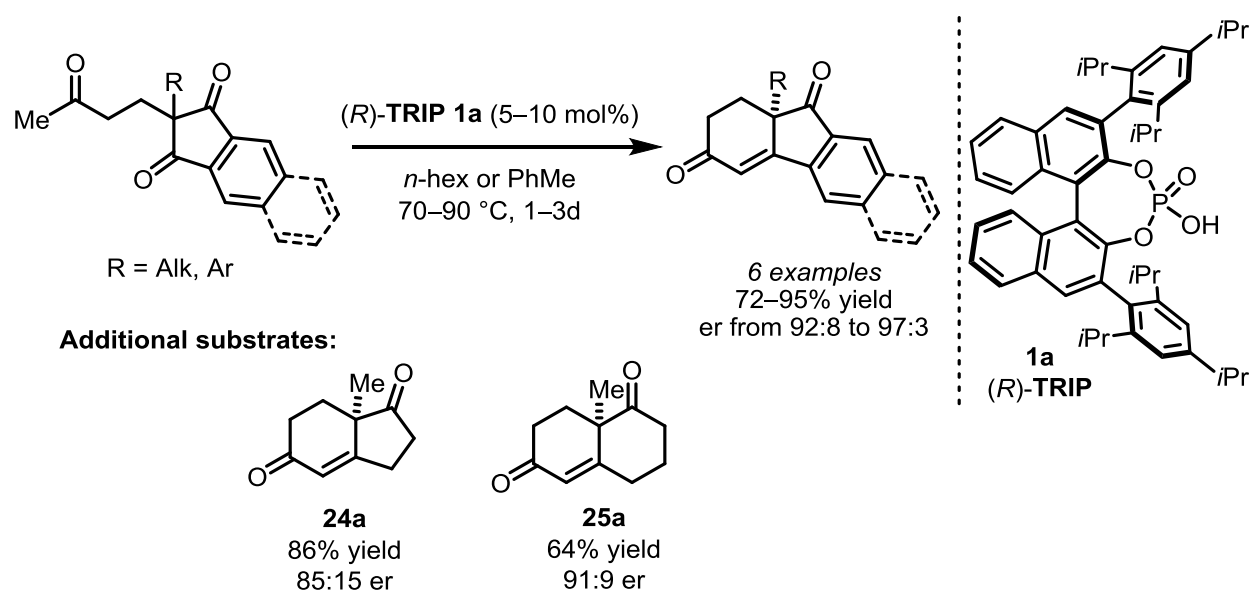
In 1971 Hajos and Parrish at Hoffmann La Roche reported the proline-catalyzed intramolecular aldol reaction of triketones **20a** and **21a** to give aldols **22a** and **23a**, which upon treatment with an acid produced the desired endiones **24a** (Hajos–Parrish ketone) and **25a** (Wieland–Miescher ketone), with good yields and enantioselectivities.^{[76][77]} Independently, Eder, Sauer and Wiechert from Schering, reported a similar proline-catalyzed reaction. Employing higher catalyst loadings, elevated temperatures and perchloric acid as an additive gave the target ketones **24a** and **25a** in a single step (Scheme 2.7).^[78] This proline-catalyzed desymmetrization of *meso*-1,3-diones is nowadays referred to as the Hajos–Parrish–Eder–Sauer–Wiechert (HPESW) reaction.^[79]



Scheme 2.7: Hajos-Parrish-Eder-Sauer-Wiechert reactions.

This reaction was a powerful alternative to the total dominance of transition metals catalysis in asymmetric synthesis. The mechanism, including the characterization of the transition state, was elucidated by Houk and List.^[80] For many reasons the synthetic potential of proline-catalyzed reactions was overlooked for the next approximately 30 years,^[3, 81] although the HPESW reaction was applied in several total syntheses, such as *ent*-deoxycholic acid,^[82] (+)-adrenosteron,^[83] (+)-cortistatin A^[84] and scabronin G^[85] to name only a few.

Although significant efforts were dedicated to extending and improving the scope and enantioselectivity of the HPESW reaction, it has not made to a large-scale industrial synthesis. Especially the synthesis of Wieland-Miescher ketone (**25a**), which under proline catalysis was only obtained in lower enantioselectivity compared to Hajos-Parrish ketone (**24a**), was particularly challenging since it required several crystallization steps to obtain it in enantiopure form.^[86] One remarkable application of this catalytic system was the extension of chiral Brønsted acid-catalyzed Robinson annulations of β -keto esters,^[87] Akiyama *et al.* reported a chiral Brønsted acid-catalyzed version of the HPESW reaction (Scheme 2.8).^[60] Using TRIP as the catalysts, the targeted tri- and tetracyclic products could be obtained in high yields (up to 94%) and enantioselectivities (er from 92:8 to 97:3). However, using **20a** and **21a** as the starting materials afforded the Hajos-Parrish ketone (**24a**) and the Wieland-Miescher ketone (**25a**) in lower enantioselectivities (85:15 er and 91:9 er, respectively).

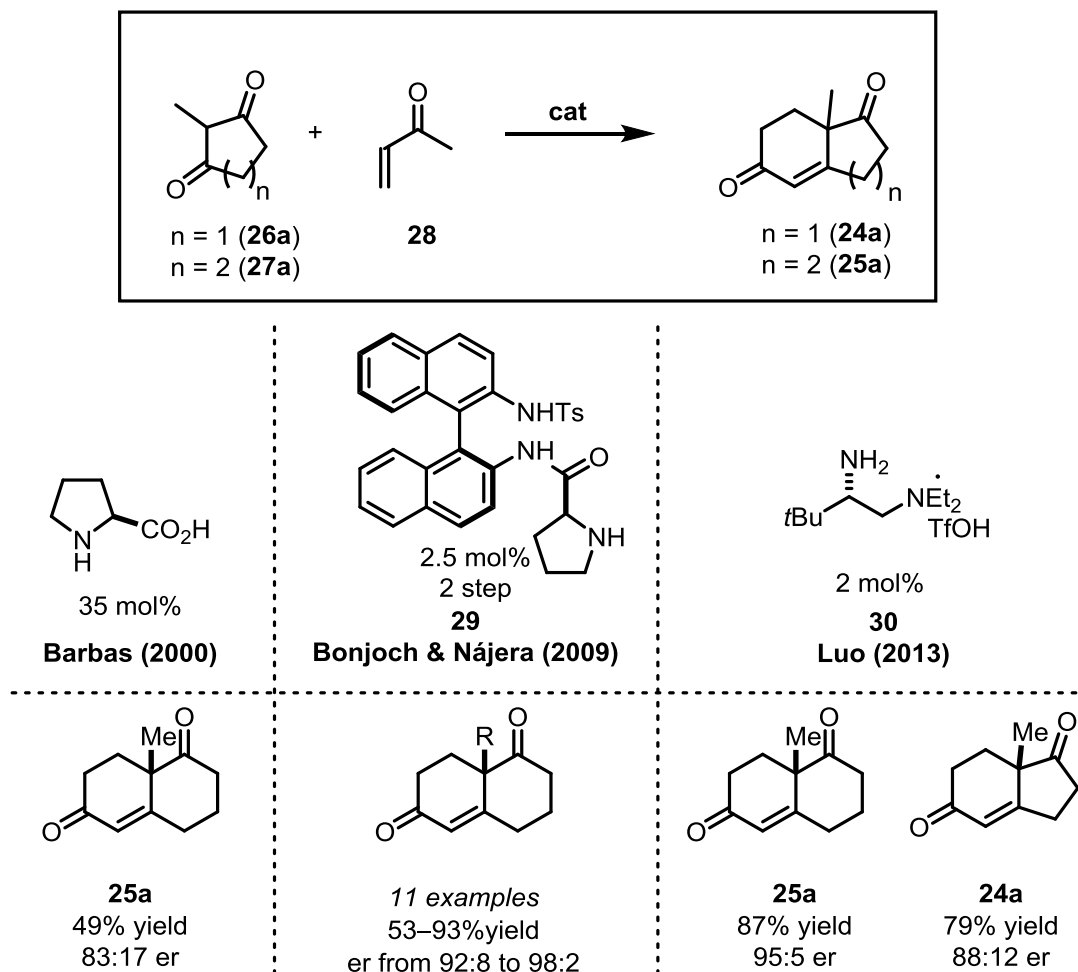


Scheme 2.8: TRIP-catalyzed HPESW reaction.

Although these developments overcame some limitations of the classical HPESW approach, such as high catalysts loadings, use of high boiling solvents and moderate to low enantioselectivity, the synthesis of triketones **20a** and **21a** was still required. A more economical and practical approach could be the direct Robinson annulation of the corresponding 2-substituted 1,3-diketones. However only few examples of such Robinson reactions were reported (Scheme 2.9): In 1997 Barbas *et al.* reported an antibody catalyzed synthesis of the Wieland-Miescher ketone.^[88] Despite the high enantioselectivity (er >97.5:2.5) and the antibody efficiently catalyzing the cyclodehydration step, only modest catalytic performance was obtained for the initial Michael reaction.

Importantly, L-proline itself is sufficiently potent to catalyze the Robinson annulation without erosion of enantioselectivity (49% yield, 88:12 er), as was reported by the same group shortly after the discovery of the proline-catalyzed intermolecular aldol reaction.^[89] In a more recent publication Bonjoch and Nájera described the application of BINAM derived catalysts **29** in a solvent free Robinson annulation of **27a**.^[90] Unfortunately, the catalyst was inactive for the initial Michael reaction resulting in a two-step one-pot procedure. Luo *et al.* reported that primary amine catalyst **30** enabled the synthesis of various Wieland-Miescher ketones in high yields (up to 87%) and excellent enantioselectivities (er from 92:8 to 96:4).^[91] Despite longer reaction times (typically 3–6 d at 2 mol% catalyst loading) a synthesis at 100 g scale pointed to its practical limitation: Although the Wieland-Miescher ketone (**25a**) could be isolated in excellent yield and

enantiomeric excess (90%, 95:5 er) an additional crystallization step was required to obtain the product as a single enantiomer (60% overall yield, 99.5:0.5 er). Therefore, increasing the yield and enantioselectivity of Hajos–Parrish and Wieland–Miescher ketones *via* Robinson annulation remained a synthetic challenge.



Scheme 2.9: Reported catalytic systems for the Robinson annulation of 1,3-diketones.

2.4 Catalytic Asymmetric α -Aminations of Ketones

α -Amino ketones and related β -amino alcohols are common structural motifs in natural products, pharmaceuticals, ligands or chiral auxiliaries that are often approached by organic synthesis (Figure 2.9).^[92] For example the synthesis of ketamine^[93] has recently attracted significant attention because this highly potent anesthetic is now considered for treating clinical depression.^[94] Because (*S*)-ketamine is up to four times more potent than its enantiomer its efficient asymmetric synthesis is of high relevance for pharmaceutical industry.^[95]

Conventional synthetic strategies of β -amino alcohols take advantage of chiral pool reagents (*e.g.* via reduction of amino acids). Alternatively, since these motifs incorporate two nucleophilic functional groups, common approaches relied upon opening of aziridines or epoxides.^[92d] It is therefore not surprising that asymmetric access of these structures is often achieved by Sharpless oxyamination^[96] and subsequent oxidation.

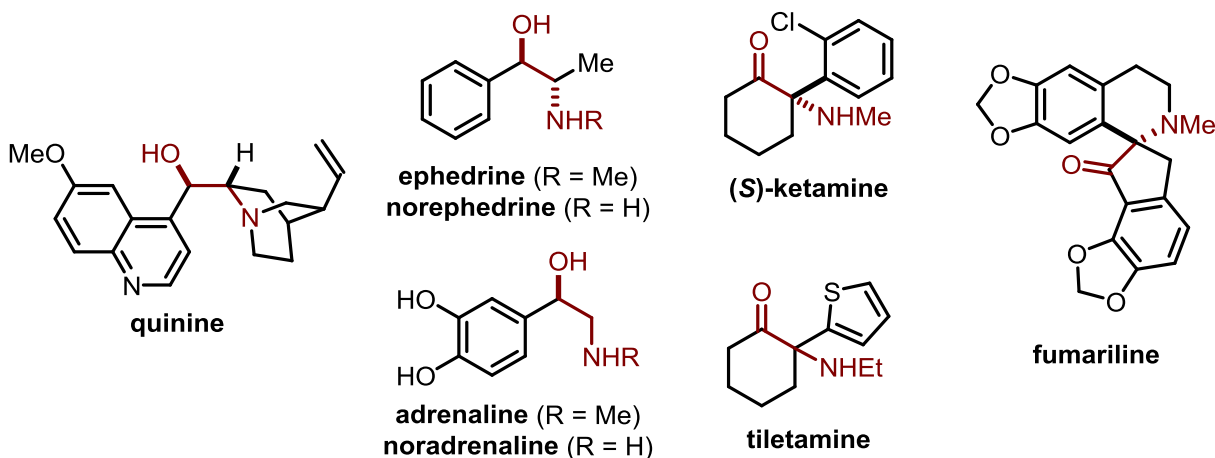
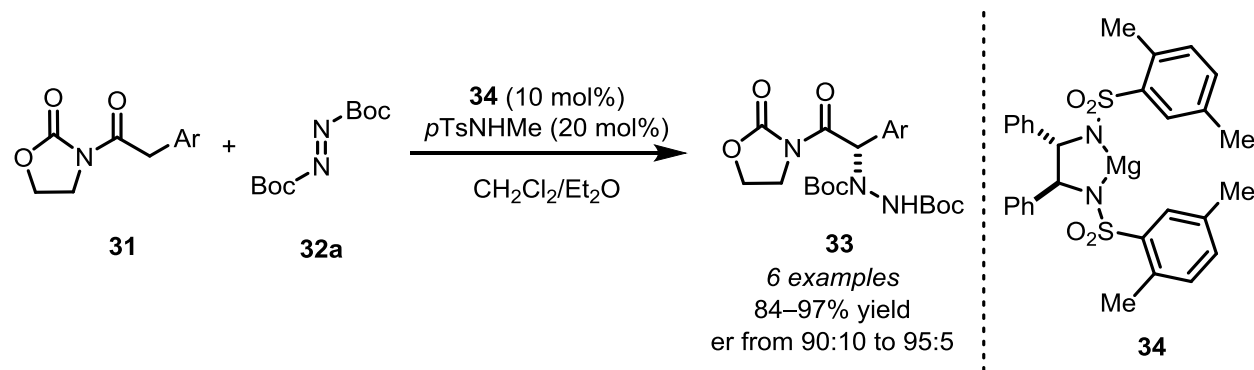


Figure 2.9: Selected examples of enantiopure α -amino ketones and β -amino alcohols in natural products and pharmaceuticals.

Although enantioselective electrophilic amination of carbonyl compounds was reported,^[97] the first catalytic version only appeared in 1997, when Evans *et al.* showed that chiral magnesium complex **34** enables the addition of aryl carboximides **31** to azodicarboxylate **32a** affording the target compounds in up to 97% yield and up to 95:5 er (Scheme 2.10). Later, numerous methods utilizing azodicarboxylates, *N*-hydroxycarbamates or nitrosobenzene as electrophilic reagents were reported. However, they usually relied on activated starting materials such as vinyl esters and ethers, nitroacetates, oxindoles, α -fluorinated ketones, β -keto or α -cyano carbonyl compounds.^[92b, 92c, 98]

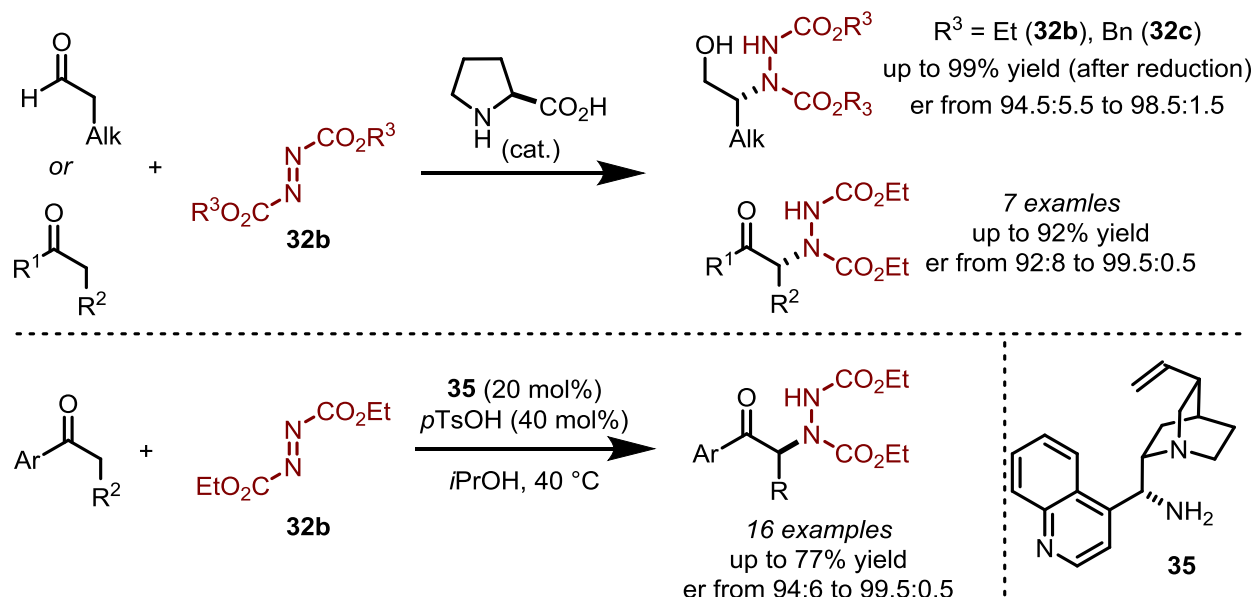


Scheme 2.10: First catalytic asymmetric electrophilic amination of carbonyl compounds by Evans *et al.* [99]

In 2002 List^[100] and Jørgensen^[101] independently reported the L-Proline catalyzed amination of unbranched aldehydes with diazocarboxylates that, upon subsequent reduction, produced corresponding protected 1,2-hydrazino alcohols in excellent yield and enantioselectivity (Scheme 2.11). Shortly after, Jørgensen confirmed the generality of this synthetic approach by extending it to unbranched cyclic and acyclic ketones.^[102] Because of higher steric hindrance aryl ketones remained challenging substrates. However, Chen and coworkers could overcome this limitation by reducing the steric bulk of the catalysts (Scheme 2.11).^[103] Applying 10 mol% of chincona alkaloid derived catalysts **35** the desired products could be obtained in good to moderated yields (up to 77%) and excellent enantioselectivities (up to 99:1 er). Recently, Wasa *et al.* reported a frustrated Lewis Acid/Brønsted base catalyst enabling the direct enantioselective α -amination of unsubstituted aryl ketones.^[104] Also, α -diazoesters were used as electrophilic amination reagents in a scandium-catalyzed example by Feng.^[50]

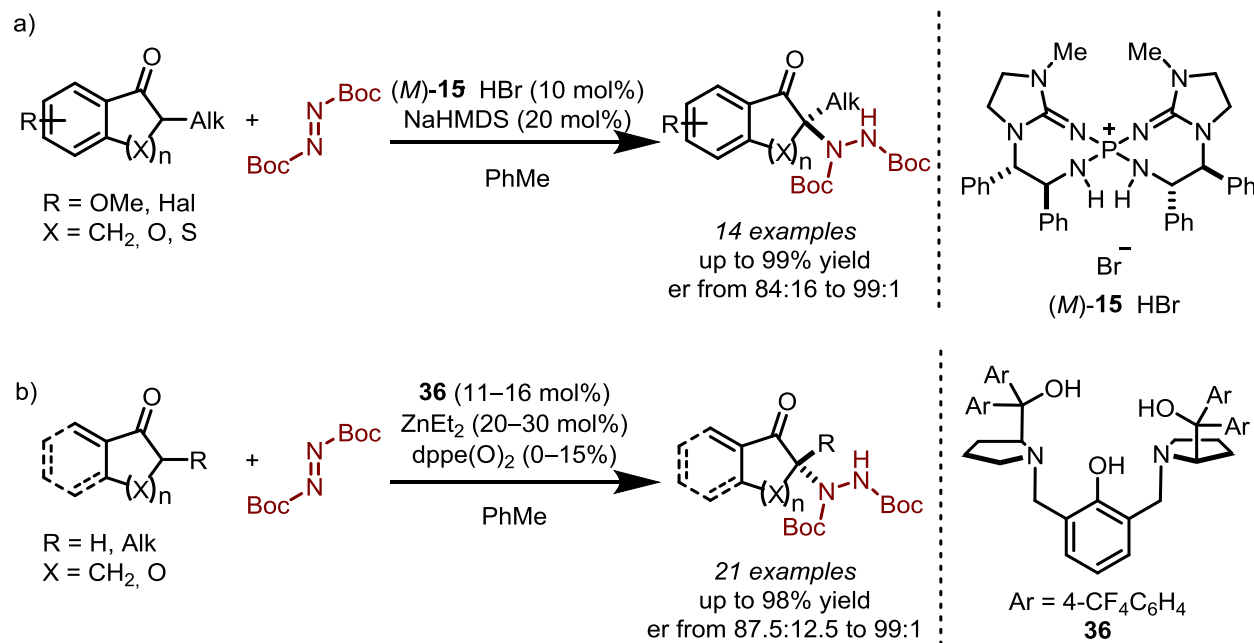
Already in 2003 Bräse *et al.* expanded the scope of L-Proline-catalyzed reactions to the direct amination of α,α -disubstituted aldehydes.^[105] Using diazocarboxylates as an electrophilic nitrogen source the targeted products were isolated in good yields (50–87%) and enantioselectivities (er from 88:12 to 93:7). Because the formation of the corresponding enamine intermediate is strongly sterically hindered higher catalyst loadings (50 mol%) and longer reaction times were required. Furthermore, one of the α -substituents should be an aryl group since otherwise the enantioselectivity was decreased down to 64:36 er. Because of importance produced α -amino aldehydes, significant efforts were directed towards improving the reaction performance.^[98i] Several systems employing secondary^[106] as well as primary amine catalysts^[107] were developed and the corresponding products further applied in the total synthesis of

biologically active compounds, such as BIRT-377, (*S*)-AIDA or (*S*)-APICA by the Barbas group.^[108]



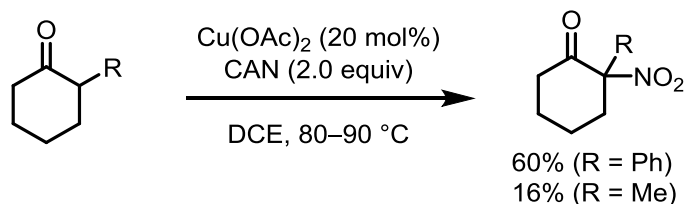
Scheme 2.11: Direct enantioselective α-amination reactions of unbranched aldehydes and ketones.

Despite excellent results achieved for α-branched aldehydes, electrophilic aminations of α-branched ketones *via* enamine catalysis suffered from the low reactivity and unfavorable steric hindrance. Only very recently alternative approaches enabling the access to corresponding α-amino ketones in a catalytic and enantioselective fashion were developed. The low acidity of α-alkyl ketones was circumvented by Terada *et al.* by employing chiral bis(guanidino)iminophosphoranes as organosuperbases.^[53a] Upon activation with NaHMDS, these compounds could deprotonate 2-alkyltetralones and their analogues and afford the desired products in excellent yields (up to >99%) and enantioselectivities (er from 84:16 to 99:1) (Scheme 2.12 a). Recently, Trost *et al.* showed that the Zn-ProPhenol system can promote the direct amination of branched and unbranched ketones (Scheme 2.12 b).^[47b] Because strongly basic conditions were applied, these methods were limited to tetralone-derivatives and their analogues since one side of the ketone should be blocked in order to prevent the side reaction *via* the less hindered unsubstituted position.



Scheme 2.12: Amination of α -branched aryl ketones using a) organosuperbase **15** and b) Zn-ProPhenol.

This challenge was recently addressed by Zhang *et al.* in a non-enantioselective copper catalyzed direct nitration of α -branched ketones using CAN as the oxidant (Scheme 2.13),^[109] that suffered from side reactions and moderate to low yields of target compounds. The authors suggested that the reaction proceeds *via* oxidation of *in situ* formed cerium enolates to form α -acyl radicals which are then quenched by NO₂ resulting from the decomposition of CAN. The reaction could also proceed in the absence of copper, however higher yields were obtained in presence of 20 mol% of Cu(OAc)₂ presumably due to enhanced enolate formation.



Scheme 2.13: Direct α -nitration of α -branched cyclic ketones.

In summary, despite extensive experimental efforts, direct catalytic and enantioselective amination of simple α -branched ketones remains a synthetic challenge.

2.5 Direct α -Oxidations of Ketones

α -Hydroxy carbonyls are common motifs in natural products and pharmaceuticals and are therefore highly appealing synthetic targets (Figure 2.10).^[110] The developed direct synthetic approaches include the reaction of *in situ* generated enolates with (chiral) electrophilic oxygen sources as oxaziridines^[111] or use of the Vedejs reagent (MoOPH)^[112] or oxidation of the corresponding vinyl ethers (Rubottom oxidation).^[113]

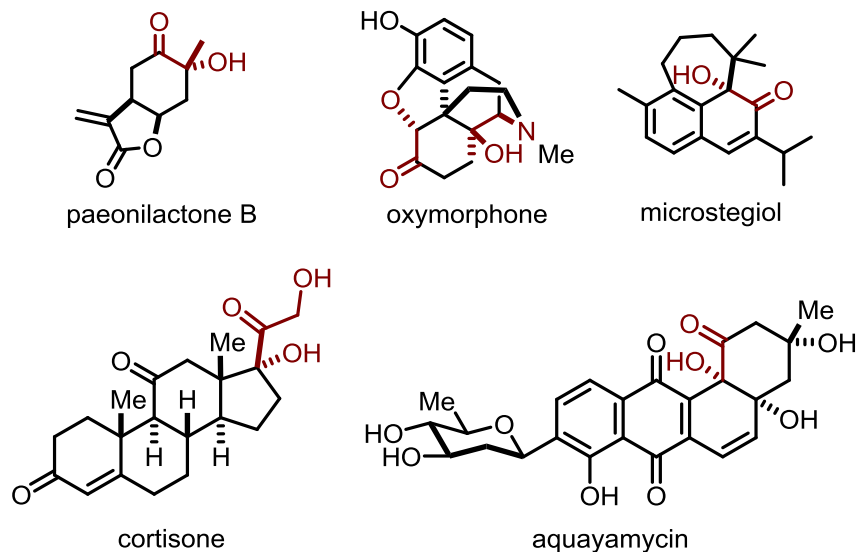


Figure 2.10: Selected natural products and pharmaceuticals bearing the α -hydroxy ketone moiety.

2.5.1 Direct α -Hydroxylations of Simple α -Branched Ketones

Hydroxylation of simple α -branched ketones remains challenging, not only because of the lower α -C–H acidity, but also because it is necessary to control the branched *vs* unbranched regioselectivity. Only few methods could address this issue (Figure 2.11). Although not catalytic, but still remarkable methods were published by Schulz^[114] and Zhang,^[115] that, presumably rely upon carbocationic pathway (for details, see section 2.5.6). They used water as a nucleophilic oxygen source together with strong oxidants such as electron deficient quinones or aminoyl radical salts. Whereas the scope of latter method was limited to 2-aryl cyclohexanones, the former method also allowed the reaction with challenging acyclic ketones. Recently, direct catalytic methods employing either Pd^[116], Cu^[117] or strong bases as Cs₂CO₃^[118] and molecular oxygen as the oxidant were developed, although no metal-free methods for the direct hydroxylation of unactivated α -branched ketones have been reported.

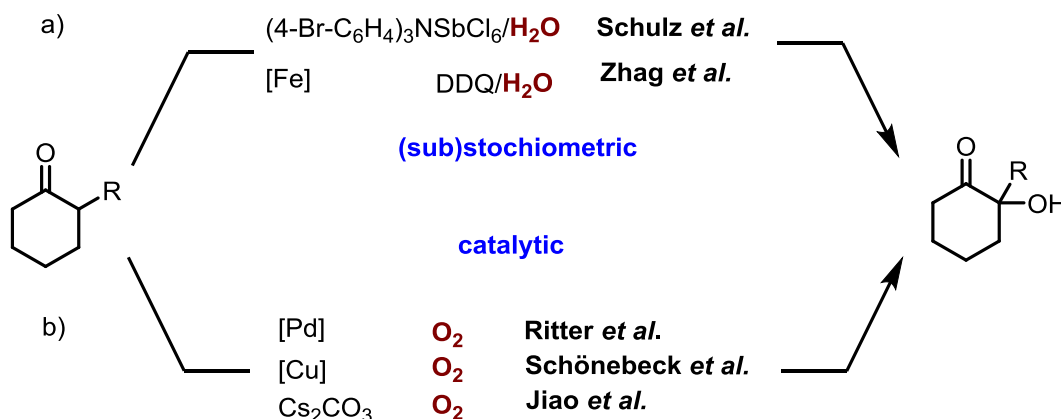
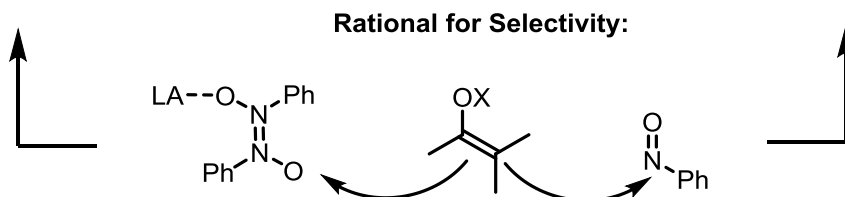
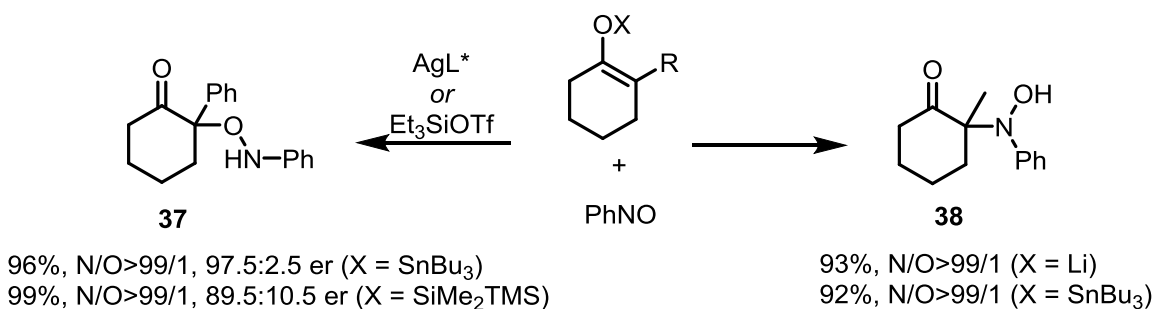


Figure 2.11: Recent methods for the direct hydroxylation of simple α -branched ketones using 2-substituted cyclohexanone as example: a) stoichiometric/(sub)stoichiometric reagents and b) catalytic systems employing molecular oxygen.

2.5.2 Catalytic Asymmetric Aminoxylation Reactions

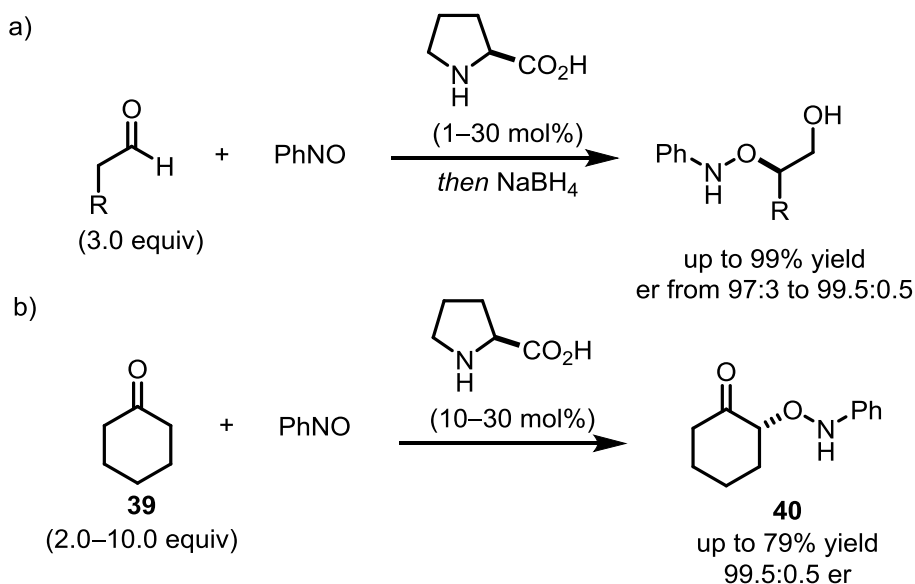
In contrast to activated carbonyl compounds, such as β -keto carbonyl derivatives, direct asymmetric hydroxylation of simple aldehydes and ketones is an imminent challenge in asymmetric catalysis.^[92a, 92b, 119] It is not surprising that methods taking advantage of nature's chiral pool,^[120] chiral reagents^[111] or chiral auxiliaries^[121] were commonly employed. Alternative approaches utilizing methods initially developed for asymmetric epoxidations/dihydroxylations of olefins, *e.g.* the Sharpless dihydroxylation^[122] or the Jacobsen-Katsuki^[123] and Shi-epoxidations,^[124] in Rubottom-type reactions of preformed vinyl ethers and esters provided a workaround solution.

Recently, Yamamoto and co-workers reported on Lewis acid catalyzed aminoxylation reactions using silyl vinyl ethers or tin enolates with nitrosobenzene as the oxidant. High *O/N* selectivity was observed and the corresponding hydroxy ketones could be obtained in an additional step using CuSO_4 as catalyst (Scheme 2.14).^[125] Interestingly, the *O/N* selectivity changed depending on the employed conditions: in presence of a Lewis acid the reaction exclusively proceeded *via O*-attack, whereas in the absence of Lewis acid *N*-attack was preferred. As nitroso compounds exist in an equilibrium of monomer and dimer forms,^[126] the reactions selectivity was explained by the Lewis acid shifting this equilibrium towards the formation of the dimer. Nevertheless, these indirect methods require 1 to 2 additional synthetic steps including prefunctionalization of the starting material.



Scheme 2.14: Lewis acid catalyzed reaction of vinyl ethers or esters with nitrosobenzene by Yamamoto *et al.* (LA = Lewis acid).

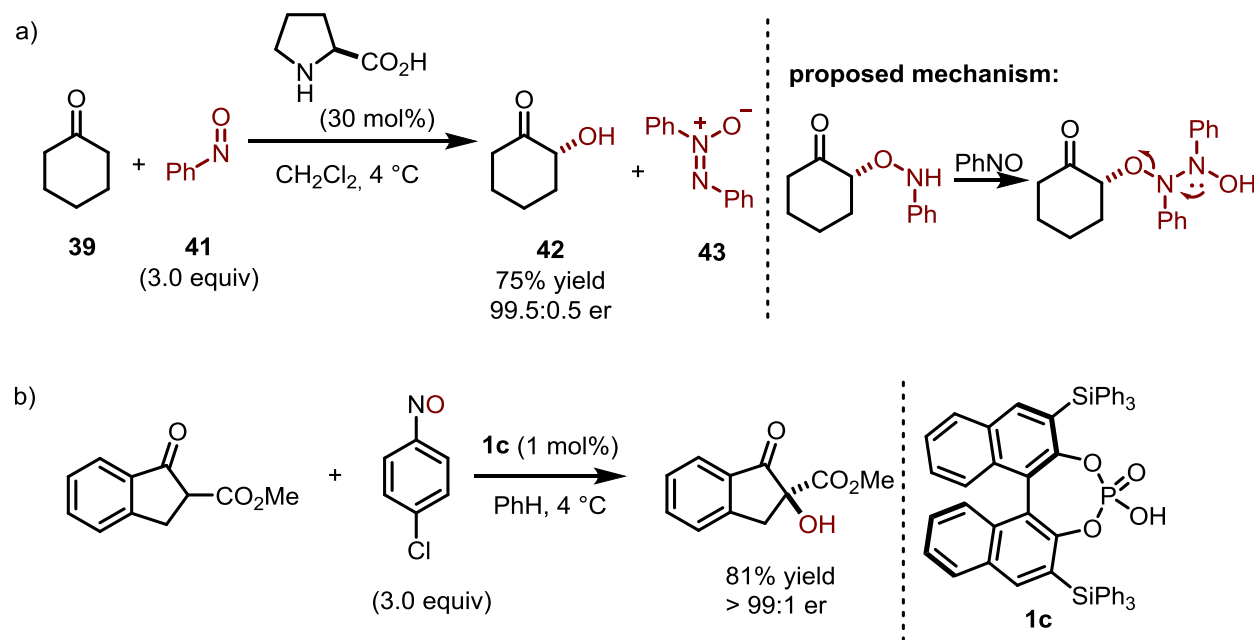
Inspired by these reports, direct and enantioselective aminoxylation reactions of simple carbonyl compounds were also employed within the context of organocatalysis (Scheme 2.15).^[92c, 127] In 2003, MacMillan,^[128] Hayashi^[129] and Zhong^[130] independently reported the reaction of linear aldehydes with nitrosobenzene using L-Proline as the catalyst affording corresponding products in excellent yields and enantioselectivities ($\geq 97:3$ er). Only *O*-selective attack of the *in situ* formed enamine onto nitrosobenzene was obtained, however a threefold excess of the aldehyde compared to nitrosobenzene was required to avoid self-condensation. Extension of the scope towards cyclic ketones,^[102, 131] acyclic ketones and α -branched aldehydes was possible although their *O/N*-selectivity was compromised.^[132] Furthermore, the selectivity can be inverted by reducing the acidity of the catalyst.^[98k, 133] Due to the intrinsic limitations of enamine catalysis similar reactions with α -branched ketones have not been reported.^[131b]



Scheme 2:15: Organocatalytic α -aminoxylation of a) aldehydes and b) ketones.

While exploring the desymmetrization of *meso*-cyclohexanones *via* L-Proline catalyzed aminoxylation, Barbas *et al.* discovered the direct formation of corresponding hydroxy ketones in the presence of excessive amounts of nitrosobenzene (Scheme 2.16 a).^[134] The following mechanism assuming a dual role of nitrosobenzene was proposed: Nitrosobenzene was supposed to act as an oxidant furnishing the corresponding aminoxylation intermediate; additionally, the second nitrosobenzene equivalent reduced the N–O bond affording azoxybenzene (**43**) as a side product. This proved to be a generic mechanism for proline-catalyzed aminoxylation reactions also observed in reactions with aldehydes and cyclohexanones.

More recently Zhong *et al.* applied this approach to the direct hydroxylation of β -keto carbonyl compounds using chiral phosphoric acid **1c** as the catalysts (Scheme 2.16 b), that afforded the target products in good yields (up to 88%) and good to excellent enantioselectivities (er up to >99:1).^[135] Acyclic substrates were also tolerated under the reaction conditions, albeit the yields and enantioselectivities were compromised.



Scheme 2.16: Aminoxylation/N–O reduction sequence catalyzed by a) L-Proline and b) chiral Brønsted acid **1c**.

2.5.3 Alternative Approaches

In the recent years, several alternative approaches for the direct synthesis of α -hydroxy carbonyl compounds, such as *via* phase-transfer catalysis (PTC), have been developed. PTC enables enantioselective hydroxylations of ketones using molecular oxygen and an excess of reductant (*e.g.* $\text{P}(\text{OEt})_3$).^[136] However, the reactions were carried out in strongly basic conditions and therefore their scope was limited to α,α' -substituted ketones, *e.g.* acetophenone-derivatives, 2-substituted indanones or tetralones.

Alternative strategies made use of singlet oxygen, hypervalent iodine reagents, oxaziridines or benzoyl peroxide and use chiral secondary amines as catalysts^[92c]. However, these methods were limited to unbranched carbonyl compounds and apart of two publications on the reaction of α -branched aldehydes by List^[137] and Jacobsen^[138] groups, direct hydroxylation of branched substrates (especially of simple α -branched ketones) was not reported.

The majority of reactions discussed here proceed *via* ionic mechanisms. Alternative synthetic methods relying on α -carbonyl radicals generated through formal H-atom abstraction, *e.g.* by the combination of acetone and *t*-butyl hydro peroxide require rather harsh reaction conditions.^[139] Therefore, the last part of this section will focus on an exciting alternative method

of generating α -carbonyl radicals *via* single electron oxidation of enols under mild reaction conditions.

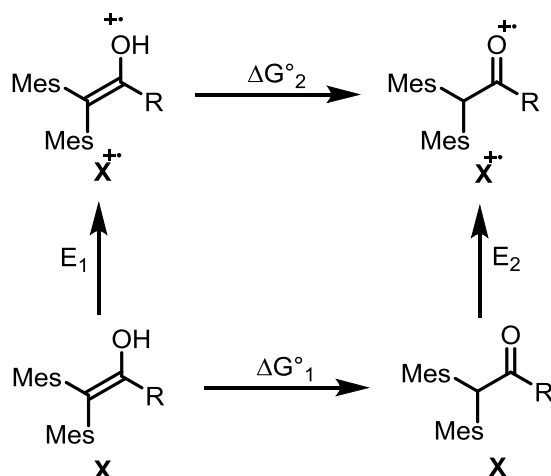
2.5.4 Oxidation of Enols

Surprisingly, the one-electron oxidation chemistry of carbonyl groups is barely investigated.^[140] Intra-^[141] and intermolecular^[142] oxidative transformations involving one-electron oxidation of enolates were applied in total synthesis of (\pm)-hirsutene,^[143] acremoauxin A, oxazinin 3^[144] and palau'amine.^[145] One-electron oxidation of enamines, so-called SOMO catalysis, is a well-established methodology for the asymmetric α -functionalization of simple aldehydes and ketones.^[146] Because of rapid tautomerization into thermodynamically favorable ketone forms, mechanistic studies on the oxidation of enols are scarce. It is therefore not surprising that their more stable and highly electron rich analogues, such as vinyl ethers,^[147] silyl vinyl ethers^[148] and vinyl esters^[149] are much better explored.

2.5.5 Properties of Enol Cation Radicals

Neutral ketones are thermodynamically more stable than their enol-tautomers. However, theoretical and experimental studies suggested that, in contrast to one-electron reduction, enol cation radicals are more stable than corresponding ketone ions under single electron oxidation.^[150] One plausible explanation is that bond energies (C=O vs C=C) are higher in enols (Figure 2.2). However, significant geometrical changes of enols upon one-electron oxidation (elongation of the C–C bond from 1.35 Å to 1.44 Å and shortening of the C–O bond from 1.37 Å to 1.30 Å), suggest that the electron is removed from the π -orbital. These structural changes do not occur in corresponding ketones, as the electron is presumably removed from the oxygen lone pair. Removing an electron from the π -system requires less energy than from an oxygen lone pair and leads to inversed stability of ketone and enol radical cations.^[140a, 151]

Thermodynamic data acquired for stable β,β -mestiyl enols indicated that similar behavior is also observed in solution (Figure 2.12)^[152] and suggested two plausible pathways for the formation of enol cation radicals: 1) Oxidation of the ketone and subsequent 1,3-hydrogen migration or 2) selective oxidation of the enol present in the tautomer equilibrium. However, *ab initio* calculations suggested higher energy barriers for the rearrangement of aldehyde and keto radical cations, hence strongly favoring the latter pathway.^[140a]



R =	E_1/V	E_2/V	$\Delta G^\circ_1/\text{kcal mol}^{-1}$	$\Delta G^\circ_2/\text{kcal mol}^{-1}$
H	1.00	1.98	-3.1	-25.7
<i>t</i> Bu	0.98	1.85	2.6	-17.7

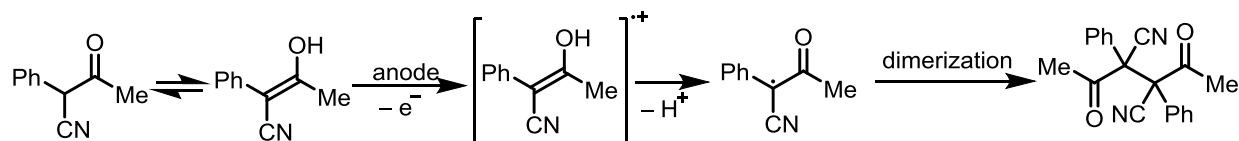
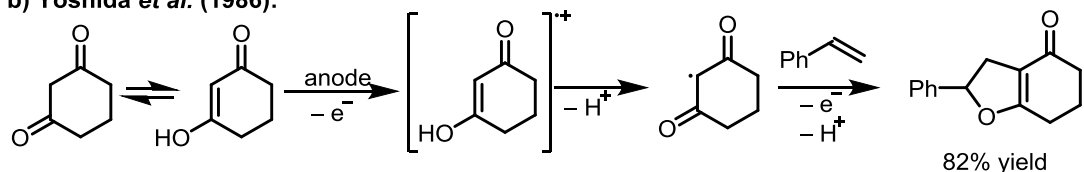
Figure 2.12: Thermodynamic data on oxidation of the keto/enol tautomeric equilibrium in solution. *Note:* As only irreversible oxidations were obtained, these numbers can be only viewed as good estimate.^[152]

Therefore oxidation potential of enols is ~ 1 V lower compared to corresponding ketones, which, in turn, suggests that applying only a mild oxidant could ensure a selective oxidation of enols present in the tautomeric equilibrium. Furthermore, recent studies demonstrated that hydrogen bonding can further decrease the oxidation potential of enols by another 0.5 V.^[153]

2.5.6 Reactions of Enol Cation Radicals

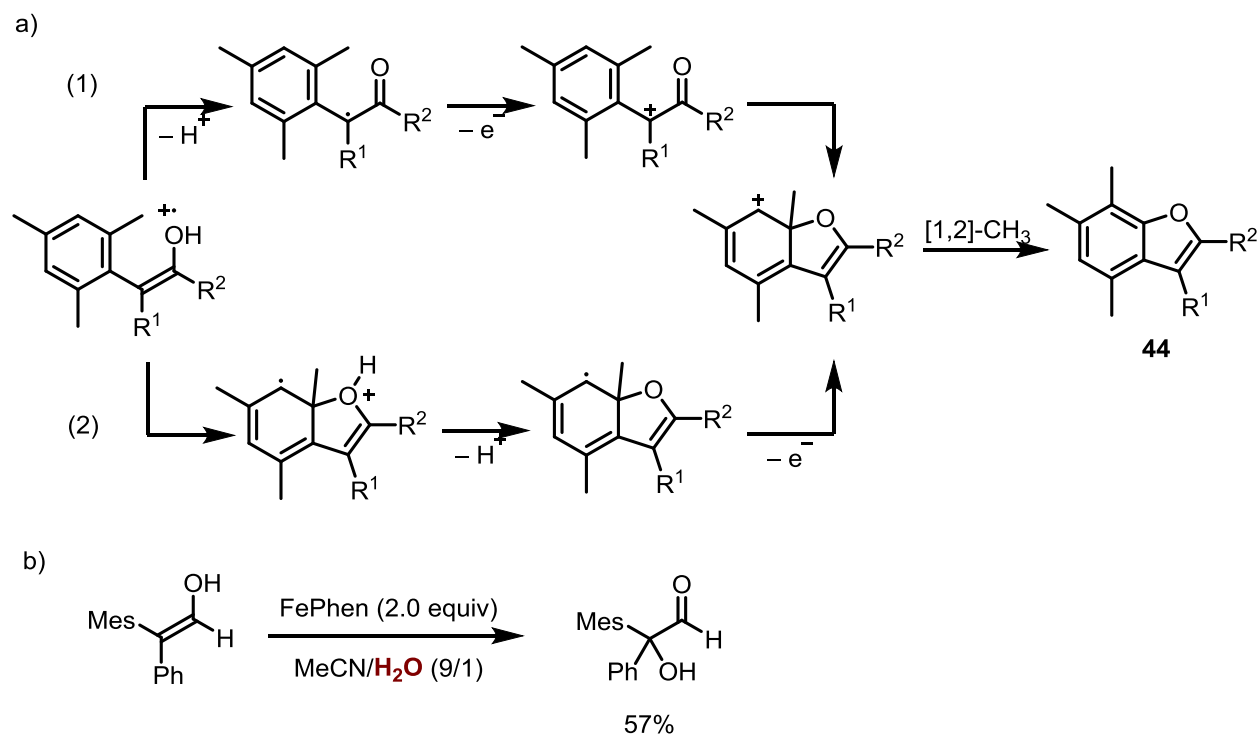
Despite using activated ketones, pioneering work of Moing, Le Guillanton and Simonet, reporting the dimerization of α -cyano ketones under anodic conditions,^[154] and Yoshida, reporting oxidative [2+3] cycloadditions of 1,3-diketones and olefins,^[155] have demonstrated the synthetic potential of selective enol oxidation (Scheme 2.17). Both mechanisms assumed the formation of α -carbonyl radicals upon oxidation of the enol and subsequent deprotonation; however the exact mechanism was not elucidated. Since both tautomers are present in the reaction medium an alternative reaction pathway *via* oxidation of the ketone could not be ruled out.

a) Moing, Le Guillanton, Simonet (1982):

b) Yoshida *et al.* (1986):**Scheme 2.17:** Early examples of synthetic application of enol cation radicals.

Schmittel *et al.* could overcome this limitation by investigating strongly sterically hindered mesityl-substituted carbonyl compounds of which the kinetically stabilized enol as well as the corresponding ketone could be obtained in tautomerically pure form.^[152, 156] Oxidizing β - and β,β -diemesityl substituted enols with two equivalents of an appropriate outer-sphere one-electron oxidant, *e.g.* triarylammonium salts or iron(III) phenantroline (FePhen), lead to benzofuranes (**44**) (Scheme 2.18 a). Same products could be generated by cyclic voltammetry under preparative electrooxidation conditions. The studies proposed two plausible mechanisms: (1) Upon oxidation, the enol cation radical was deprotonated and produced an α -carbonyl radical, which underwent second oxidation, cyclisation and 1,2-methyl migration. Although the intramolecular cyclization of the enol cation radical could not be excluded (2), oxidation of less hindered enols in the presence of a nucleophile, *e.g.* methanol or water, produced corresponding α -substituted carbonyl compounds (Scheme 2.18 b) and indicated the presence of a carbocationic intermediate. This formal Umpolung of ketones, however with simpler substrates, was independently discovered by Schulz *et al.*^[114]

Due to the short life-time of enol cation radicals their electrochemical characterization deemed impossible. The life-time of a radical resulting from the corresponding enol ether is in the order of seconds, which indicates that proton loss creating α -carbonyl radicals could be the primary reaction pathway.^[140a]



Scheme 2.18: a) Proposed mechanisms for the oxidative formation of benzofuranes (**44**) and b) α -hydroxylation in presence of water.

2.5.7 Proton Coupled Electron Transfer

The observed net reaction leading to the ketone α -radical is a hydrogen atom transfer (HAT) from the enol to the oxidant. In these reactions a formal homolytic cleavage of the X–H bond of a donor and recombination of the resulting hydrogen atom with the corresponding acceptor generates neutral free radicals which undergo subsequent reactions. The thermodynamic driving force for HAT reactions is proportional to the difference of the strengths of broken and newly formed bonds. The transfer only takes place if the donor and the acceptor are having similar bond dissociation free energies (BDFE). Since most synthetically interesting functional groups feature bond strengths exceeding $100 \text{ kcal mol}^{-1}$ and the reduction generates, due to the vicinal position to a radical, X–H bonds with significantly lower BDFEs, the synthetic utility of HAT, with some exceptions, is strongly limited (Figure 2.13). The weakest known metal-hydride species $\text{H–V(CO)}_4(\text{dppb})$ has a V–H BDFE of ca. 50 kcal mol^{-1} ,^[157] and it is therefore still too strong for reductive activation of common organic π -systems.^[158]

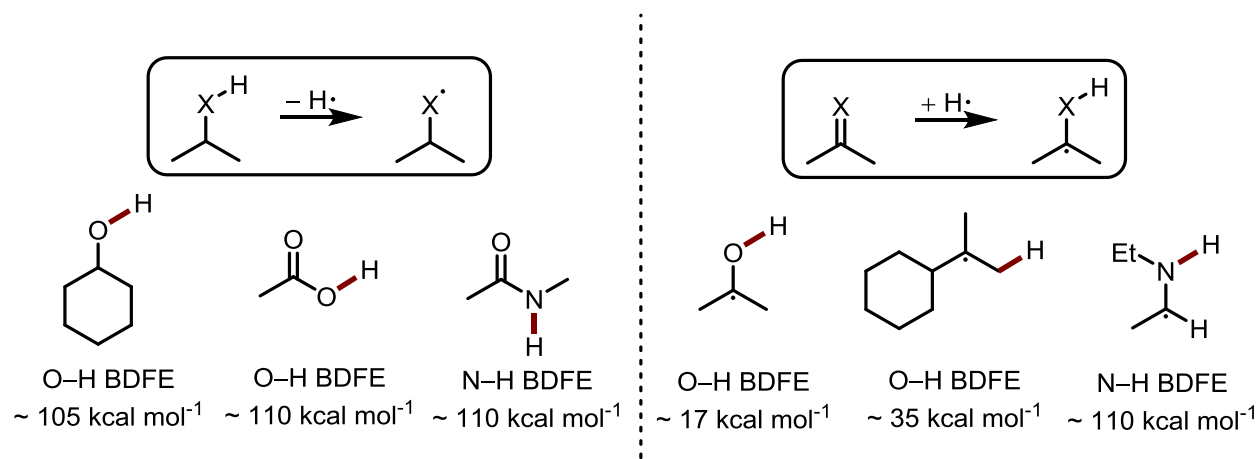


Figure 2.13: Selected BDFEs of common organic functional groups.^[158]

According to Bordwell *et al.*, factors contributing to the BDFE of a given bond can be analyzed in a thermodynamic cycle (Figure 2.14).^[159] The homolytic bond cleavage can be considered as a sum of the heterolytic bond cleavage (characterized by its pK_a) and the energy required to reduce/oxidize the formally formed ions to corresponding radical species and the hydrogen atom. This ultimately suggests that, in order to weaken the X–H bond of a hydrogen atom donor, either pK_a or redox potential should be altered. Since within the same molecule these parameters are inversely correlated, a rational design of the reagent remains challenging.

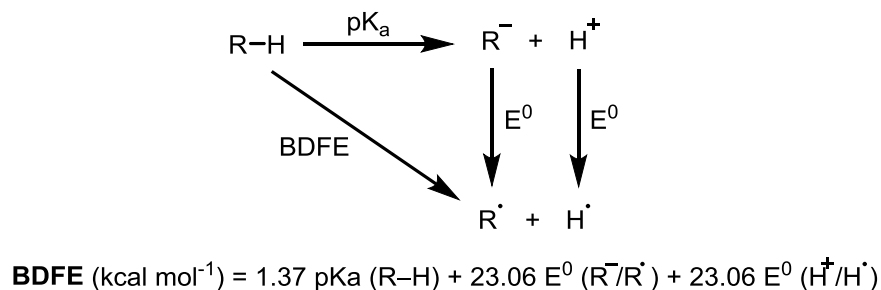


Figure 2.14: Thermodynamic cycle for the determination of BDFEs according to Bordwell.^[159]

In a HAT mechanism proton and electron result from the same bond, in a multisite proton coupled electron transfer (PCET) process they originate from spatially separated independent donors: a Brønsted acid and a single electron oxidant. Since products are neutral free radicals, PCET is similar to traditional HAT; however it is not affected by its thermodynamic constraints and therefore could enable the activation of previously energetically inaccessible functional groups.

Although no bond is homolytically cleaved during PCET process, according to Mayer *et al.* a conceptually similar thermodynamic cycle should still be valid (Figure 2.15).^[160] In this case the sum of pK_a and redox potentials gives an “effective” BDFE which quantifies the ability of any acid/reductant to function as a hydrogen atom donor. Furthermore, the pK_a and the redox potentials are now featured by two independent molecules and can be adjusted according to the requirements.

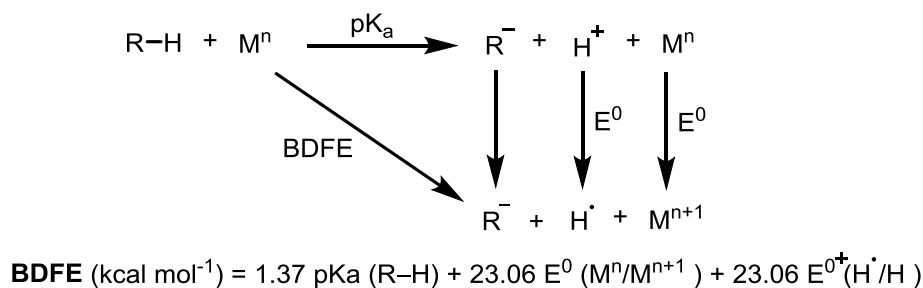


Figure 2.15: Thermodynamic cycle for the determination of BDFEs of multisite PCET according to Mayer.^[160]

PCET allows tunable access to more powerful HAT reagents; but it also enables highly selective and orthogonal bond activation. In contrast to conventional HAT processes, whose selectivity is mainly determined by the bond strength, pre-coordination *via* hydrogen bonding and distance of electron- ($> 10 \text{ \AA}$) and proton-transfer ($1\text{--}2 \text{ \AA}$) are dominant factors for PCET.

Besides favorable thermodynamic advantages PCET is also kinetically favored over the competing stepwise pathways (Figure 2.16). It circumvents high energy intermediates and reactions could be carried out under much milder conditions (in respect to pK_a or potentials) than required for particular substrates.

Nevertheless, competition between HAT and PCET might occur, as for example with aromatic ketones.^[161]

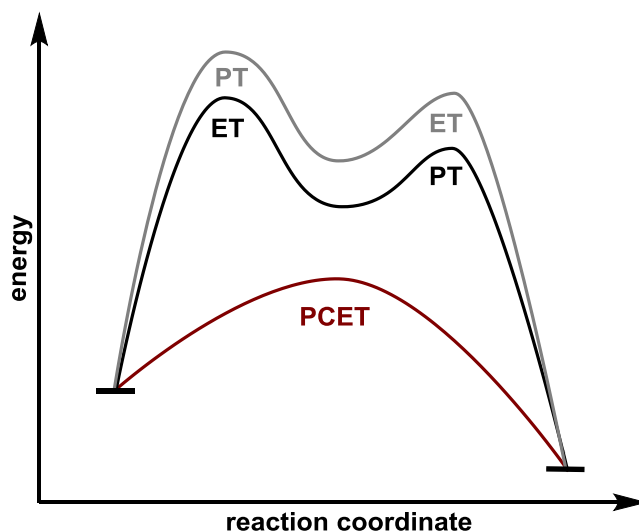
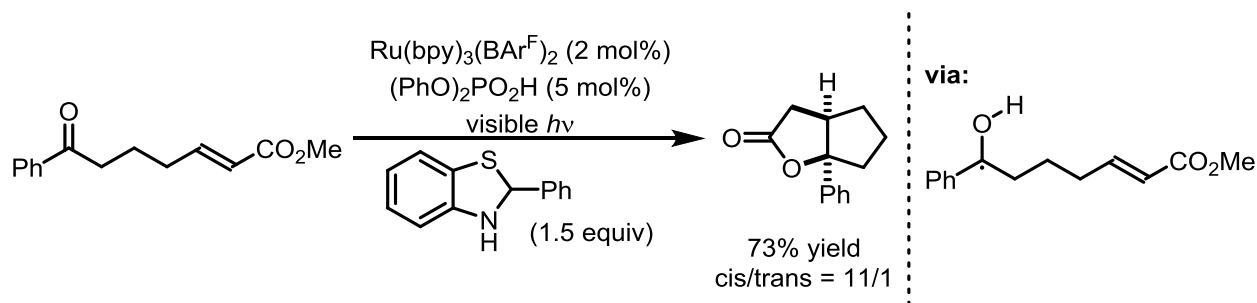


Figure 2.16: Reaction coordinate demonstrating kinetic advantages of PCET relative to the corresponding stepwise processes.^[158, 162]

2.5.8 Recent Applications of PCET in Asymmetric Catalysis

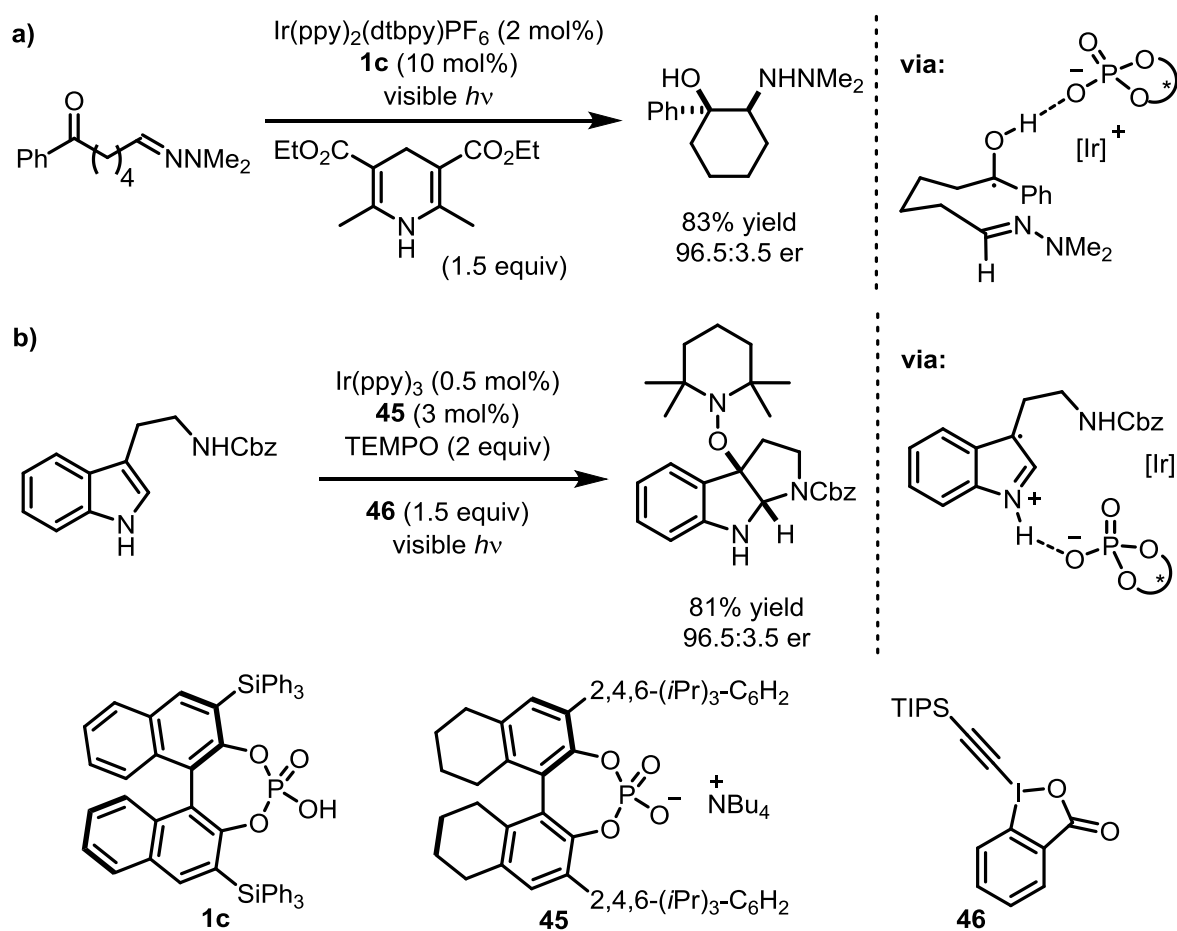
PCET mechanism is best known for its role in biological energy conversion during respiration and photosynthesis.^[163] Due to rising interest in photoredox catalysis, PCET has also been recognized as method of chemical synthesis.^[158, 162, 164] In 2013, Knowles *et al.* reported a reduction of ketones to corresponding ketyl radicals and their subsequent coupling with olefins to furnish substituted cyclopentanes (Scheme 2.19).^[165] The key factor in the successful reduction of BDFE of the ketone to the one of ketyl radicals ($\sim 26 \text{ kcal mol}^{-1}$) was the combination of a ruthenium-based photoredox catalyst and a Brønsted acid.



Scheme 2.19: Ketyl-olefin coupling reported by Knowles *et al.*^[165]

By following this seminal work, PCET has expanded into new application areas. Notable examples are the activation of N–H bond in amides, carbamates and sulfonamides^[166], the O–H bond in alcohols^[167] or the S–H bond in thiols.^[168] However, until recently, only few enantioselective applications were reported. Knowles and co-workers performed reductive

coupling of ketones and hydrazones (Scheme 2.20 a).^[169] Similar to their previous report on ketyl-olefin couplings, a ketyl radical was generated *via* PCET using a photoredox catalysts and a chiral phosphoric acid. A subsequent C–C bond forming step and quenching of the resulting *N*-centered radical with a Hantzsch ester furnished the targeted cyclic amino alcohols in good to excellent yields (up to 96%) and enantioselectivities (er from 83.5:16.5 to 98:2). More recently the same group reported a photocatalytic method for the synthesis of indole radical cations which could be intercepted by TEMPO to furnish alkoxyamine-substituted pyrroloindoles in good yields (up to 80%) and enantioselectivities (er from 93.5:6.5 to 96:4).^[170] In this case a single-electron reduction was the key step and a combination of photoredox catalyst and chiral phosphate ensured high levels of reactivity and selectivity. Further derivatization of the obtained products using a catalytic single-electron oxidation/mesolytic cleavage sequence in presence of nucleophiles was demonstrated.



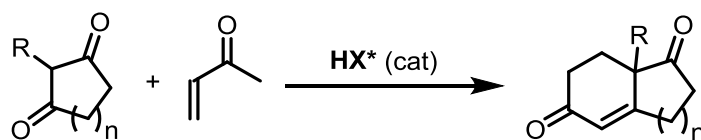
Scheme 2.20: Enantioselective a) coupling of ketones and hydrazones and b) synthesis of indole radical cations.

Meggers group reported a combination of their previously developed chiral-at-rhodium Lewis acid and a photocatalyst enabling enantioselective access to β -amino carbonyl-derivatives from α,β -unsaturated 2-acyl imidazoles and *N*-aryl carbamates.^[171] According to the proposed reaction mechanism an *N*-centered radical was generated *via* PCET together with the radical resulting from single electron reduction of rhodium-coordinated α,β -unsaturated 2-acyl imidazole. Subsequent radical recombination afforded the desired products in excellent yields (up to 99%) and enantioselectivities (er from 97:3 to 99:1). The same group reported an asymmetric variant of a PCET/1,5-HAT sequence for the remote C–H alkylation of amides initially reported by Knowles^[172] and Rovis.^[173]

.

3 Objectives

The Hajos–Parrish–Eder–Sauer–Wiechert reaction is an iconic transformation in organocatalysis and a benchmark for evaluating newly developed amine catalysts. Furthermore, the obtained products have been used as starting materials in numerous total syntheses. As already mentioned in section 2.3, Akiyama showed that this intramolecular aldol reaction can be catalyzed by a chiral phosphoric acid.^[60] However, in order to obtain high enantiomeric excess, specific activated substrates had to be used. In this context we wondered if we could find a solution to this problem and achieve the direct and highly enantioselective synthesis of Hajos–Parrish and Wieland–Miescher ketones, starting from readily available 2-substituted-1,3-diketones and methyl vinyl ketone (Figure 3.1).



Scheme 3.1: Envisioned enantioselective Robinson annulation of cyclic 1,3-diketones.

The direct α -functionalization of α -branched ketones is a major challenge in asymmetric catalysis and only few systems for the *in situ* generation of reactive enolate equivalents have been reported. These systems typically operate under basic conditions and typically favor the formation of the corresponding kinetic products. Therefore, they are restricted to substrates in which one side of the ketone is blocked. In this context we wondered if Brønsted acid-catalyzed enolization (*enol catalysis*) could enable the formation of the more substituted enols, thus giving enantioselective access to α,α -disubstituted ketones. In parallel to our studies on the chiral phosphoric acid-catalyzed Michael addition of unactivated branched ketones to enones *via enol catalysis*,^[63, 174] we also decided to pursue α -heterofunctionalization reactions, which could grant us an efficient access to highly valuable synthetic building blocks.

In particular, direct α -amination appeared as highly attractive approach because it opens a straight forward synthetic route towards enantiomerically pure α -amino ketones and β -amino alcohols, which are ubiquitous structures in natural products and pharmaceuticals. Despite the poor atom-economy, azodicarboxylates were envisioned as suitable electrophilic amination reagents, since they are highly reactive and commercially available (Figure 3.1).

We further aimed at extending the scope of *enol catalysis* to C–O bond forming reactions (Figure 3.1). As previously described, α -hydroxy ketones are also important and ubiquitous motifs that could be obtained by direct hydroxylation of ketones. Beyond controlling the enantioselectivity, the major challenge in such transformations is the choice of an appropriate electrophilic oxygen source.

The α -arylation of aldehydes, β -keto esters, substituted indoles or 2-naphtols *via* the conjugate addition to 1,4-benzoquinones is a well-established methodology in asymmetric organocatalysis.^[175] As an extension of our previous work on *enol catalysis*, we further considered a phosphoric acid-catalyzed addition of cyclic ketones to benzoquinones (Figure 3.1).

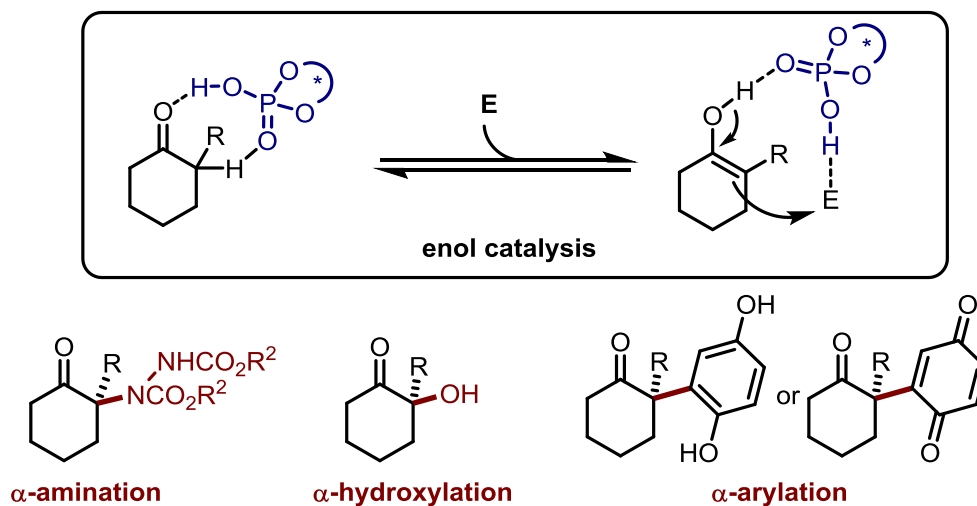


Figure 3.1: Proposed activation mode of *enol catalysis* and envisioned transformations.

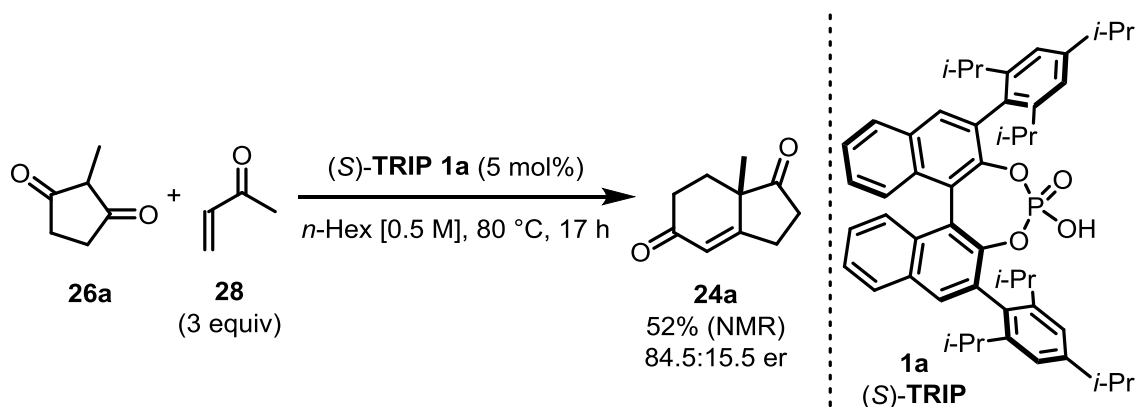
4 Results and Discussion

4.1 Brønsted Acid-Catalyzed Asymmetric Robinson Annulations

The work presented in this section was done with support by Dr. Desislava Petkova.

4.1.1 Initial Studies

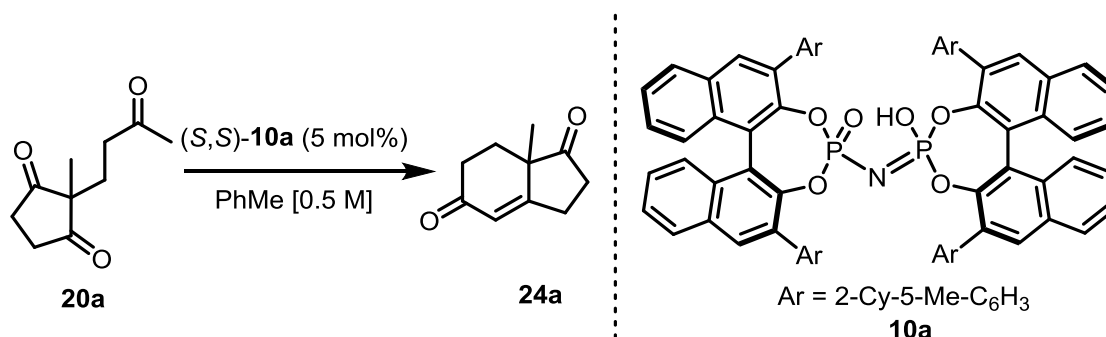
In an initial experiment 1,3-diketone **26a** was subjected to an excess of methyl vinyl ketone (**28**) and (*S*)-TRIP (**1a**) as the catalyst and the desired product could be obtained in 52% NMR-yield and 84.5:15.5 er (Scheme 4.1). Comparing this with Akiyama's results (86% yield, 85:15 er starting from the corresponding triketone intermediate)^[60] suggested that the one-pot Robinson annulation should be possible under Brønsted acidic conditions and the reaction proceeds with negligible erosion of enantioselectivity.



Scheme 4.1: Initial experiment on the Brønsted acid-catalyzed asymmetric Robinson annulation. Absolute configuration assigned according to Akiyama *et al.*

In order to simplify the initial process of screening for optimal reaction conditions, we decided to first focus on the enantiodetermining aldol reaction starting from triketone **20a** and to later apply the optimized conditions to the one-pot sequence described above. In addition to phosphoric acids, we evaluated the performance of various IDP catalysts. Out of the tested substitution patterns of 3,3'-aryl substituents, *ortho*-substitution proved to be the most crucial in respect to enantioselectivity. Using catalysts **10a**, the targeted product was obtained in high enantioselectivities, yet in low yields (Table 4.1). Despite several attempts to further optimize the conditions through additives and application of temperature programs, the yields could not be improved. Furthermore, when these conditions were applied to the envisioned complete Robinson

annulation sequence, the product was obtained in only 22% yield and reduced enantioselectivity (94:6 er) after prolonged reaction time (5 d).



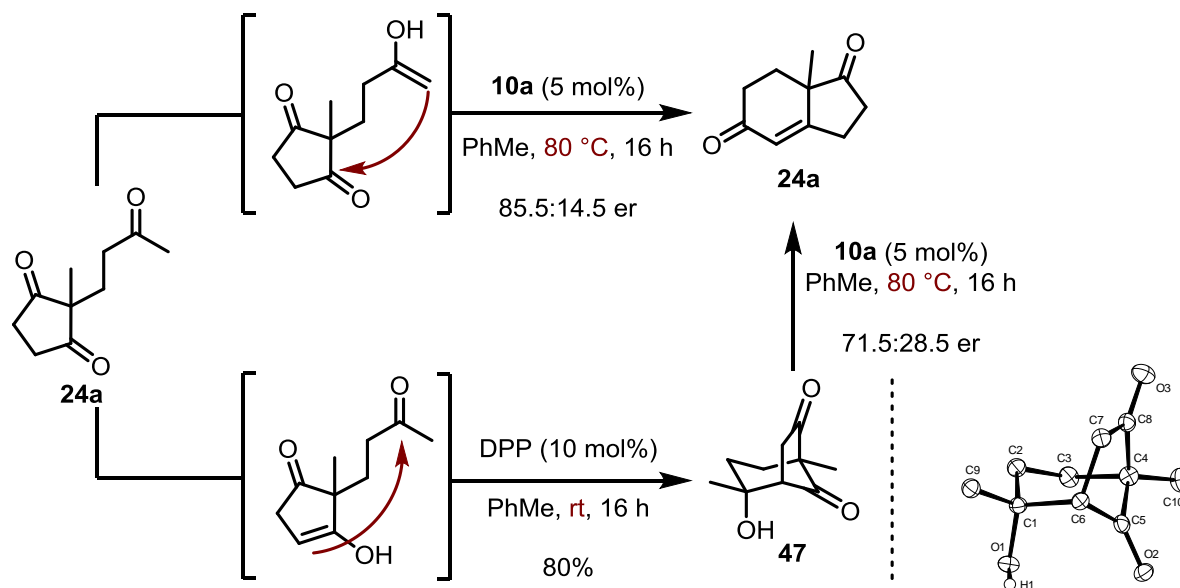
Entry	T/°C	time	yield ^a	er
1	80	3 h	35%	85.5:14.5
2	50	24 h	34%	87:13
3	rt	48 h	17%	98:2

Table 4.1: Selected conditions for the Brønsted acid-catalyzed aldol reaction toward the Hajos-Parrish ketone. ^aDetermined by ¹H NMR analysis of the crude reaction mixture using Ph₃CH as internal standard.

Especially at low temperatures, the compound **47**, resulting from the attack of the enol formed at the cyclopentanone onto the methyl ketone, was identified as the main side product of this transformation (Scheme 4.2). Since equilibrium constants for the enolization of primary ketones (*e.g.* acetone, pK = 7.20) and cyclopentanone (pK = 7.20) are similar, it is likely that both aldol reactions occur at similar rates, but the low solubility of **47** in nonpolar solvents shifts the equilibrium towards this undesired aldol product. Furthermore, IDPs furnished higher amounts of undesired **47** than phosphoric acids. This could be explained by the catalysts structure, where monomeric phosphoric acids provide an open cavity while highly confined active site of the IDPs forces the flexible substrate into a more staggered conformation.

Since the irreversible elimination of the alcohol in **47** is disfavored according to Bredt's rule^[176] and aldol reactions are *per se* reversible, we wondered if the byproduct could be converted to the targeted Hajos-Parrish ketone **24a**. Indeed, when **47** was subjected to the reaction conditions using catalysts **10a** at elevated temperatures, diketone **24a** could be obtained, albeit with reduced enantioselectivity (71.5:28.5 er). Therefore we concluded that the reaction should be performed at elevated temperatures. Furthermore, the optimal catalysts should possess

a proper confined environment, which does catalyze the desired transformation enantioselectively without erosion of chemoselectivity.



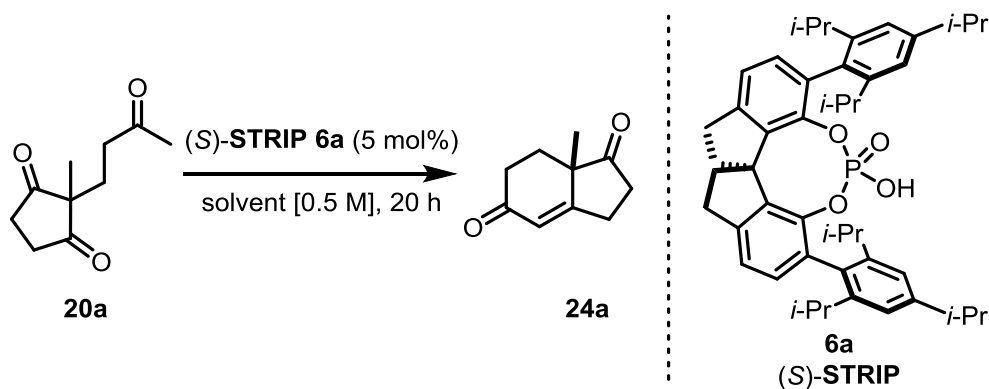
Scheme 4.2: Preparation, reactivity and X-ray crystal structure of **47**.

4.1.2 Breakthrough and Fine-Tuning of Reaction Conditions

A breakthrough was achieved by switching from BINOL-derived TRIP to SPINOL-derived STRIP, which produced the target compound in up to 95.5:4.5 er and synthetically useful yields (Table 4.2).

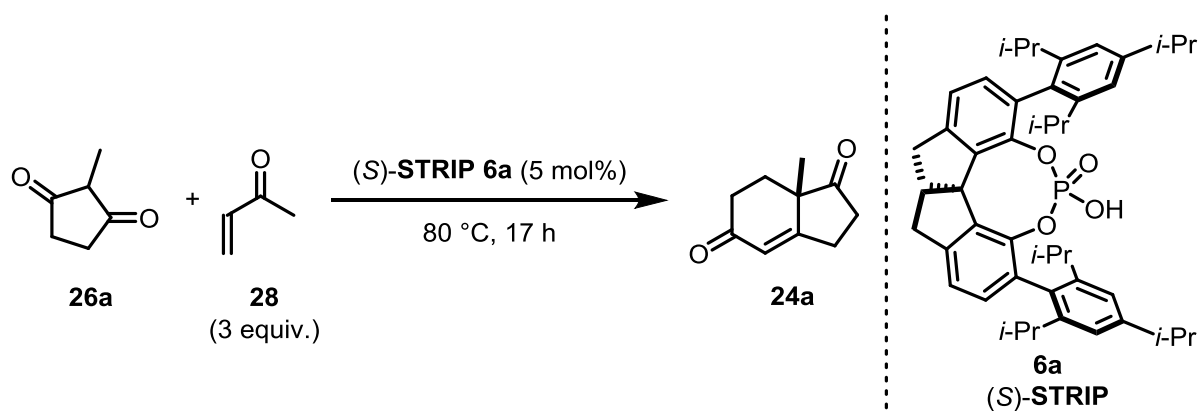
With these promising results in hand, we turned our attention toward our initial goal, the full Robinson annulation. Unfortunately, this approach turned out to be rather challenging. Despite several attempts, yields of the target material did not exceed 10%, although the enantioselectivities were high (Table 4.3, Entries 1, 2 and 4). One possible explanation is that, because of their high polarity, 1,3-diketones are poorly soluble in non-polar solvents.. A possible solution would be to either add an acidic co-catalysts or phase-transfer catalysts forming soluble ion-pairs. This, however, did not improve the yield and enantioselectivity (Entry 3 and 5). Interestingly, even though the reaction barely proceeds in water (Entry 6), to our delight, the addition of water as a co-solvent strongly improved the yields without erosion of enantioselectivity (Entry 7). It is known that the initial Michael reaction proceeds in water under acidic conditions, however the solubility of the formed triketone **20a** was low. Therefore, we

speculated that our phosphoric acid catalyst, besides promoting enolization, also acts as a phase transfer catalyst. The addition of dibutylhydroxytoluene (BHT) to prevent the polymerization of methyl vinyl ketone at elevated temperatures further improved the yields without deterioration of enantioselectivity (Entry 8; 38% NMR-yield, 98:2 er).



Entry	solvent	T/°C	yield ^a	er
1	PhMe	80	47%	94:6
2	CyH	80	41%	95:5
3	<i>n</i> -Hex	80	62%	95.5:4.5
4	<i>n</i> -Hex	60	7%	97.5:2.5

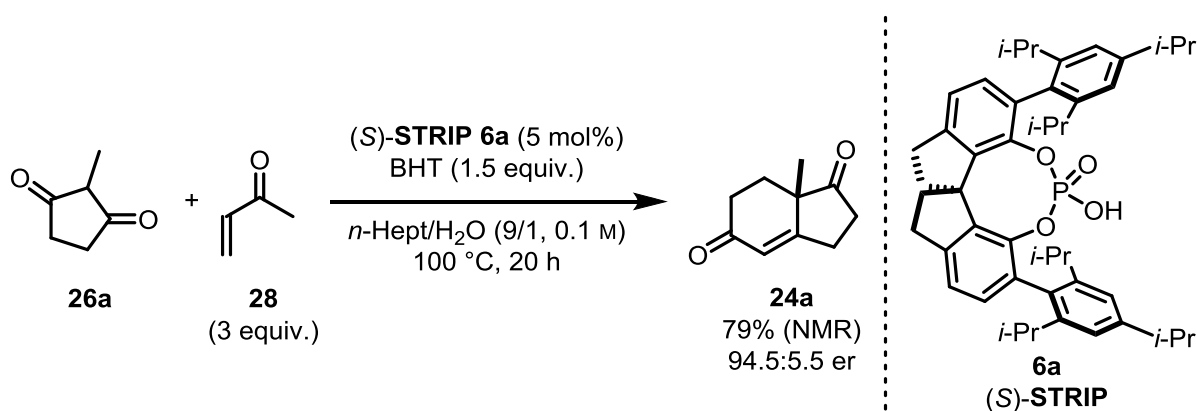
Table 4.2: Optimization of reaction conditions using (S)-STRIP as the catalyst. ^aDetermined by ¹H NMR analysis of the crude reaction mixture using Ph₃CH as internal standard.



Entry	solvent	C/M	yield ^a	er	comment
1	<i>n</i> -Hex	0.5	2%	98.5:1.5	-
2	<i>n</i> -Hex	0.25	4%	98.5:1.5	-
3	<i>n</i> -Hex	0.5	8%	96.5:3.5	10 mol% of BzOH added
4	<i>n</i> -Hept	0.5	4%	98.5:1.5	-
5	<i>n</i> -Hept	0.25	7%	n.d.	10 mol% of TBAB added
6	H ₂ O	0.25	3%	n.d.	-
7	<i>n</i> -Hept/H ₂ O (2/1)	0.3	19%	98:2	-
8	<i>n</i>-Hept/H₂O (2/1)	0.3	38%	98:2	1.5 equiv of BHT added

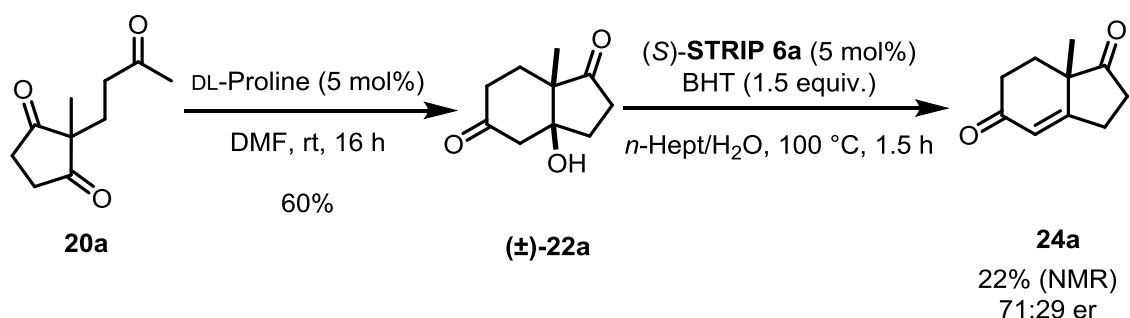
Table 4.3: Initial results on the Robinson annulation using (S)-STRIP as the catalysts. The best result is highlighted in bold. ^aDetermined by ¹H NMR analysis of the crude reaction mixture using Ph₃CH as internal standard.

The yields were further increased by performing the reaction at higher temperatures (100 °C) and higher ratio of *n*-Hept/H₂O (9/1). The amount of BHT was not critical; however, at least 1 equivalent had to be used to efficiently suppress polymerization. The optimized reaction conditions are presented in Scheme 4.2.



Scheme 4.2: Optimized reaction conditions.

Interestingly, decreasing the catalyst loading from 5 mol% to 2.5 mol% decreased the yield, yet slightly enhanced the enantioselectivity. This highlighted a trend which we already observed during our optimization studies: lower yields, under otherwise similar or identical reaction conditions, coincided with higher enantioselectivities. Although the magnitude of changes was rather small, it prompted us to consider a kinetic resolution pathway which favors the desired enantiomer in the final dehydration step. Therefore, racemic ketol (\pm)-**22a** was prepared using DL-Proline (Scheme 4.3). Indeed, when (\pm)-**22a** was subjected to the optimized reaction conditions an enantioenrichment favoring the obtained major enantiomer was observed. However, a possible DKR mechanism cannot be excluded at this point.



Scheme 4.3: Investigations into the kinetic resolution of ketol (\pm)-**22a**.

4.1.3 Preliminary Substrate Scope

Although these results were highly promising, a preliminary substrate scope showed that, under given conditions, the reaction scope lacked generality (Figure 4.1). Whereas the Hajos-Parrish ketone (**24a**) could, as was already shown, be synthesized in good yield and

enantioselectivity (79% NMR-yield and 94.5:4.5 er), its benzyl-derivative showed not only lower reactivity but also selectivity (64% NMR-yield and 91:9 er). Gratifyingly, when extending the ring size of the used 1,3-diketone, the Wieland-Miescher ketone (**25a**) could be obtained in 83% isolated yield and 98:2 er.

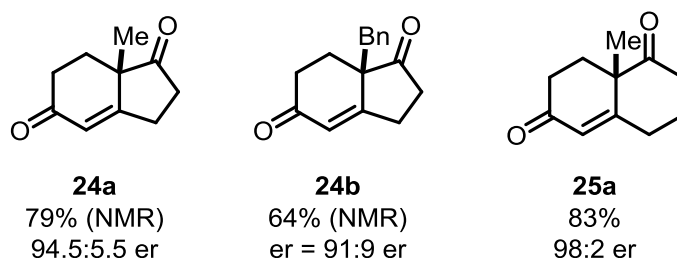
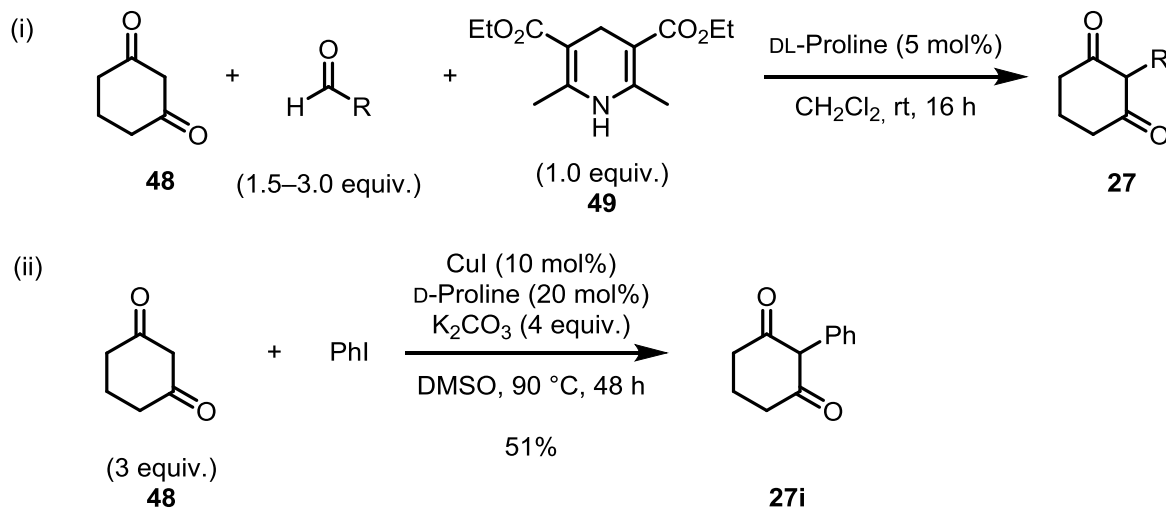


Figure 4.1: Preliminary substrate scope.

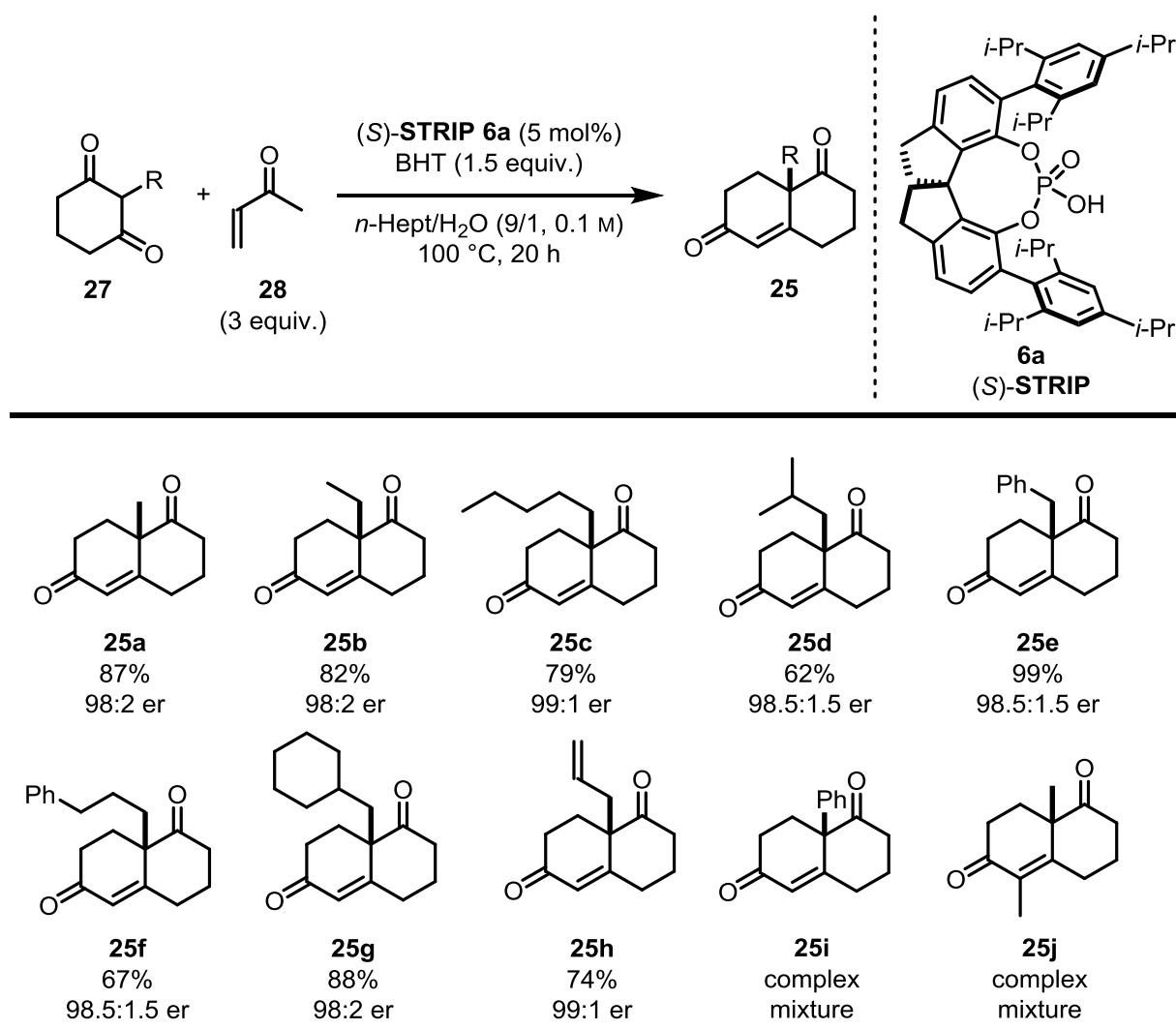
With these results in hand, we then decided to investigate the generality of our transformation toward various Wieland-Miescher ketone derivatives. The starting materials were obtained in a one pot aldol/conjugate reduction sequence of cyclohex-1,3-dione (**48**) and a corresponding aldehyde in presence of Ethidine (**49**) using DL-Proline as catalysts (Scheme 4.4). Phenyl-substituted substrate **27i** was synthesized *via* copper(I)-catalyzed coupling of cyclohex-1,3-dione (**48**) and iodobenzene.



Scheme 4.4: General procedures for the synthesis of the starting materials.

To our delight, under the reaction conditions nearly all tested substrates gave the expected products in good to excellent yields (62–99%) and excellent enantioselectivities (>98:2 er)

(Scheme 4.5). Current limitations are aryl-substituted substrates, such as **27i**, and other vinyl ketones, since both lead to in complex reaction mixtures (**25i** and **25j**).



Scheme 4.5: Preliminary substrate scope of Wieland-Miescher ketones.

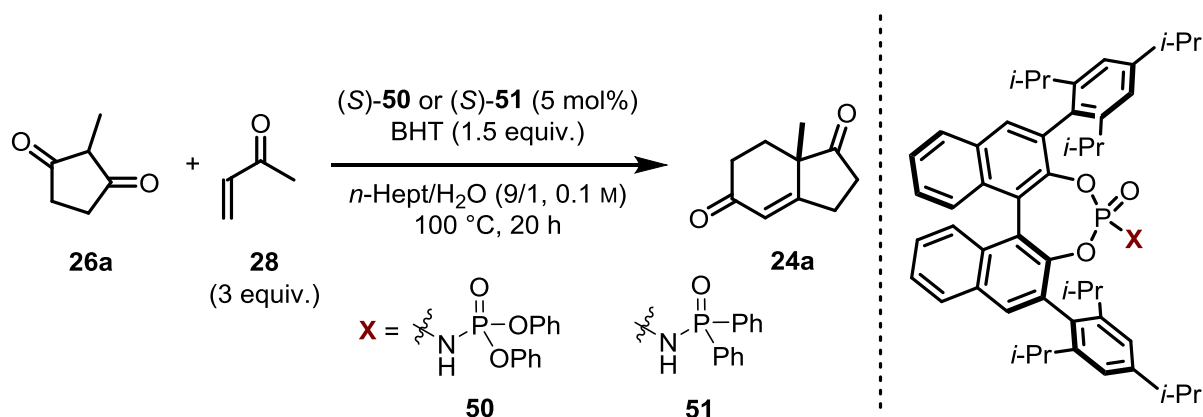
4.1.4 Revisiting the Catalyst Structure

Having disclosed an efficient system for the synthesis of Wieland-Miescher ketones, we turned our attention back to underperforming Hajos-Parrish ketones. From our previous studies we concluded that the selectivity issue cannot be solved by further modifying the reaction conditions and therefore we decided to further optimize the catalyst structure. We identified three starting points for further catalyst development: 1) the active site, 2) the 3,3'-substituents and 3) the catalyst backbone. Out of these three possibilities, the first two seemed to us to be the most

facile, since we could take advantage of well-established BINOL chemistry and then extend our positive experience to the SPINOL-backbone.

Modification of the Active Site

As described above, IDP catalysts showed no significant improvement regarding the enantioselectivity compared to TRIP. This could be explained by the high confinement and rigid structure generated by the two BINOL-backbones. We therefore tested bisphosphorylimide **50** and *N*-phosphinyl phosphoramidate **51**,^[177] in which one of the BINOL-moieties is substituted by aryl/aryloxy groups. Unfortunately, enantioselectivity was not improved (Entries 1–4, Table 4.4). We assume that the active site of these catalysts is stretching too far out of the cavity and therefore limiting the required interaction of substrate and substituents in the 3,3'-position of the catalysts.

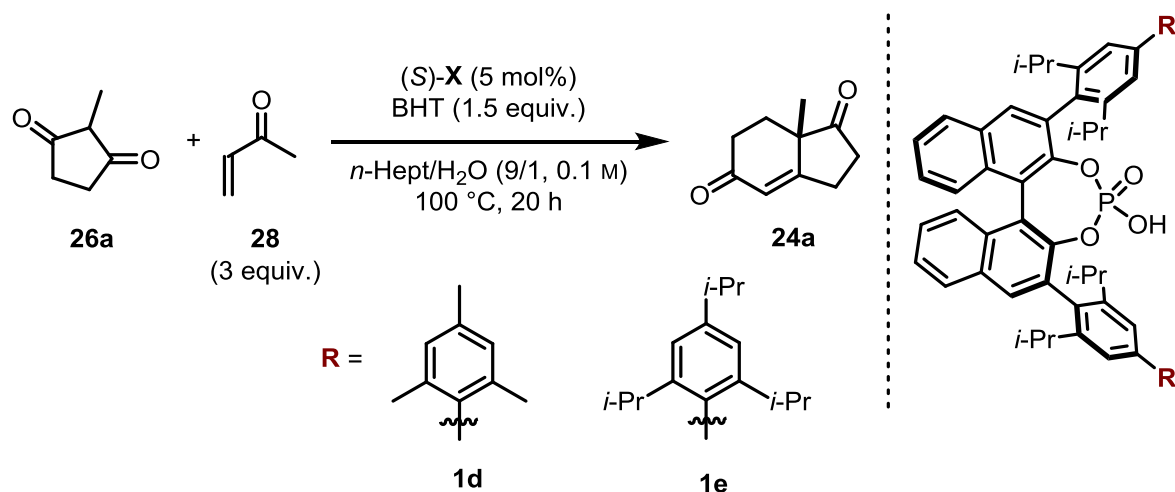


Entry	catalyst	yield ^a	er	comment
1	50	75%	76:34	-
2	50	86%	82:18	without H ₂ O
3	51	73%	75:25	-
4	51	68%	75.5:24.5	without H ₂ O
5	TRIP (1a)	74%	78:22	-
6	TRIP (1a)	51%	83:17	without H ₂ O

Table 4.4: Evaluation of bisphosphorylimides and *N*-phosphinyl phosphoramidates as catalysts.
^aDetermined by ¹H NMR analysis of the crude reaction mixture using Ph₃CH as internal standard.

Modification of the 3,3'-Substituents

As this line of research turned out to be unsuccessful, we further focused on the modification of the 3,3'-substituents. Akiyama recently reported phosphoric acids **1d** and **1e** (Table 4.5), in which the biphenyls, due to the large substituents, approach a torsion angle of 90°. [178] This has the consequence that one of the *ortho*-substituents of the second aryl-moiety reaches into the active site of the catalysts thus making it more confined. Indeed, promising enantioselectivities without significant erosion of yields were obtained (Table 4.5). However, the attempted cross-coupling towards the corresponding SPINOL-derived phosphoric acids did not lead to the target product.



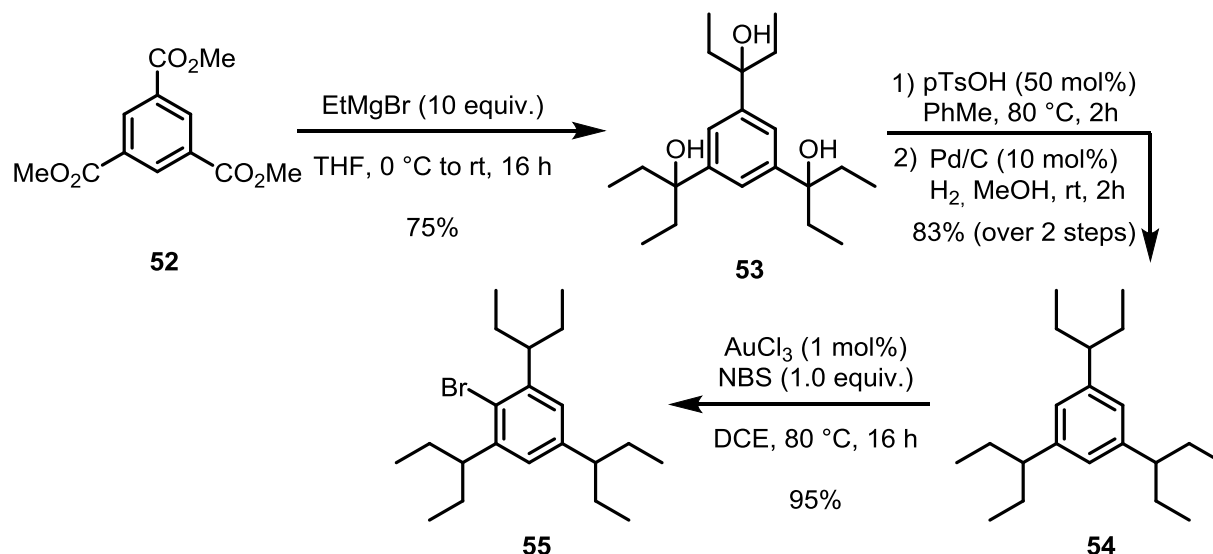
Entry	catalyst	yield ^a	er	comment
1	1d	71%	78.5:21.5	-
2	1d	48%	84:16	without H ₂ O
3	1e	66%	87:13	-
4	1e	55%	88.5:11.5	without H ₂ O
5	TRIP (1a)	74%	78:22	-
6	TRIP (1a)	51%	83:17	without H ₂ O

Table 4.5: Evaluation of novel substituents in 3,3'-position of BINOL-derived phosphoric acids..

^aDetermined by ¹H NMR analysis of the crude reaction mixture using Ph₃CH as internal standard.

In parallel we attempted to increase the steric bulk of the TRIP-substituent by extending the isopropyl to 3-isopentyl groups. The synthesis of bromide **55** was achieved in 4 consecutive

steps from commercially available trimethyl benzene-1,3,5-tricarboxylate (**52**) (Scheme 4.6). Addition of ethylmagnesium bromide to **52**, followed by sequential acid-catalyzed elimination and hydrogenation furnished 1,3,5-tri(pentan-3-yl)benzene (**54**) in 83% yield.. Selective mono-bromination was achieved in 95% yield using gold(III)-chloride and freshly recrystallized NBS.



Scheme 4.6: Synthesis of 2-bromo-1,3,5-tri(pentan-3-yl)benzene (**55**).

This sequence provided us with sufficient material for subsequent trials toward cross-coupling to MOM-protected 3,3'-bisiso BINOL. We chose the Negishi cross-coupling since by this method C–H bond activation at the alkyl chains could be minimized. Despite successful lithiation and transmetalation to zinc the cross-coupling was unsuccessful. In all cases only remaining starting material was detected by ^1H NMR analysis of crude reaction mixtures.

Modification of the Catalyst Backbone

Because previous strategies were not successful, we proceeded with further modifications of the catalyst backbone. In 2007 Zhou *et al.* reported the synthesis of spirobitetraline-derived chiral phosphoramidite ligands and their application in asymmetric hydrogenations.^[179] Comparing the crystal structures of spirobiindane-derived diol (SPINOL, **56**) and the spirobitetraline-derived diol (**57**), suggested that the additional carbon atoms increased the dihedral angles and O–O distances (Figure 4.2 a). This indicated that a potential catalyst, having aryl-substituents in the 3,3'-position, would not only have a more twisted structure but also a shorter spatial distance of the 3,3'-substituents and therefore a more confined active site.

Calculations performed with both corresponding structures having TRIP substitutes in the 3,3'-position supported this assumption (Figure 4.2 b).

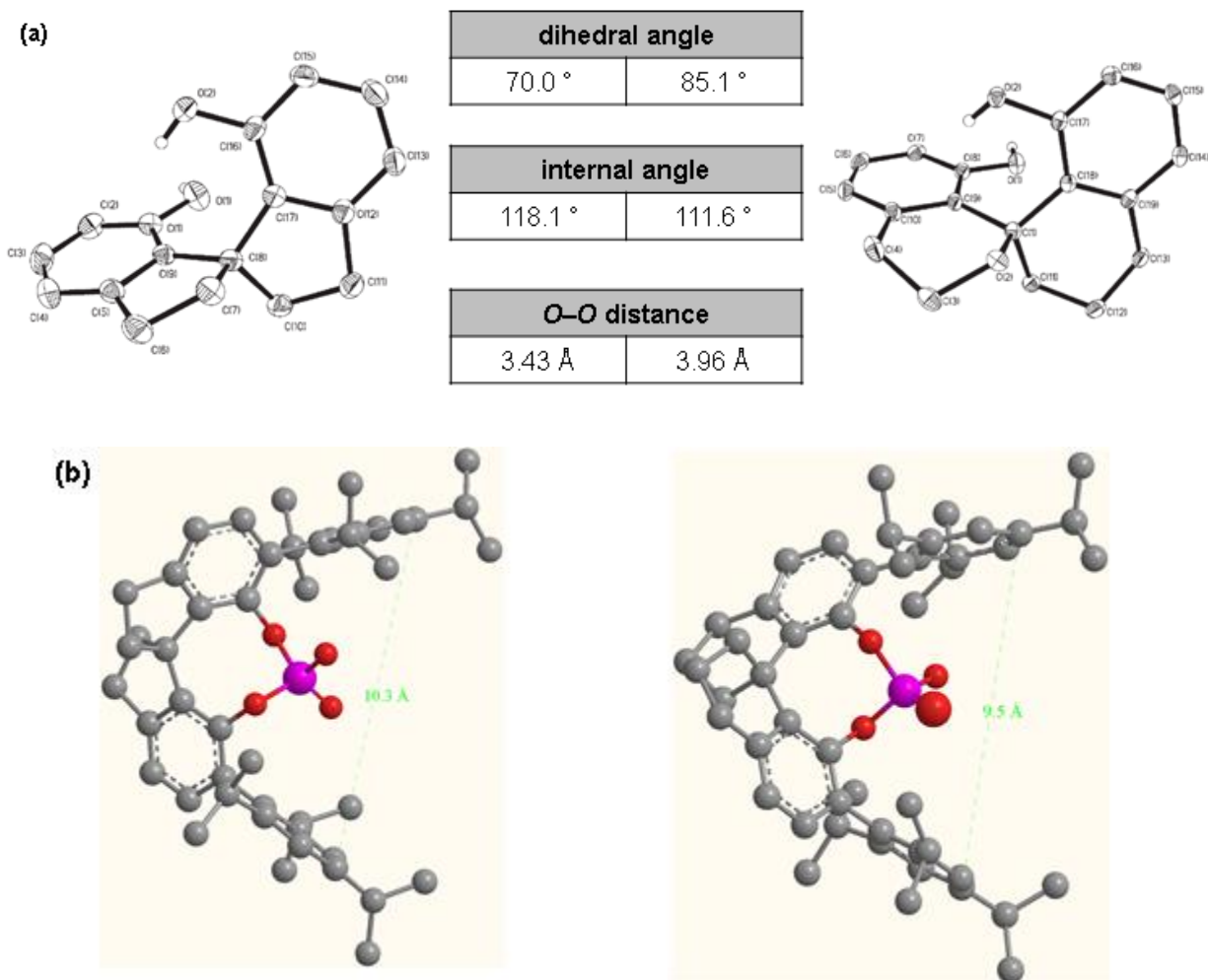
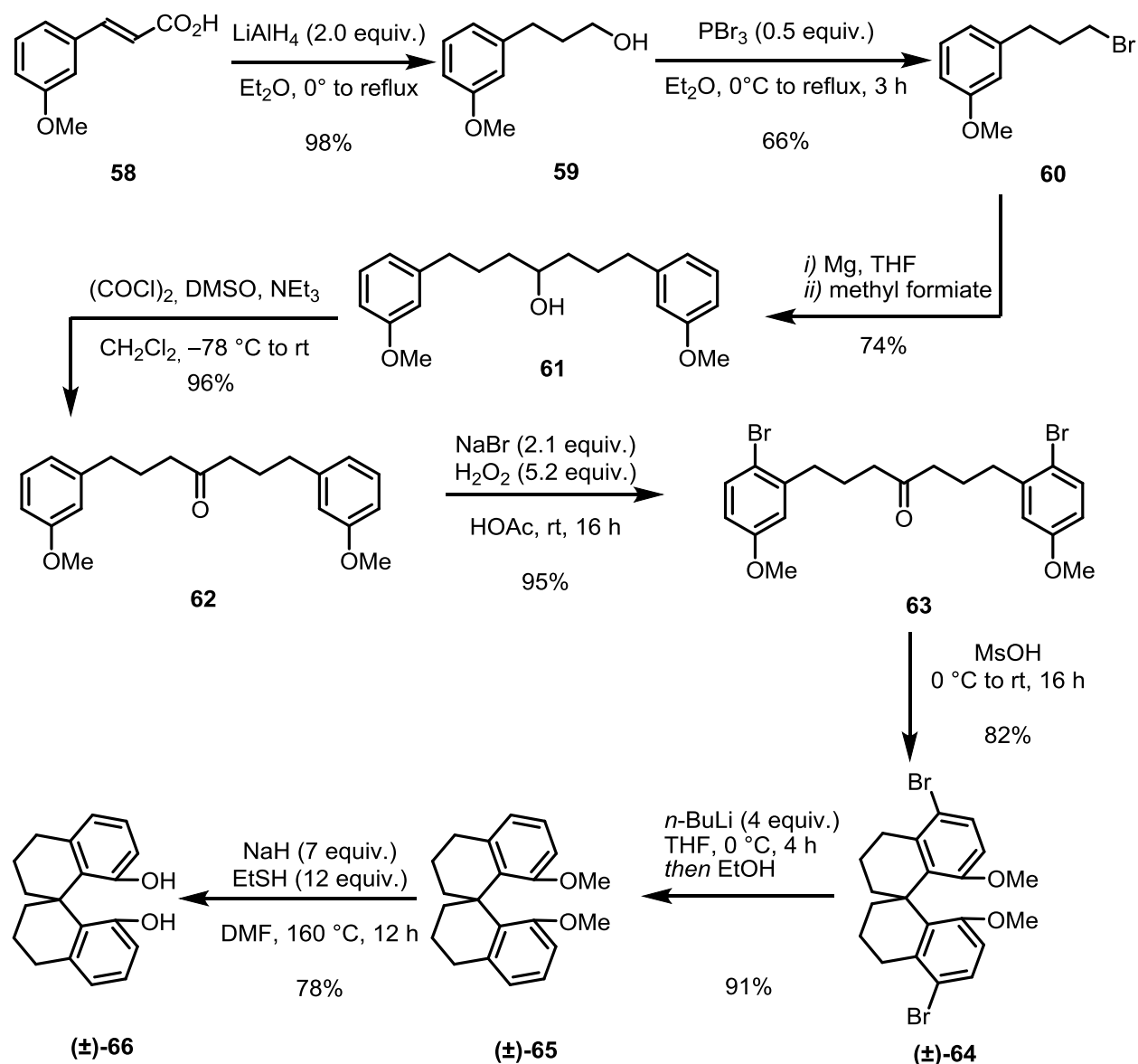


Figure 4.2: (a) Comparison of key elements of the crystal structures of spirobiindane-derived diol (SPINOL, left, **56**) and spirobitetraline-derived diol (right, **57**). (b) Calculated structures of the corresponding phosphoric acids, bearing the TRIP-substituent in 3,3'-position. Calculations were performed at the B3LYP-level of theory in the gasphase. Protons are removed for better visibility.

We therefore attempted the synthesis of diol **66** as described by Zhou *et al.* (Scheme 4.7). Lithium aluminum hydride reduction of 3-methoxy cinnamic acid (**58**) gave alcohol **x** in quantitative yield. Subsequent treatment with phosphorus tribromide furnished bromide **60**, which was transformed into the corresponding *Grignard* reagent and quenched with methyl formate to give alcohol **61** in 49% yield over three steps. *Swern* oxidation and subsequent bromination using sodium bromide and hydrogen peroxide in acetic acid resulted in compound **63** in 82% yield. The bromines functioned as a protecting group for the subsequent Friedel–

Crafts-alkylation because they blocked the more reactive *para*-position. The Friedel–Crafts step required additional optimization, as the original conditions resulted in complex mixtures containing only trace amounts of the desired product. However, performing the reaction in methansulfonic acid at 0 °C produced (±)-**64** in 82% yield. Removal of the bromines *via* metalation/protonation and deprotection using sodium ethanethiolate finally gave the target racemic diol (±)-**66**.

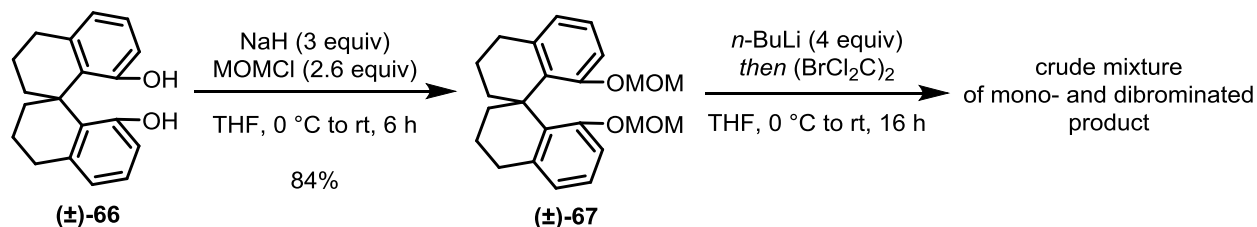


Scheme 4.7: Synthesis of (±)-**66**.

Separation of the enantiomers can be achieved by esterification of (±)-**66** with (1*S*)-(+)-10-camphersulfonyl chloride followed by chromatographic separation of the corresponding

diastereomers.^[179] However, this process required two additional synthetic steps and separation of the diastereoisomers was not straightforward. Our attempts to separate the enantiomers by preparative HPLC were unsuccessful: it was only achieved at the analytical scale. As an alternative, we decided to continue the synthesis and separate the final phosphoric acids, because for these compounds separation on ion exchange columns looked more promising.

To install substituents at the 3,3'-positions, we attempted the synthesis of the corresponding bromides *via* directed *ortho*-lithiation/bromination sequence. Presumably because of inefficient coordination by the methoxy groups, the direct deprotonation of (\pm)-**65** using *n*-BuLi and TMEDA was unsuccessful. Quenching of the crude reaction mixture with D₂O did not show deuterium incorporation. Attempts to brominate the unprotected diol (\pm)-**66** with NBS resulted in complex mixtures of products containing various amounts of bromine (up to four). A promising initial result was obtained by treating the MOM-protected diol (\pm)-**67** with *n*-BuLi followed by 1,2-dibromo-1,1,2,2-tetrachloroethane. In a small-scale experiment an inseparable mixture of mono- and di-brominated product was detected (Scheme 4.8). Further optimization of this reaction conditions should enable the access in synthetically useful yields.



Scheme 4.8: MOM-protection and initial attempts toward bromination.

4.1.5 Conclusions

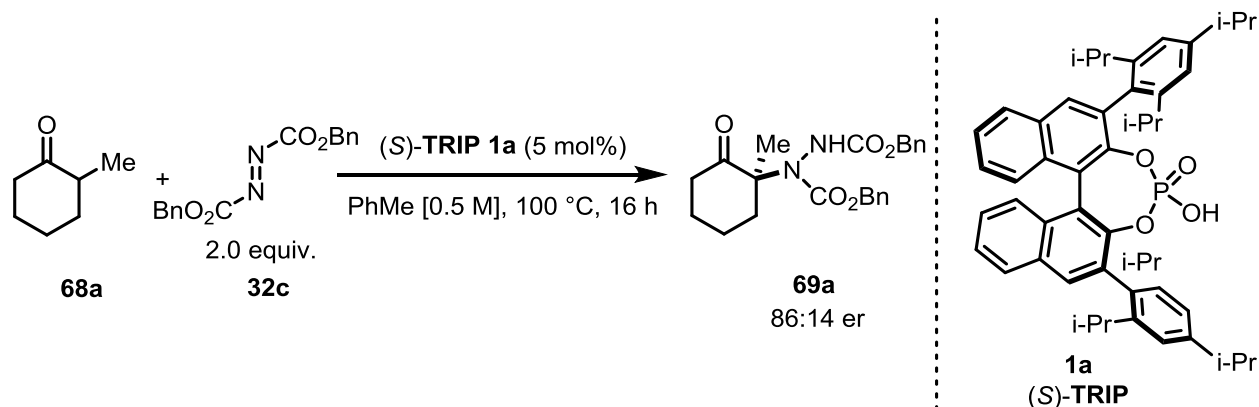
We developed a Brønsted acid-catalyzed enantioselective Robinson annulation of cyclic 1,3-diketones with methyl vinyl ketone. Using STRIP as the catalyst gave access to various derivatives of the Wieland-Miescher ketone in good to excellent yields and excellent enantioselectivities ($\geq 98:2$ er). Unfortunately, derivatives of the Hajos-Parrish ketone were obtained in lower enantioselectivity. To address this challenge, synthetic efforts towards a presumably more confined bis-tetraline-derived phosphoric acid were taken.

4.2 Catalytic Asymmetric α -Amination of α -Branched Ketones via Enol Catalysis^[180]

The work presented in this section was done with support by Dr. Gabriele Pupo. Towards the end of this study, a conceptually similar work with complimentary scope was published by Toste *et al.*^[181]

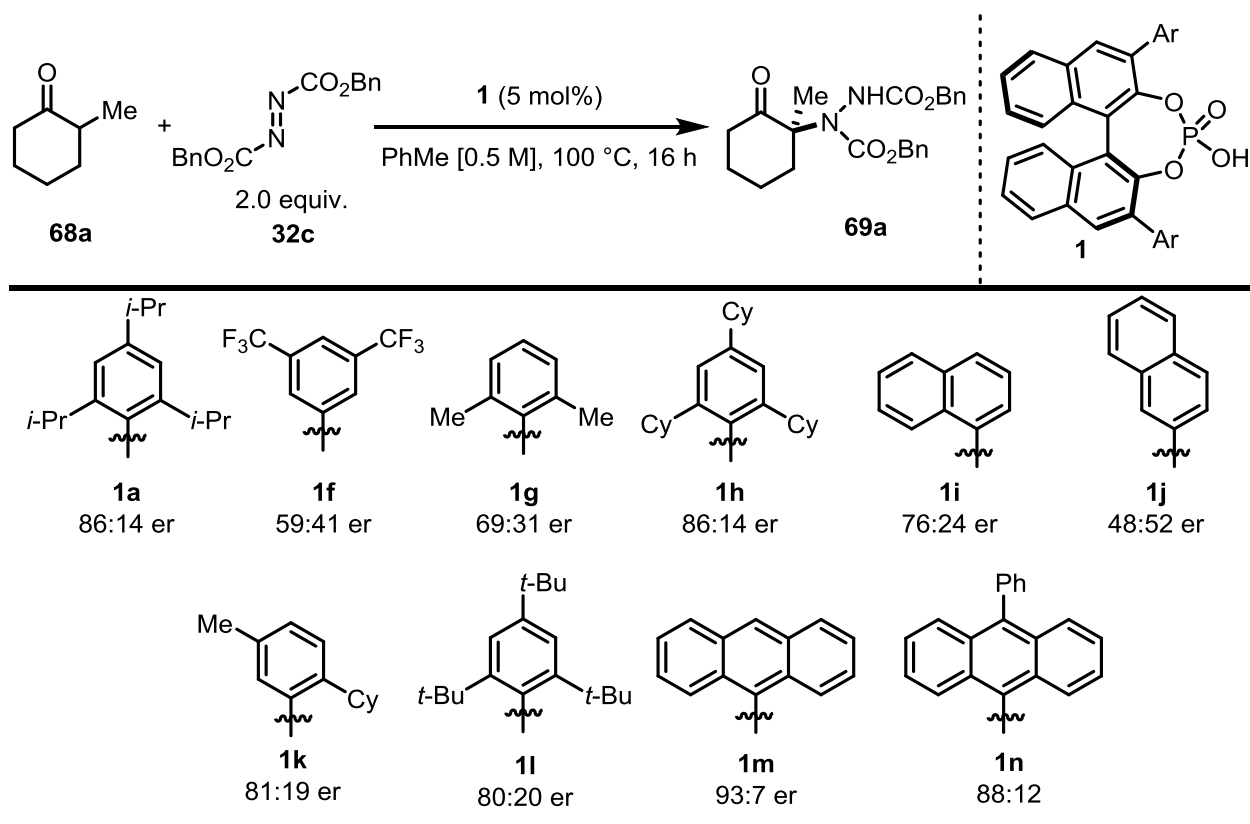
4.2.1 Optimization Studies

We began our investigation by employing 2-methyl cyclohexanone (**68a**) and dibenzoyl azodicarboxylate (**32c**) as model substrates. Performing the reaction at 100 °C and using (*S*)-TRIP (**1a**) as catalysts resulted in full conversion of the starting material and the desired product **69a** was obtained in promising 86:14 er (Scheme 4.9).



Scheme 4.9: Initial result for the asymmetric α -amination of α -branched ketones.

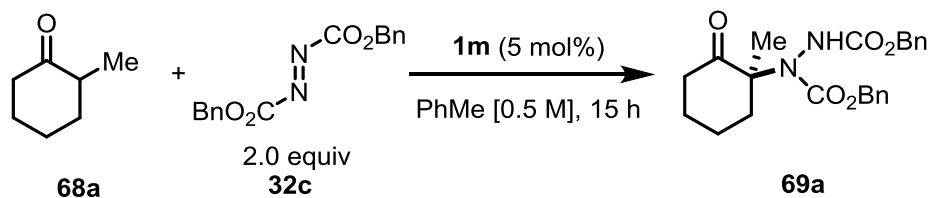
These promising results prompted us to evaluate the catalytic abilities of other phosphoric acids (Scheme 4.10). Having bulky groups in the *ortho*-position of the 3,3'-substituent turned out to be beneficial regarding the enantioselectivity, *i.e.* out of the tested phosphoric acids, **1f** and **1j**, both not having any *ortho*-substituent, catalyzed the reaction with the lowest enantioselectivity (59:41 er and 48:52 er, respectively). Changing the three *i*-Pr groups of TRIP (**1a**) to either cyclohexyl- or *t*-Bu-groups^[182] did not improve enantioselectivities (**1h**, 86:14 er and **1l**, 80:20 er, respectively). Gratifyingly, 9-anthracenyl substituted phosphoric acid **1m** delivered the desired product in excellent 93:7 er. Other catalyst motifs resulted either in very low reactivity (IDP) or racemic product (DSI).



Scheme 4.10: Screening of catalysts.

Performing the reactions at 100 °C afforded complex reaction mixtures and control experiments showed that the azodicarboxylate was decomposing to several unidentified products. Lowering the temperature resulted in a cleaner reaction profile and improved the enantioselectivity: Reaction at room temperature gave the desired ketone in 64% isolated yield and 97:3 er (Table 4.5, Entry 3). *Note:* For better consistency, the reaction was stopped after 15 h; although TLC analysis of the crude reaction mixture indicated the presence of unreacted starting material.

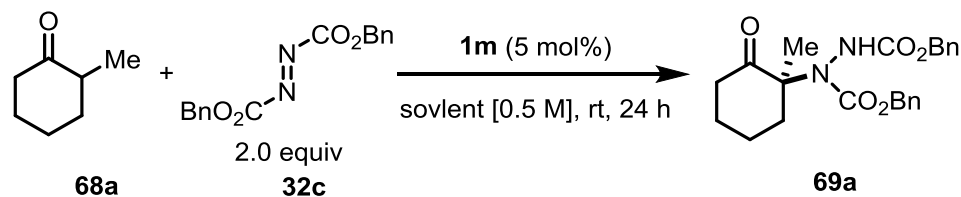
Because of the rotamers, the NMR spectrum of **69a** contained extremely broad signals and hence yields based on an internal standard could not be accurately determined. Instead, conversion of the starting material based on an internal standard was used as an indicator for reactivity.



Entry	T/°C	yield ^a	er
1	100	n.d.	93:7
2	60	76%	95.5:4.5
3	rt	64%	97:3

Table 4.5: Effect of temperature. ^aDetermined by purification of the crude reaction mixture by preparative TLC.

A solvent screening revealed that the choice of solvent mainly affected reactivity, whereas enantioselectivity remained the same (Table 4.6). Due to the higher enantioselectivity, acetonitrile was chosen as a solvent for further studies.

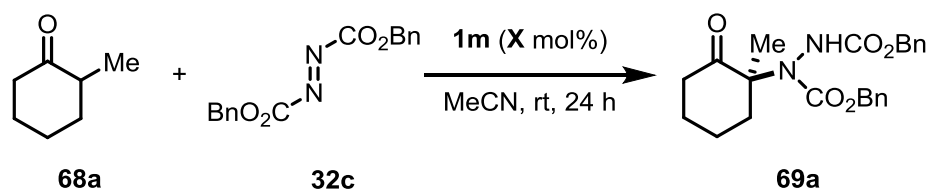


Entry	solvent	conversion ^a	er
1	PhMe	96%	96.5:3.5
2	CH ₂ Cl ₂	96%	98:2
3	EtOAc	68%	97.5:2.5
4	MTBE	50%	97:3
5	DMSO	13%	n.d.
6	acetone	28%	98:2
7	MeCN	74%	98.5:1.5

Table 4.6: Screening of solvents. ^aDetermined by ¹H NMR analysis of the crude reaction mixture using Ph₃CH as internal standard.

Reactivity was improved by increasing the concentration (Table 4.7, Entry 1 and 2). Remarkably, the reaction also proceeded under neat conditions, however with slightly lower

enantioselectivity (Entry 3). Catalysts loading could be reduced from 5 mol% to 1 mol%, however longer reaction times were required to reach full conversion of the starting material (Entry 4). The amount of azodicarboxylate could be reduced to 1.2 equivalents without deterioration of selectivity or yield (Entry 5). Under fully optimized conditions, the desired product was obtained in 85% yield and 99:1 er (Entry 6).



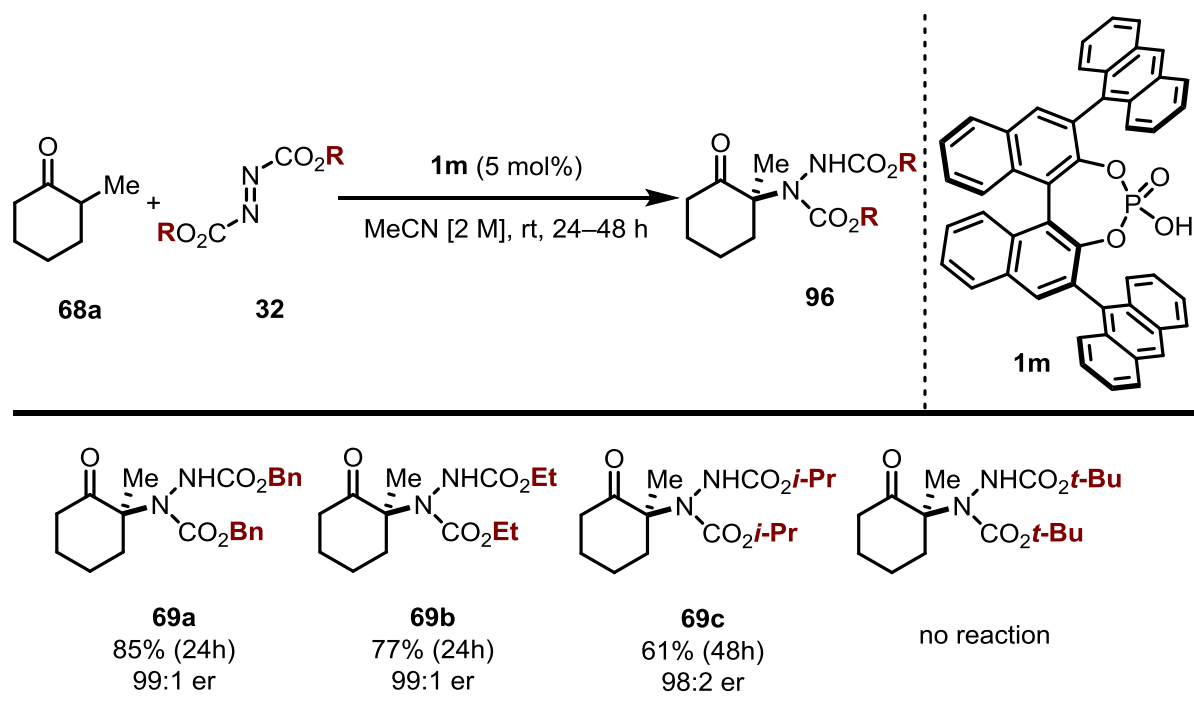
Entry	M	mol% 1m	equiv. 32a	conversion ^a	er
1	0.5	5	2	74%	98.5:1.5
2	1.0	5	2	93%	98.5:1.5
3	neat	5	2	>95%	95.5:4.5
4	0.5	1	2	28%	99:1
5	0.5	5	1.2	68%	98.5:1.5
6	2	5	1.2	(85%)	99:1

Table 4.7: Further optimization of reaction parameters. Isolated yields are given in parenthesis.

^aDetermined by ¹H NMR analysis of the crude reaction mixture using Ph₃CH as internal standard.

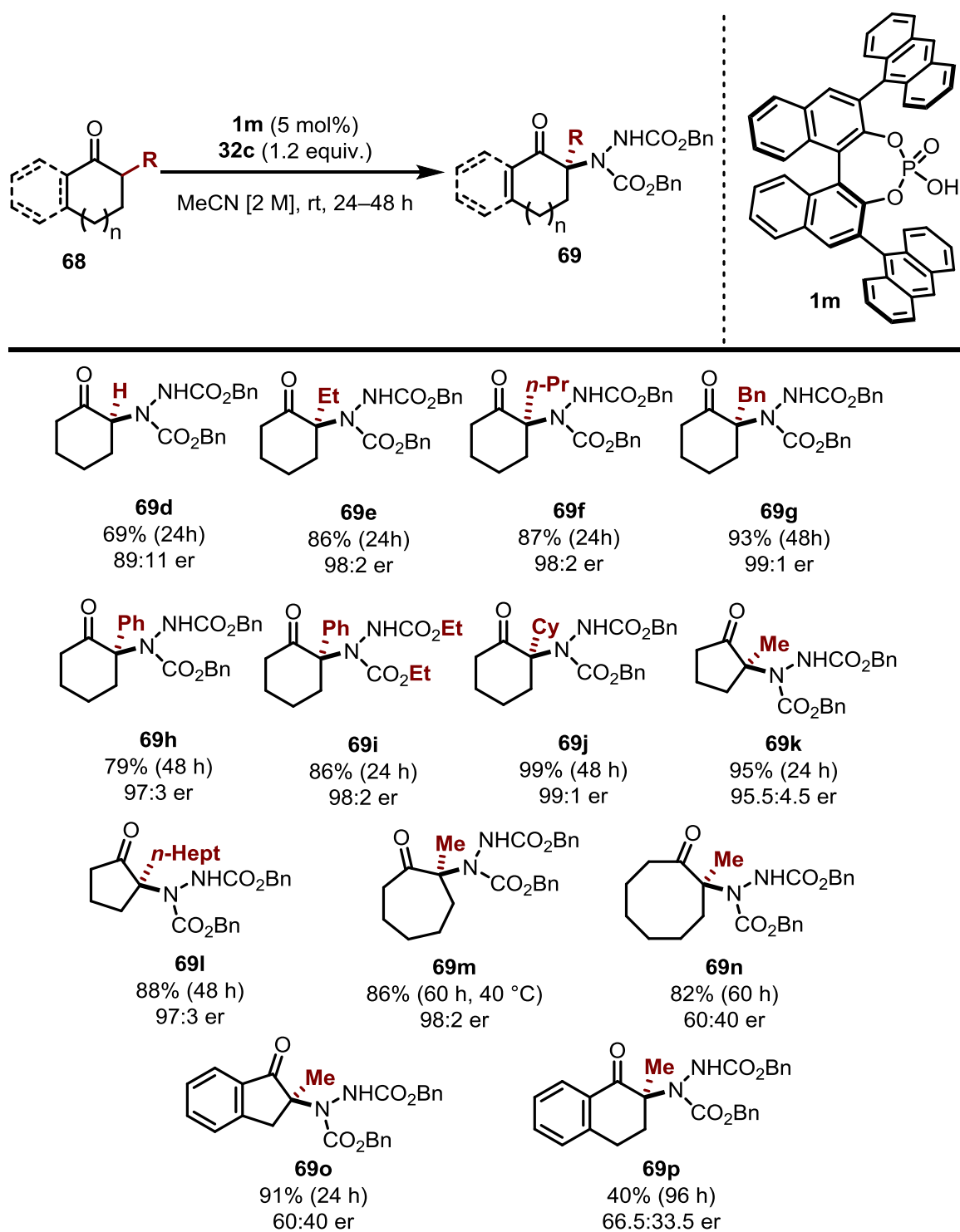
4.2.2 Substrate Scope

Having identified optimal reaction conditions, we focused our attention on the substrate scope. In addition to **32c**, other azodicarboxylates, *e.g.* DEAD (Et, **32b**) and DIAD (*i*-Pr, **32d**), were tested as electrophiles. Gratifyingly, the corresponding α -hydrazino ketones were obtained in good yields and excellent enantioselectivities (>98:2 er). Using *Boc*-protected hydrazine (DBAD, **32a**) no desired product was observed even at elevated temperatures (Scheme 4.11).



Scheme 4.11: Scope of azodicarboxylates.

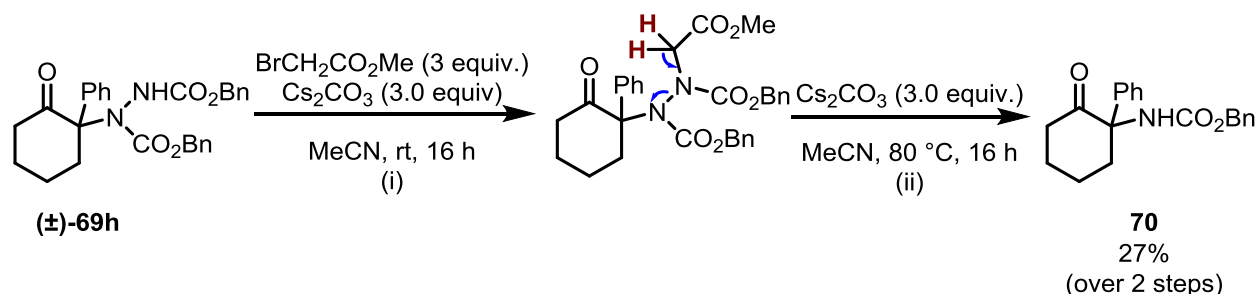
A variety of 2-alkyl- and 2-aryl-substituted ketones were tolerated by the system, delivering the desired products in excellent yields and enantioselectivities (Scheme 4.12). Furthermore, the method could also be expanded to 2-alkyl substituted cyclopentanones (**69k** and **69l**). Remarkably, cyclohexanone itself turned out to be a suitable substrate and the corresponding mono-aminated product **69d** was obtained in 69% yield and 89:11 er. Gratifyingly, no racemization was observed, emphasizing the selectivity of this catalytic system. The developed method was also scalable: The reaction of 2-phenyl cyclohexanone (**76**) and DEAD (**32b**) delivered the corresponding product in 77% yield and 97.5:2.5 er at 1 mmol scale. However, reduced reactivity and selectivity were obtained using 1-indanone and 1-tetralone derived substrates.



Scheme 4.12: Scope of ketones. The absolute configuration of products was assigned according to **69d**.

4.2.3 Synthesis of Carbamate-Protected α -Amino Ketones

Although being very convenient electrophilic amination agents, azodicarboxylates produce a disadvantageous N–N bond. Usually, this bond is cleaved under reductive conditions (*e.g.* using Rayne Ni/H₂ or SmI₂), which is not compatible with the ketone moiety in α -hydrazino ketones and all of our attempts using a variety of heterogeneous hydrogenation catalysts led to full decomposition. Magnus group recently reported an alternative approach giving carbamate-protected α -amino ketones *via* an (i) alkylation and (ii) E₁cB elimination sequence.^[183] Using this reaction conditions α -amino ketone **70** was isolated in 27% yield over two steps (Scheme 4.13).

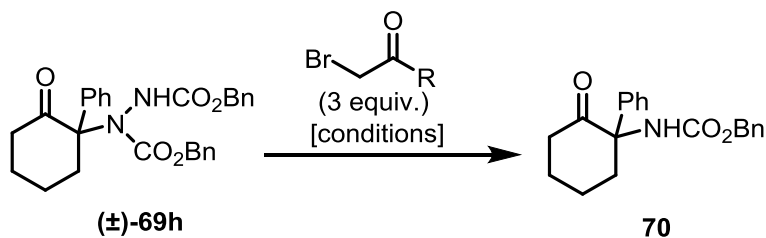


Scheme 4.13: Initial attempt for N–N bond cleavage of carbamate-protected hydrazine derivatives via E₁cB mechanism.

Although formally being a two-step procedure, the transformation can be performed in one-pot without additional work up or purification of the intermediate. Using α -hydrazino ketone (\pm) -**69h**, we further optimized this cleavage reaction (Table 4.8). Using the standard reaction conditions, the target product was obtained in 14% yield (Entry 1). Changing the base from Cs₂CO₃ to KOH marginally improved the yield (Entry 2). Applying higher amounts of base, changing the order of addition or modifying the alkylating agent resulted in no improvements (Entries 3–5).

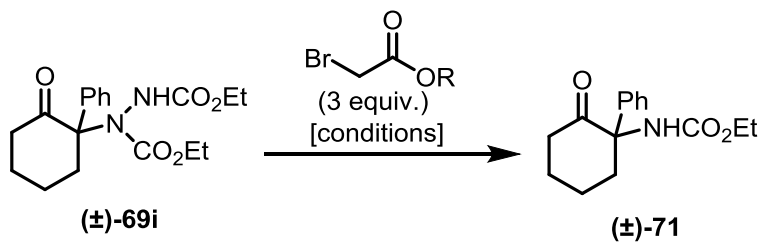
We reasoned that steric bulk of the two benzoyl carbamates hinders the elimination step and therefore leads to decomposition of the corresponding alkylated intermediate. In order to overcome this, we decided to switch from dibenzoyl protected α -hydrazino ketone **69h** to diethoxy protected **69i** (Table 4.9). Indeed, similar trends were obtained as before, yet the isolated yields were higher. Under standard reaction conditions, the desired product could be isolated in 24% yield (Entry 1). In contrast to our previous results, only decomposition of starting material was observed when changing the base to KOH (Entry 2). Increasing the temperature to

70 °C and changing the ester group from methyl to ethyl turned was beneficial and the corresponding ketone was isolated in 39% yield (Entries 3 and 4).



Entry	conditions	R	yield
1	Cs ₂ CO ₃ (6 equiv.); 16 h at 50 °C	OMe	14%
2	KOH (6 equiv.); 16 h at 50 °C	OMe	16%
3	KOH (30 equiv.); 50 °C	OMe	0%
4	Cs ₂ CO ₃ (6 equiv.); 72 h at 50 °C then 8 h at 80 °C	NMe ₂	traces
5	Cs ₂ CO ₃ (6 equiv.); 72 h at 50 °C	OEt	0%

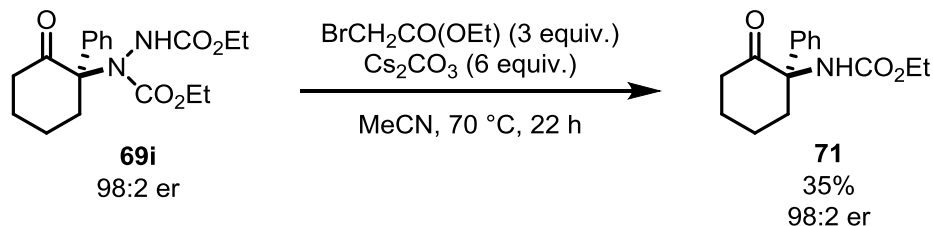
Table 4.8: Optimization of reaction conditions for the one-pot N–N bond cleavage. Isolated yields are presented.



Entry	conditions	R	yield
1	Cs ₂ CO ₃ (6 equiv.); 16 h at 50 °C	Me	24%
2	KOH (6 equiv.); 16 h at 50 °C	Me	traces
3	Cs ₂ CO ₃ (6 equiv.); 16 h at 70 °C	Me	36%
4	Cs ₂ CO ₃ (6 equiv.); 16 h at 70 °C	Et	39%

Table 4.9: Optimization of reaction conditions for the one-pot N–N bond cleavage. Isolated yields are presented.

Finally, the above mentioned conditions were applied to the synthesis of carbamate protected α -amino ketone **71**, which was isolated in 35% yield and without erosion of enantioselectivity (Scheme 4.14).



Scheme 4.14: Cleavage of the N–N bond under redox neutral conditions.

4.2.4 Conclusions

In summary, a direct asymmetric α -amination of α -branched ketones *via* enol catalysis was developed. In the presence of a chiral phosphoric acid, the higher substituted enol was exclusively formed and subsequently reacted with azodicarboxylates to produce α -hydrazino ketones in excellent yields (40–99%) and enantioselectivities (up to 99:1 er). Preliminary results on the cleavage of the disadvantageous N–N bond under redox neutral conditions provided direct access to enantiomerically enriched carbamate-protected α -amino ketones. The reaction probably proceeds *via* a transition state (Figure 4.3) in which the phosphoric acid not only promotes enolization but also activates the electrophile through protonation.

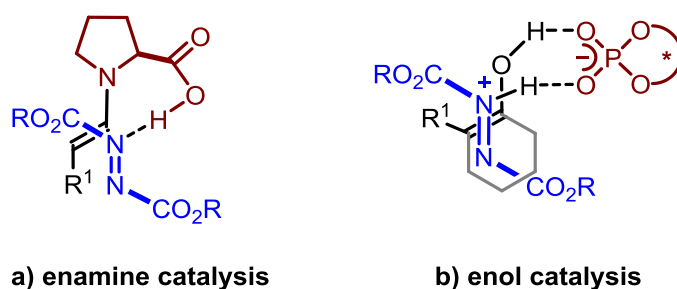


Figure 4.3: a) Proposed transition states for the α -amination of a) aldehydes *via* enamine catalysis and b) α -branched ketones *via* enol catalysis.

4.3 The Direct α -Hydroxylation of Cyclic α -Branched Ketones *via* Enol Catalysis

The work presented in this section was done in collaboration with Dr. Gabriele Pupo and Stefanie Dehn. The calculations presented here were performed by Dr. Giovanni Bistoni at the Max-Planck-Institut für Chemische Energiekonversion (CEC) and the Max-Planck-Institut für Kohlenforschung.

4.3.1 Oxidative Cleavage of α -Branched Ketones

While conceiving the project, we were inspired by the work of Cordova *et al.*, who reported the direct hydroxylation of simple aldehydes and ketones *via* enamine catalysis using *in situ* generated singlet oxygen.^[184] Although some aspects of this work are under debate, a recent study conclusively showed that such transformations are indeed possible using aldehydes as the starting materials.^[185] We therefore began our investigations by irradiating a solution of 2-methyl cyclohexanone (**68a**), catalytic amounts of DPP and Rose Bengal (**72**) with visible light under an atmosphere of oxygen (Figure 4.4 a). Unfortunately, under various reaction conditions, ¹H NMR analysis of the crude reaction mixture did not reveal desired α -hydroxy ketone even in trace amounts. However, a new compound, which we could identify as 6-oxoheptanoic acid (**73**), was detected (Figure 4.4 b).

Addition of radical scavengers (*e.g.* BHT) or reducing agents (*e.g.* triethylphosphite) did not have any effect, suggesting that the reaction proceeds *via* an ionic mechanism with no or very short lived peroxide-containing intermediates. We therefore believe that this reaction proceeds *via* a [2+2] cycloaddition of the enol and the generated singlet oxygen to form **74**, which is not stable under the reaction conditions and opens to give **73a** (Scheme 4.15). At first glance, this transformation might not appear as synthetically useful; however, when cyclohexanone is used as a substrate, this would enable a rather efficient access to adipic acid– an industrial precursor to nylon.

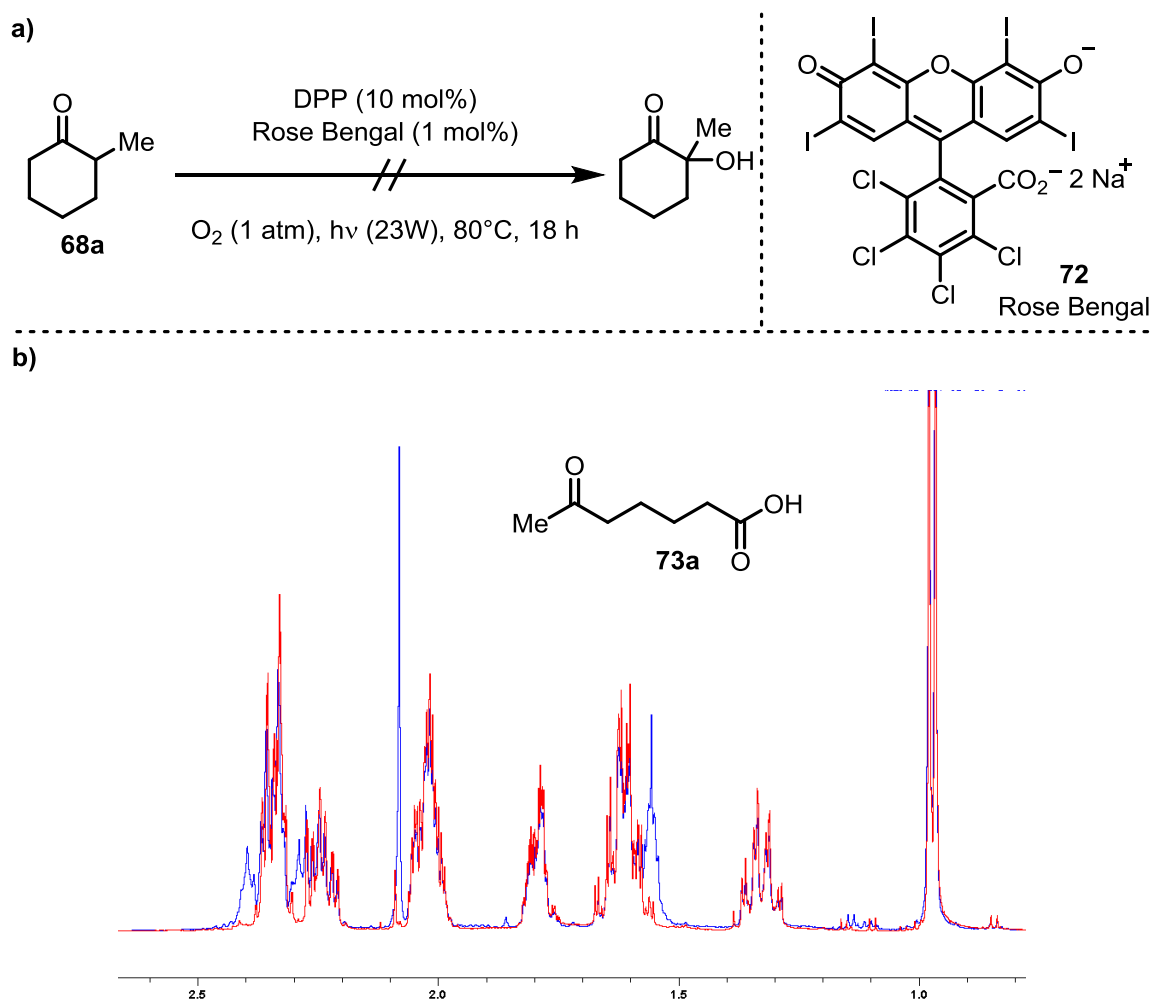
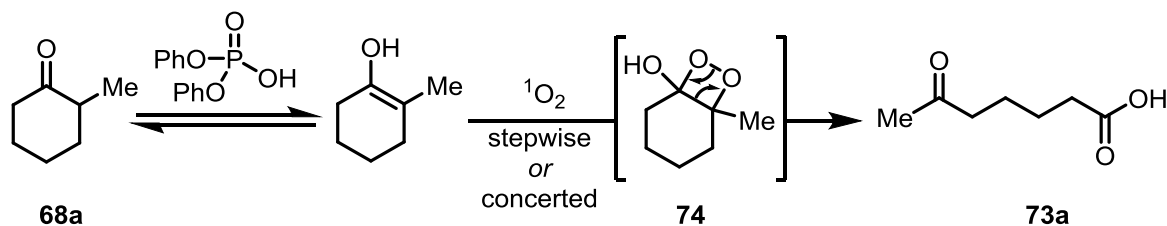


Figure 4.4: (a) Selected conditions for the initial experiments of the direct α -hydroxylation of α -branched ketones using singlet oxygen. (b) (*blue*) Part of the crude ^1H NMR of the reaction. (*red*) ^1H NMR spectra of 2-methyl cyclohexanone (**68a**).



Scheme 4.15: Proposed reaction mechanism for the formation of **73a**.

Unfortunately, only low conversions of **68a** (up to 30%) were obtained using our initial conditions. Another major issue was the reproducibility: A simple modification of reaction conditions such as changing the reaction vial strongly affected the outcome. Reproducibility (but

not the yield) was improved by changing the light source from a normal household light bulb to an LED power block, containing six connected 20 W LEDs (Figure 4.5). We therefore decided to further optimize the reaction conditions using 2-methyl cyclohexanone (**68a**) as the starting material.

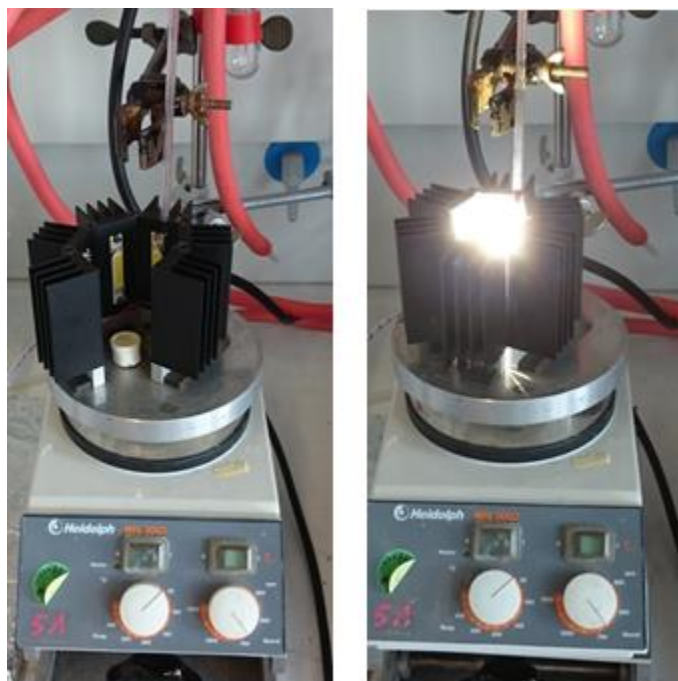
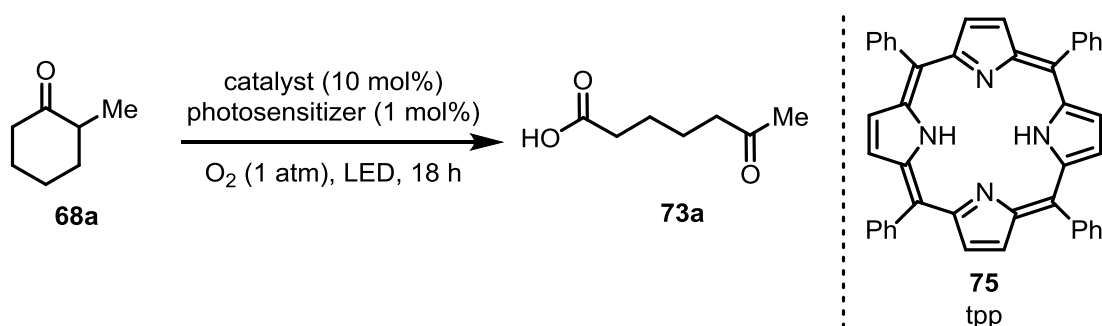


Figure 4.5: Reaction set up using six connected 20 W LEDs. When closed, the temperature inside the core could reach 110 °C.

An initial screening of photosensitizers revealed that using tetraphenylporphyrin (tpp, **75**) significantly increases the yield (74%, Table 4.9 Entry 2). Other common acids, such as triflic acid and methanesulfonic acid or other phosphoric acids also catalyzed the reaction, albeit the yields were lower (Entries 5–7).

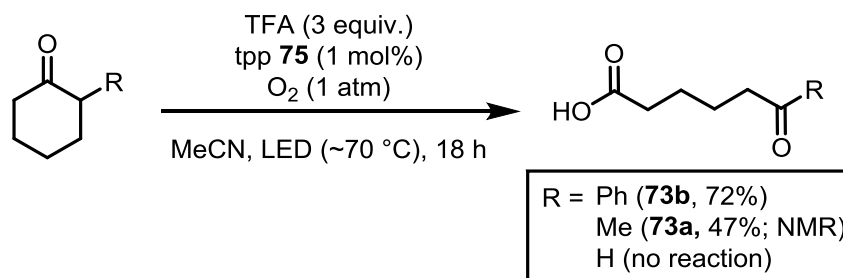
Screening of catalyst loading and the amount of photosensitizer did not show any further improvement and therefore we attempted the isolation of the products. This proved to be challenging as the visibility of such compounds on TLC is low, thus hindering isolation by flash column chromatography. Acid/base extractions of the crude reaction mixture gave inseparable mixtures of product and catalyst. We attempted *in situ* esterification of the carboxylic acid moiety. However, the isolated yields of the corresponding esters never exceeded 42%.



Entry	solvent	photosensitizer	catalyst	yield ^a
1	MeCN	Rose Bengal	DPP	47%
2	MeCN	tpp	DPP	74%
3	PhMe	tpp	DPP	40%
4	DMF	tpp	DPP	<5%
5	MeCN	tpp	TfOH	9%
6	MeCN	tpp	H ₃ PO ₄	24%
7	MeCN	tpp	MeSO ₃ H	45%

Table 4.9: Summary of reaction optimization. Best result is highlighted in bold. ^aDetermined by ¹H NMR analysis of the crude reaction mixture using Ph₃CH as internal standard.

Finally, we could overcome this drawback by applying over-stoichiometric amounts of TFA, which, due to its low boiling point, was easily removed under reduced pressure. **73b**, the oxidation product of 2-phenyl cyclohexanone, was isolated in 72% yield by simple acid/base extraction of the crude reaction mixture and subsequent removal of all volatiles under reduced pressure (Scheme 4.16). Unfortunately, using cyclohexanone as the starting material did not result in any detectable amounts adipic acid.

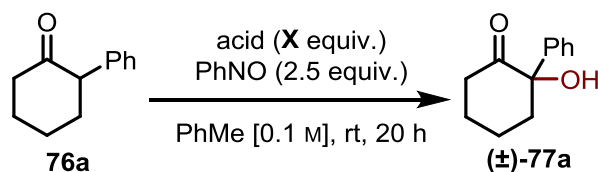


Scheme 4.16: Optimized reaction conditions and preliminary scope of the oxidative cleavage of ketones.

4.3.2 Development of a Non-Enantioselective Direct α -Hydroxylation of α -Branched Cyclic Ketones

Since the desired α -hydroxy ketones were not afforded *via* the reaction with singlet oxygen, we shifted our interest towards other electrophilic oxygen reagents. Oxaziridines, such as the Davis' oxaziridine, seemed to be a straight forward approach for C–O bond formation. However, since a stoichiometric amount of a *N*-tosyl imine is produced as side product in course of the reaction the corresponding Mannich reaction would affect the yield of desired product.^[181] Furthermore, additional synthesis / purification steps would be required to obtain the labile oxaziridines. Nitrosobenzene, on the other hand, is stable, commercially available and has been used as an oxidant in organocatalytic aminoxylations of simple aldehydes and ketones. In fact, in the presence of a Brønsted acid, second equivalent of nitrosobenzene can act as a reductant and directly afford the desired hydroxyl carbonyl compounds *via* tandem aminoxylation/N–O bond cleavage sequence (Scheme 2.16 a).^[134] We also reasoned that the synthetic advantage of a single step procedure outweighs the moderate atom economy and therefore decided to investigate the non-enantioselective direct α -hydroxylation of α -branched ketones using nitrosobenzene.

We started on by using 2-phenyl cyclohexanone (**76**) as a model. Considering our experiences with oxidative cleavage of ketones, a selection of common acids in stoichiometric and catalytic amounts were tested (Table 4.10). Over-stoichiometric amount of a strong acid is required for the reaction; no reaction took place in acetic acid and low conversions were observed using its more acidic mono- and di-chlorinated derivatives (Entries 1–3). Optimal results were obtained when using 3 equiv. of trichloroacetic acid (TCA), affording the target hydroxyl ketone in 60% isolated yield. Although full conversion of the starting material was observed using TFA or *p*TsOH, lower yields of **77a** were observed (Entries 5 and 6). Reduced amounts of TCA resulted in lower conversion rates (Entries 7 and 8). On the other hand, higher amount of TCA, lead to no improvement (Entries 9 and 10). Since clean reaction profiles were observed in all cases, we suspected that moderate yields could be explained by the formation of some polymer.

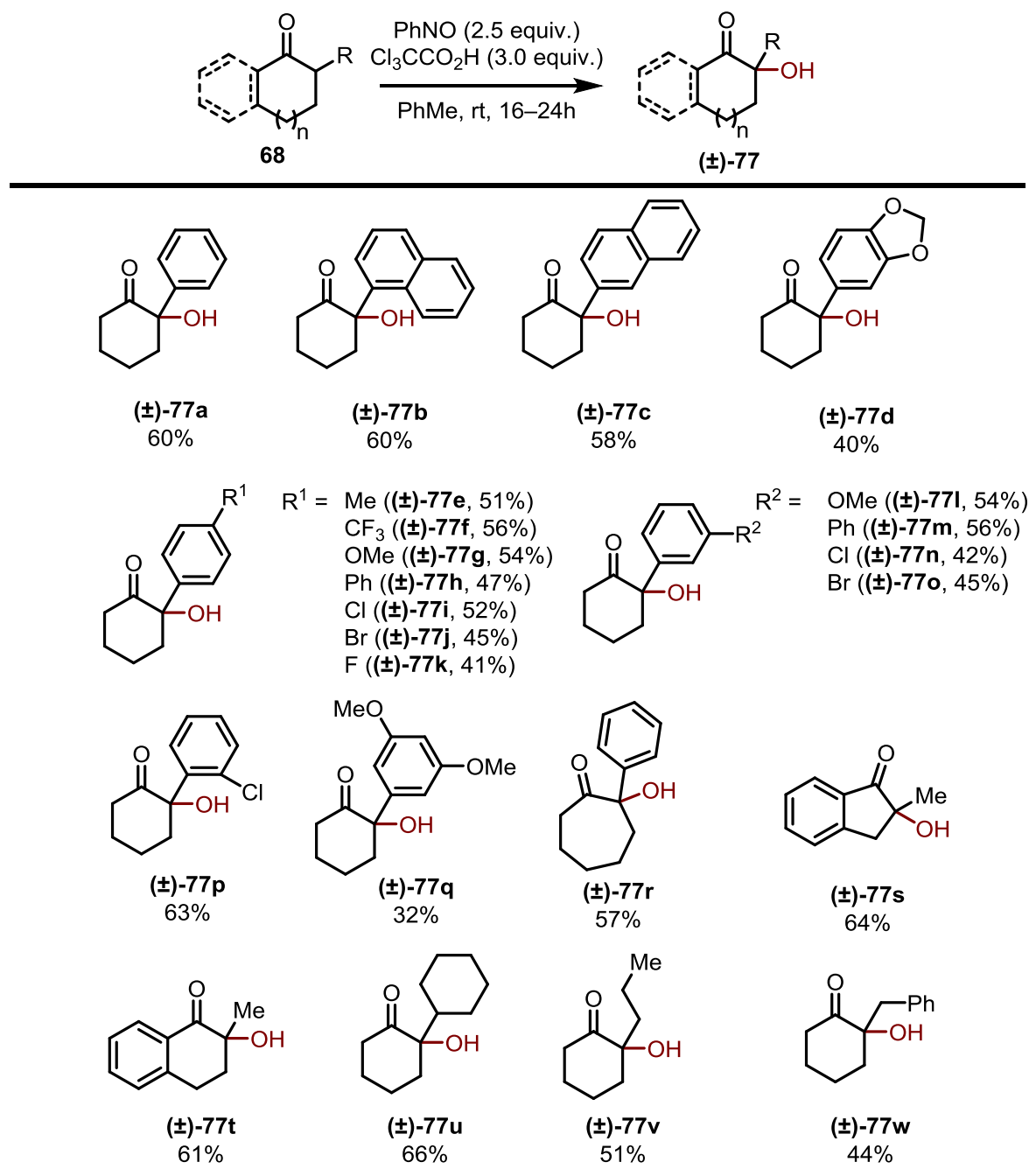


Entry	acid	equiv acid	conversion ^a	yield ^a
1	AcOH	3	n.r.	-
2	ClCH ₂ CO ₂ H	3	<10%	traces
3	Cl ₂ CHCO ₂ H	3	76%	28%
4	TCA	3	>95%	(60%)
5	TFA	3	>95%	(37%)
6	<i>p</i> TsOH	3	>95%	37%
7	TCA	0.5	65%	41%
8	TCA	2	77%	53%
9	TCA	4	>95%	(60%)
10	TCA	5	>95%	(56%)

Table 4.10: Optimization of reaction conditions for the non-enantioselective direct α -hydroxylation of α -branched ketones. Isolated yields in parentheses. Best result highlighted in bold. ^aDetermined by ¹H NMR analysis of the crude reaction mixture using Ph₃CH as internal standard.

Next, we set out to explore the scope of this transformation. To our delight, the reaction proved to be rather general: a variety of cyclic α -aryl and α -alkyl ketones readily reacted under these reaction conditions, giving the desired products in moderate to good yields (Scheme 4.12). Regarding the substitution on the α -aryl moiety, no significant electronic effect was observed (*e.g.* (±)-**77f** vs (±)-**77g**, 56% vs 54% yield). *ortho*-Substituted α -aryl cyclohexanones, which were difficult substrates in our previous studies, could be transformed to their corresponding hydroxy ketones in good yields ((±)-**77b** and (±)-**77p**). 2-Methyl indanone and tetralone were also well tolerated and produced the desired products in 64% and 61% yield, respectively ((±)-**77s** and (±)-**77t**). Furthermore, challenging α -alkyl cyclohexanones readily reacted under the optimized reaction conditions ((±)-**77u**–(±)-**77w**). While using α -phenyl cycloheptanone as the starting material gave the desired product (±)-**77r** in 57% yield, the corresponding

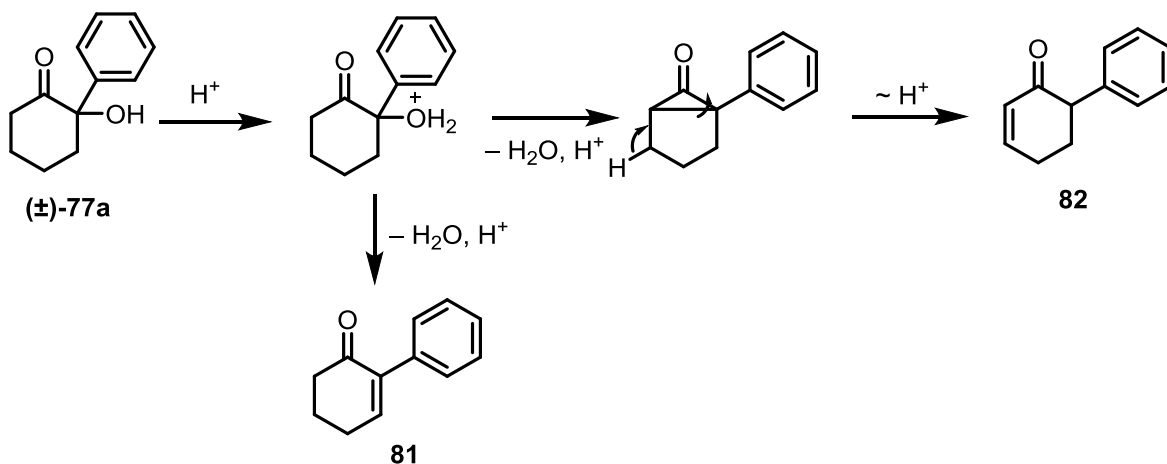
cyclopentanone resulted in a complex mixture of products; also acyclic ketones did not react.



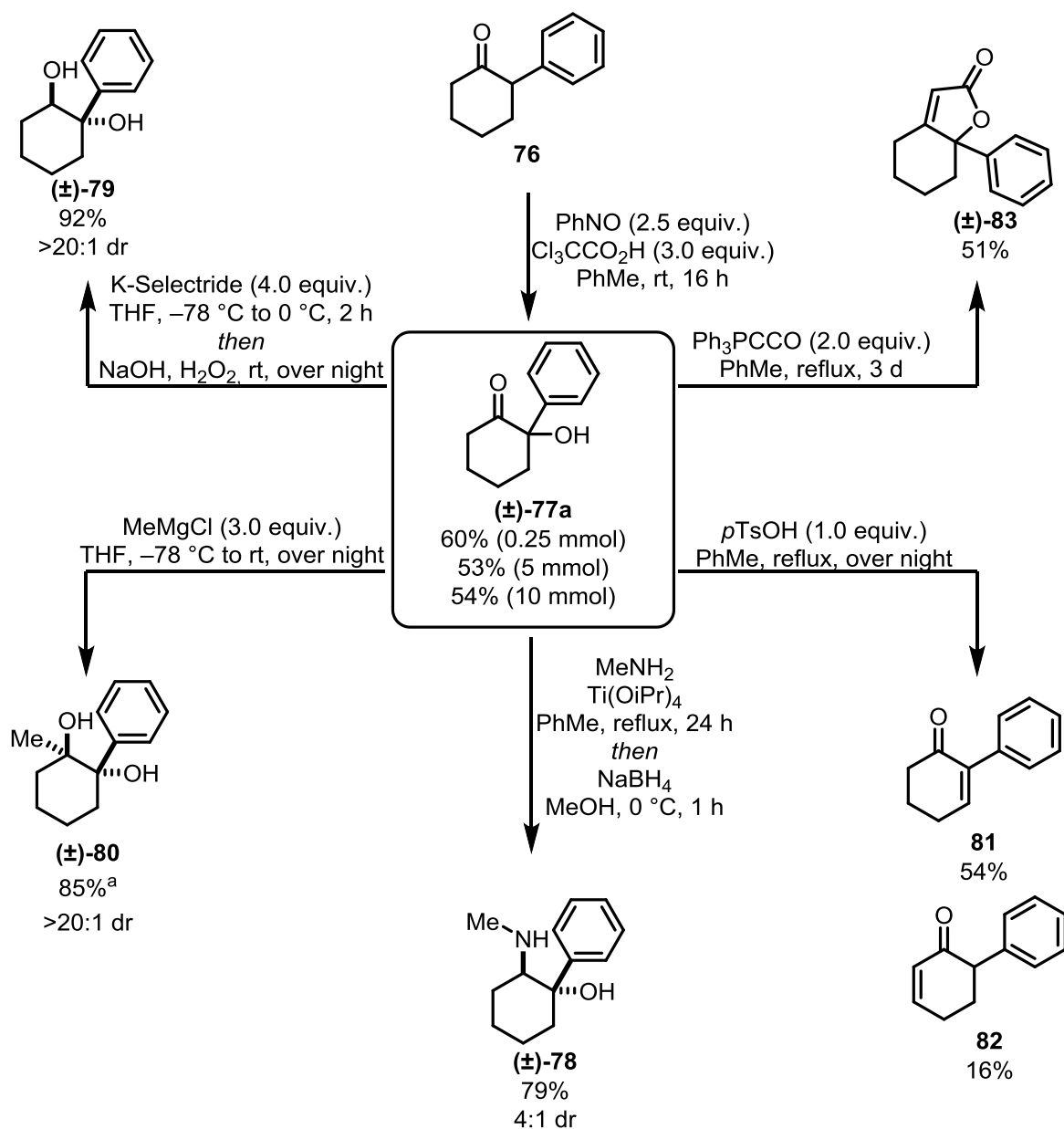
Scheme 4.12: Scope of the non-enantioselective α -hydroxylation of α -branched ketones.

The robustness of our method was demonstrated by scale-up experiments with the model substrate. Gratifyingly, (**(±)-77a**) could be obtained at a maximum tested scale of 10 mmol without deterioration of yield (Scheme 4.18). To demonstrate the practical utility of obtained compounds, product (**(±)-77a**) was further derivatized to a variety of synthetically useful functionalities.

Namely, amino alcohol (\pm)-**78** was obtained *via* reductive amination. Reduction of (\pm)-**77a** using K-Selectride[®] gave diol (\pm)-**79** in excellent yield and diastereoselectivity. Notably, using NaBH₄ as the reductant resulted in similar yields, yet lower selectivity of the product (4:1 dr by ¹H NMR analysis of the purified product). Treatment of (\pm)-**77a** with methyl magnesium chloride resulted in diol (\pm)-**80** as single diastereomer. Unfortunately, the product was contaminated with trace amounts of unreacted starting material, presumably due to enolate formation. Elimination under acidic conditions gave enone **81** in 54% yield alongside with 16% of its regioisomer **82**, which presumably was formed *via* a Favorskii-rearrangement-type reaction (a proposed reaction mechanism is shown in Scheme 4.18). Finally, treatment with the Bestmann-ylide^[186] afforded lactone (\pm)-**83**, providing an efficient access to dihydroactinidolide-type structures (Scheme 4.19).^[187]



Scheme 4.18: Proposed reaction mechanism for the formation of **82**.



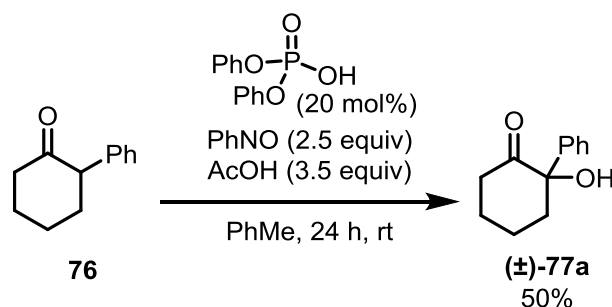
Scheme 4.19: Scale-up experiment and derivatizations of (±)-77a. ^aIsolated as an inseparable mixture with unreacted starting material (¹H NMR ratio: (±)-80/(±)-77a = 5.6/1).

4.3.3 Development of a Direct Enantioselective α -Hydroxylation of α -Branched Cyclic Ketones

The experimental work described in this section was done in collaboration with Dr. Gabriele Pupo. Full optimization studies can be found in his PhD thesis and are therefore only briefly summarized here.^[174]

4.3.3.1 Optimization of Reaction Conditions

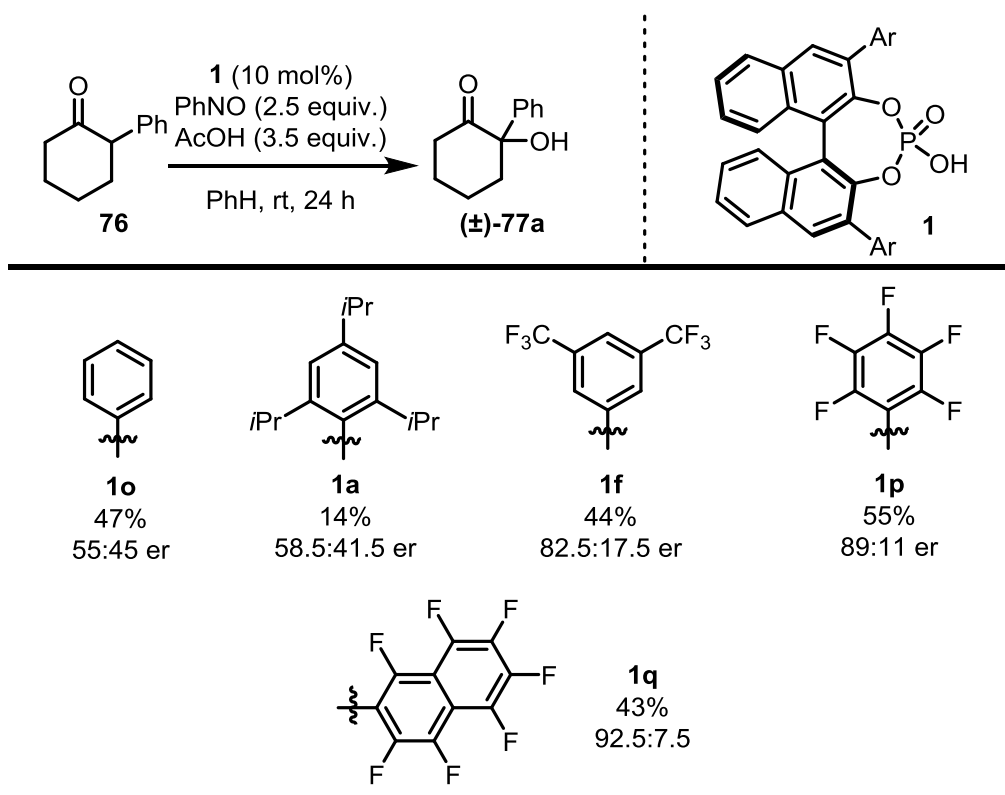
Having established a protocol for the non-enantioselective direct α -hydroxylation of α -branched cyclic ketones, we proceeded towards the development of an enantioselective variant. Initial experiments towards a catalytic version using 2-phenyl cyclohexanone (**76**) as the starting material showed that addition of catalytic amounts of DPP to the reaction mixture containing acetic acid enabled the hydroxylation of **76** in promising 50% yield (Scheme 4.20). *Note:* No background reaction using acetic acid was observed.



Scheme 4.20: Initial experiment on the development of a catalytic direct α -hydroxylation.

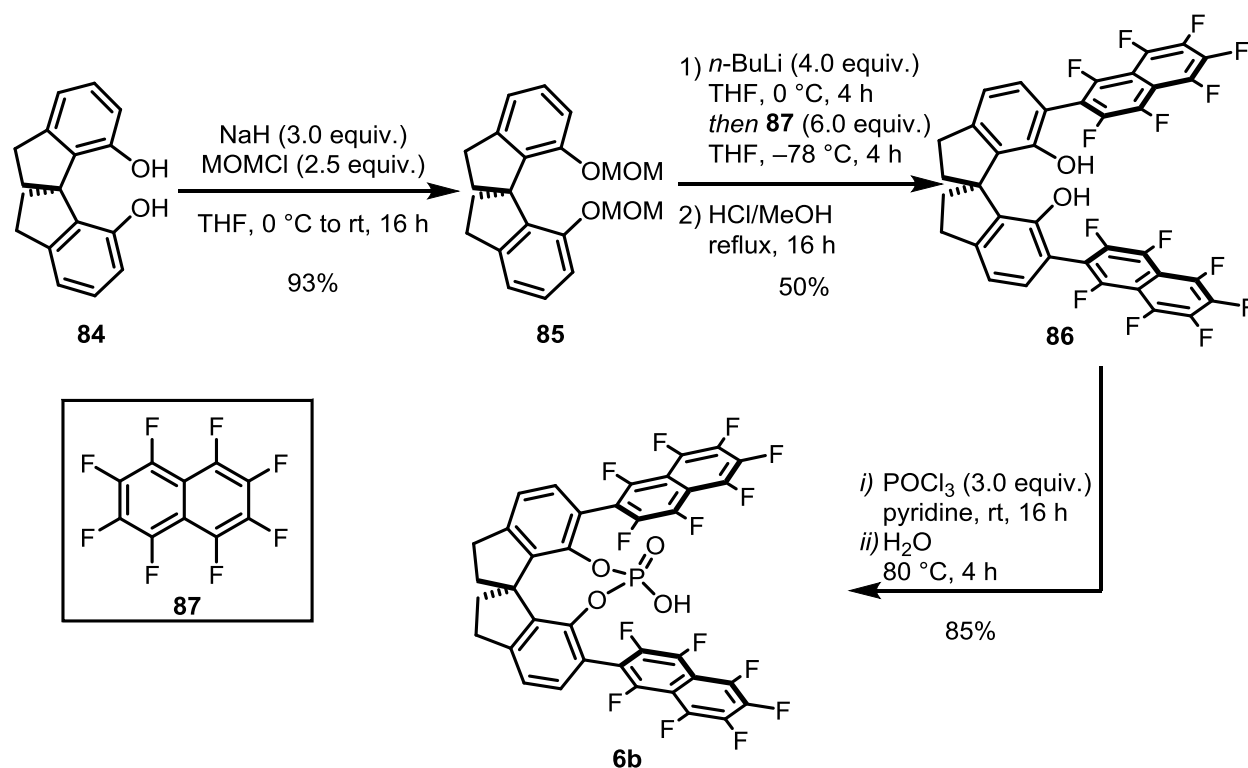
Already preliminary optimization studies showed that the addition of acetic acid and use of aromatic solvents was beneficial for both, yield and enantioselectivity.^[174] Other nitrosobenzene-derivatives neither improved the yield nor selectivity.^[174] Furthermore, in contrast to *meta*- or *para*-substituted aryl groups, *ortho*-substituted aryl groups in the 3,3'-position of the catalyst reduced the yield and enantioselectivity. For example, using (*S*)-TRIP as the catalyst, (**±**)-**77a** could only be obtained in 14% yield and 58.5:41.5 er. Interestingly, electron-withdrawing aryl groups in the 3,3'-position was beneficial, *i.e.* catalyst **1f** afforded (**±**)-**77a** in 44% yield and 82.5:17.5 er. A further increase in the yield and enantioselectivity was obtained when catalyst **1p**, bearing a perfluorinated naphthyl-substituent, was used, giving the desired product in 55% yield and 89:11 er. Following this lead, a series of catalysts with perfluorinated

aryl groups was prepared and tested, resulting in optimal catalyst **1q**, which gave the hydroxy ketone (\pm)-**77a** in 43% yield and 92.5:7.5 er.



Scheme 4.21: Screening of BINOL-derived phosphoric acids for the direct α -hydroxylation of α -branched cyclic ketones. NMR yields, determined by analysis of the ^1H NMR of the crude reaction mixture using Ph_3CH as internal standard are presented.

Due to its more rigid and confined structure we envisioned that the corresponding SPINOL-derived catalysts would further improve the enantiomeric excess of the desired product. Similar to the preparation of **1q**, (*R*)-SPINOL (**84**) was first MOM-protected (Scheme 4.22). Directed lithiation with *n*-BuLi and, subsequent quenching with **87** at -78°C followed by MOM-deprotection using HCl in methanol afforded **86** in overall 50% yield. The lithiation/ $\text{S}_{\text{N}}\text{Ar}$ /deprotection sequence was challenging and required additional optimization. Despite several attempts, this step could not be performed with more than 200 mg of **85**. The synthesis was completed upon reaction with phosphoryl chloride and subsequent hydrolysis.



Scheme 4.22: Synthesis of SPINOL-derived phosphoric acid **6b**.

The exclusive selectivity of the S_NAr reaction was confirmed by comparing shifts and multiplets observed in the ¹⁹F NMR with published spectra obtained in simpler systems.^[188] **6b** was isolated as crude mixture of rotamers, as was also confirmed by HPLC analysis. Interconversion and equilibration in solution was observed by ³¹P NMR in CDCl₃ (Figure 4.5). However, using DMSO-D₆ as the solvent hindered this process, thus allowing full characterization and quantification of all three rotamers by ¹H,¹⁹F-HOESY experiments (Figure 4.6).

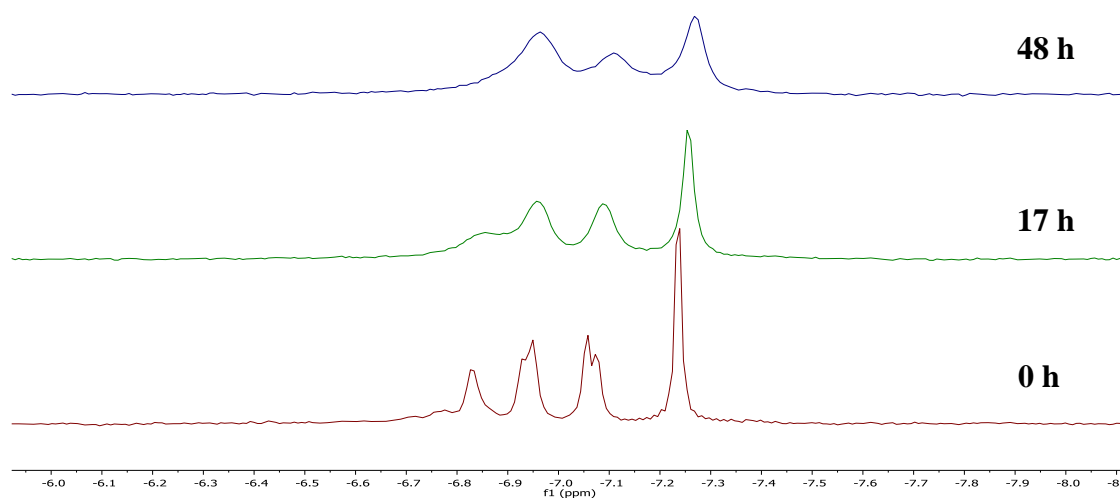
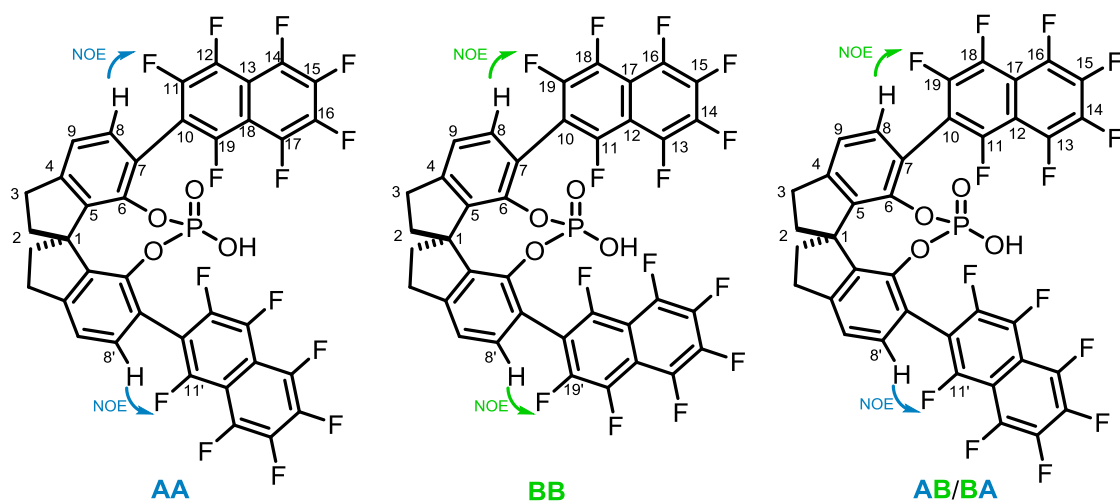


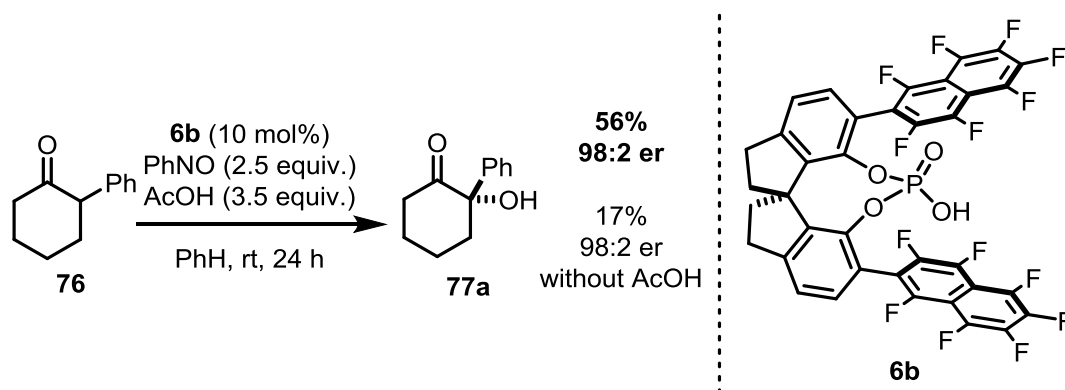
Figure 4.5: Time-dependent ^{31}P NMR study of **6b**.



Name	Position of Substituents	Relative Intensity	Sets of Signals
AA	F11 next to H8	0.5	1
BB	F19 next to H8	1	1
AB/BA	F11 and F19 next to H8	1.5 (0.75 + 0.75)	2

Figure 4.6: Obtained results of the ^1H , ^{19}F -HOESY experiments in $\text{DMSO}-\text{D}_6$.

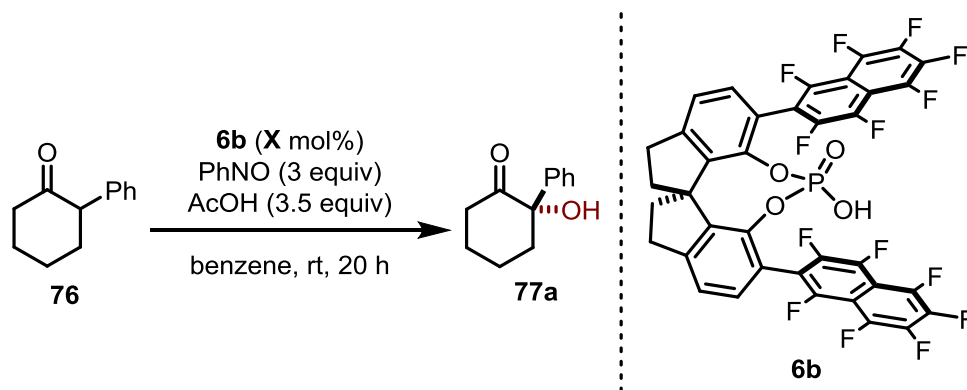
When catalyst **6b** was used under our optimized reaction conditions, the hydroxy ketone **77a** was obtained in 56% isolated yield and 98:2 er (Scheme 4.22). Despite the moderate yield, the starting material was fully converted (as assessed by ^1H NMR analysis of the crude reaction mixture). Interestingly, in the absence of acetic acid the **77a** was obtained with the same level of enantioselectivity, yet significantly lowers yields.



Scheme 4.22: Application of SPINOL-derived phosphoric acid **6b** in the enantioselective α -hydroxylation of cyclic α -branched ketones.

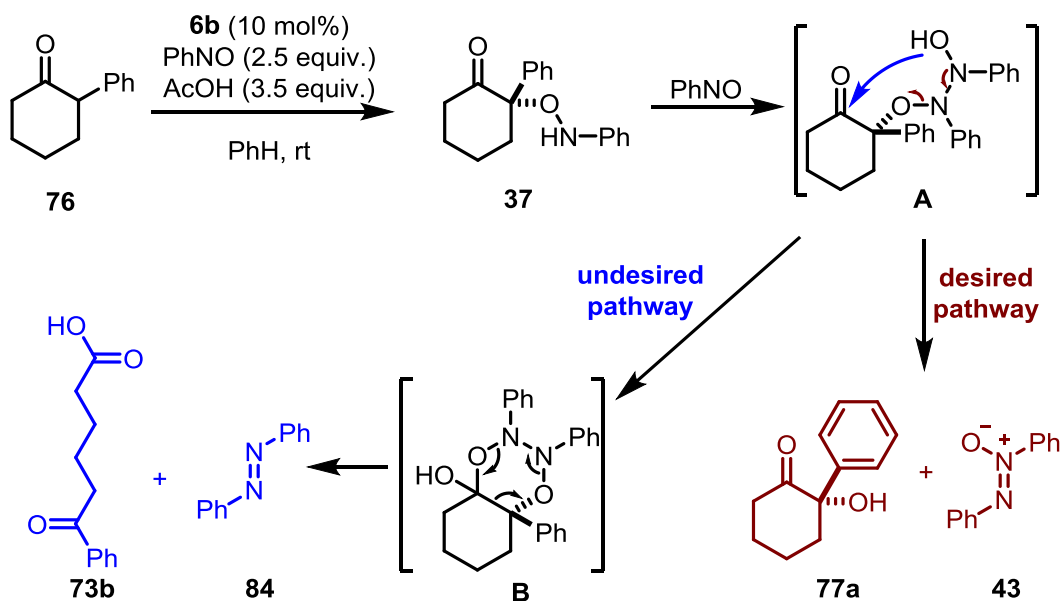
Next we set to revise the reaction conditions and adjust them to optimal catalyst (Table 4.11). Higher catalyst loadings and increased concentration improved the yields (Entries 1–4). Decreasing the amount of nitrosobenzene from 3 to 2.2 equivalents resulted in no erosion of yield or selectivity (Entry 5).

Through careful analysis of the ^1H NMR of the crude reaction mixtures, we identified 6-oxo-6-phenylhexanoic acid (**73b**) as a major side product together with expected azoxybenzene (**43**) and trace amounts of azobenzene (**84**). A plausible mechanism is shown in Scheme 4.23. The aminoxylated ketone **37** formed under the reaction conditions reacted with a second equivalent of nitrosobenzene forming intermediate **A**. In the desired pathway (red), **A** underwent N–O bond cleavage forming the targeted product and azoxybenzene. **A** can also form ketal intermediate **B** (blue), which, following C–C bond cleavage, gives acid **73b** and azobenzene (**84**).



Entry	cat. loading	concentration	conversion ^a	yield ^a	er
1	5 mol%	0.1 M	72%	41%	98:2
2	5 mol%	0.2 M	78%	40%	98:2
3	10 mol%	0.5 M	91%	56%	97:3
4	10 mol%	1.0 M	92%	57%	97.5:2.5
5 ^b	10 mol%	0.5 M	83%	55%	97.5:2.5

Table 4.11: Final optimization of reaction parameters. ^aDetermined by ¹H NMR analysis of the crude reaction mixture using Ph₃CH as internal standard. ^b2.2 equiv of PhNO used.

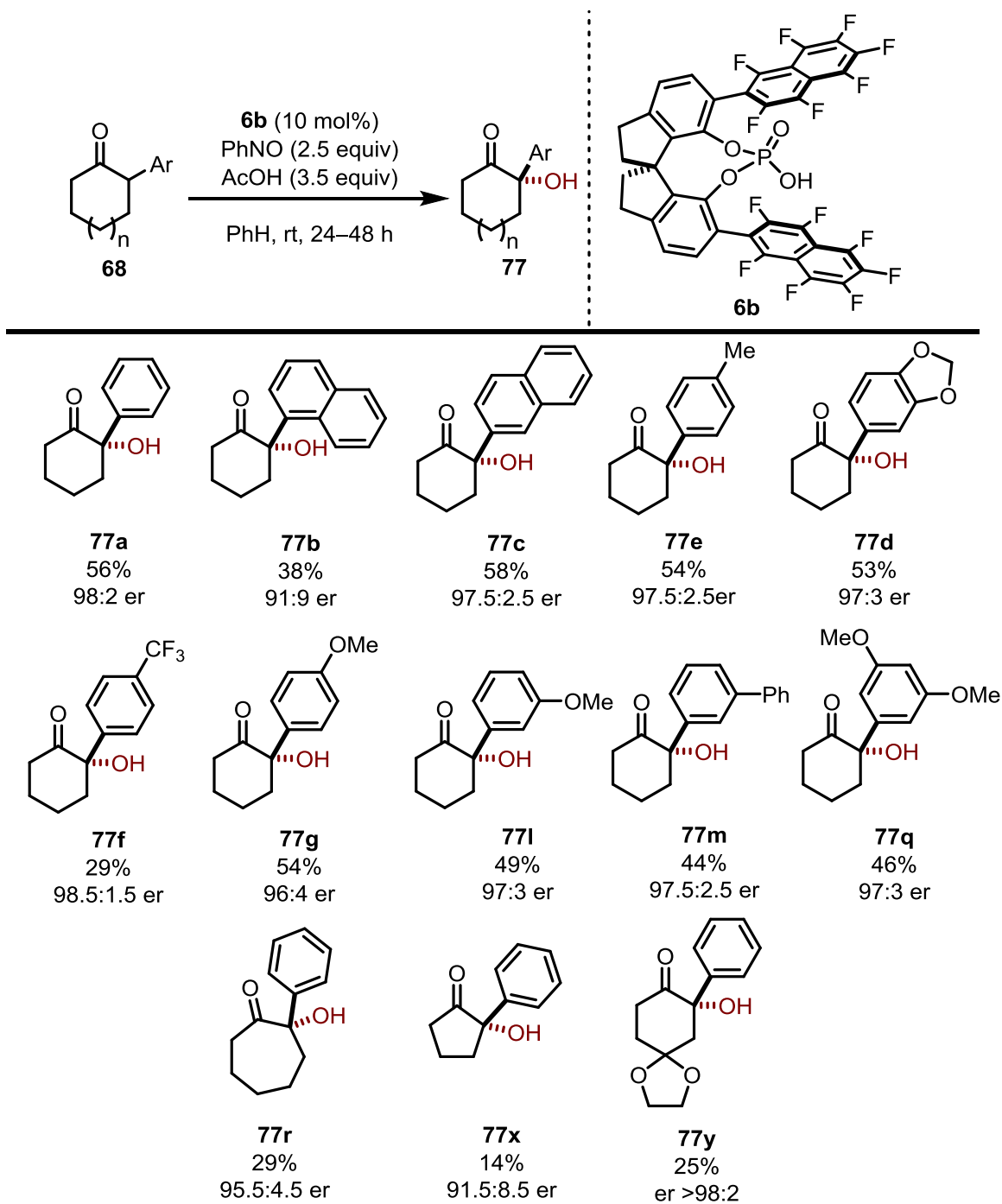


Scheme 4.23: Plausible reaction mechanism including the formation of **73b**.

Extensive studies showed that the formation of **73b** can be avoided by slow addition of nitrosobenzene to the reaction solution, however without improving the target product yield ($\leq 56\%$). After evaluating various methods, we concluded that the speed of addition, *via* either a syringe pump or portion-wise, did not have any significant influence yield and we therefore decided to use the latter protocol for practical reasons.

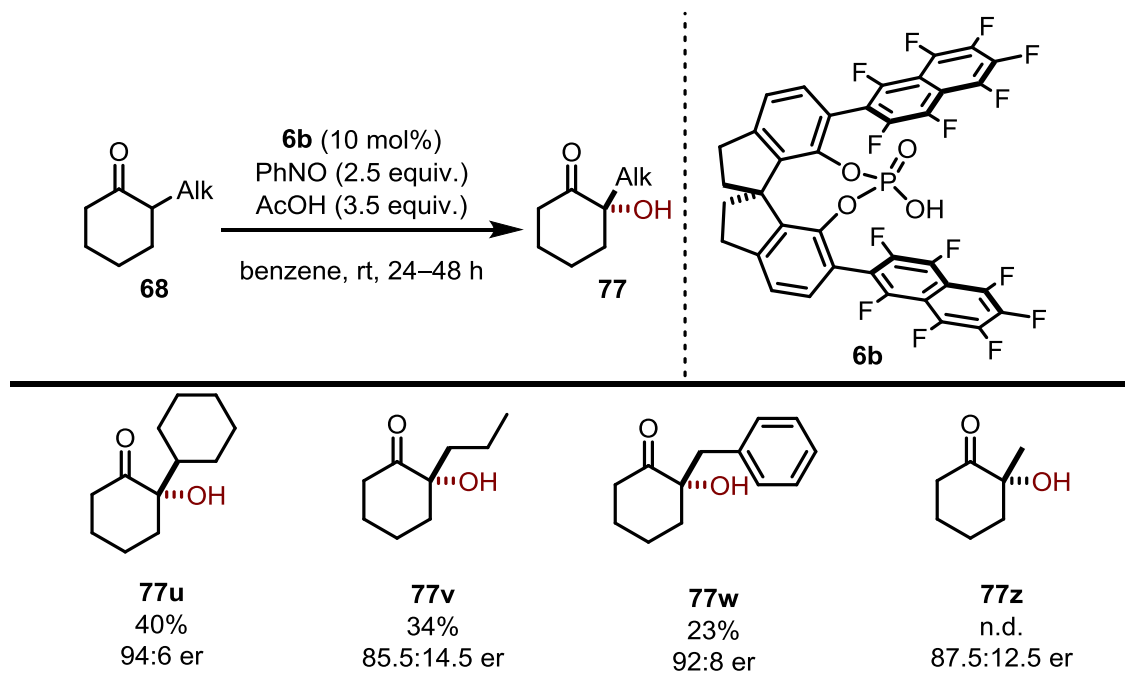
4.3.3.2 Substrate Scope and Application

We further examined the scope of this transformation (Scheme 4.24). Various cyclohexanones bearing electron-rich and electron-poor aromatic substituents in the 2-position readily reacted producing the corresponding hydroxy ketones in moderate yields and excellent enantioselectivities. Regarding electronic effects, electron-rich substrates resulted in similar yields as the model ketone **77a**. A ketone with an electron-withdrawing substituent gave the corresponding product in reduced yield, yet higher enantioselectivity (**77f**, 29% yield, 98.5:1.5 er). While no reaction was observed when employing a ketone with an *ortho*-substituted α -aryl group, substituents in the *meta*- or *para*-position were well tolerated. Despite its strong steric hindrance, 2-(1-naphthyl) cyclohexanone was also compatible with the protocol (**77b**, 38% yield, 91:9 er). Ketones with different ring sizes afforded the targeted products in lower yields and enantioselectivities (**77r**, 29% yield, 95.5:4.5 er and **77u**, 14% yield, 91.5:8.5 er). Due to partial hydrolysis of the ethylene glycol protecting group, hydroxy ketone **77v** could only be isolated in 25% yield but excellent enantioselectivity ($>98:2$ er). Whereas using 2-methyl indanone resulted in racemic product, no reaction was observed using 2-methyl tetralone (not shown).



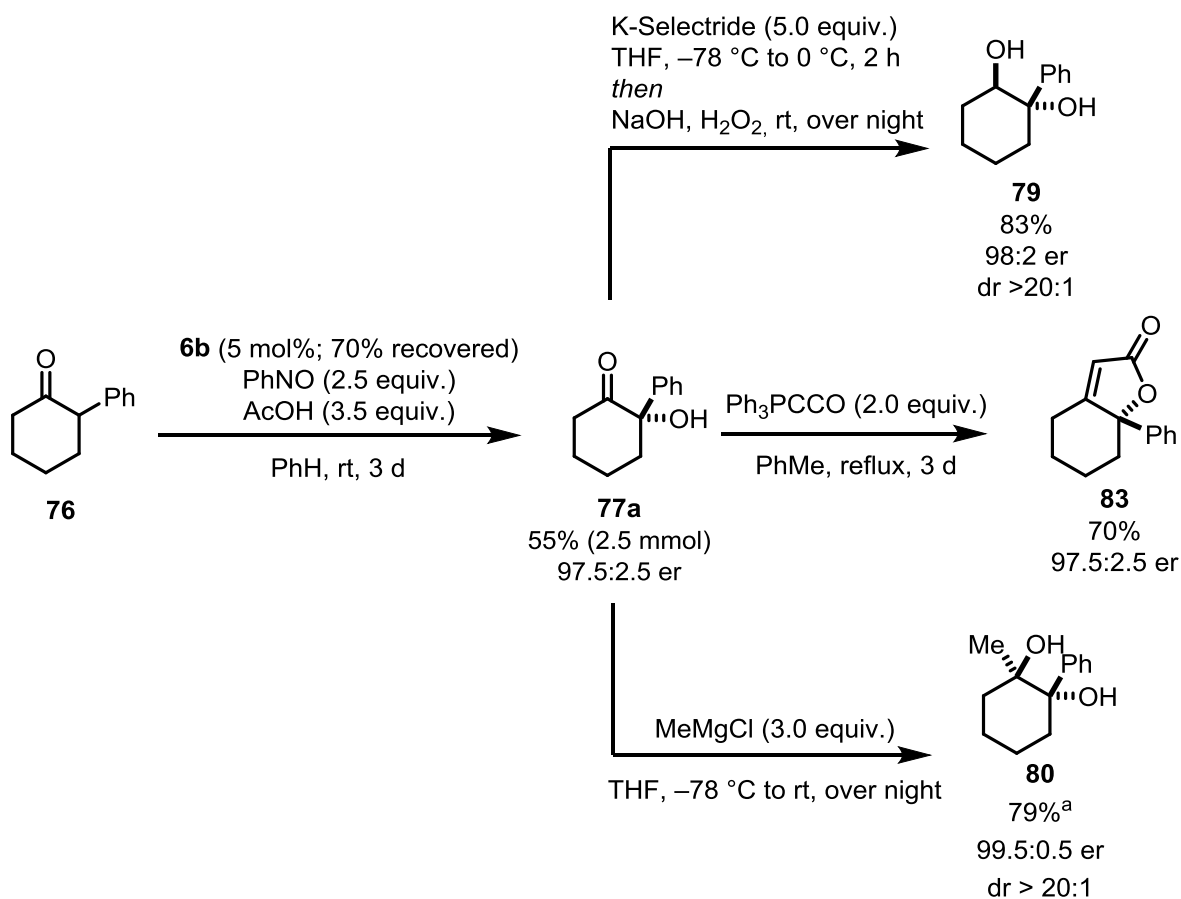
Scheme 4.24: Substrate scope of α -aryl cyclic ketones. The absolute configuration was confirmed by X-ray analysis of the crystal structure of **77a** and assigned by analogy for the other substrates.

2-alkyl cyclohexanones delivered the desired products in lower yields and enantioselectivities (Scheme 4.25). Interestingly, in the tested series, a branched alkyl group performed best (**77u**).



Scheme 4.25: Scope of α -alkyl cyclohexanones.

The robustness of our method was shown in a scale up experiment. On a maximum tested scale of 2.5 mmol, **77a** was isolated without erosion of the yield or enantioselectivity using a decreased catalysts loading (Scheme 4.25). In analogy with the results shown in Scheme 4.18, hydroxy ketone **77a** was transformed to diols **79** and **80** and to unsaturated ester **83** in good yields and without deterioration of enantioselectivity.



Scheme 4.25: Scale up experiment and derivatizations of **77a**. ^aIsolated as an inseparable mixture with remaining starting material (¹H NMR ratio: **80/77a** = 5.8:1)

4.3.3.3 Preliminary Mechanistic Studies

The discrepancy between the conversion of starting material and observed yields prompted further mechanistic studies. Catalyst degradation was excluded by ¹⁹F and ³¹P NMR analysis of the crude reaction mixture. Furthermore, reactions using stoichiometric amounts of catalyst resulted in the same yield as the catalytic ones (52% NMR-yield). We further discovered that background formation of azoxybenzene adds to the inaccurate mass balance. Issues regarding the mass balance were insofar surprising to us, as the ¹H NMR spectra of the crude reaction mixtures usually indicated a clean reaction profile.

NMR-studies showed that the products were stable under the reaction conditions. However, when DPP was used as the catalyst, slow degradation to an unknown compound occurred. A parallel reaction between the starting material and azoxybenzene (**43**) was excluded, although slow conversion towards **73b** was observed in combination with azobenzene (**84**).

Following the reaction by ^1H NMR, we noticed its rate changed after 50–60% conversion of the starting material, suggesting a possible kinetic resolution. Indeed, when the reaction was stopped after 5 h, the unreacted starting material (**76**) was reisolated in 23% yield and 90:10 er (Figure 4.7 a). Kinetic experiments using DPP as the catalysts showed that the rate was independent of nitrosobenzene concentration (Figure 4.7 b). Together, this suggested that the rate-determining step of this reaction is the enolization.

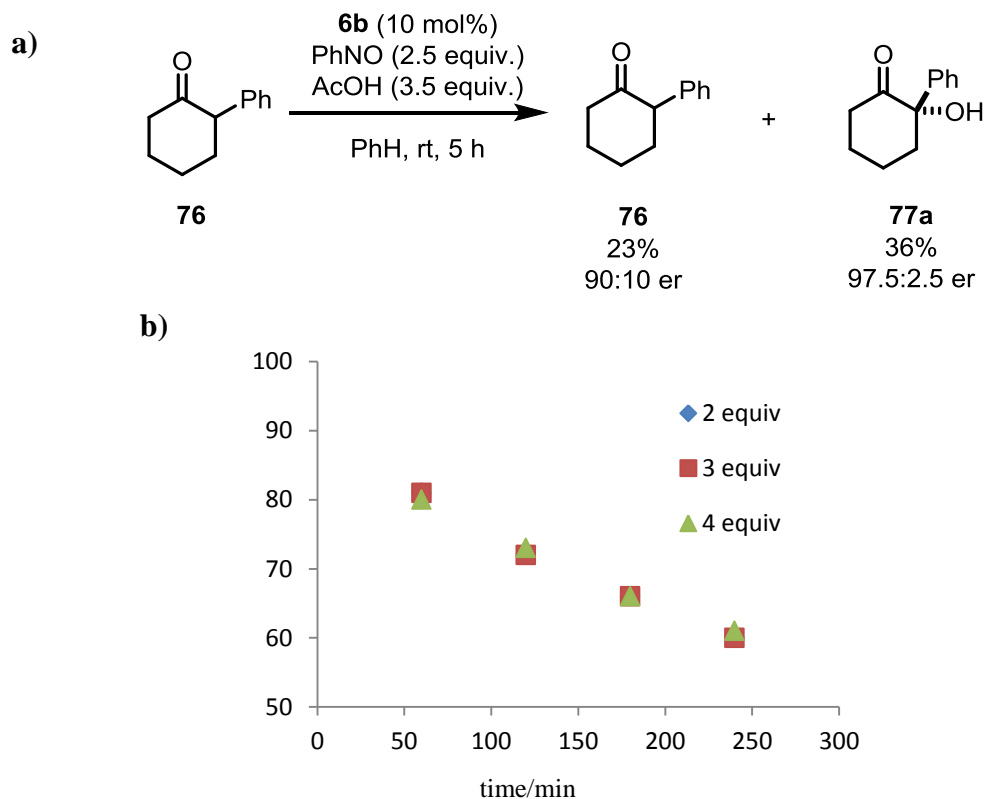
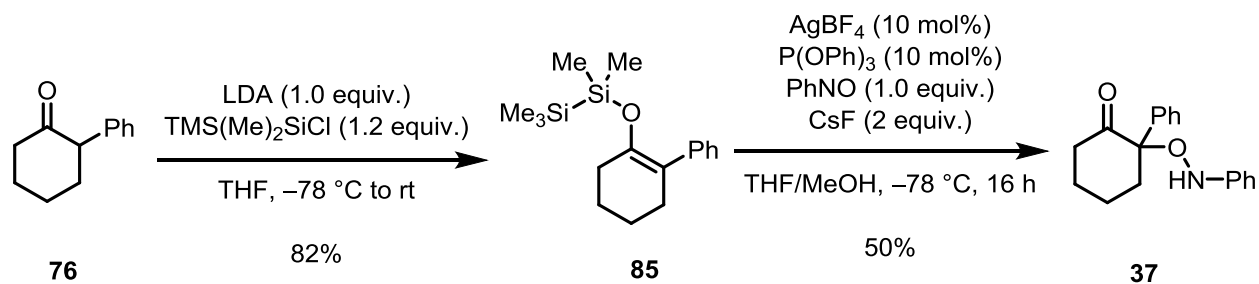


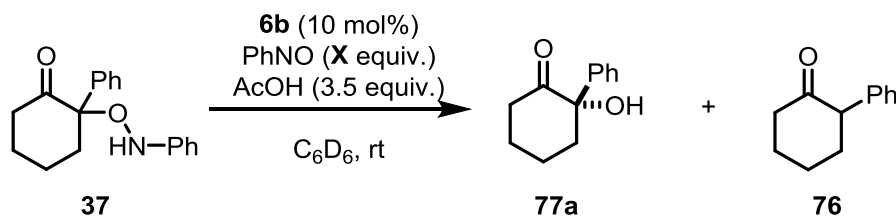
Figure 4.7: a) Test for kinetic resolution and kinetic measurements using different concentrations of nitrosobenzene regarding b) the conversion of the starting material (in %).

We continued our mechanistic investigation by probing the N–O bond cleaving step. The synthesis of the proposed intermediate **43** proved to be challenging; however, was finally accomplished by a silver-mediated addition of silyl vinyl ether **85** reported by Yamamoto *et al* (Scheme 4.27).^[125c]



Scheme 4.27: Synthesis of aminosylated ketone **37**.

The transformation into hydroxy ketone **77a** was investigated by subjecting **37** to the reaction conditions and analyzing the resulting mixture by ¹H NMR (Table 4.11). Although we never detected **37** by NMR, we proved that it is a possible intermediate in the reaction sequence. A rapid reaction of **37** to **77a** was obtained when stoichiometric amounts of nitrosobenzene were used (Entries 1 and 2). Employing smaller amounts (0.5 equiv.) resulted in a slower reaction, yet higher yields during the initial phase (Entry 3). A longer reaction time led to full consumption of starting material (Entry 4). In all cases, no enantioenrichment of hydroxy ketone **77a** was observed, suggesting that the initial nitroso aldol reaction is enantiodetermining. Interestingly, the formation of 2-phenyl cyclohexanone (**76**) was observed in absence of nitrosobenzene, suggesting that the initial aminosylation reaction is reversible (Entries 5 and 6). Surprisingly, enrichment of the opposite enantiomer, suggesting that the complex of catalyst and desired enantiomer of **37** is thermodynamically less stable and therefore more prone to undergo retro-aminosylation reaction, was observed. The slower reaction rates obtained in the absence of catalyst suggested that the phosphoric acid is involved in the N–O bond cleaving step (Entry 7).



Entry	X	time	37 ^a	77a ^a	76 ^a	er of 77a
1	1.0	3 h	traces	64%	-	-
2	1.0	24 h	traces	68%	-	50:50
3	0.5	3 h	18%	78%	-	-
4	0.5	24 h	traces	64%	-	50:50
5	0	3 h	58%	14%	7%	-
6	0	24 h	27%	41%	10%	45:55
7 ^b	0.5	3 h	50%	36%	2%	-

Table 4.11: Preliminary investigations on the N–O bond cleavage reaction. ^aDetermined by ¹H NMR analysis of the crude reaction mixture using Ph₃CH as internal standard. ^bNo catalyst used.

4.3.3.4 Computational Study

To gain further insight into the reaction mechanism, computational studies at the DLPNO-CCSD(T)/def2-TZVPPD + SMD(benzene)//PBE-D3 (BJ)/def2-svp level of theory were performed using 2-phenyl cyclohexanone (**76**) and catalysts (*R*)-**6b** as substrates. The lowest energy pathway is depicted in Figure 4.7. As the addition of acetic acid had no influence on enantioselectivity, it was not considered the presented calculations.

At the outset, we focused on the mechanism and the regioselectivity (less vs more substituted enol) of the phosphoric acid catalyzed enolization step. Our calculations suggest initial protonation of the ketone to form complex **RC** which then undergoes a double hydrogen transfer mechanism *via* **TS1** or **TS1'** to form the corresponding enol-catalyst complexes **C** or **C'**. The formation of the desired more substituted enol (**C**) is not only kinetically (**TS1** is 3.6 kcal/mol lower than **TS1'**), but also thermodynamically favored (**C** is 6.2 kcal/mol lower in energy than **C'**). The kinetic preference can be explained by the Hammond-postulate, suggesting

a late transition state which is therefore geometrically similar to the product. As the calculated energy difference between **RC** and **TS1** is the largest, enolization is rate limiting, which is in good agreement with our kinetic experiments.

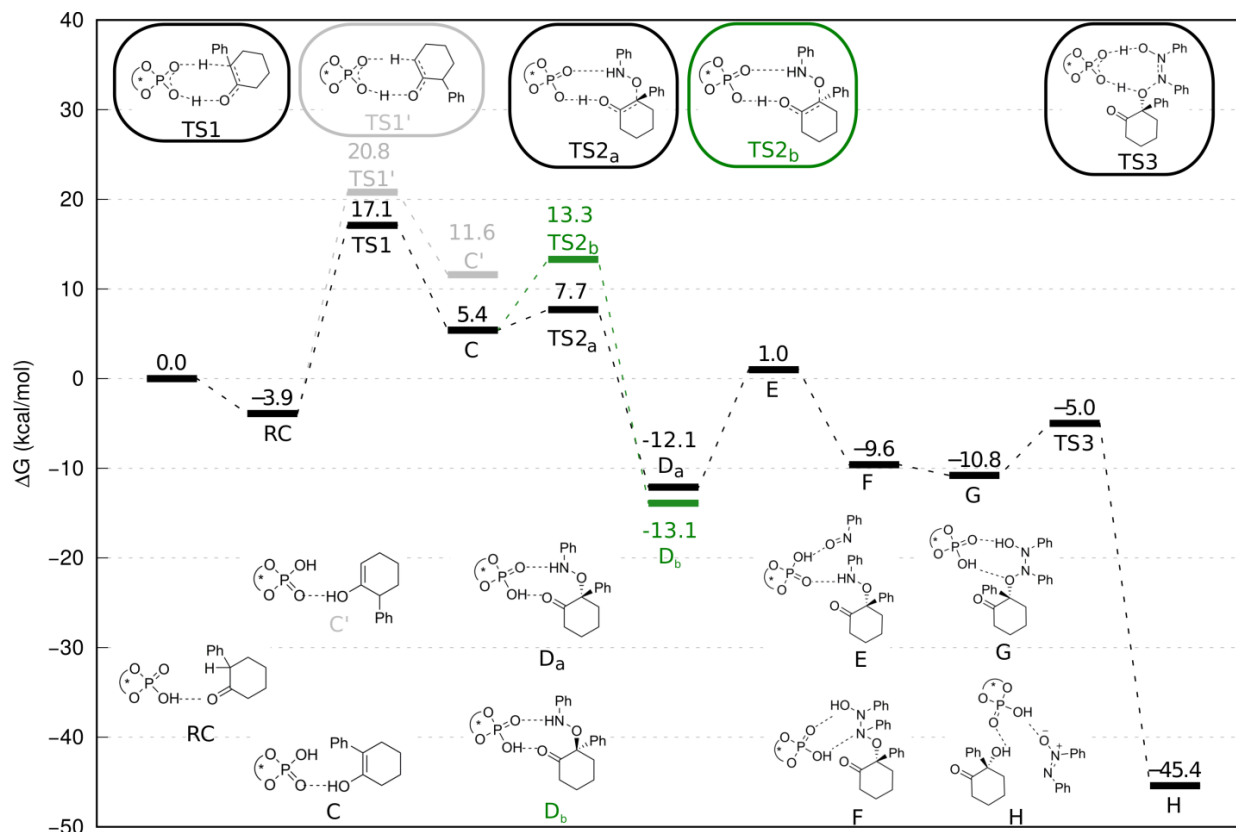


Figure 4.7: ΔG profile for the direct asymmetric α -hydroxylation of **76**. The reference energy corresponds to the dissociated species at infinite separation

Starting from **C**, the transformation towards aminoxylated ketone **37** was attempted. This step is challenging for theory as it potentially involves charged intermediates and the coexistence of catalyst rotamers have to be taken into account. Nevertheless, our studies show that this step proceeds via initial protonation of the nitrogen of the nitrosobenzene (nitrogen protonation was found to be thermodynamically favored by 4.2 kcal/mol compared to oxygen) and subsequent attack of the enol-catalyst complex onto the oxygen. The transition state of the (*S*)-enantiomer, the same one obtained in our synthetic studies, is favored by 5.6 kcal/mol (**TS2_a** vs **TS2_b**), which is in a good agreement with the experimentally determined 98:2 er. Interestingly, the energy barrier leading to the obtained (*S*)-enantiomer is only 2.3 kcal/mol, whereas the one leading to the opposite enantiomer is 7.9 kcal/mol. Considering the aminoxylated ketone **37**, the obtained (*S*)-

enantiomer is thermodynamically less stable than the opposite (1 kcal/mol), explaining the enrichment of the opposite enantiomer in our synthetic studies starting from (\pm)-**37**.

By employing the recently developed Local Energy Decomposition (LED), electrostatic interactions between the catalyst and the reactants are believed to stabilize **TS2a** over **TS2b** and steric repulsion is presumably responsible for the enantioselectivity. A representation of both transition states is depicted in Figure 4.8.

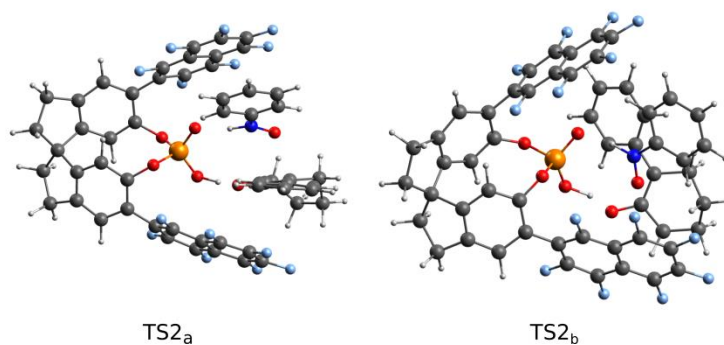


Figure 4.8: Representation of the enantiodetermining transition states **TS2a** and **TS2b**.

As observed synthetically, the final steps towards the targeted hydroxy ketone are rapid. Interaction of complex **D_b** with an additional molecule of nitrosobenzene eventually leads to complex **F** which gives, after a rearrangement involving a hydrogen bond shift (**G**), the final product (**H**) with a very small energy barrier (**TS3**).

4.3.4 Conclusions

In summary, we have investigated and developed systems for direct oxidations of cyclic α -branched ketones under acidic conditions. Depending on the oxidant used, the reaction outcome varied. When using singlet oxygen, an oxidative cleavage forming a compound bearing a carboxylic acid and a ketone moiety occurred. In contrast, in excess of nitrosobenzene the corresponding hydroxy ketones were formed *via* a aminoxylation /N–O bond cleavage sequence. Further modifications of reaction conditions allowed us to use a chiral phosphoric acid as the catalyst, affording the desired products in moderate yields and excellent enantioselectivities. Derivatization of the obtained products supported the synthetic utility of our presented method. Kinetic and mechanistic experiments complemented with high-end computational studies provided insight into the mechanism of the proposed reaction sequence.

4.4 α -Oxidation of Cyclic Ketones with 1,4-Benzoquinones via Enol Catalysis^[189]

The work presented in this section was done in collaboration with Barry Oppelaar.

We envisioned the direct arylation of ketones *via enol catalysis* using 1,4-benzoquinones as the reactions partners. Surprisingly, the reaction between 2-phenyl cyclohexanone (**76**) and 1,4-benzoquinone (**86**) using DPP as the catalyst yielded only trace amounts of the expected 1,4-addition products (**87a** or **87b**) and exclusively produced formal 1,6-addition product ((\pm)-**88a**) (Figure 4.9).

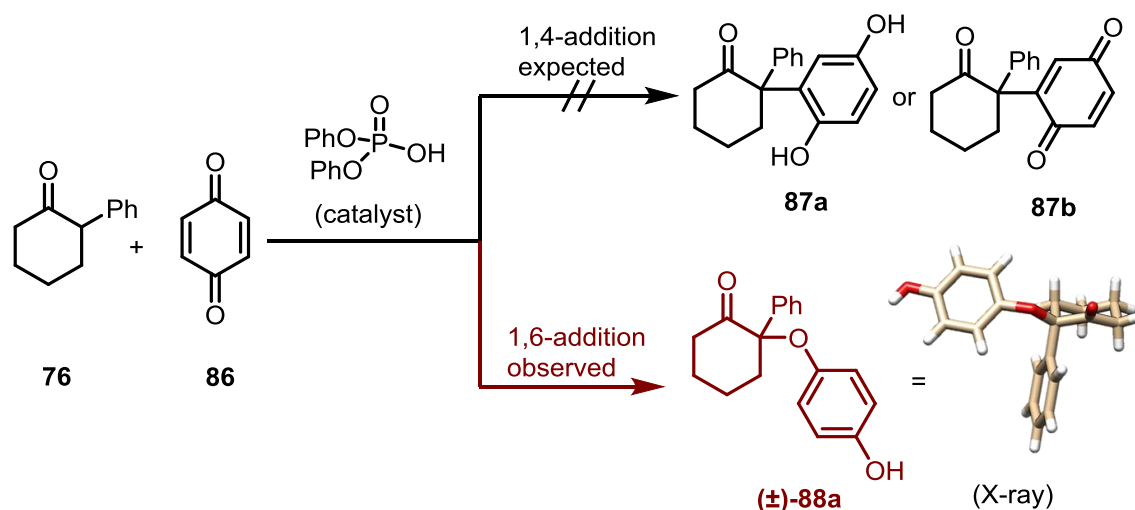


Figure 4.9: Discovery of the phosphoric acid-catalyzed 1,6-addition of branched ketones to 1,4-benzoquinone.

Related structures have been observed in the oxidation of silyl vinyl ethers to enones using 2,3-dichloro-5,6-1,4-benzoquinone (DDQ) as the oxidant (Figure 4.10).^[190] In this case, the desired enone is formed spontaneously *via* elimination from the intermediate derived from the 1,4-addition of the silyl vinyl ether to DDQ. However, if the silyl vinyl ether is sterically demanding, lower yields of the targeted enone are obtained and the product of the 1,6-addition (*O*-product) is instead observed. Extensive kinetic experiments by the Mayr group explained this observation by the reduced rate of the *C*-attack and the hindered elimination from the corresponding intermediate.^[190c] Proceeding *via* an ionic mechanism, the 1,4-addition is reversible and therefore the irreversible formation of the thermodynamically favorite *O*-product is preferred, thus inhibiting the formation of the enone. Measured rate constants and a negative result in a radical clock experiment suggest that the formation of the *O*-product proceeds *via* a

single electron transfer (SET)/inner sphere electron transfer (ISET) mechanism. This is supported by studies of the Renaud group, who investigated the *O*- vs *C*-selectivity of radical addition to 1,4-benzoquinone.^[191]

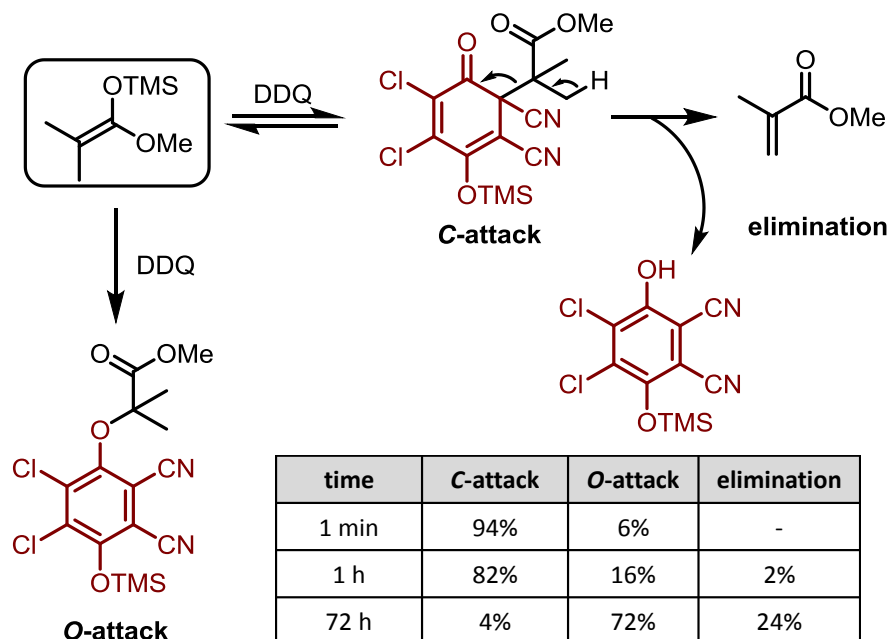


Figure 4.10: Mechanism of the oxidation of silyl vinyl ethers with DDQ.^[190c]

Nevertheless, these reactions have been considered merely as curiosities, since they require preformed enol equivalents, strong oxidants and have not been approached in a catalytic or an enantioselective fashion. In light of its uniqueness and potential utility, we decided to explore this unusual transformation.

4.4.1 Exploration of the Reactivity

We began our investigations by exploring the non-asymmetric transformation in more detail. At first, we evaluated the catalytic potential of other commonly used organic acids using 2-phenyl cyclohexanone (**76**) and 1,4-benzoquinone (**86**) as the starting materials (Table 4.12). Using a high excess of **86**, DPP, the least acidic acid among the tested ones, performed best in terms of yield and chemoselectivity. Namely, when using DPP as catalyst, the targeted aryloxyketone could be isolated as the single product in 60% yield; whereas using *p*TsOH resulted in a mixture of 1,6/1,4-addition products (combined yield of 37% yield, 1,6/1,4 = 16:1).

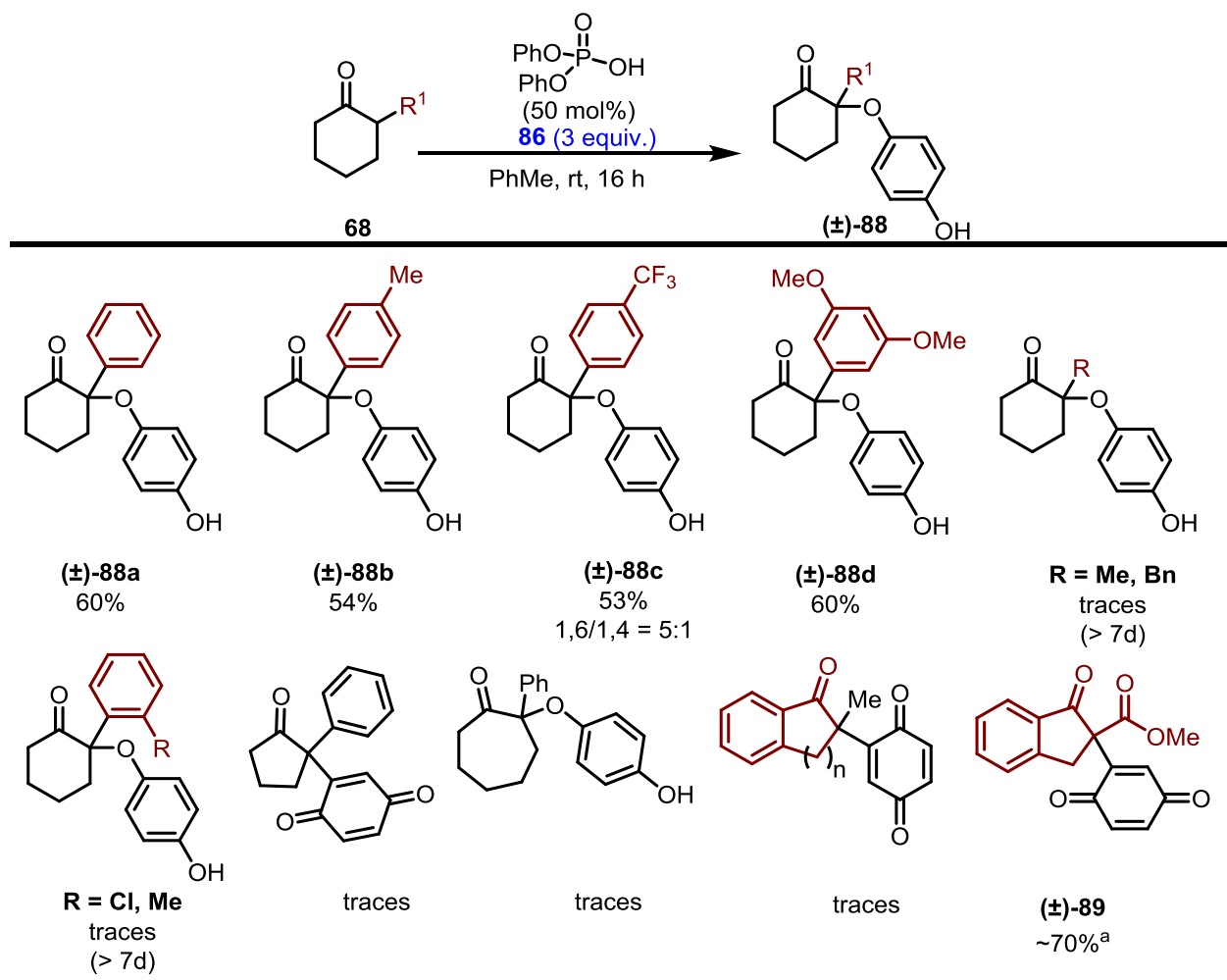
O=C1CCCCC1c2ccccc2
 $\xrightarrow[\text{PhMe, rt, 16 h}]{\text{acid 86 (3 equiv.)}}$
O=C1CCCCC1(c2ccccc2)Oc3ccc(O)cc3

76 **(±)-88a**

Entry	acid	equiv.	yield ^a
1	TFA	0.5	traces
2	TFA	1.0	8%
3	TCA	0.5	traces
4	TCA	1.0	14%
5	<i>p</i> TsOH	0.5	38% (46%)
6	<i>p</i> TsOH	1.0	37%
7	DPP	0.5	(60%)

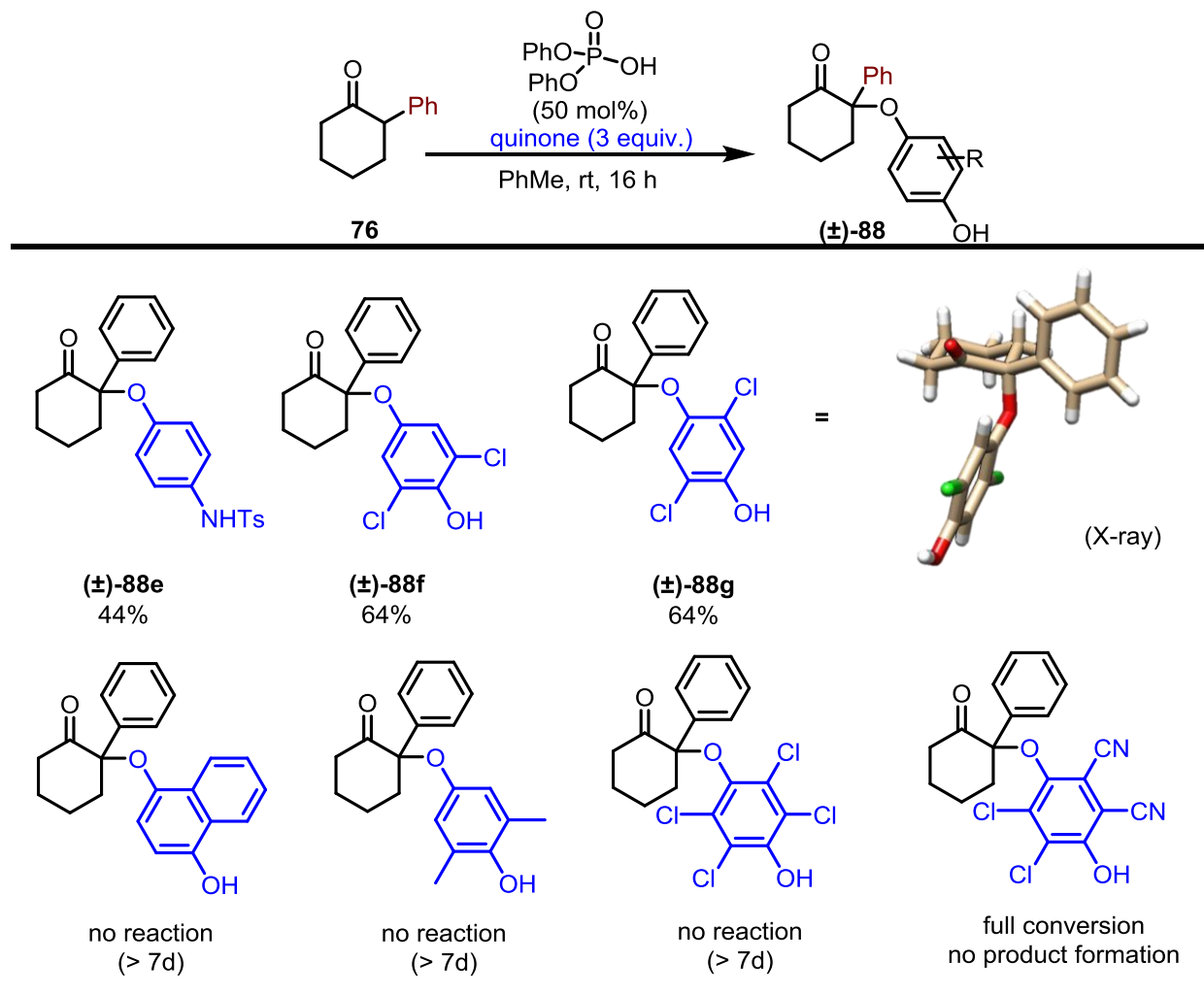
Table 4.12: Evaluation of conventional acids as catalysts for the 1,6-addition of 2-phenyl cyclohexanone (**76**) to 1,4-benzoquinone (**86**). ^aDetermined by ¹H NMR analysis of the crude reaction mixture using Ph₃CH as internal standard. Isolated yields in parentheses.

Using the above mentioned conditions, we then switched our attention towards the generality of the transformation, initially focusing on the ketone scope (Scheme 4.28). While α -aryl ketones readily reacted ((**±**)-**88a**–(**±**)-**88d**), α -alkyl ketones resulted only in trace amounts of the desired products, even at prolonged reaction times and higher temperatures. Regarding substitution on the α -aryl group, *meta*- and *para*-substituents were well accepted and the resulting products could be obtained in similar yields ((**±**)-**88b** and (**±**)-**88d**). In contrast, substituents in the *ortho*-position yielded only trace amounts of the targeted products. Regarding electronic effects, an electron-withdrawing substituent lead to diminished yields and selectivity, *i.e.* ketone (**±**)-**88c** was isolated as an inseparable mixture of the corresponding 1,6- and 1,4-addition products. The reaction turned out to be limited to cyclohexanones, as only trace amounts of either the 1,6- or the 1,4-addition products were obtained using ketones with different ring sizes. The same results were obtained using either indanone or tetralon-derived ketones. Using an indanone-derived β -keto ester as starting material resulted in the exclusive formation of the oxidized product from 1,4-addition (**89**), which could only be isolated as inseparable mixture with hydroquinone, presumably due to partial formation of a charge-transfer complex.



Scheme 4.28: Ketone scope of the non-asymmetric 1,6-addition reaction. ^aIsolated as an inseparable mixture with hydroquinone.

Regarding different benzoquinones, sterics as well as electronics have a crucial influence on the outcome of the reaction (Scheme 4.29). While electron-poor quinones, *e.g.* 2,5- and 2,6-dichloro benzoquinone readily reacted to form the corresponding products in good yields ((±)-**88f** and (±)-**88g**), electron-rich quinones, such as 1,4-naphthaquinone or 2,6-dimethyl quinone, resulted in no conversion of the starting material. This is presumably due to the increased steric hindrance, as the same result was obtained using chloranil, a strong oxidizing agent.^[192] When DDQ was used, full conversion of the ketone was obtained, however no detectable amounts of the desired product were formed. As confirmed by the ¹³C NMR shifts, the *O*-alkylated product could be exclusively obtained using the 4-amino phenol-derived quinone (±)-**88e**.

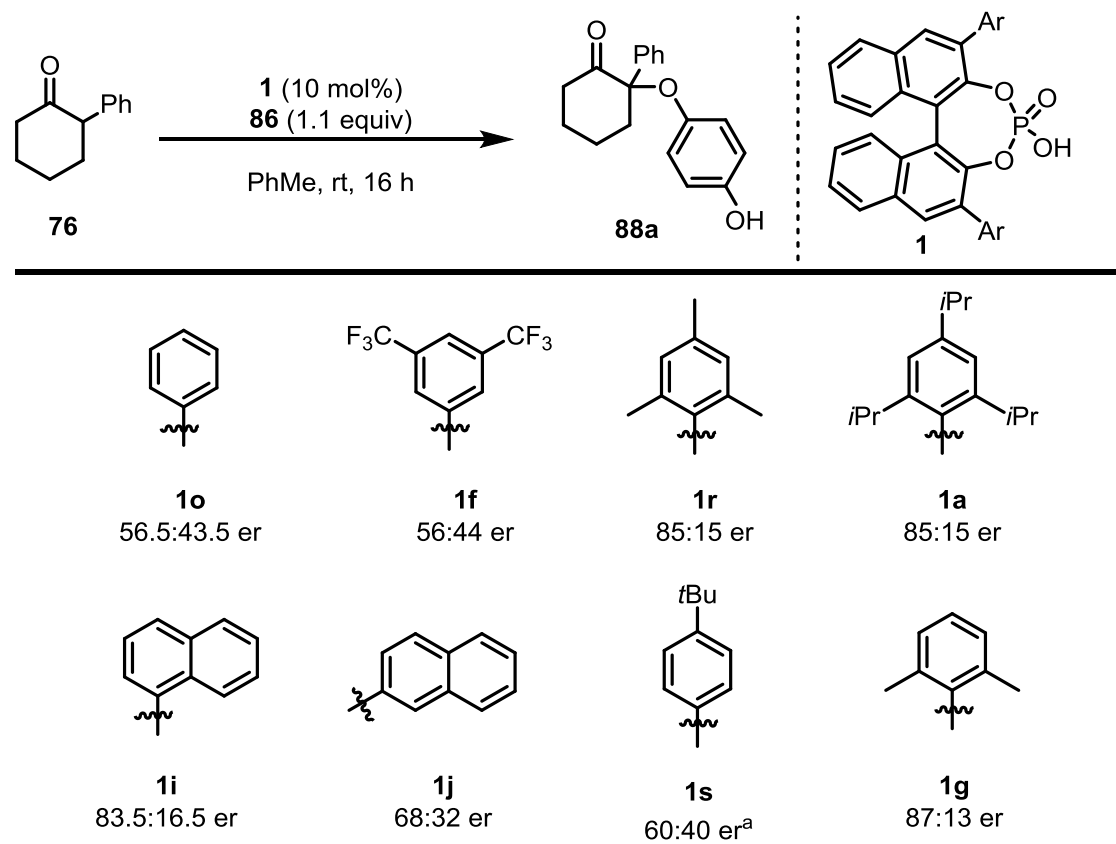


Scheme 4.29: Benzoquinone scope of the non-asymmetric 1,6-addition reaction.

4.4.2 Exploration of the Asymmetric Transformation

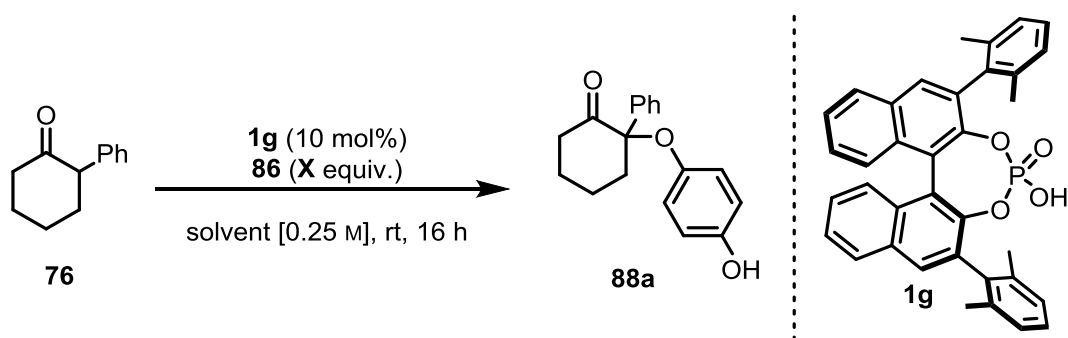
With these results in hand we attempted the development of an asymmetric variant of this transformation using 2-phenyl cyclohexanone (**76**) and 1,4-benzoquinone (**86**) as the starting materials. In an initial round of catalyst screening, we wanted to demonstrate that enantioinduction by a chiral phosphoric acid is possible (Scheme 4.30). Considering substitution patterns of the aryl-moiety in 3,3'-position of the BINOL backbone, *meta*-substituents did not have any beneficial effect on selectivity (compare catalysts **1o** and **1f**). A substituent in the *para*-position gave a slight increase in enantioselectivity; however, the corresponding reaction had to be performed at a higher temperature due to the low reactivity (catalyst **1s**). Substitution in the *ortho*-position had the highest impact on the outcome of the reaction. Namely, 1-naphthyl- and

ortho,ortho-dimethyl-substituted catalysts **1i** and **1g** delivered the corresponding aryloxyated product in already promising enantioselectivities (83.5:16.5 er and 87:13 er, respectively). Similar enantiomeric excess was obtained with TRIP, albeit with only trace amounts of product (**1a**, 85:15 er).



Scheme 4.30: Initial catalyst screening. ^aPerformed at 40 °C.

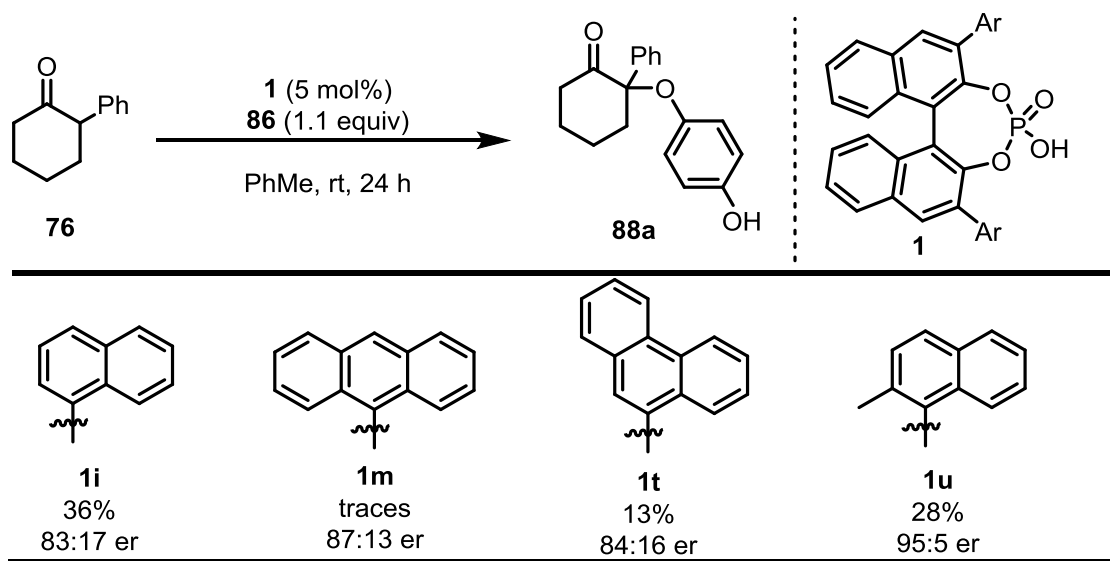
Using *ortho,ortho*-dimethyl substituted catalyst **1g**, further parameters were briefly screened (Table 4.13). No reaction was observed when the concentration was diluted to 0.1 M. Increasing the amount of 1,4-benzoquinone from 1.1 to 3.0 equivalents did not improve the yield, however an erosion in enantioselectivity was obtained (Entries 2–4). While maintaining the level of enantioselectivity, the yield was improved using toluene as the solvent (Entry 10). The addition of acetic acid inhibited the reaction (Entry 11) and no improvement was obtained by increasing the reaction temperature from room temperature to 50 °C.



entry	solvent	A	yield ^a	er	comment
1	CH ₂ Cl ₂	1.1	traces	-	0.1 M
2	CH ₂ Cl ₂	1.1	22%	87:13	
3	CH ₂ Cl ₂	2	23%	79:21	
4	CH ₂ Cl ₂	3	21%	78:22	
5	DCE	1.1	16%	82:18	
6	MeCN	1.1	n.r.	-	
7	CHCl ₃	1.1	21%	78.5:21.5	
8	Et ₂ O	1.1	n.d.	81:19	
9	CyH	1.1	n.d.	86:14	
10	PhMe	1.1	42%	85.5:14.5	
11	CH ₂ Cl ₂	1.1	traces	n.d.	3.5 equiv AcOH added
12	CH ₂ Cl ₂	1.1	28%	86:14	At 50 °C

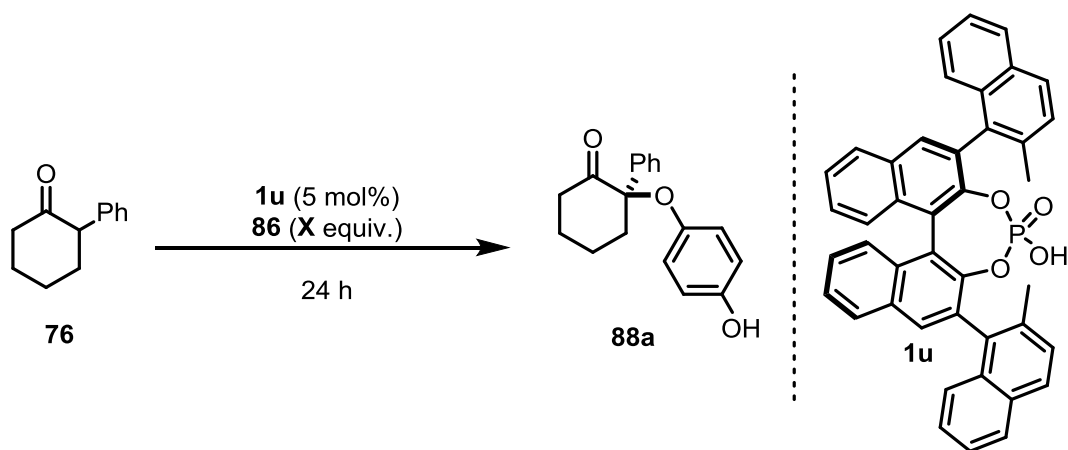
Table 4.13: Initial screening of conditions. Best result in highlighted in bold. ^aDetermined by ¹H NMR analysis of the crude reaction mixture using Ph₃CH as internal standard.

These initial results prompted us to reinvestigate the structure of the catalyst. As 1-naphthyl substitution proved to be promising, we focused our attention in the second round of catalysts optimization on related structural motifs (Scheme 4.31). To our delight, 2-methyl-1-naphthyl substituted catalyst **1u** delivered the targeted product in 28% yield and 95:5 er. Notably, **1u** was used as a mixture of rotamers. The separation *via* semi-prep HPLC is reported, however was not successful in our hands.^[193]



Scheme 4.31: Screening of 1-naphthyl-derived substituted phosphoric acids. Yields determined by ^1H NMR analysis of the crude reaction mixture using Ph_3CH as internal standard.

With the optimized catalyst in hands, we attempted to refine the reaction conditions in order to improve the yield. The results of these efforts are summarized in Table 4.14. A significant improvement was obtained by changing the solvent from toluene to benzene (Entries 1 and 2). 6-oxo-6-phenylhexanoic acid (**73b**), the product of over-oxidation, was identified as one major side product. Performing the reaction at 0 °C inhibited its formation and slightly increased the yield of the target ketone (Entry 3). The mechanism for the formation of **73b** is unclear; however, traces of it can be observed when some of the obtained products (**88**) were stored over a long period of time under air and at room temperature. As previously shown, increasing the concentration was beneficial regarding the yield and the desired product was isolated in 50% yield and 96:4 er (Entry 4). Finally, increasing the amount of 1,4-benzoquinone to 3 equivalents provided **88a** in 67% isolated yield and 96:4 er (Entries 5 and 6)

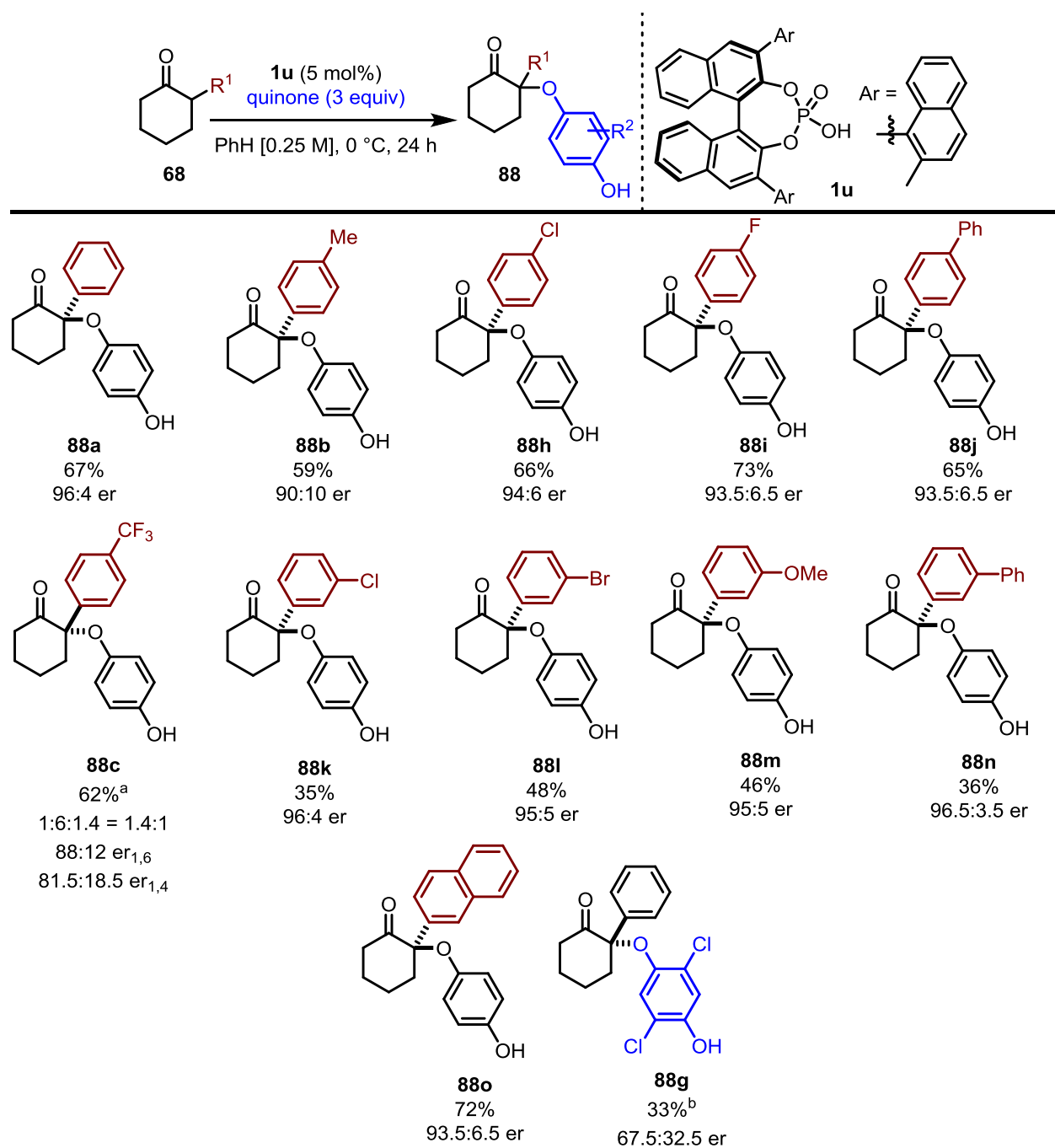


entry	solvent	T	M	X	yield ^a	er
1	PhMe	rt	0.25	1.1	28%	95:5
2	PhH	rt	0.25	1.1	38%	95:5
3	PhH	0 °C	0.25	1.1	42%	95:5
4	PhH	0 °C	0.5	1.1	(50%)	96:4
5	PhH	0 °C	0.5	3	(67%)	96:4
6	PhH	0 °C	0.5	5	(59%)	96:4

Table 4.14: Refinement of reaction conditions. Best result highlighted in bold. ^aDetermined by ¹H NMR analysis of the crude reaction mixture using Ph₃CH as internal standard. Isolated yield in parentheses.

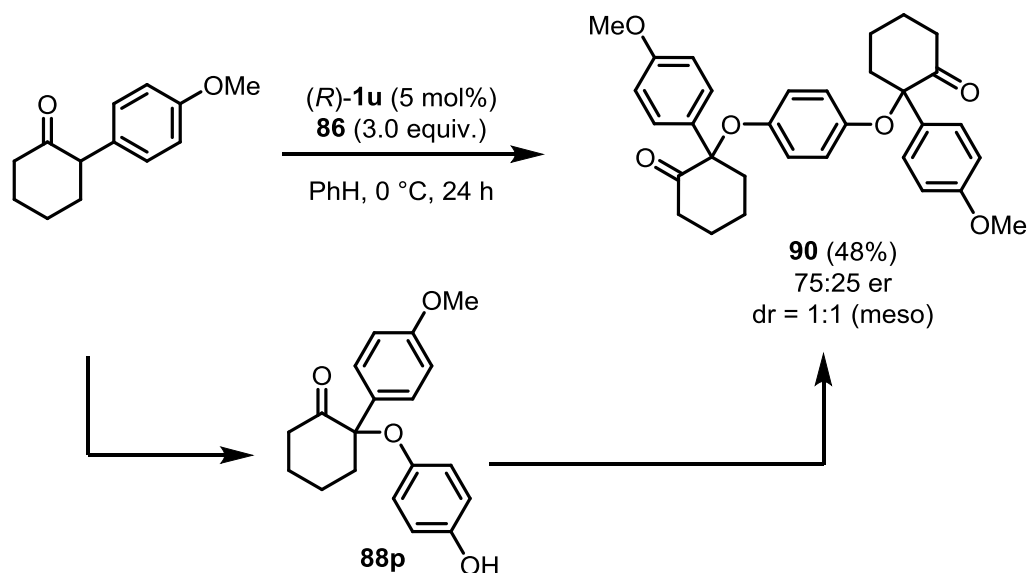
Having found what seemed to be optimal reaction conditions, we turned our attention towards the scope of this asymmetric transformation (Scheme 4.32). Similar to the non-enantioselective variant, this method is limited to α -aryl ketones. Despite several attempts to overcome this drawback by rescreening more acidic catalysts or varying the reaction conditions, no reaction using cyclic α -alkyl ketones or cyclohexanone was observed. Nevertheless, *para*-substituents on the α -aryl group were well tolerated under the optimized reaction conditions and the corresponding products were isolated in similar yields and enantioselectivities as the model substrate (**88a–88j**). While substituents in the *meta*-position gave the targeted products in lower yield yet increased enantioselectivities (**88k–88n**), *ortho*-substituted α -aryl ketones did not show any reactivity. An electron-withdrawing substituent led to decreased chemoselectivity, *i.e.* ketone **88c** could only be isolated as an inseparable mixture of the 1,4- and 1,6-addition products with diminished enantioselectivity. Gratifyingly, 2-naphtyl cyclohexanone readily reacted under the optimized reaction conditions giving **88o** in 72% yield and 93.5:6.5 er. Besides 2,5-dichloro-1,4-

benzoquinone (**88g**, 33%, 67.5:32.5 er), the use of other 1,4-benzoquinone derivatives or ketones with different ring sizes resulted in either no reaction or complex mixtures.



Scheme 4.32: Scope of the phosphoric acid-catalyzed 1,6-addition of α -branched ketones (**76**) to benzoquinones (**86**). Isolated yields presented. ^aUsing (*S*)-**1u**, 3 d reaction time. ^bUsing (*S*)-**1u**, 4 d reaction time at room temperature.

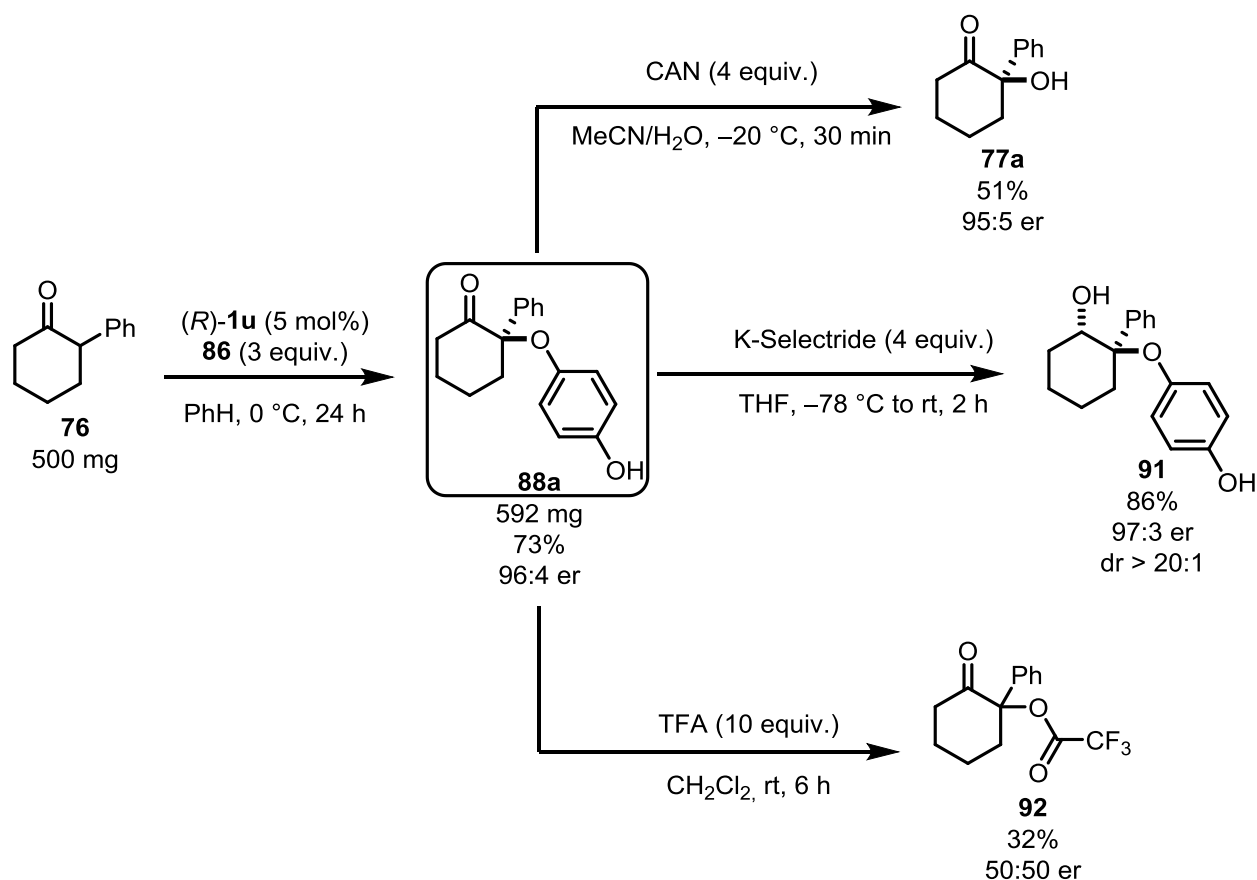
A surprising observation was made when *para*-methoxy substituted 2-phenyl cyclohexanone was used as the starting material. Formation of the desired product **88p** was observed; however it was not stable under the reaction conditions and reacted further to form dimer **90** as an equimolar mixture of diastereoisomers (Scheme 4.33).



Scheme 4.33: Reaction using a *para*-methoxy substituted 2-aryl ketone as the starting material.

Despite several attempts, the crystallization of the enantioenriched substrates could not be achieved. Therefore the absolute configuration of the products was determined in analogy to literature known α -hydroxy ketone **77a** (*vide infra*).

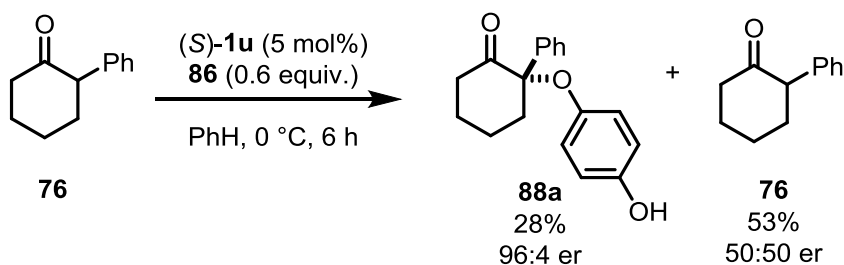
A scale up experiment using 500 mg of 2-phenyl cyclohexanone (**76**) proceeded smoothly and gave **88a** without deterioration of yield or enantioselectivity (Scheme 4.34). Gratifyingly, the introduced hydroquinone moiety was converted to a synthetically-useful hydroxy group under oxidative conditions similar to those applied for the removal of PMP protecting groups.^[194] Alcohol **91** was obtained as single diastereomer after reduction of **88a** with K-Selectride. Interestingly, in presence of an excess of TFA, the hydroquinone moiety was transformed into the corresponding TFA protected hydroxy ketone **92** with complete loss of chiral information.



Scheme 4.34: Scale up and derivatization experiments.

4.4.3 Study of the Reaction Mechanism

When considering the mechanism of this reaction, several aspects have to be taken into account. (1) No reaction was observed in the absence of a phosphoric acid catalyst. (2) The scope was limited to α -aryl ketones; *i.e.* low reactivity was observed when α -alkyl ketones were used as starting materials. (3) Reactivity was only obtained when electron-neutral or -poor benzoquinones were used as reaction partners. On the other hand, some strongly activated benzoquinones, such as chloranil, were not reacting presumably due to steric reasons. (4) The reaction selectively produced the C–O bond and the 1,4-addition products were only obtained in trace amounts. Finally, (5) the reisolated starting material was racemic, suggesting that, in contrast to our direct hydroxylation, phosphoric acid-catalyzed enolization was not rate determining (Scheme 4.35).



Scheme 4.35: Results of the test for kinetic resolution.

To gain further insight into the reaction mechanism, we attempted a different-excess-experiment. Accordingly, the protocol for the non-enantioselective variant of this reaction was performed using different amounts of 1,4-benzoquinone (**86**) and the progress was followed over time by analyzing aliquots taken from the crude reaction mixture with ^1H NMR. Catalyst loading of 25 mol% was applied in order to slow down the reaction rate, as full consumption of the starting material within 3 h was obtained when 50 mol% of DPP were used. The plot visualizing product formation over time is depicted in Figure 4.11. The visible change in the kinetic profile suggested, that the rate limiting step involved benzoquinone and therefore the enolization, as it only incorporates ketone and catalyst, was not rate limiting. *Note:* Due to the low solubility of 1,4-benzoquinone in benzene, the reaction mixtures obtained using 2 and 3 equivalents of 1,4-benzoquinone were saturated throughout the duration of the measurement, thus leading to similar slopes.

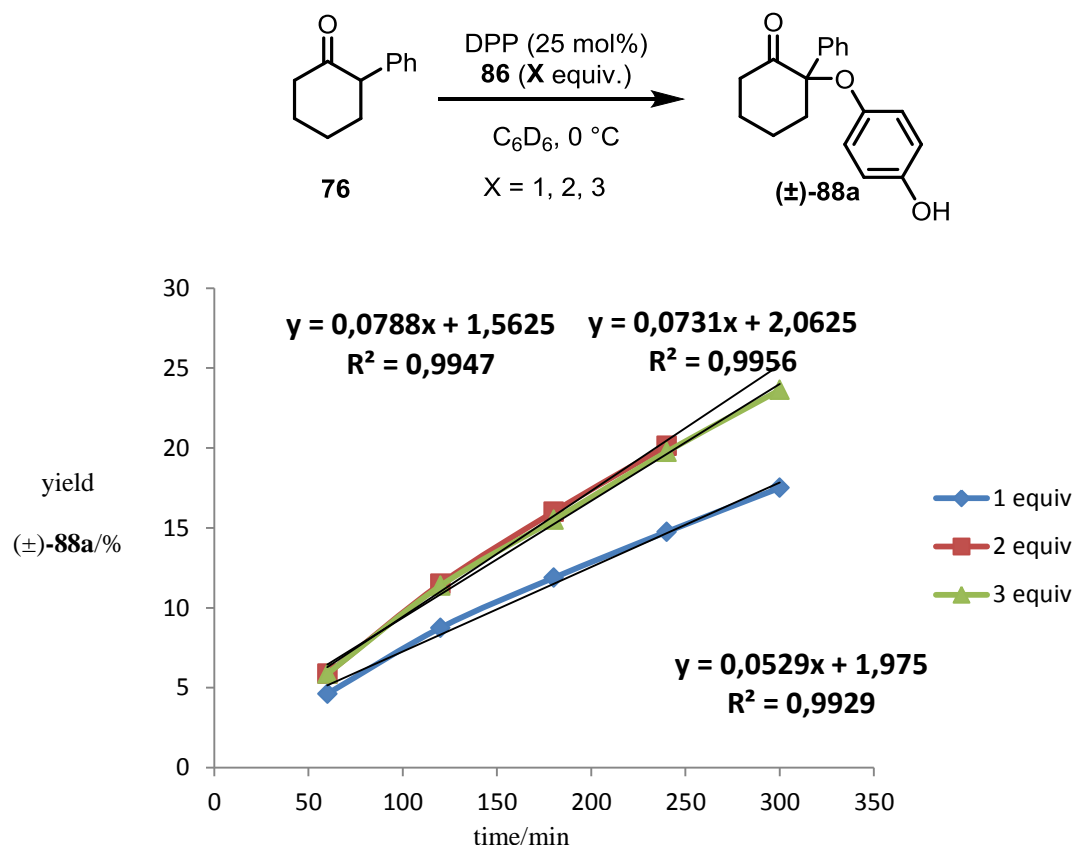


Figure 4.11: Effect of 1,4-benzoquinone molar excess.

In contrast to the conversion of starting material, product formation could be approximated as linear within the initial 300 min of reaction time. We therefore envisioned that a Hammett plot might give us further information on the electronic nature of the rate determining transition step. Thus, a series of competition experiments, comparing the initial rates of para-*X* substituted α -aryl ketones to 2-phenyl cyclohexanone (**76**, X = H) was conducted. The experiments were performed by subjecting the corresponding substrate alongside 2-phenyl cyclohexanone using the standard protocol (25 mol% catalysts loading) and analyzing aliquots, taken every 60 min by ^1H NMR using an internal standard. The corresponding plots are depicted in Figure 4.12. *Note:* except X = Me every experiment was conducted twice, hence the larger data set.

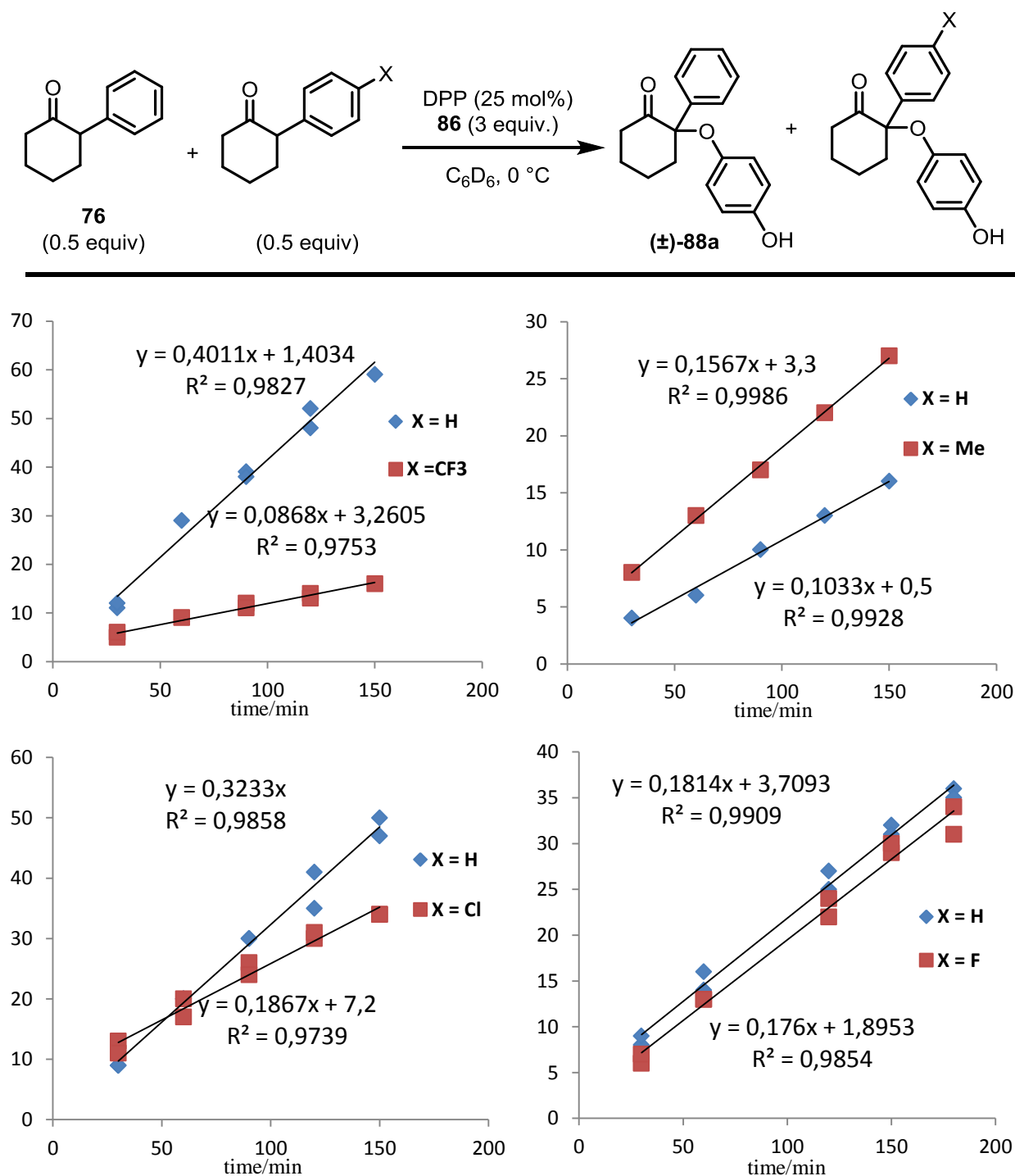


Figure 4.12: Relative kinetic data of *para*-substituted α -aryl cyclohexanones compared to 2-phenyl cyclohexanone (**76**). Note: Non-normalized ratios determined by 1H NMR analysis of the crude reaction mixture compared to Ph_3CH as internal standard are presented on the y-axis.

The slope for each relative kinetic profile was determined using EXCEL. From this data, the $\log(k_X/k_H)$ could be calculated and plotted against the corresponding Hammett parameters (σ , σ^+ , σ^-) taken from the literature (Figure 4.13).^[195]

X	σ	σ^+	σ^-	$\log(k_X/k_H)$
H	0	0	0	0
CF ₃	0,54	0,61	0,65	-0,66
Me	-0,19	-0,31	-0,17	0,18
Cl	0,23	0,11	0,19	-0,24
F	0,06	-0,07	-0,03	-0,01

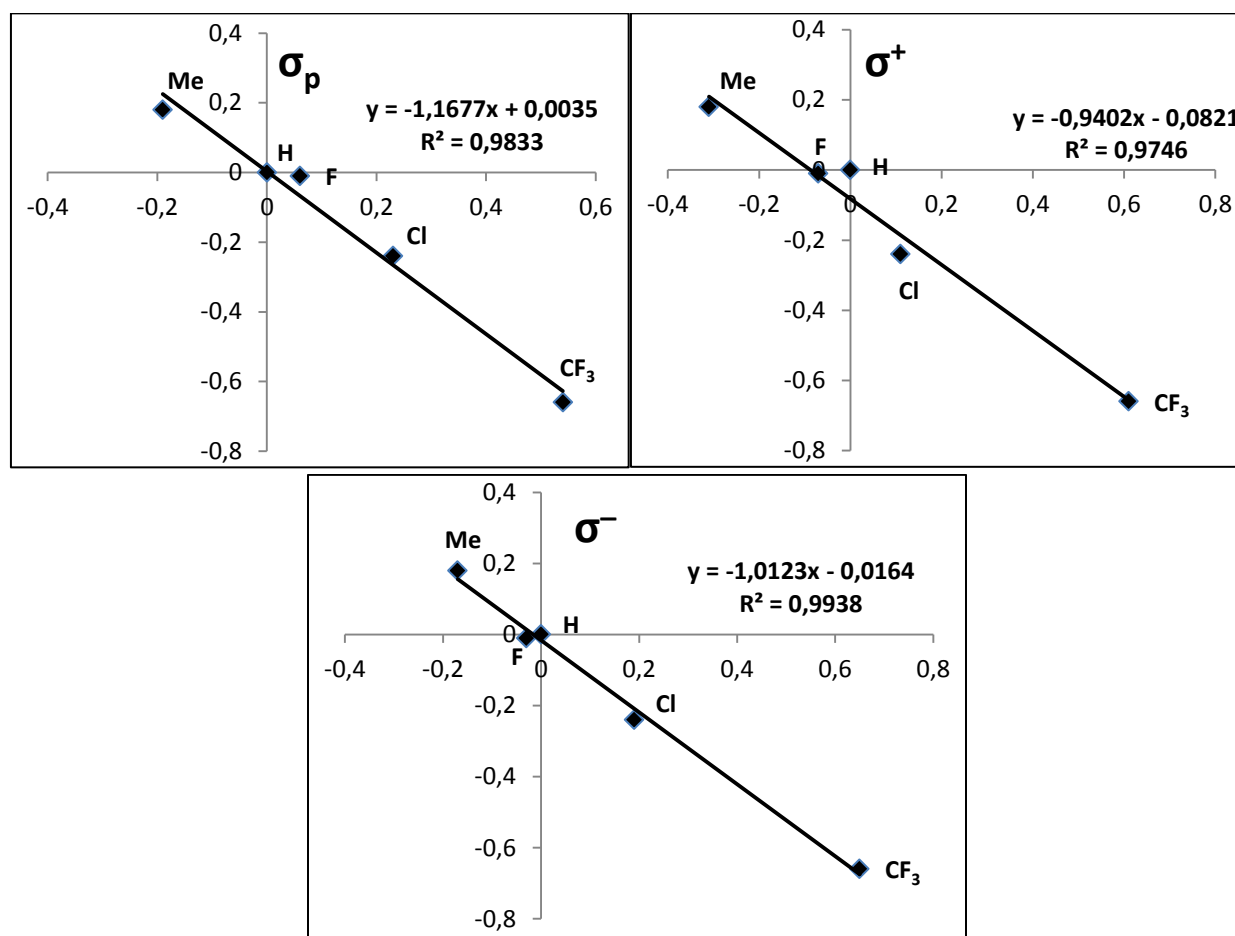
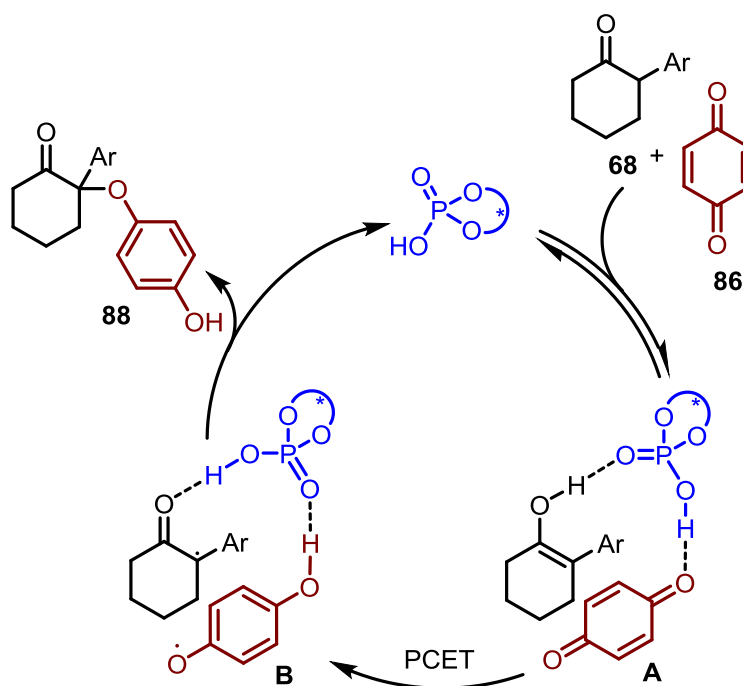


Figure 4.13: Hammett analysis. a) Determined $\log(k_X/k_H)$ values and the corresponding Hammett parameters. b) Plot using σ . c) Plot using σ^+ . d) Plot using σ^- .

The decrease rate of product formation using electron-withdrawing substituents leads to negative ρ -values (slopes) in all three Hammett plots. This indicates a reduction of negative charge/buildup of positive charge in the rate determining transition state. As all three Hammett plots showed similar R^2 -values, indicating the quality of the estimated trend line, no significant influence of mesomeric or inductive effects was evident.

The conclusion of the obtained results leads to the proposed reaction mechanism depicted in Scheme 4.35. Phosphoric acid catalyzed enolization of the ketone followed by coordination of the benzoquinone derivative forms complex **A**. This complex undergoes a proton coupled electron transfer (PCET) to form diradical complex **B**. In this scenario the employed phosphoric acid simultaneously acts as acid, protonating the benzoquinone, and as base, deprotonating the enol. This oxidation step is in good agreement with the obtained negative ρ -values in the Hammett plots and the extensive kinetic studies by Mayr *et al.* suggesting that related products are formed *via* a SET/ISET mechanism.^[190c] Subsequent radical-radical recombination furnishes the targeted product and releases the catalyst.



Scheme 4.35: Proposed reaction mechanism.

At this point, we cannot exclude the possibility that the oxidation step from **A** to **B** occurs *via* an electron transfer and subsequent proton transfer (or *vice versa*). However, this is less likely

as the difference in the BDFEs of the O–H groups of phenols (as an extreme case of an enol, 88.3 kcal mol⁻¹/DMSO) and of the semiquinone radical (65.2 kcal mol⁻¹/DMSO) is too high to allow a HAT-type mechanism.^[160] The existence of radical intermediates could synthetically not be verified as experiments in the presence of radical quenchers, such as BHT or TEMPO, only reduced the rate of product formation but did not inhibited the reaction itself. Such experiments can only be positive if diffusion of both radicals is faster than the recombination, suggesting that, in our case, the radical recombination, due to the tight complex **B**, occurs very rapidly. This is in line with the ISET mechanism suggested by Mayr *et al.*^[190c] According to oxidation potentials of enol cation radicals using stable enols obtained *via* cyclovoltametry, the oxidation of α -keto radicals, similar to the one proposed in complex **B**, is even more facile than the initial radical formation. In these cases, the formed carbocation could be intercepted by nucleophiles such as methanol.^[140e] However in our case only reduced rates, presumably due to interrupted hydrogen bonding, and no further side products could be obtained in the presence of an excess amount of methanol.

4.4.4 Conclusions

In summary, we report the first direct, catalytic and asymmetric α -aryloxylation of ketones *via enol catalysis*. Using 1,4-benzoquinones as the reaction partners, various α -branched cyclic ketones underwent selective formal 1,6-addition, forming exclusively the C–O bond in good to moderate yields (up to 73%) and enantioselectivities (up to 96.5:3.5 er). Preliminary mechanistic studies are in line with a phosphoric acid promoted proton coupled electron transfer.

5 Summary

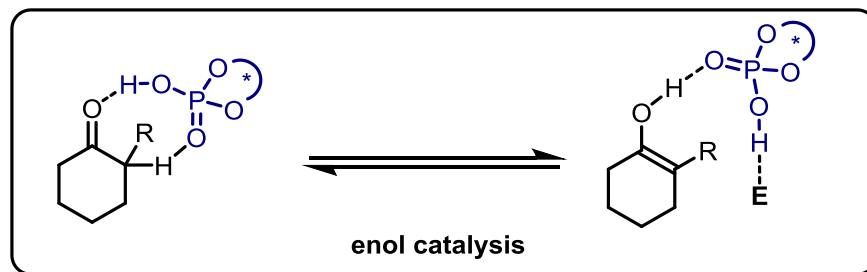
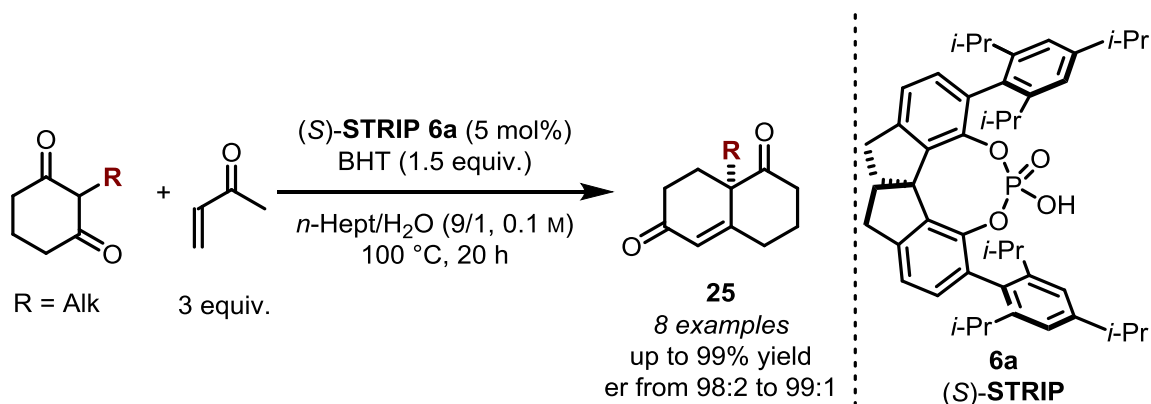


Figure 5.1: Proposed activation mode of *enol catalysis* (E = electrophile).

Despite of being a rather obvious approach, Brønsted acid-catalyzed enolizations have so far barely found application in asymmetric catalysis. Although a few systems for enantioselective α -functionalization of unactivated α -branched ketones have been reported, they usually rely on tetralone analogs and, hence, omitting the challenge of the regioselectivity. Over the last years, others and our groups independently demonstrated that *enol catalysis* can overcome these limitations.^[62-63, 65-66, 181] Indeed, the more substituted enol is exclusively formed under phosphoric acid catalysis giving enantioselective access to synthetically promising α,α -disubstituted ketones (Figure 5.1). We demonstrated the generality of this methodology by applying it to a variety of enantioselective C–C, C–N and C–O bond forming reactions using simple α -branched and unbranched ketones as substrates.

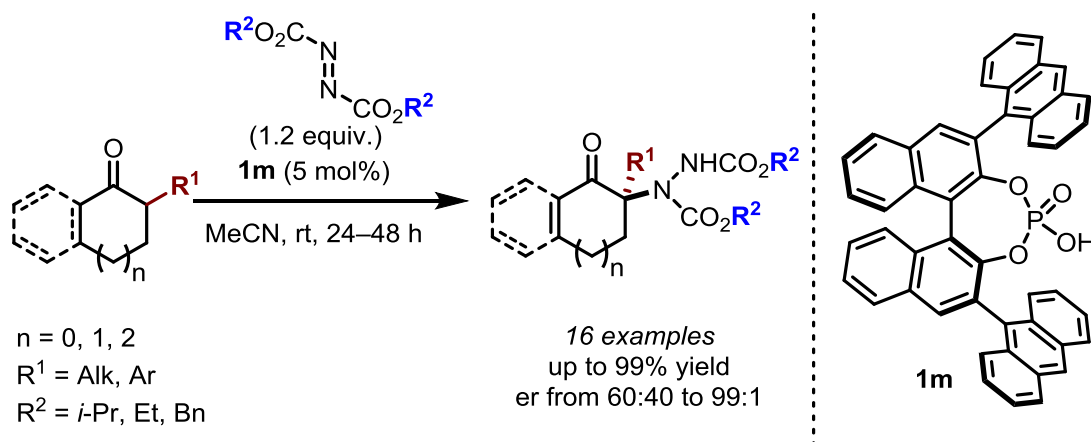


Scheme 5.1: Enantioselective synthesis of Wieland–Miescher ketones *via* Brønsted acid-catalyzed Robinson annulation.

Inspired by the results from Akiyama group, we developed a highly enantioselective Robinson annulation of 1,3-diketones giving derivatives of the synthetically valuable Wieland–Miescher ketone (**25**) in good to excellent yields (up to 99%) and enantioselectivities ($\geq 98:2$ er)

(Scheme 5.1).^[60] Our approach has two key features: First, we used a biphasic water-containing solvent system that assists the initial Michael reaction. Second, we employed the confined spirocyclic biindane-derived phosphoric acid STRIP (**6a**). In contrast to previously reported catalytic systems, our method delivers the targeted products in shorter reaction times (~24 h) even at low catalysts loadings (down to 1 mol% tested) without significant erosion of enantioselectivity or yield. Promising results in the synthesis of the corresponding Hajos-Parrish ketones prompted us to attempt the synthesis of a novel bitetralane-derived backbone, whose catalytic properties are currently being investigated.

Next, we disclosed the direct amination of α -branched cyclic ketones *via enol catalysis* employing diazocarboxylates as electrophilic aminating agents (Scheme 5.2). Using catalytic amounts of a chiral phosphoric acid, the target products could be obtained in excellent yields (up to 99%) and enantioselectivities (up to 99:1 er). Remarkably, cyclohexanone proved to be a suitable substrate and the corresponding product showed no racemization under the optimized reaction conditions emphasizing the selectivity of our method. The obtained products could be further transformed to *N*-carbamate protected α -amino ketones without affecting of enantioselectivity.

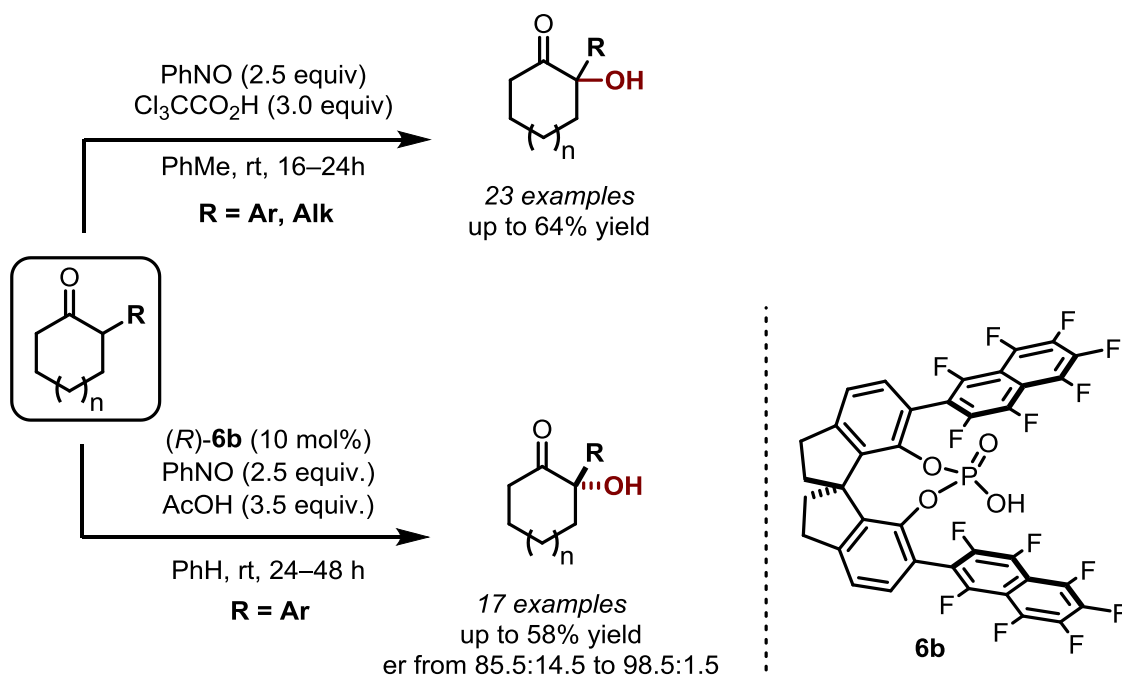


Scheme 5.2: Direct α -amination of α -branched ketones *via enol catalysis*.

Then, we turned our attention towards the direct hydroxylation of cyclic α -branched ketones. Initial attempts employing singlet oxygen as an electrophilic oxygenating agent failed: we only observed the oxidative cleavage of the *in situ* formed enols. The products bearing a

carboxylic acid and ketone moiety, were presumably formed *via* an unstable 1,2-dioxetane intermediate, formed by either stepwise or concerted [2+2] cycloaddition.

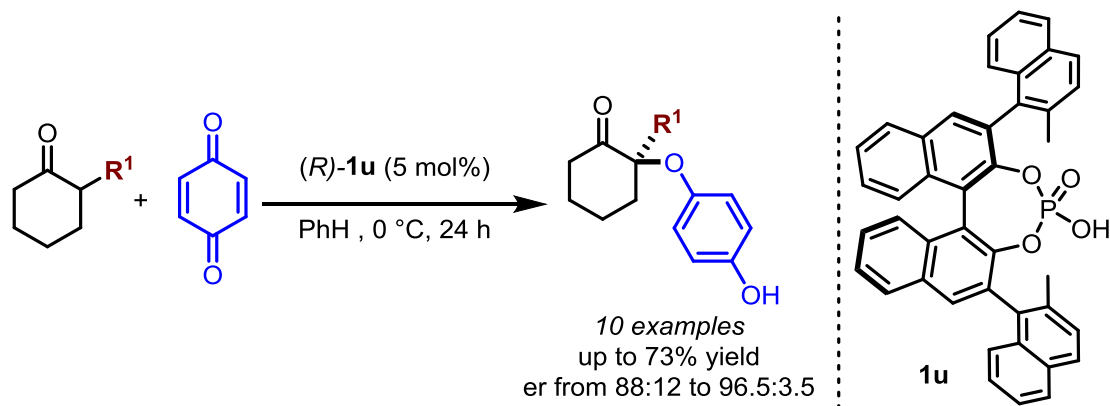
The targeted direct hydroxylation was achieved by using nitrosobenzene as an oxidant. In initial experiments we developed a non-enantioselective variant using trichloroacetic acid (TCA) as a promoter (Scheme 5.3). A variety of cyclic α -branched ketones readily reacted under the optimized reaction conditions giving the target α -hydroxy ketones in good yields (up to 66%). The developed system is scalable, as was demonstrated by preliminary experiments at a 10 mmol scale, and also enabled the reaction of challenging α -alkyl ketones.



Scheme 5.3: Direct α -hydroxylation of α -branched ketones under acidic conditions.

Employing the novel SPINOL-derived phosphoric acid **6b** as a catalysts enabled the first enantioselective direct α -hydroxylation of α -branched cyclic ketones *via enol catalysis*, giving the corresponding products in moderate yields (up to 56%) yet excellent enantioselectivities (up to 98.5:1.5 er) (Scheme 5.3). Initial mechanistic experiments together with computational studies supported the proposed aminoxylation/N–O bond cleavage sequence and gave first insights into the mechanism of phosphoric acid-catalyzed enolizations. Our findings support a mechanism, in which acidic P–OH and basic P=O are involved in the enolization step.

Furthermore, *enol catalysis* enabled an unprecedented direct α -aryloxylation of α -branched cyclic ketones using 1,4-benzoquinones as reaction partners (Scheme 5.4). This transformation was discovered by serendipity and we further developed its asymmetric variant furnishing the corresponding products in good yields (up to 73%) and excellent enantioselectivities (up to 96.5:3.5 er). Initial mechanistic studies suggested, that this transformation proceeds *via* a proton coupled electron transfer (PCET) mechanism.



Scheme 5.4: Direct α -aryloxylation of α -branched ketones *via enol catalysis*.

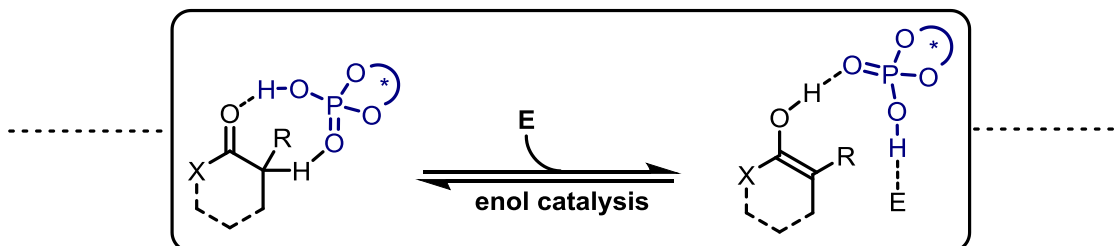
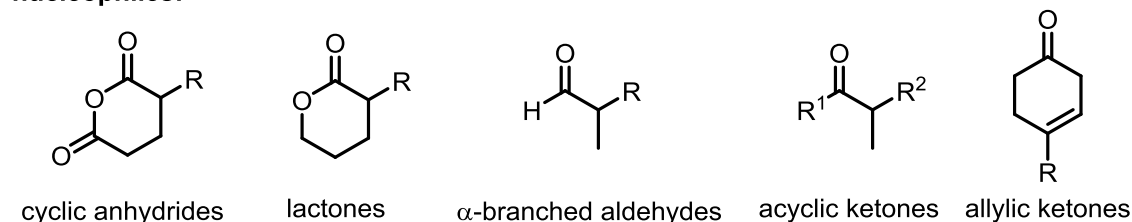
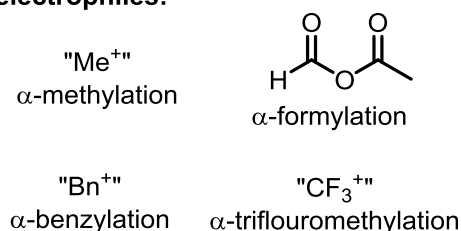
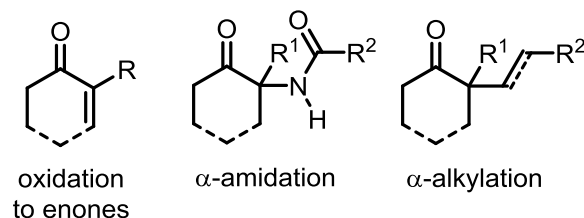
6 Outlook

Although *enol catalysis* proved to be an efficient method for the direct asymmetric α -functionalization of α -branched cyclic ketones several limitations and challenges require further development of the method:

(1) The scope is limited to addition reactions and the feasibility of substitution reactions has yet to be explored. Because of their high synthetic value, direct α -methylation/benzylations and α -trifluoromethylations of carbonyl compounds are highly appealing challenges and catalytic asymmetric variants are scarce.^[196] Additionally, deracemization strategies, either through selective deuteration or in combination with enzymes (*e.g.* lipases) can also be envisioned.

(2) The scope of nucleophiles is currently limited to cyclic ketones and expansion towards linear ketones is highly desired. A major challenge regarding these substrates would be the control of *E/Z*-geometry of the enol, as these diastereomers may lead to opposite enantiomers. In a more distant future, the scope should be expanded towards other carbonyl compounds, such as aldehydes, lactones or cyclic anhydrides. Although the functionalization of α -branched aldehydes using chiral primary amines as catalysts is well-established, a complementary method promises many unexpected transformations. Vinylogous reactions, starting either from enones or allylic ketones, might allow the remote control of distal stereocenters.

(3) We have demonstrated that the combination of chiral phosphoric acids and appropriate oxidants enables the formation of α -carbonyl radicals *via* single-electron oxidation of *in situ* formed enols. Future studies should broaden the scope of such transformations by investigating other reaction partners, such as alkenes or nitriles, and other oxidants. For example, the direct and selective oxidation of ketones to enones would be a particularly important goal since it promises to circumvent the drawbacks of commonly used Saegusa-Ito oxidations. Alternatively, using of electrochemical methods would be an appealing alternative to stoichiometric oxidants.

nucleophiles:**electrophiles:****via oxidation:****Figure 6.1:** Envisioned further transformations using *enol catalysis*.

In order to address some of these challenges, we already preformed a few initial experiments on the Brønsted-acid catalyzed Robinson annulation of α-branched aldehydes (**93**) and methyl vinyl ketone (**28**) (Figure 6.2). This is a challenging reaction for enamine catalysis as a selective reaction of two competing carbonyl groups is involved, although systems utilizing bifunctional catalysts were reported recently.^[197] To our delight, 5 mol% of a chiral phosphoric acid delivered the targeted cyclohexanones (**94**) in good yields and promising enantioselectivities (up to 92:8 er). 2-Aryl substituted aldehydes were preferred substrates, presumably due to the higher *E/Z*-ratio of the formed enol. Unfortunately, cyclohexanone **94e**, which is a key intermediate in the total synthesis of retigeranic acid.^[198] could only be obtained in low yield and compromised selectivity. Nevertheless, these studies suggest that, in principle, it should be possible to extend the scope of *enol catalysis* towards linear carbonyl groups. Further optimization studies are currently ongoing.

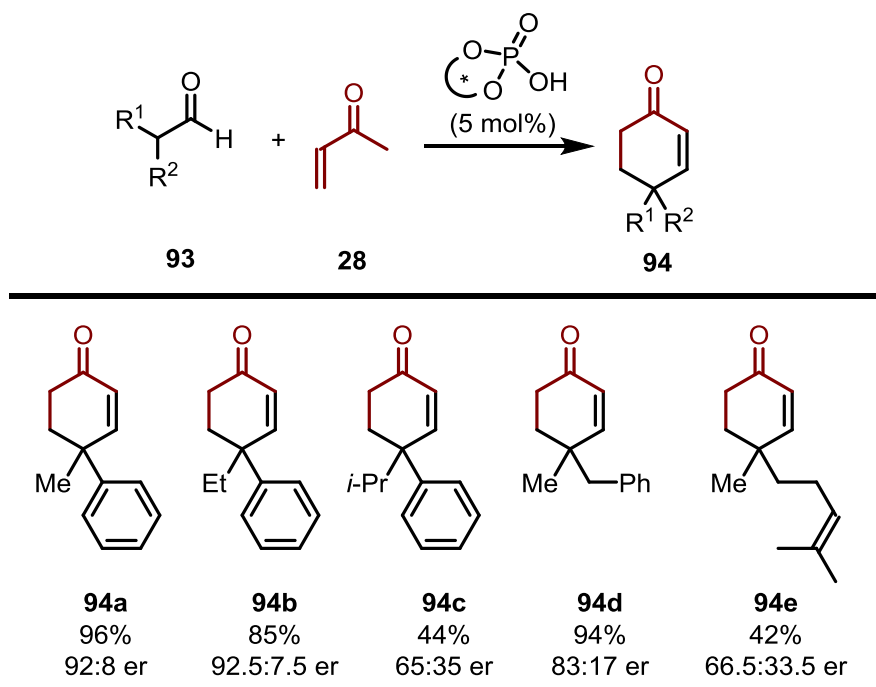


Figure 6.2: Preliminary results on the Brønsted acid-catalyzed Robinson annulation of α -substituted aldehydes. Yields determined by ^1H NMR analysis of the crude reaction mixture using Ph_3CH as internal standard.

7 Experimental Section

7.1 General Experimental Conditions

Chemicals

Chemicals (Abcr, Acros, Aldrich, Gelest, Fluka, Fluorochem, Strem, TCI) were purchased as reagent grade and used without further purification unless indicated otherwise. Nitrosobenzene was purified by recrystallization ($-20\text{ }^{\circ}\text{C}$, ethanol). 1,4-Benzoquinone was recrystallized from boiling hexanes. All ketones were purified by flash column chromatography (hexanes/EtOAc) prior to use.

Solvents

Solvents (CH_2Cl_2 , CHCl_3 , Et_2O , THF, toluene) were dried by distillation from an appropriate drying agent in the technical department of the Max-Planck-Institut für Kohlenforschung and received in Schlenk flasks under argon. The other solvents (acetone, benzene, cyclohexane, chlorobenzene, 1,4-dioxane, DME, DMF, DMSO, EtOAc, EtOH, MeCN, MeOH, MTBE, NMP, *n*-Bu₂O, *n*-hexane, *n*-octane, *n*-pentane, pyridine, α,α,α -trifluorotoluene, xylenes) were purchased from commercial suppliers and dried over molecular sieves.

Inert Gas

Dry argon was purchased from Air Liquide with >99.5% purity.

Glassware

All non-aqueous reactions were performed in oven-dried ($85\text{ }^{\circ}\text{C}$) or flame-dried glassware under Argon. Solvents were removed under reduced pressure at $40\text{ }^{\circ}\text{C}$ using a rotary evaporator and drying under high vacuum (10^{-3} mbar).

Thin Layer Chromatography

Thin-layer chromatography (TLC) was performed using silica gel pre-coated plastic sheets (Polygram SIL G/UV254, 0.2 mm, with fluorescent indicator; Macherey-Nagel), which were visualized with a UV lamp (254 or 366 nm) and phosphomolybdic acid (PMA). PMA stain: PMA (20 g) in EtOH (200 mL). Preparative thin-layer chromatography was performed on silica gel

pre-coated glass plates SIL G-25 UV254 and SIL G-100 UV254 with 0.25 mm and 1.0 mm SiO₂ layers (Macherey-Nagel).

Flash Column Chromatography

Flash column chromatography (FCC) was carried out using Merck silica gel (60 Å, 230–400 mesh, particle size 0.040–0.063 mm) using technical grade solvents. Elution was accelerated using compressed air. All reported yields, unless otherwise specified, refer to spectroscopically and chromatographically pure compounds.

Nomenclature

Nomenclature follows the suggestions proposed by the computer program ChemBioDraw (15.0.0.106) of CBD/Cambridgesoft.

Nuclear Magnetic Resonance Spectroscopy

¹H, ¹³C, ¹⁹F, ³¹P nuclear magnetic resonance (NMR) spectra were recorded on a Bruker AV-500, AV-400 or DPX-300 spectrometer in a suitable deuterated solvent. The solvent employed and respective measuring frequencies are indicated for each experiment. Chemical shifts are reported with tetramethylsilane (TMS) serving as a universal reference of all nuclides and with two or one digits after the comma. The resonance multiplicity is described as s (singlet), d (doublet), t (triplet), q (quadruplet), p (pentet), hept (heptet), m (multiplet), and br (broad). All spectra were recorded at 298 K unless otherwise noted, processed with Bruker TOPSPIN 2.1 or MestReNova 11.0.2 suite of programs, and coupling constants are reported as observed. The residual deuterated solvent signal relative to tetramethylsilane was used as the internal reference in ¹H NMR spectra (e.g. CDCl₃ = 7.26 ppm), and are reported as follows: chemical shift δ in ppm (multiplicity, coupling constant *J* in Hz, number of protons). ¹³C, ¹⁹F, ³¹P NMR spectra were referenced according to Ξ - values (IUPAC recommendations 2008) relative to the internal references set in ¹H NMR spectra (e.g. ¹³C: Me₄Si, ¹⁹F: CCl₃F, ³¹P: H₃PO₄ each 0.00 ppm). All spectra are broadband decoupled unless otherwise noted.

Mass Spectrometry

Electron impact (EI) mass spectrometry (MS) was performed on a Finnigan MAT 8200 (70 eV) or MAT 8400 (70 eV) spectrometer. Electrospray ionization (ESI) mass spectrometry was

conducted on a Bruker ESQ 3000 spectrometer. High resolution mass spectrometry (HRMS) was performed on a Finnigan MAT 95 (EI) or Bruker APEX III FTMS (7T magnet, ESI). The ionization method and mode of detection employed is indicated for the respective experiment and all masses are reported in atomic units per elementary charge (m/z) with an intensity normalized to the most intense peak.

Specific Rotations

Specific rotations were measured with a Rudolph RA Autopol IV Automatic Polarimeter at the indicated temperature with a sodium lamp (sodium D line, $\lambda = 589$ nm). Measurements were performed in an acid resistant 1 mL cell (50 mm length) with concentrations (g/(100 mL)) reported in the corresponding solvent.

High Performance Liquid Chromatography

High performance liquid chromatography (HPLC) was performed on Shimadzu LC-20AD liquid chromatograph (SIL-20AC auto sampler, CMB-20A communication bus module, DGU-20A5 degasser, CTO-20AC column oven, SPD-M20A diode array detector), Shimadzu LC-20AB liquid chromatograph (SIL-20ACHT auto sampler, DGU-20A5 degasser, CTO-20AC column oven, SPD-M20A diode array detector), or Shimadzu LC-20AB liquid chromatograph (reverse phase, SIL-20ACHT auto sampler, CTO-20AC column oven, SPD-M20A diode array detector) using Daicel columns with a chiral stationary phase. All solvents used were HPLC-grade solvents purchased from Sigma-Aldrich. The column employed and respective solvent mixtures are indicated for each experiment.

Preparative High Performance Liquid Chromatography

Preparative high performance liquid chromatography (Prep-HPLC) was performed on a Shimadzu LC-8A/10A liquid chromatograph (FRC-10A fraction collector, SPD-10-AVP diode array detector). All solvents used were HPLC-grade solvents purchased from Sigma-Aldrich. The column employed and respective solvent mixtures are indicated for each experiment.

Gas Chromatography

Gas chromatography (GC) analyses on a chiral stationary phase were performed on HP 6890 and 5890 series instruments (split-mode capillary injection system, flame ionization detector (FID)),

hydrogen carrier gas). All the analyses were conducted in the GC department of the Max-Planck-Institut für Kohlenforschung. The conditions employed are described in detail in the individual experiments.

Gas Chromatography Mass Spectroscopy

Gas chromatography-mass spectrometry (GC-MS) analyses were recorded on an Agilent Technologies 6890N Network GC System equipped with a 5973 Mass Selective Detector, Gerstel Multi-Purpose Sampler MPS2, and a Macherey-Nagel Optima 5 column (30 m length, 0.25 mm i. D.) and an Agilent Technologies 7890A GC System equipped with a 5975C VL MSD mass selective detector, Gerstel Multi-Purpose Sampler MPS2, and a Macherey-Nagel Optima 5 column (30 m length, 0.25 mm i.D.).

Liquid Chromatography Mass Spectrometry

Liquid chromatography-mass spectrometry (LC-MS) was performed on a Shimadzu LC-MS 2020 liquid chromatograph. All solvents used were HPLC-grade solvents purchased from Sigma-Aldrich. The column employed, the respective solvent mixture, and the MS parameters are indicated for each experiment. Elemental Analysis Elemental analysis (EA) was performed on a Vario Elementar EL (CHN) and an Ionchromatograph Metrohm IC 883 (SP).

7.2 General Procedures for Synthesis of 2-Aryl Ketones

Commercially unavailable 2-substituted aryl ketones were synthesized according to the following unoptimized procedures.

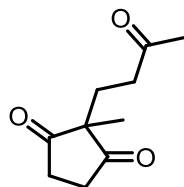
Procedure 1: Under an atmosphere of dry argon, an oven-dried Schlenk flask was charged with Cs_2CO_3 (2.2 equiv.), $\text{Pd}_2(\text{dba})_3$ (0.5 mol%) and Xantphos (1.2 mol%). After evacuating and backfilling the flask with argon three times, dry dioxane (1 M), the corresponding aryl bromide/iodide (1 eq) and cyclohexanone (2 equiv.) were added and the mixture was stirred at 80 °C for 24 h. After cooling down to room temperature, the reaction mixture was diluted with Et_2O and washed with water. The aqueous layer was extracted with Et_2O (3x), the combined organic layers were dried over Na_2SO_4 and the solvent was removed under reduced pressure. The crude product was purified by flash column chromatography (SiO_2 , hexanes/ EtOAc = 100/0 then 10/1). If required, an additional purification with toluene as eluent was performed.

Procedure 2: At –78 °C, *n*-BuLi (2 equiv., 2.5 M in *n*-hexane) was added to a solution of the corresponding aryl bromide (2 equiv.) in THF (0.25 M) and the resulting solution was stirred for 1 h at this temperature. Then cyclohexene oxide (1 equiv.) and $\text{BF}_3 \cdot \text{Et}_2\text{O}$ (1.5 equiv.) were added and the resulting solution stirred for additional 3 h at –78 °C. The reaction mixture was quenched by addition of sat. aq. NaHCO_3 solution, warmed to room temperature and diluted with ethyl acetate. The layers were separated and the organic layer was washed with 2 N NaOH solution and brine. The combined organic layers were dried over Na_2SO_4 and the solvent removed under reduced pressure. The crude product was purified by flash column chromatography (SiO_2 , hexanes/ EtOAc = 100/0 then 10/1). Under an atmosphere of dry argon the obtained product was dissolved in dry DMSO (0.25 M). Dry triethylamine (10 equiv.) and sulfur trioxide-pyridine complex (3 equiv.) were then added and the resulting mixture was stirred overnight at room temperature. The reaction was quenched with water and extracted with CH_2Cl_2 . The combined organic layers were dried over Na_2SO_4 and the solvent was removed under reduced pressure. The crude product was purified by flash column chromatography (SiO_2 , hexanes/ EtOAc = 100/0 then 10/1).

7.3 Brønsted Acid-Catalyzed Asymmetric Robinson Annulations

7.3.1 Characterization of Intermediates

2-Methyl-2-(3-oxobutyl)cyclopentane-1,3-dione (**20a**)^[199]



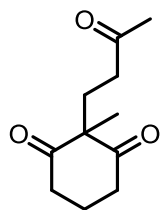
Procedure: To a solution of 2-methyl-cyclopentane-1,3-dione (1.12 g, 10.0 mmol, 1.0 equiv.) in MeCN (15 mL) NEt₃ (5.0 ml, 35.9 mmol, 3.6 equiv.) and Methylvinylketone (0.97 mL, 12.0 mmol, 1.2 equiv.) were added and the resulting mixture was stirred over night at room temperature. The solvents were removed under reduced pressure and the crude product was purified by column chromatography (SiO₂, hexanes/EtOAc = 1/1) to give **20a** as a colorless oil (1.26 g, 69%).

¹H NMR (500 MHz, CDCl₃): δ = 2.87–2.71 (m, 4H), 2.44 (t, J = 7.2 Hz, 2H), 2.09 (s, 3H), 1.88 (t, J = 7.2 Hz, 2H), 1.09 (s, 3H).

¹³C NMR (125 MHz, CDCl₃): δ = 216.0, 208.1, 55.2, 37.5, 34.8, 30.2, 27.9, 19.2.

HRMS (ESIpos): m/z calculated for C₁₀H₁₄NaO₃ [M+Na]⁺: 205.0835, found 205.0835.

2-methyl-2-(3-oxobutyl)cyclohexane-1,3-dione (**21a**)^[199]



Procedure: To a solution of (1.26 g, 10.0 mmol, 1.0 equiv.) in MeCN (15 mL) NEt₃ (5.0 ml, 35.9 mmol, 3.6 equiv) and Methylvinylketone (0.97 mL, 12.0 mmol, 1.2 equiv) were added and the resulting mixture was stirred over night at room temperature. The solvents were removed

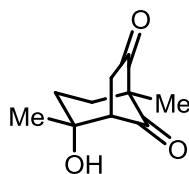
under reduced pressure and the crude product was purified by column chromatography (SiO₂, hexane/EtOAc = 1/1) to give **21a** as a colorless oil (1.91 g, 97%).

¹H NMR (500 MHz, CDCl₃): δ = 2.74–2.59 (m, 4H), 2.33 (t, *J* = 7.6 Hz, 2H), 2.10 (s, 3H), 2.07–1.96 (m, 3H), 1.94–1.85 (m, 1H), 1.23 (s, 3H).

¹³C NMR (125 MHz, CDCl₃): δ = 210.2, 207.7, 64.5, 38.5, 37.9, 30.1, 29.7, 20.2, 17.7.

HRMS (ESIpos): *m/z* calculated for C₁₁H₁₆NaO₃ [M+Na]⁺: 219.0992, found 219.0991.

(1S,2R,5S)-2-hydroxy-2,5-dimethylbicyclo[3.2.1]octane-6,8-dione (47a)



Procedure: A solution of **20a** (200 mg, 1.10 mmol, 1.0 equiv.) and DPP (27.5 mg, 10 mol%) in anhydrous toluene (1 mL) was stirred at room temperature overnight. Filtration of the crude reaction mixture yielded the targeted product as white solid (159 mg, 80%).

¹H NMR (500 MHz, CDCl₃): δ = 2.78 (d, *J* = 7.4 Hz, 1H), 2.63 (dd, *J* = 19.3, 7.4 Hz, 1H), 2.55 (dd, *J* = 19.3 Hz, 0.9 Hz, 1H), 2.13 (ddd, *J* = 12.8, 12.8, 6.7 Hz, 1H), 1.92 (s, 1H), 1.84 (ddd, *J* = 12.8, 5.4, 1.9 Hz, 1H), 1.78–1.65 (m, 2H), 1.40 (s, 3H), 1.07 (s, 3H).

¹³C NMR (125 MHz, CDCl₃): δ = 214.0, 211.2, 80.7, 58.3, 57.5, 42.7, 38.5, 32.3, 28.6, 11.9.

HRMS (ESIpos): *m/z* calculated for C₁₀H₁₄NaO₃ [M+Na]⁺: 205.0835, found 205.0837.

X-Ray data for **47a**:

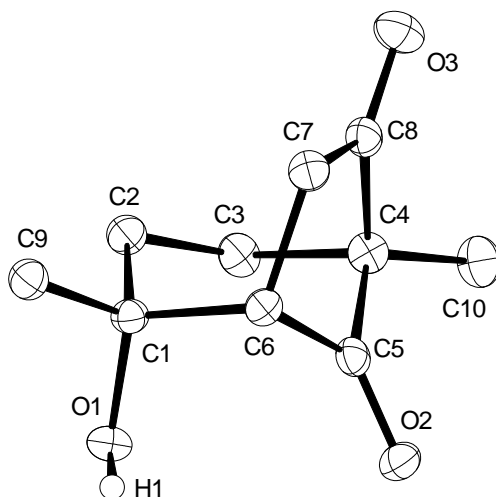


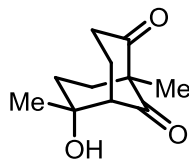
Table 1. Crystal data and structure refinement.

Identification code	9339		
Empirical formula	$C_{10}H_{14}O_3$		
Color	colorless		
Formula weight	182.21 g · mol ⁻¹		
Temperature	100 K		
Wavelength	1.54178 Å		
Crystal system	ORTHORHOMBIC		
Space group	Pna2₁, (no. 33)		
Unit cell dimensions	a = 11.9662(5) Å	α= 90°.	
	b = 10.6428(4) Å	β= 90°.	
	c = 7.0712(3) Å	γ= 90°.	
Volume	900.54(6) Å ³		
Z	4		

Density (calculated)	1.344 Mg · m ⁻³	
Absorption coefficient	0.808 mm ⁻¹	
F(000)	392 e	
Crystal size	0.16 x 0.15 x 0.05 mm ³	
θ range for data collection	5.563 to 67.474°.	
Index ranges	-14 ≤ h ≤ 14, -12 ≤ k ≤ 12, -8 ≤ l ≤ 7	
Reflections collected	19694	
Independent reflections	1551 [R _{int} = 0.0393]	
Reflections with I>2σ(I)	1497	
Completeness to θ = 67.474°	99.8 %	
Absorption correction	Gaussian	
Max. and min. transmission	0.96 and 0.89	
Refinement method	Full-matrix least-squares on F ²	
Data / restraints / parameters	1551 / 1 / 125	
Goodness-of-fit on F ²	1.090	
Final R indices [I>2σ(I)]	R ₁ = 0.0296	wR ² = 0.0711
R indices (all data)	R ₁ = 0.0310	wR ² = 0.0720
Absolute structure parameter	-0.12(9)	
Extinction coefficient	0.0069(10)	
Largest diff. peak and hole	0.170 and -0.139 e · Å ⁻³	

Table 2. Bond lengths [Å] and angles [°].

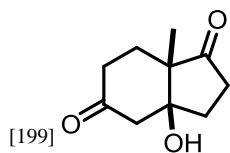
O(2)-C(5)	1.218(3)	O(3)-C(8)	1.223(3)
O(1)-C(1)	1.442(3)	C(8)-C(4)	1.516(3)
C(8)-C(7)	1.511(3)	C(10)-C(4)	1.510(3)
C(6)-C(7)	1.538(3)	C(6)-C(5)	1.507(3)
C(6)-C(1)	1.567(3)	C(2)-C(1)	1.526(3)
C(2)-C(3)	1.528(3)	C(4)-C(5)	1.515(3)
C(4)-C(3)	1.569(3)	C(1)-C(9)	1.516(3)
O(3)-C(8)-C(4)	124.7(2)	O(3)-C(8)-C(7)	125.3(2)
C(7)-C(8)-C(4)	109.99(18)	C(7)-C(6)-C(1)	112.76(17)
C(5)-C(6)-C(7)	102.02(17)	C(5)-C(6)-C(1)	105.67(17)
C(1)-C(2)-C(3)	113.71(17)	C(8)-C(4)-C(3)	105.63(17)
C(10)-C(4)-C(8)	115.93(19)	C(10)-C(4)-C(5)	117.10(19)
C(10)-C(4)-C(3)	112.6(2)	C(5)-C(4)-C(8)	101.18(18)
C(5)-C(4)-C(3)	102.75(17)	C(8)-C(7)-C(6)	104.27(18)
O(2)-C(5)-C(6)	127.5(2)	O(2)-C(5)-C(4)	126.2(2)
C(6)-C(5)-C(4)	106.20(18)	O(1)-C(1)-C(6)	108.68(16)
O(1)-C(1)-C(2)	105.88(18)	O(1)-C(1)-C(9)	109.81(18)
C(2)-C(1)-C(6)	108.77(18)	C(9)-C(1)-C(6)	111.36(18)
C(9)-C(1)-C(2)	112.14(18)	C(2)-C(3)-C(4)	113.08(19)

(1S,5S,6R)-6-hydroxy-1,6-dimethylbicyclo[3.3.1]nonane-2,9-dione (47b)

Procedure: The product was obtained as a side product.

¹H NMR (500 MHz, CDCl₃): δ = 2.70–2.64 (m, 1H), 2.61–2.52 (m, 1H), 2.45–2.35 (m, 1H), 2.13–2.00 (m, 3H), 1.93–1.72 (m, 3H), 1.69–1.61 (m, 1H), 1.38 (s, 3H), 1.17 (s, 3H).

¹³C NMR (125 MHz, CDCl₃): δ = 211.7, 211.4, 79.0, 62.6, 57.1, 38.3, 37.1, 32.6, 28.1, 19.4, 16.6.

(±)-(3aS,7aS)-3a-hydroxy-7a-methylhexahydro-1H-indene-1,5(4H)-dione (22a)

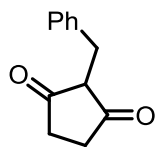
Procedure: To a stirred solution of **20a** (200 mg, 1.09 mmol, 1.0 equiv.) in DMF (1 mL) DL-proline (6.3 mg, 5 mol%) was added and the resulting solution was stirred overnight at room temperature. The reaction was quenched by addition of brine and extracted with EtOAc (3x). The combined organic layers were washed with brine, dried over Na₂SO₄, the solvent was removed under reduced pressure and the crude product was purified by column chromatography (SiO₂, hexane/EtOAc = 1/1) to give **22a** as a colorless oil (120 mg, 60%).

¹H NMR (500 MHz, CDCl₃): δ = 2.63 (d, *J* = 0.8 Hz, 2H), 2.61–2.52 (m, 1H), 2.48–2.40 (m, 2H), 2.33 (dt, *J* = 14.5, 4.9, 0.8 Hz, 1H), 2.08–1.97 (m, 2H), 1.79 (ddd, *J* = 14.3, 11.6, 5.1 Hz, 1H), 1.75–1.67 (m, 2H), 1.27 (s, 3H).

7.3.2 Synthesis of 2-Substituted 1,3-Diketones

General procedure: To a solution of the aldehyde (3 equiv.), HEH (1 equiv.) and 1,3-cyclohexandione/1,3-cyclopentandione (1 equiv) in CH_2Cl_2 (2 mL/mmol) was added DL-Proline (0.2 equiv.). The resulting mixture was stirred over night at room temperature and subsequently directly purified by column chromatography (SiO_2 , hexanes/EtOAc = 3/1 \rightarrow 1/1).

2-benzylcyclopentane-1,3-dione (**26b**)



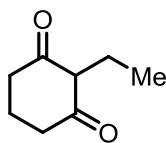
The general procedure was performed on a 2 mmols scale, giving **26b** as a colorless solid; 206 mg (54%).

^1H NMR (300 MHz, $\text{MeOH}-\text{D}_4$): δ = 7.22–7.14 (m, 4H), 7.13–7.07 (m, 1H), 4.91 (s, 1H), 3.42 (s, 2H), 2.51 (s, 4H).

^{13}C NMR (125 MHz, CDCl_3): δ = 141.5, 129.4, 129.1, 126.7, 118.1, 31.4, 27.6.

HRMS (APPIpos): m/z calculated for $\text{C}_{12}\text{H}_{13}\text{O}_2$ $[\text{M}+\text{H}]^+$: 189.0910, found 189.0911.

2-ethylcyclohexane-1,3-dione (**27b**)

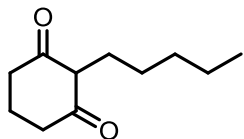


The general procedure was performed on a 5 mmols scale, giving **27b** as a colorless solid; 260 mg (37%).

^1H NMR (300 MHz, $\text{MeOH}-\text{D}_4$): δ = 4.58 (s_{br} , 1H), 2.39 (t, J = 6.3 Hz, 4H), 2.25 (q, J = 7.4 Hz, 2H), 1.93 (p, J = 6.4 Hz, 2H), 0.90 (t, J = 7.4 Hz, 3H).

HRMS (ESIpos): m/z calculated for $C_8H_{13}O_2$ $[M+H]^+$: 141.0910, found 141.0910.

2-pentylcyclohexane-1,3-dione (27c)

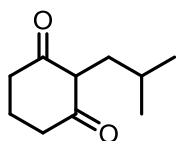


The general procedure was performed on a 3 mmols scale, giving **27c** as a colorless solid; 418 mg (76%).

1H NMR (500 MHz, DMSO- D_6) δ = 10.20 (s, 1H), 2.29 (s, 4H), 2.11 (t, J = 7.2 Hz, 2H), 1.81 (p, J = 6.4 Hz, 2H), 1.36–1.14 (m, 6H), 0.84 (t, J = 7.1 Hz, 3H).

^{13}C NMR (126 MHz, DMSO) δ = 114.8, 31.4, 28.0, 22.1, 21.4, 20.6, 14.0. (Carbonyls are not visible due to rapid tautomerization)

2-isobutylcyclohexane-1,3-dione (27d)

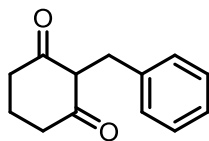


The general procedure was performed on a 3 mmols scale, giving **27d** as a colorless solid; 129 mg (38%).

1H NMR (500 MHz, DMSO- D_6) δ = 10.16 (s, 1H), 2.47–2.12 (m, 4H), 2.03 (d, J = 7.3 Hz, 2H), 1.82 (p, J = 6.4 Hz, 2H), 1.66 (dp, J = 13.6, 6.8 Hz, 1H), 0.78 (d, J = 6.7 Hz, 6H).

^{13}C NMR (126 MHz, DMSO) δ = 114.3, 30.8, 27.6, 22.9, 21.1. (Carbonyls are not visible due to rapid tautomerization)

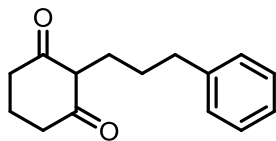
HRMS (ESIpos): m/z calculated for $C_{10}H_{16}O_2Na$ $[M+Na]^+$: 191.1042, found 191.1042.

2-benzylcyclohexane-1,3-dione (27e)

The general procedure was performed on a 3 mmols scale, giving **27e** as a colorless solid; 347 mg (57%).

¹H NMR (500 MHz, DMSO- D_6) δ = 10.56 (s, 1H), 7.30–7.02 (m, 5H), 3.47 (s, 2H), 2.36 (s, 4H), 1.85 (p, J = 6.4 Hz, 2H).

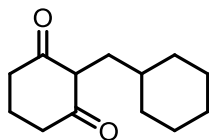
HRMS (ESIpos): m/z calculated for $C_{13}H_{14}O_2Na$ $[M+Na]^+$: 225.0886, found 225.0884.

2-(3-phenylpropyl)cyclohexane-1,3-dione (27f)

The general procedure was performed on a 3 mmols scale, giving **27f** as a colorless solid; 556 mg (80%).

¹H NMR (500 MHz, DMSO- D_6) δ = 10.28 (s, 1H), 7.34–7.08 (m, 5H), 2.56–2.49 (m, 2H), 2.43 (m, 2H), 2.19 (q, J = 9.2, 8.4 Hz, 4H), 1.81 (p, J = 6.5 Hz, 2H), 1.58–1.50 (m, 2H).

¹³C NMR (126 MHz, DMSO) δ = 143.0, 128.6, 128.6, 125.9, 115.0, 35.9, 30.7, 22.0, 21.1. (Carbonyls are not visible due to rapid tautomerization)

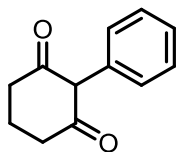
2-(cyclohexylmethyl)cyclohexane-1,3-dione (27g)

The general procedure was performed on a 5 mmols scale, giving **27g** as a colorless solid; 517 mg (50%).

¹H NMR (300 MHz, MeOH-D₄) δ = 4.58 (s, 1H), 2.40 (t, J = 6.4 Hz, 4H), 2.13 (d, J = 7.2 Hz, 2H), 2.03–1.87 (m, 2H), 1.75–1.53 (m, 2H), 1.39 (ddp, J = 10.9, 7.0, 3.5 Hz, 1H), 1.25–1.08 (m, 3H), 0.91 (dt, J = 15.3, 11.0 Hz, 2H).

HRMS (ESIpos): m/z calculated for C₁₃H₂₁O₂ [M+H]⁺: 209.1536, found 209.1537.

2-phenylcyclohexane-1,3-dione (**28**)



To a solution of CuI (61.3 mg, 0.32 mmol, 10 mol%), L-proline (78.2 mg, 0.68 mmol, 20 mol%), K₂CO₃ (1.97 g, 14.3 mmol, 4.0 equiv.) and 1,3-cyclohexandione (1.20 g, 10.7 mmol, 3.0 equiv) in DMSO (17 mL) was added iodobenzene (0.40 mL, 3.57 mmol, 1.0 equiv). The resulting reaction mixture was heated to 90 °C for 48 h. After cooling down to room temperature the mixture was poured into aq. HCl (1 M). The phases were separated, and the organic layer was extracted with EtOAc (3 × 20 mL). The combined organic extracts were washed with brine and dried over Na₂SO₄, filtered and the solvent was removed in vacuo. Purification by FCC (SiO₂, hexanes/EtOAc) afforded **28** as a yellow solid (344 mg, 51%)

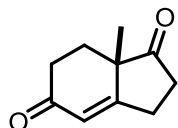
¹H NMR (300 MHz, CDCl₃) δ = 7.54–7.41 (m, 2H), 7.40–7.32 (m, 1H), 7.23–7.16 (m, qH), 2.63 (t, J = 6.3 Hz, 2H), 2.51 (dd, J = 7.4, 6.0 Hz, 2H), 2.17–2.03 (m, 2H).

7.3.3 Characterization of Products

General procedure: 1,3-Diketone (0.2 mmol, 1.0 equiv.), BHT (66.1 mg, 0.3 mmol, 1.5 equiv.) and STRIP **6a** (7.2 mg, 5 mol%) were placed in a headspace vial and *n*-heptane (1.8 mL), H₂O (0.2 mL) and methylvinyl ketone (49 μ L, 0.6 mmol, 3.0 equiv) were added. The vial was closed

and the resulting mixture was stirred at 100 °C for 24 h at 1000 rpm. After cooling down to room temperature the crude mixture was directly purified by FCC (hexanes/EtOAc = 2/1).

7a-methyl-2,3,7,7a-tetrahydro-1H-indene-1,5(6H)-dione (24a)

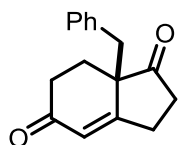


¹H NMR (500 MHz, CDCl₃): δ = 6.00–5.95 (m, 1H), 2.96 (dddd, J = 17.0, 11.1, 10.0, 2.5 Hz, 1H), 2.84–2.71 (m, 2H), 2.59–2.38 (m, 3H), 2.11 (ddd, J = 13.5, 5.2, 2.2 Hz, 1H), 1.86 (td, J = 13.8, 5.4 Hz, 1H), 1.32 (s, 3H).

HRMS (ESIpos): m/z calculated for C₁₀H₁₂NaO₂ [M+Na]⁺: 187.0729, found 187.0729.

HPLC (Chiralcel OD-3, *n*-heptane/*i*PrOH = 95/5, flowrate: 1.0 ml/min, λ = 240 nm): t_{major} = 15.67 min, t_{minor} = 16.99 min.

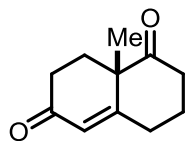
(R)-7a-benzyl-2,3,7,7a-tetrahydro-1H-indene-1,5(6H)-dione (24b)



¹H NMR (500 MHz, CDCl₃): δ = 7.31–7.24 (m, 3H), 7.12–7.05 (m, 2H), 6.06 (d, J = 2.4 Hz, 1H), 3.11–3.01 (m, 2H), 2.60–2.39 (m, 3H), 2.34–2.18 (m, 3H), 2.09–1.98 (m, 1H), 1.84 (td, J = 13.8, 5.7 Hz, 1H).

¹³C NMR (125 MHz, CDCl₃): δ = 217.8, 198.2, 169.4, 135.7, 129.7, 128.8, 128.5, 127.7, 125.3, 54.3, 42.5, 37.1, 33.0, 29.4, 28.3.

HPLC (Chiralcel OD-3, *n*-heptane/*i*PrOH = 95/5, flowrate: 1.0 ml/min, λ = 240 nm): t_{minor} = 8.58 min, t_{major} = 8.59 min.

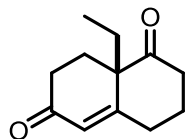
(S)-8a-methyl-3,4,8,8a-tetrahydronaphthalene-1,6(2H,7H) (25a)

Appearance: yellowish solid; 31.1 mg (87%); 98:2 er.

¹H NMR (500 MHz, CDCl₃): δ = 5.86 (d, J = 1.8 Hz, 1H), 2.77–2.67 (m, 2H), 2.54–2.42 (m, 4H), 2.19–2.09 (m, 3H), 1.71 (tq, J = 13.3, 4.3 Hz, 1H), 1.45 (s, 3H).

¹³C NMR (125 MHz, CDCl₃): δ = 211.2, 198.4, 165.9, 126.9, 50.8, 37.8, 33.8, 31.9, 29.8, 23.4, 23.1.

HPLC (Chiralcel OD-3, *n*-heptane/*i*PrOH = 95/5, flowrate: 1.0 ml/min, λ = 240 nm): t_{minor} = 11.6 min, t_{major} = 12.9 min.

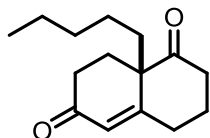
(S)-8a-ethyl-3,4,8,8a-tetrahydronaphthalene-1,6(2H,7H)-dione (25b)

Appearance: yellowish solid; 31.6 mg (82%); 98.5:1.5 er.

¹H NMR (500 MHz, CDCl₃): δ = 5.86 (d, J = 1.2 Hz, 1H), 2.84–2.74 (m, 1H), 2.65 (dt, J = 15.0, 6.2 Hz, 1H), 2.52–2.30 (m, 4H), 2.27–2.20 (m, 1H), 2.19–2.11 (m, 1H), 2.06–1.96 (m, 2H), 1.88–1.78 (m, 1H), 1.75–1.63 (m, 1H), 0.85 (t, J = 7.3 Hz, 3H).

HRMS (ESIpos): m/z calculated for C₁₂H₁₆NaO₂ [M+Na]⁺: 215.1042, found 215.1043.

HPLC (Chiralpak AD-3, *n*-heptane/*i*PrOH = 95/5, flowrate: 1.0 ml/min, λ = 240 nm): t_{major} = 7.6 min, t_{minor} = 8.4 min.

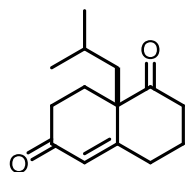
(S)-8a-pentyl-3,4,8,8a-tetrahydronaphthalene-1,6(2H,7H)-dione (25c)

Appearance: yellowish solid; 37.2 mg (79%); 99:1 er.

¹H NMR (500 MHz, CDCl₃): δ = 5.86 (d, J = 1.8 Hz, 1H), 2.80 (dddd, J = 15.3, 13.6, 5.2, 2.0 Hz, 1H), 2.65 (td, J = 14.5, 6.1 Hz, 1H), 2.52–2.30 (m, 4H), 2.23 (ddd, J = 14.5, 4.9, 4.0 Hz, 1H), 2.19–2.10 (m, 1H), 2.04 (dddd, J = 14.6, 13.2, 5.4, 1.1 Hz, 1H), 1.96–1.85 (m, 1H), 1.81–1.63 (m, 1H), 1.37–1.18 (m, 5H), 1.06 (dddd, J = 13.9, 12.5, 6.4, 3.5 Hz, 1H), 0.87 (t, J = 7.0 Hz, 3H).

¹³C NMR (125 MHz, CDCl₃): δ = 210.3, 198.5, 166.3, 126.2, 55.1, 38.5, 35.6, 33.7, 32.1, 32.1, 25.7, 24.2, 23.7, 22.5, 14.1.

HPLC (Chiralpak AD-3, *n*-heptane/*i*PrOH = 95/5, flowrate: 1.0 ml/min, λ = 240 nm): t_{major} = 6.17 min, t_{minor} = 7.14 min.

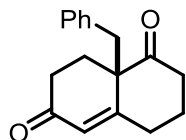
(R)-8a-isobutyl-3,4,8,8a-tetrahydronaphthalene-1,6(2H,7H)-dione (25d)

Appearance: yellowish solid; 27.2 mg (62%); 98.5:1.5 er.

¹H NMR (500 MHz, CDCl₃): δ = 5.77 (d, J = 1.8 Hz, 1H), 2.80–2.67 (m, 2H), 2.47–2.36 (m, 3H), 2.34–2.20 (m, 2H), 2.13–1.98 (m, 2H), 1.85 (ddd, J = 14.6, 6.5, 1.3 Hz, 1H), 1.72–1.56 (m, 3H), 0.88 (d, J = 6.6 Hz, 3H), 0.79 (d, J = 6.6 Hz, 3H).

¹³C NMR (125 MHz, CDCl₃): δ = 211.1, 198.4, 166.9, 126.2, 55.4, 44.5, 38.9, 33.8, 32.1, 26.0, 25.0, 24.9, 24.2, 23.9.

HPLC (Chiralcel OD-3, *n*-heptane/*i*PrOH = 95/5, flowrate: 1.0 ml/min, λ = 240 nm): t_{major} = 6.7 min, t_{minor} = 8.5 min.

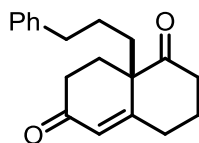
(R)-8a-benzyl-3,4,8,8a-tetrahydronaphthalene-1,6(2H,7H)-dione (25e)

Appearance: yellowish solid; 50.6 mg (99%); 98.5:1.5 er.

¹H NMR (500 MHz, CDCl₃): δ = 7.32–7.23 (m, 3H), 7.09–7.03 (m, 2H), 6.03–5.85 (m, 1H), 3.18 (q, J = 13.7 Hz, 2H), 2.75–2.61 (m, 2H), 2.60–2.48 (m, 2H), 2.43–2.23 (m, 2H), 2.22–1.96 (m, 3H), 1.71 (qt, J = 13.2, 4.4 Hz, 1H).

¹³C NMR (125 MHz, CDCl₃): δ = 210.1, 198.3, 165.1, 135.7, 129.7, 128.8, 127.7, 127.2, 56.0, 42.9, 39.3, 33.7, 32.8, 27.7, 23.2.

HPLC (Chiralpak AD-3, *n*-heptane/*i*PrOH = 95/5, flowrate: 1.0 ml/min, λ = 240 nm): t_{major} = 9.3 min, t_{minor} = 10.4 min.

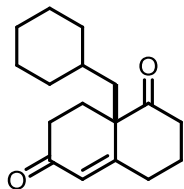
(S)-8a-(3-phenylpropyl)-3,4,8,8a-tetrahydronaphthalene-1,6(2H,7H)-dione (25f)

Appearance: orange oil; 37.7 mg (67%); 98.5:1.5 er.

¹H NMR (500 MHz, CDCl₃): δ = 7.31–7.25 (m, 3H), 7.22–7.17 (m, 1H), 7.15–7.10 (m, 2H), 5.83 (d, J = 1.8 Hz, 1H), 2.69 (dddd, J = 15.4, 13.6, 5.3, 1.9 Hz, 1H), 2.61 (td, J = 7.2, 2.4 Hz, 2H), 2.53–2.33 (m, 4H), 2.30–2.16 (m, 2H), 2.13–1.99 (m, 2H), 1.90 (dddd, J = 13.8, 12.3, 4.5, 1.1 Hz, 1H), 1.77 (ddd, J = 14.2, 12.5, 4.6 Hz, 1H), 1.71–1.59 (m, 2H), 1.46–1.36 (m, 1H).

¹³C NMR (125 MHz, CDCl₃): δ = 210.2, 198.4, 166.0, 141.1, 128.6, 128.5, 126.4, 126.3, 54.9, 38.4, 35.7, 34.4, 33.6, 32.0, 25.9, 25.7, 23.6.

HPLC (Chiralpak AD-3, *n*-heptane/*i*PrOH = 95/5, flowrate: 1.0 ml/min, λ = 240 nm): t_{major} = 17.12 min, t_{minor} = 21.22 min.

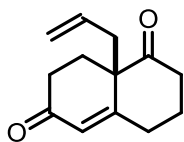
(R)-8a-(cyclohexylmethyl)-3,4,8,8a-tetrahydronaphthalene-1,6(2H,7H)-dione (25g)

Appearance: orange oil; 45.8 mg (88%); 98:2 er.

¹H NMR (500 MHz, CDCl₃): δ = 5.83 (d, J = 1.7 Hz, 1H), 2.80 (tdd, J = 14.3, 12.0, 5.7 Hz, 2H), 2.55–2.41 (m, 3H), 2.39–2.34 (m, 1H), 2.33–2.25 (m, 1H), 2.16 (dtq, J = 13.8, 5.4, 2.5 Hz, 1H), 2.10–2.01 (m, 1H), 1.89 (ddd, J = 14.9, 6.2, 1.4 Hz, 1H), 1.77–1.48 (m, 7H), 1.37–0.82 (m, 6H).

HRMS (ESIpos): m/z calculated for C₁₇H₂₄O₂Na [M+Na]⁺: 283.1668; found 283.1670.

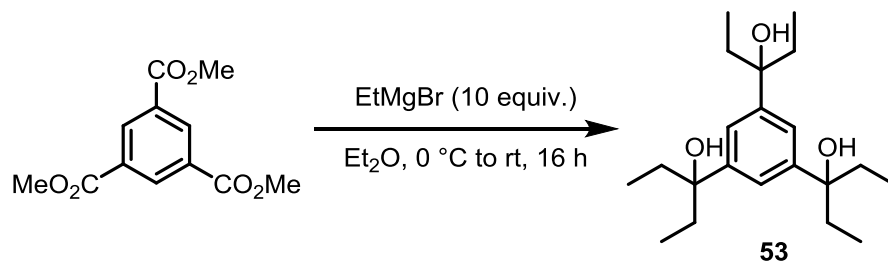
HPLC (Chiralcel OD-3, *n*-heptane/*i*PrOH = 95/5, flowrate: 1.0 ml/min, λ = 240 nm): t_{major} = 5.97 min, t_{minor} = 7.66 min.

(R)-8a-allyl-3,4,8,8a-tetrahydronaphthalene-1,6(2H,7H)-dione (25h)

Appearance: orange oil; 25.0 mg (74%); 99:1 er.

¹H NMR (500 MHz, CDCl₃): δ = 5.89 (d, J = 1.9 Hz, 1H), 5.59 (ddt, J = 16.1, 10.8, 7.4 Hz, 1H), 5.18–5.06 (m, 2H), 2.83–2.72 (m, 1H), 2.70–2.61 (m, 2H), 2.58–2.47 (m, 3H), 2.44–2.39 (m, 2H), 2.28–2.12 (m, 2H), 2.06 (dddd, J = 14.4, 10.3, 8.7, 1.2 Hz, 1H), 1.71 (qt, J = 13.6, 4.3 Hz, 1H).

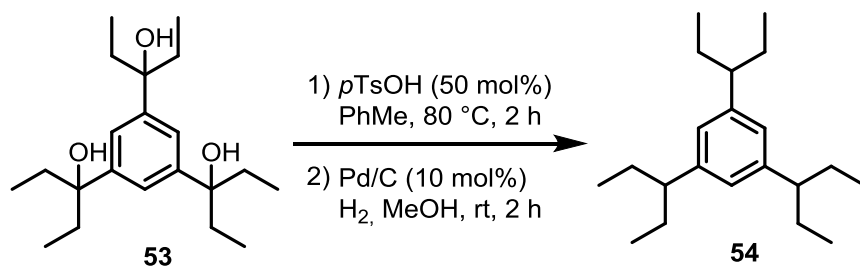
7.3.4 Modifications and Synthesis of Novel Backbones:

3,3',3''-(benzene-1,3,5-triyl)tris(pentan-3-ol) (**53**)

Procedure: A solution of trimethyl-1,3,5-benzotricarboxylate (1.50 g, 5.94 mmol, 1.0 equiv.) in diethylether (5 mL) was cooled to 0 °C and ethylmagnesium bromide (60 mL, 1 M in Et₂O, 60 mmol, 10.0 equiv) was added dropwise. The reaction was allowed to warm up overnight, quenched with aq. NH₄Cl solution and the layers were separated. The aqueous layer was extracted with Et₂O, dried over Na₂SO₄ and the solvent removed under reduced pressure. Recrystallization in hexanes gave the target product as colorless solid (1.50 g, 75%).

¹H NMR (500 MHz, CDCl₃): δ = 1.96–1.71 (m, 12H), 1.64 (s, 3H), 0.73 (t, *J* = 7.4 Hz, 18H).

HRMS (ESIpos): *m/z* calculated for C₂₁H₃₆O₃Na [M+Na]⁺: 359.2557; found 359.2559.

1,3,5-tri(pentan-3-yl)benzene (**54**)

Procedure: A solution of **53** (790 mg, 2.35 mmol, 1.0 equiv) and *p*-toluenesulfonic acid monohydrate (223 mg, 1.17 mmol, 0.5 equiv) in anhydrous toluene (20 mL) was stirred for 2 h at 80 °C. After cooling down to room temperature the crude reaction mixture was filtered through a pad of silica (hexanes as eluent) and the solvent was removed under reduced pressure. The obtained clear oil was dissolved in MeOH (24 mL), Pd/C (250 mg, 10%) was added and the resulting mixture was put under an atmosphere of hydrogen. After stirring at room

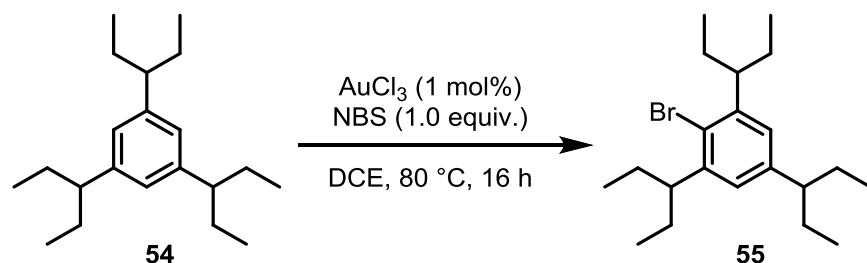
temperature for 2 h the reaction mixture was filtered through a pad of celite, the solvent was removed giving **54** as clear oil (535 mg, 79%).

^1H NMR (500 MHz, CDCl_3): δ = 6.66 (s, 3H), 2.24 (tt, J = 9.0, 5.4 Hz, 3H), 1.66 (dqd, J = 12.8, 7.4, 5.4 Hz, 6H), 1.57–1.46 (m, 6H), 0.74 (t, J = 7.3 Hz, 18H).

^{13}C NMR (125 MHz, CDCl_3): δ = 145.0, 124.9, 49.8, 29.5, 12.3.

HRMS (EI): m/z calculated for $\text{C}_{21}\text{H}_{36}$ $[\text{M}]^+$: 288.2817; found 288.2817.

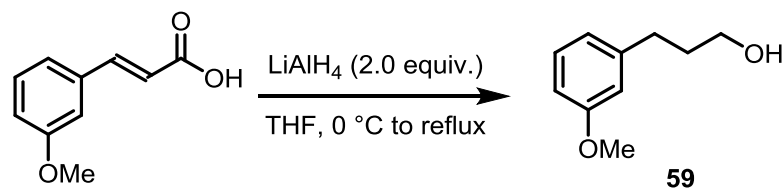
1,3,5-tri(pentan-3-yl)benzene (**55**)



Procedure: Under an atmosphere of dry argon a solution of **54** (740 mg, 2.56 mmol, 1.0 equiv.), AuCl_3 (8 mg, 1 mol%) and freshly recrystallized NBS (461 mg, 2.59 mmol, 1.0 equiv.) in anhydrous DCE (13 mL) was stirred at 80 °C for 16 h. After cooling down to room temperature the crude reaction mixture was filtered through a pad of silica (hexanes as eluent) giving **55** as clear oil (897 mg, 95%).

^1H NMR (500 MHz, CDCl_3): δ = 6.72 (s, 2H), 3.29–3.17 (m, 2H), 2.24 (td, J = 9.3, 4.8 Hz, 2H), 1.74–1.60 (m, 6H), 1.60–1.44 (m, 6H), 0.76 (dt, J = 25.0, 7.4 Hz, 18H).

3-(3-methoxyphenyl)propan-1-ol (**59**)



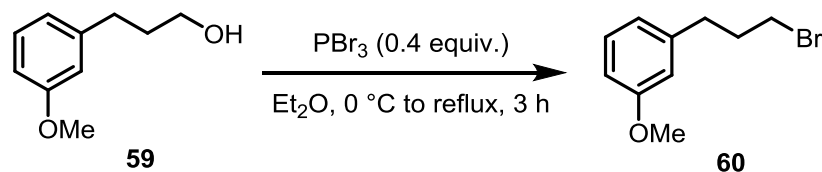
Procedure: To 3-methoxycinnamic acid (5.00 g, 28.1 mmol, 1.0 equiv) in THF (20 mL) lithium aluminum hydride (57.0 mL, 1 M in THF, 57.0 mmol, 2.0 equiv) was added at 0 °C. After completion the resulting solution was refluxed overnight. After cooling down to 0 °C sat. aq. NH₄Cl solution was added until the no hydrogen formation was visible, additional Et₂O was added if necessary. After addition of an excess of MgSO₄ the resulting heterogeneous mixture was filtered, excessively washed with Et₂O and the solvent removed under reduced pressure to give **59** (4.60 g, 98%) as colorless oil.

¹H NMR (500 MHz, CDCl₃): δ = 7.23–7.17 (m, 1H), 6.84–6.70 (m, 3H), 3.80 (s, 3H), 3.68 (t, *J* = 6.4 Hz, 2H), 2.73–2.64 (m, 2H), 1.95–1.85 (m, 2H), 1.32 (s, 1H).

¹³C NMR (125 MHz, CDCl₃): δ = 159.8, 143.6, 129.6, 129.5, 121.0, 114.4, 111.3, 62.5, 55.3, 34.3, 32.3.

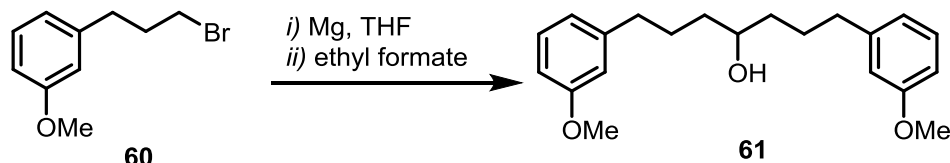
HRMS (ESIpos): *m/z* calculated for C₁₀H₁₄O₂Na [M+Na]⁺: 189.0886; found 189.0886.

1-(3-bromopropyl)-3-methoxybenzene (**60**)



Procedure: To a stirred solution of **59** (4.60 g, 27.7 mmol, 1.0 equiv) in Et₂O (30 mL) was added PBr₃ (1.04 mL, 11.1 mmol, 0.4 equiv.) at 0 °C. The mixture was heated to reflux for 3 h and then quenched with water and partitioned between Et₂O and aqueous NaHCO₃. The organic extract was dried over Na₂SO₄ and concentrated. The residue was purified by FCC (SiO₂, pentane/MTBE = 3/1) to give **60** (4.20 g, 66% yield) as colorless oil.

¹H NMR (500 MHz, CDCl₃): δ = 7.24–7.18 (m, 1H), 6.83–6.73 (m, 3H), 3.81 (s, 3H), 3.40 (t, *J* = 6.6 Hz, 2H), 2.76 (t, *J* = 7.3 Hz, 2H), 2.21–2.12 (m, 2H).

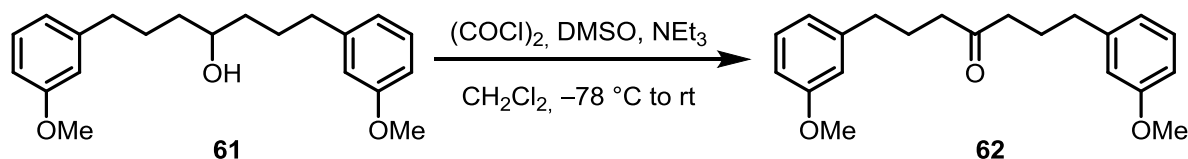
1,7-bis(3-methoxyphenyl)heptan-4-ol (61)^[179]

Procedure: A solution of ethyl formate (1.67 mL, 20.8 mmol, 1.0 equiv.) was added slowly to a stirred solution of 3-(3-methoxyphenyl)-propylmagnesium bromide in THF (120 mL), which was prepared from **60** (10.0 g, 43.6 mmol, 2.1 equiv.) and magnesium (1.26 g, 52.0 mmol, 2.5 equiv.), at 0 °C. Upon completion the reaction mixture was stirred at room temperature overnight. The reaction mixture was cooled to 0°C by and sat. aq. NH₄Cl solution was added. The organic layer was extracted with ethyl acetate (3x100 mL) and dried over Na₂SO₄. The solvent was removed under reduced pressure, and the residue was purified by FCC (SiO₂, hexanes/EtOAc = 3/1) to afford **61** (5.05 g, 74%) as colorless oil.

¹H NMR (500 MHz, CDCl₃): δ = 7.22–7.15 (m, 2H), 6.82–6.68 (m, 6H), 3.80 (d, *J* = 0.7 Hz, 6H), 3.68–3.59 (m, 2H), 2.69–2.52 (m, 4H), 1.85–1.70 (m, 2H), 1.70–1.58 (m, 2H), 1.56–1.39 (m, 4H), 1.30–1.23 (m, 1H).

¹³C NMR (125 MHz, CDCl₃): δ = 159.8, 144.2, 129.4, 121.0, 114.3, 111.1, 71.8, 55.3, 37.2, 36.1, 27.5.

HRMS (ESIpos): *m/z* calculated for C₂₁H₂₈O₃Na [M+Na]⁺: 351.1931; found 351.1930.

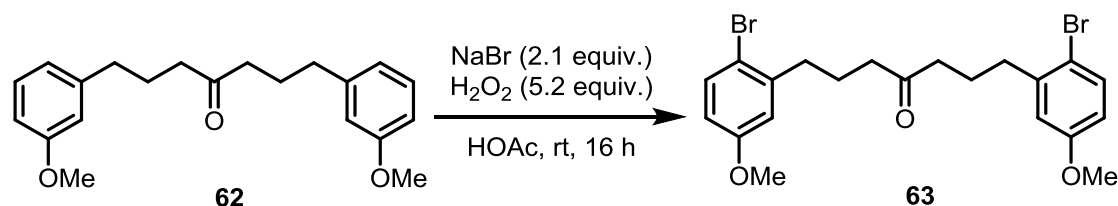
1,7-bis(3-methoxyphenyl)heptan-4-one (62)^[179]

Procedure: Dimethyl sulfoxide (1.5 mL, 21.1 mmol, 1.3 equiv.) was added dropwise to a stirred solution of oxalyl chloride (1.6 mL, 18.6 mmol, 1.1 equiv.) in CH₂Cl₂ (60 mL) at -78°C. The mixture was stirred for 15 min, and a solution of **61** (5.5 g, 16.7 mmol, 1.0 equiv) in CH₂Cl₂ (15 mL) was added dropwise. The resulting mixture was stirred for an additional 30 min at -78 °C, triethylamine (9.3 mL, 66.7 mmol, 4.0 equiv.) was added dropwise. After stirring at -78 °C for

additional 15 min and at room temperature for 2 h, water was added, the organic layer was separated and the aqueous layer was extracted with CH_2Cl_2 . The combined organic layers were washed successively with aq. HCl (1 M), saturated Na_2CO_3 and dried over Na_2SO_4 . After removal of the solvent, the residue was purified by FCC (SiO_2 , hexanes/EtOAc = 10/1) affording **62** (5.26 g, 96%) as colorless oil.

^1H NMR (500 MHz, CDCl_3): δ = 7.19 (t, J = 7.8 Hz, 2H), 6.78–6.69 (m, 6H), 3.79 (s, 6H), 2.58 (t, J = 7.5 Hz, 4H), 2.38 (t, J = 7.4 Hz, 4H), 1.93–1.85 (m, 4H).

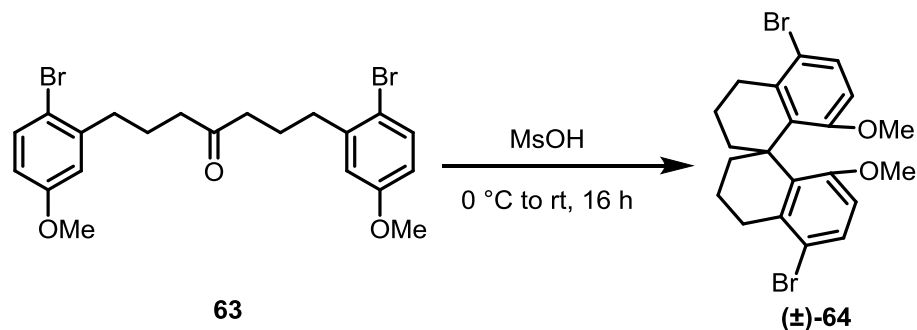
1,7-bis(2-bromo-5-methoxyphenyl)heptan-4-one (63**)** ^[179]



Procedure: A solution of H_2O_2 (aq., 35%, 2.15 mL, 22.2 mmol, 5.2 equiv.) in acetic acid (10 mL) was added dropwise to a stirred solution of **62** (1.38 g, 4.22 mmol, 1.0 equiv.) and NaBr (0.91 g, 8.88 mmol, 2.1 equiv.) in acetic acid (20 mL). The mixture was stirred at room temperature overnight. The solvent was removed under reduced pressure and the residue was dissolved in CH_2Cl_2 , washed with water and dried over Na_2SO_4 . The solvent was removed under reduced pressure and the crude product was purified by FCC (SiO_2 , hexanes/EtOAc = 10/1) affording **63** (1.95 g, 95%) as a white solid.

^1H NMR (500 MHz, CDCl_3): δ = 7.40 (d, J = 8.7 Hz, 2H), 6.76 (d, J = 3.0 Hz, 2H), 6.63 (dd, J = 8.7, 3.1 Hz, 2H), 3.77 (s, 6H), 2.73–2.66 (m, 2H), 2.47 (t, J = 7.3 Hz, 2H), 1.95–1.86 (m, 2H).

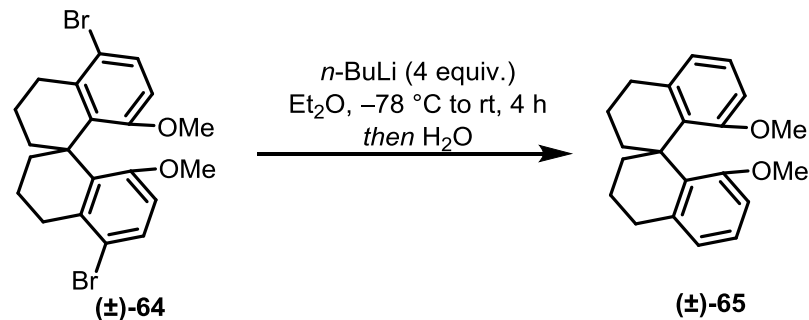
^{13}C NMR (125 MHz, CDCl_3): δ = 210.3, 159.1, 142.1, 133.4, 116.2, 115.0, 113.5, 55.6, 42.0, 35.6, 24.0.

5,5'-dibromo-8,8'-dimethoxy-3,3',4,4'-tetrahydro-2H,2'H-1,1'-spirobi[naphthalene] ((±)-64)^[179]

Procedure: **63** (1.9 g, 3.92 mmol, 1.0 equiv.) was added to MsOH (15 mL) at 0 °C. The reaction was allowed to warm up overnight. After, the crude reaction mixture was poured onto ice and extracted with CH₂Cl₂. The combined organic layers were dried of Na₂SO₄ and the solvent was removed under reduced pressure. The crude product was purified by FCC (hexanes/CH₂Cl₂ = 9/1) giving (±)-**64** (1.50 g, 82%) as a white solid.

¹H NMR (500 MHz, CDCl₃): δ = 7.28 (d, *J* = 8.7 Hz, 2H), 6.47 (dd, *J* = 8.8, 0.8 Hz, 2H), 3.17 (s, 6H), 3.07 (ddt, *J* = 16.9, 4.3, 2.0 Hz, 1H), 2.60 (dddd, *J* = 16.8, 12.8, 5.5, 0.9 Hz, 2H), 2.10–2.02 (m, 2H), 1.96 (dtd, *J* = 13.2, 3.4, 1.8 Hz, 2H), 1.90–1.72 (m, 4H).

¹³C NMR (125 MHz, CDCl₃): δ = 156.3, 138.6, 138.3, 129.3, 116.6, 112.2, 55.6, 40.38, 33.8, 31.6, 19.9.

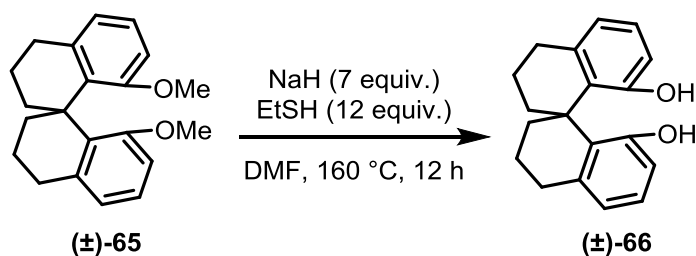
8,8'-dimethoxy-3,3',4,4'-tetrahydro-2H,2'H-1,1'-spirobi[naphthalene] ((±)-65)^[179]

Procedure: To a stirred solution of (±)-**64** (1.49 g, 3.20 mmol 1.0 equiv.) in anhydrous Et₂O (25 mL) was slowly added *n*-BuLi (2.3 M in hexane, 7 mL, 16.1 mmol, 5 equiv.) at –78 °C. After

stirring the reaction at 0 °C for 2 h it was further warmed to room temperature and stirred for further 2 h. Afterwards the reaction mixture was quenched by slow addition of H₂O (5 mL) at 0 °C. The solvent was removed under reduced pressure and the residue was extracted with CH₂Cl₂. The combined organic layers were washed with water and dried over Na₂SO₄. After removal of the solvent, the residue was purified by FCC (SiO₂, CH₂Cl₂/hexanes = 9/1) affording (±)-**65** (900 mg, 91%) as a white solid.

¹H NMR (500 MHz, CDCl₃): δ = 6.98 (t, *J* = 7.8 Hz, 2H), 6.72 (dq, *J* = 7.6, 1.0 Hz, 2H), 6.58 (dt, *J* = 8.0, 1.1 Hz, 2H), 3.20 (s, 6H), 2.92–2.74 (m, 4H), 2.13–2.05 (m, 2H), 1.98 (dtd, *J* = 13.3, 3.3, 2.0 Hz, 2H), 1.80 (tq, *J* = 11.2, 3.2 Hz, 4H).

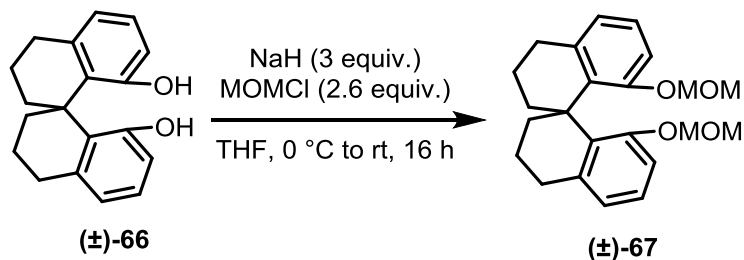
3,3',4,4'-tetrahydro-2H,2'H-1,1'-spirobi[naphthalene]-8,8'-diol ((±)-66**)** ^[179]



Procedure: To a suspension of NaH (467 mg, 11.7 mmol, 12.0 equiv.) in DMF (8 mL), EtSH (0.5 mL, 6.81 mmol, 7.0 equiv.) was added slowly while cooling by an ice bath. (±)-**65** (300 mg, 0.97 mmol, 1.0 equiv.) was added in one portion, and the mixture was stirred at 160 °C for 12 h. The reaction was quenched by adding aq. HCl (1 M) at 0 °C, extracted with EtOAc and dried over Na₂SO₄. After removal of the solvent, the residue was purified by FCC (hexanes/CH₂Cl₂ = 9/1) giving (±)-**66** (213 mg, 78%) as a white solid.

¹H NMR (500 MHz, CDCl₃): δ = 7.02 (t, *J* = 7.8 Hz, 2H), 6.71 (dq, *J* = 7.5, 1.0 Hz, 2H), 6.58 (dd, *J* = 8.0, 1.3 Hz, 2H), 4.75 (s, 2H), 2.87–2.81 (m, 4H), 2.13–2.07 (m, 2H), 2.00–1.91 (m, 2H), 1.81 (ttd, *J* = 13.8, 5.9, 2.7 Hz, 4H).

HRMS (ESIpos): *m/z* calculated for C₁₉H₂₀O₂Na [M+Na]⁺: 303.1355; found 303.1353.

8,8'-bis(methoxymethoxy)-3,3',4,4'-tetrahydro-2H,2'H-1,1'-spirobi[naphthalene] ((±)-67)

Procedure: To a suspension of NaH (86 mg, 2.15 mmol, 3.0 equiv.) in THF (1.4 mL), (±)-66 (200 mg, 0.71 mmol, 1.0 equiv.) in THF (0.6 mL) was added at 0 °C. The reaction was stirred at 0 °C for another 6 h, then chloro(methoxy)methane (0.15 mL, 1.88 mmol, 2.6 equiv.) was added. After stirring at room temperature overnight, the reaction was quenched by addition of water and diluted with EtOAc. The layers were separated and the aqueous layer was extracted with EtOAc. The combined organic layers were dried over Na₂SO₄, the solvent removed under reduced pressure and the crude product was purified by FCC (hexanes/CH₂Cl₂ = 9/1) to give (±)-67 (221 mg, 84%) as a white solid.

¹H NMR (500 MHz, CDCl₃): δ = 6.94 (t, *J* = 7.8 Hz, 2H), 6.79–6.74 (m, 4H), 4.58 (d, *J* = 6.8 Hz, 2H), 4.46 (d, *J* = 6.8 Hz, 2H), 2.95 (s, 6H), 2.90–2.76 (m, 4H), 2.21–2.11 (m, 2H), 2.07–1.98 (m, 2H), 1.88–1.77 (m, 4H).

¹³C NMR (125 MHz, CDCl₃): δ = 154.8, 139.6, 136.1, 125.5, 122.3, 112.8, 94.1, 55.3, 39.5, 35.1, 31.3, 20.4.

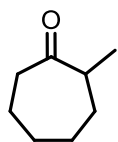
HRMS (EI): *m/z* calculated for C₂₃H₂₈O₄ [M]⁺: 368.1988; found 368.1986.

7.4 Catalytic Asymmetric α -Amination of α -Branched Ketones *via* Enol Catalysis

7.4.1 Synthesis of Starting Materials

General procedure for the α -alkylation of cyclic ketones: At $-78\text{ }^{\circ}\text{C}$ a solution of the ketone in dry THF (30 mL) was added dropwise within 15 min to a stirred solution of LiHMDS (1.0 M in THF). The resulting mixture was stirred at $-78\text{ }^{\circ}\text{C}$ for 30 min, then MeI (1.3 equiv.) was added and stirring was continued for a further 30 min. The reaction mixture was allowed to warm to room temperature overnight and quenched by dropwise addition of sat. aq. NH_4Cl . The aqueous layer was extracted with Et_2O ; the combined organic extracts were dried over Na_2SO_4 and concentrated under reduced pressure. Purification of the resulting residue by FCC (SiO_2 , pentane/ Et_2O) affords the targeted α -alkyl ketones.

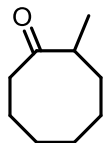
2-methylcycloheptan-1-one



The general procedure was performed using cycloheptanone (950 μL , 8.00 mmol) giving the desired product (613 mg, 61%) as clear oil.

^1H NMR (500 MHz, CDCl_3): δ = 2.64–2.54 (m, 1H), 2.52–2.43 (m, 2H), 1.91–1.75 (m, 3H), 1.68–1.55 (m, 1H), 1.48–1.30 (m, 3H), 1.06 (dd, J = 7.0, 1.1 Hz, 3H).

2-methylcyclooctan-1-one



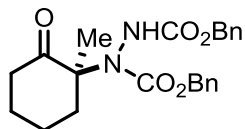
The general procedure was performed using cyclooctanone (1.00 g, 7.92 mmol) giving the desired product (426 mg, 38%) as clear oil.

^1H NMR (500 MHz, CDCl_3): δ = 2.60 (dq, J = 10.2, 6.8, 3.4 Hz, 1H), 2.47–2.35 (m, 2H), 1.98–1.84 (m, 2H), 1.78 (ddtd, J = 10.3, 8.6, 6.5, 4.3 Hz, 1H), 1.72–1.36 (m, 6H), 1.27–1.15 (m, 1H), 1.05 (d, J = 6.8 Hz, 3H).

7.4.2 Characterization of Products

General Procedure for the direct amination: To a solution of the catalyst **1m** (5 mol%) and the ketone **68** (0.2 mmol) in acetonitrile (0.1 mL) azodicarboxylate **32c** (74.6 mg, 0.24 mmol) was added and the resulting mixture was stirred at r.t. for 24h. The crude reaction mixture was directly purified by silica-gel column chromatography ($\text{CH}_2\text{Cl}_2/\text{MTBE}$ = 0% \rightarrow 5%)..

Dibenzyl (*S*)-1-(1-methyl-2-oxocyclohexyl)hydrazine-1,2-dicarboxylate (**69a**)



$[\alpha]_{\text{D}}^{25}$: +5.6 (c 1.0, CH_2Cl_2 , 99:1 er.).

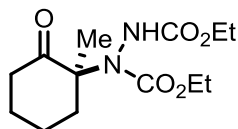
^1H NMR (500 MHz, CDCl_3): δ = 7.42–7.01 (m, 10H), 6.82–6.44 (m, 1H), 5.19–4.79 (m, 4H), 2.74–1.08 (m, 11 H).

^{13}C NMR (125 MHz, CDCl_3): δ = 209.1, 156.7, 155.8, 135.6, 135.5, 128.6, 128.5, 128.4, 128.3, 128.1, 70.7, 69.7, 68.6, 68.3, 68.0, 67.8, 39.6, 39.0, 38.3, 29.7, 29.2, 26.5, 21.8, 21.8, 21.0, 19.8.

HRMS (ESIpos): m/z calculated for $\text{C}_{23}\text{H}_{26}\text{N}_2\text{NaO}_5$ $[\text{M}+\text{Na}]^+$: 433.1734; found 433.1732.

HPLC (Chiralcel OJ-3R, $\text{MeCN}/\text{H}_2\text{O}$ = 50:50, flowrate: 1.0 ml/min, λ = 220 nm): $t_{\text{r}(\text{major})}$ = 15.2 min, $t_{\text{r}(\text{minor})}$ = 12.2 min.

Diethyl (*S*)-1-(1-methyl-2-oxocyclohexyl)hydrazine-1,2-dicarboxylate (**69b**)



$[\alpha]_D^{25}$: +15.2 (c 1.0, CH₂Cl₂, 99:1 er).

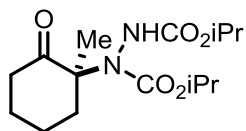
¹H NMR (500 MHz, CDCl₃): δ = 6.64–6.31 (m, 1H), 4.27–4.08 (m, 4H), 2.85–2.26 (m, 3H), 2.0–1.13 (m, 14H).

¹³C NMR (125 MHz, CDCl₃): δ = 209.4, 156.9, 156.0, 69.5, 62.9, 62.3, 62.2, 39.7, 38.9, 38.3, 29.7, 29.3, 26.6, 21.9, 21.7, 21.0, 19.8, 14.5, 14.3.

HRMS (ESIpos): m/z calculated for C₁₃H₂₂N₂NaO₅ [M+Na]⁺: 309.1421, found 309.1422.

GC (Hydrodex- γ -TBDAC; G/624, 150°C iso, 0.5 bar H₂): $t_{r(\text{major})}$ = 103.3 min, $t_{r(\text{minor})}$ = 106.3 min.

Diisopropyl (S)-1-(1-methyl-2-oxocyclohexyl)hydrazine-1,2-dicarboxylate (69c)



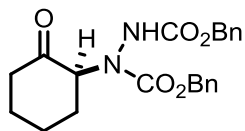
$[\alpha]_D^{25}$: +21.2 (c 1.0, CH₂Cl₂, 98:2 er).

¹H NMR (500 MHz, CDCl₃): δ = 6.58–6.17 (m, 1H), 5.07–4.77 (m, 2H), 2.96–2.34 (m, 3H), 2.08–1.39 (m, 5H), 1.38–1.12 (m, 15H).

¹³C NMR (125 MHz, CDCl₃): δ = 209.7, 156.6, 155.5, 70.1, 69.9, 39.8, 38.9, 38.4, 22.0, 21.9, 21.8, 20.8, 19.8.

HRMS (ESIpos): m/z calculated for C₁₅H₂₆N₂NaO₅ [M+Na]⁺: 337.1734, found 337.1734.

HPLC (Chiralcel OJ-3R, MeCN/H₂O = 30:70, flowrate: 0.8 mL/min, λ = 210 nm): $t_{r(\text{major})}$ = 10.3 min, $t_{r(\text{minor})}$ = 8.9 min.

Dibenzyl (S)-1-(2-oxocyclohexyl)hydrazine-1,2-dicarboxylate (69d)^[200]

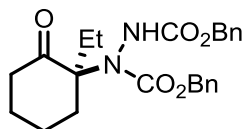
$[\alpha]_D^{25}$: +18.8 (c 1.0, CH₂Cl₂, 89:11 er).

¹H NMR (500 MHz, CDCl₃): δ = 7.40–7.20 (m, 10H), 6.95–6.55 (m, 1H), 5.25–5.00 (m, 4H), 4.98–4.61 (m, 1H), 2.55–2.15 (m, 3H), 2.13–1.47 (m, 5H).

¹³C NMR (125 MHz, CDCl₃): δ = 207.7, 156.7, 156.2, 135.8, 135.7, 128.6, 128.5, 128.4, 128.1, 127.7, 127.5, 68.6, 68.3, 67.7, 67.6, 66.9, 65.8, 65.4, 41.3, 41.1, 30.9, 30.7, 30.5, 29.7, 26.7, 26.6, 24.3.

HRMS (ESIpos): m/z calculated for C₂₂H₂₄N₂NaO₅ [M+Na]⁺: 419.1577, found: 419.1576.

HPLC (Chiralcel OD-H, *n*Hept/*i*PrOH = 90/10, flowrate: 1.0 mL/min, λ = 220 nm):
 $t_{r(\text{major})}$ = 16.9 min, $t_{r(\text{minor})}$ = 26.8 min.

Dibenzyl (S)-1-(1-ethyl-2-oxocyclohexyl)hydrazine-1,2-dicarboxylate (69e)

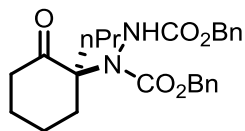
$[\alpha]_D^{25}$: +0.4 (c 1.0, CH₂Cl₂, 98:2 er).

¹H NMR (500 MHz, CDCl₃): δ = 7.39–7.21 (m, 10H), 6.59–6.20 (m, 1H), 5.25–4.95 (m, 4H), 2.92–2.13 (m, 3H), 2.07–1.32 (m, 7H), 1.09–0.70 (m, 3H).

¹³C NMR (125 MHz, CDCl₃): δ = 208.1, 156.9, 156.3, 135.6, 128.8, 128.7, 128.5, 128.4, 72.6, 68.7, 68.1, 40.4, 39.6, 37.6, 29.2, 27.8, 27.3, 22.1, 21.7, 8.8.

HRMS (ESIpos): m/z calculated for C₂₄H₂₈N₂NaO₅ [M+Na]⁺: 447.1890, found: 447.1889.

HPLC (Chiralcel OJ-3R, MeCN/H₂O = 50:50, flowrate: 1.0 mL/min, λ = 220 nm):
 $t_{r(\text{major})}$ = 17.5 min, $t_{r(\text{minor})}$ = 15.7 min.

Dibenzyl (S)-1-(2-oxo-1-propylcyclohexyl)hydrazine-1,2-dicarboxylate (69f)

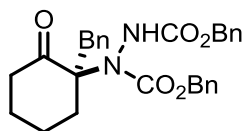
$[\alpha]_D^{25}$: +2.8 (c 1.0, CH₂Cl₂, 98:2 er).

$^1\text{H NMR}$ (500 MHz, CDCl₃): δ = 7.41–7.20 (m, 10H), 6.59–6.15 (m, 1H), 5.26–4.97 (m, 4H), 2.95–2.13 (m, 3H), 2.06–1.35 (m, 8H), 1.21–0.76 (m, 4H).

$^{13}\text{C NMR}$ (125 MHz, CDCl₃): δ = 208.1, 156.7, 156.1, 135.5, 128.6, 128.6, 128.5, 128.4, 128.2, 73.5, 72.3, 68.5, 67.9, 39.8, 39.3, 37.7, 37.0, 36.5, 29.0, 27.7, 21.9, 21.5, 17.3, 17.1, 14.7, 14.5.

HRMS (ESIpos): m/z calcd for C₂₅H₃₀N₂NaO₅ [M+Na]⁺: 461.2047, found: 461.2046.

HPLC (Chiralpak ID-3, *n*Hept/*i*PrOH = 90:10, flowrate: 1.0 mL/min, λ = 220 nm):
 $t_{\text{r(major)}}$ = 18.1 min, $t_{\text{r(minor)}}$ = 31.5 min.

Dibenzyl (R)-1-(1-benzyl-2-oxocyclohexyl)hydrazine-1,2-dicarboxylate (69g)

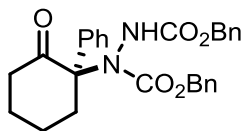
$[\alpha]_D^{25}$: +114.8 (c 1.0, CH₂Cl₂, 99:1 er).

$^1\text{H NMR}$ (500 MHz, CDCl₃): δ = 7.54–6.67 (m, 15H), 5.25–4.69 (m, 5H), 3.46–1.11 (m, 10H).

$^{13}\text{C NMR}$ (125 MHz, CDCl₃): δ = 209.6, 156.0, 137.0, 136.7, 135.6, 130.1, 129.1, 128.9, 128.8, 128.6, 128.5, 128.2, 128.1, 127.6, 127.3, 127.1, 127.0, 126.8, 72.1, 68.6, 68.3, 67.7, 39.0, 38.5, 38.1, 38.0, 37.7, 36.9, 30.0, 29.7, 20.3, 20.0.

HRMS (ESIpos): m/z calculated for C₂₉H₃₀N₂NaO₅ [M+Na]⁺: 509.2047, found: 509.2045.

HPLC (Chiralcel OJ-3R, MeCN/H₂O = 60:40, flowrate: 1.0 mL/min, λ = 220 nm):
 $t_{\text{r(major)}}$ = 8.3 min, $t_{\text{r(minor)}}$ = 9.8 min.

Dibenzyl (R)-1-(2-oxo-1-phenylcyclohexyl)hydrazine-1,2-dicarboxylate (69h)

$[\alpha]_D^{25}$: -44.0 (c 1.0, CH_2Cl_2 , 97:3 er).

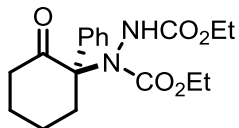
$^1\text{H NMR}$ (500 MHz, CDCl_3): δ = 7.53–7.06 (m, 15H), 6.24–5.87 (m, 1H), 5.23–4.89 (m, 4H), 3.10–2.46 (m, 3H), 2.38–2.20 (m, 1H), 2.11–1.41 (m, 4H).

$^{13}\text{C NMR}$ (125 MHz, CDCl_3): δ = 205.6, 156.1, 155.7, 135.6, 135.1, 128.8, 128.7, 128.6, 128.5, 128.3, 128.2, 128.1, 127.9, 76.4, 68.4, 67.4, 40.7, 27.9, 27.0, 26.5, 22.3.

HRMS (ESIpos): m/z calculated for $\text{C}_{28}\text{H}_{28}\text{N}_2\text{NaO}_5$ $[\text{M}+\text{Na}]^+$: 495.1890, found: 495.1892.

HPLC (Chiralpak IC-3R, $\text{MeOH}/\text{H}_2\text{O}$ = 80:20, flowrate: 1.0 mL/min, λ = 220 nm):

$t_{\text{r(major)}}$ = 10.2 min, $t_{\text{r(minor)}}$ = 8.4 min.

Diethyl (R)-1-(2-oxo-1-phenylcyclohexyl)hydrazine-1,2-dicarboxylate (69i)

$[\alpha]_D^{25}$: -36.4 (c 1.0, CH_2Cl_2 , 97.5:2.5 er).

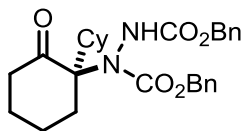
$^1\text{H NMR}$ (500 MHz, CDCl_3): δ = 7.45–7.05 (m, 5H), 6.16–5.84 (m, 1H), 4.30–3.81 (m, 4H), 2.97–2.37 (m, 3H), 2.33–2.18 (m, 1H), 2.05–1.47 (m, 4H), 1.30–0.90 (m, 6H).

$^{13}\text{C NMR}$ (125 MHz, CDCl_3): δ = 205.8, 205.5, 156.6, 156.3, 155.9, 135.5, 135.1, 128.7, 128.4, 128.0, 127.8, 76.1, 62.9, 62.4, 62.1, 62.0, 61.8, 40.9, 40.6, 35.2, 34.8, 29.7, 28.0, 26.7, 22.2, 21.8, 14.4, 14.3, 14.1.

HRMS (ESIpos): m/z calculated for $\text{C}_{18}\text{H}_{24}\text{N}_2\text{NaO}_5$ $[\text{M}+\text{Na}]^+$: 371.1577, found: 371.1578.

HPLC (Chiralcel OD-3, $n\text{Hept}/i\text{PrOH}$ = 95:5, flowrate: 1.0 mL/min, λ = 220 nm):

$t_{\text{r(major)}}$ = 9.1 min, $t_{\text{r(minor)}}$ = 7.3 min.

Dibenzyl (R)-1-(2-oxo-[1,1'-bi(cyclohexan)]-1-yl)hydrazine-1,2-dicarboxylate (69j)

$[\alpha]_D^{25}$: +23.2 (c 1.0, CH₂Cl₂, 99:1 er).

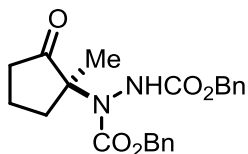
¹H NMR (500 MHz, CDCl₃): δ = 7.50–7.11 (m, 10H), 6.66–6.18 (m, 1H), 5.29–4.94 (m, 4H), 3.17–2.44 (m, 1H), 2.42–1.87 (m, 4H), 1.83–0.98 (m, 12H), 0.96–0.78 (m, 2H);

¹³C NMR (125 MHz, CDCl₃): δ = 208.1, 156.4, 135.4, 128.7, 128.6, 128.5, 128.4, 128.3, 74.3, 69.6, 68.8, 68.4, 68.0, 65.3, 43.7, 42.6, 42.2, 40.6, 40.0, 39.4, 34.6, 33.9, 29.6, 29.1, 29.0, 28.2, 27.2, 26.8, 26.7, 26.4, 26.3, 20.5, 20.3.

HRMS (ESIpos): m/z calculated for C₂₈H₃₄N₂NaO₅ [M+Na]⁺: 501.2360, found: 501.2357;

HPLC (Chiralcel OJ-3R, MeCN/H₂O = 60:40, flowrate: 1.0 mL/min, λ = 220 nm):

$t_{r(\text{major})}$ = 9.7 min, $t_{r(\text{minor})}$ = 8.8 min.

Dibenzyl (S)-1-(1-methyl-2-oxocyclopentyl)hydrazine-1,2-dicarboxylate (69k)

$[\alpha]_D^{25}$: +31.6 (c 1.0, CH₂Cl₂, 95.5:4.5 er).

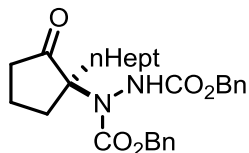
¹H NMR (500 MHz, CDCl₃): δ = 7.40–7.19 (m, 10H), 6.83–6.45 (m, 1H), 5.24–4.93 (m, 4H), 2.79–1.52 (m, 6H), 1.30–1.13 (m, 3H).

¹³C NMR (125 MHz, CDCl₃): δ = 216.1, 215.6, 156.5, 156.3, 154.8, 154.5, 135.7, 135.6, 128.6, 128.5, 128.4, 128.3, 128.2, 128.1, 127.8, 68.1, 68.0, 67.8, 34.8, 20.2, 19.9, 18.3.

HRMS (ESIpos): m/z calculated for C₂₂H₂₄N₂NaO₅ [M+Na]⁺: 419.1577, found: 419.1575.

HPLC (Chiralcel OD-3, *n*Hept/*i*PrOH = 95:5, flowrate: 1.0 mL/min, λ = 220 nm):
 $t_{r(\text{major})}$ = 17.7 min, $t_{r(\text{minor})}$ = 9.4 min.

Dibenzyl (S)-1-(1-heptyl-2-oxocyclopentyl)hydrazine-1,2-dicarboxylate (69l)



$[\alpha]_D^{25}$: -4.4 (c, CH₂Cl₂, 97:3 er).

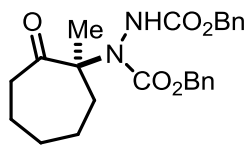
¹H NMR (500 MHz, CDCl₃): δ = 7.43–7.08 (m, 10H), 5.28–4.91 (m, 4H), 2.73–1.50 (m, 8H), 1.40–1.05 (m, 10H), 0.92–0.79 (m, 3H).

¹³C NMR (125 MHz, CDCl₃): δ = 215.2, 214.8, 156.7, 156.5, 155.2, 154.9, 135.5, 135.4, 128.6, 128.5, 128.4, 128.3, 128.3, 128.2, 128.0, 127.9, 70.6, 68.3, 68.1, 67.9, 35.5, 35.3, 34.1, 33.7, 31.8, 31.6, 30.1, 30.0, 29.7, 29.0, 23.4, 22.6, 18.2, 14.1.

HRMS (ESIpos): m/z calculated for C₂₈H₃₆N₂NaO₅ [M+Na]⁺: 503.2516, found: 503.2515.

HPLC (Chiralpak ID-3, *n*Hept/*i*PrOH = 80:20, flowrate: 1.0 ml/min, λ = 220 nm):
 $t_{r(\text{major})}$ = 6.1 min, $t_{r(\text{minor})}$ = 8.4 min.

Dibenzyl (S)-1-(1-methyl-2-oxocycloheptyl)hydrazine-1,2-dicarboxylate (69m)



$[\alpha]_D^{25}$: +7.2 (c 1.0, CH₂Cl₂, 77:23 er).

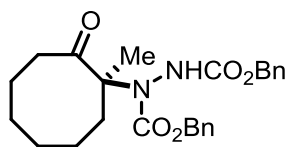
¹H NMR (500 MHz, CDCl₃): δ = 7.42–7.14 (m, 10H), 6.88–6.59 (m, 1H), 5.25–4.93 (m, 4H), 3.20–0.78 (m, 13).

^{13}C NMR (125 MHz, CDCl_3): δ = 210.3, 156.8, 156.5, 155.4, 135.5, 128.6, 128.6, 128.5, 128.5, 128.3, 128.3, 128.1, 128.1, 72.3, 71.2, 68.3, 67.9, 53.5, 40.4, 38.0, 37.1, 35.7, 30.3, 28.3, 24.7, 24.0, 23.9, 23.6, 21.6, 21.2.

HRMS (ESIpos): m/z calculated for $\text{C}_{24}\text{H}_{28}\text{N}_2\text{NaO}_5$ $[\text{M}+\text{Na}]^+$: 447.1890, found: 447.1888.

HPLC (Chiralcel OD-3, MeCN- H_2O = 50:50, flowrate: 0.9 mL/min, λ = 220 nm):
 $t_{\text{r}(\text{major})}$ = 15.1 min, $t_{\text{r}(\text{minor})}$ = 12.6 min.

Dibenzyl (S)-1-(1-methyl-2-oxocyclooctyl)hydrazine-1,2-dicarboxylate (69n)



$[\alpha]_{\text{D}}^{25}$: +5.4 (c 1.0, CH_2Cl_2 , 60:40 er).

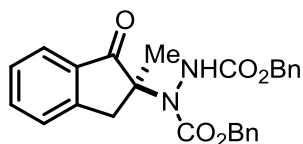
^1H NMR (500 MHz, CDCl_3): δ = 7.54–7.06 (m, 10H), 7.02–6.598(m, 1H), 5.29–4.89 (m, 4H), 3.62–2.62 (m, 1H), 2.43–0.83 (m, 14).

^{13}C NMR (125 MHz, CDCl_3): δ = 212.0, 211.6, 211.3, 157.1, 156.7, 155.8, 135.7, 135.7, 135.6, 128.8, 128.7, 128.7, 128.7, 128.6, 128.5, 128.4, 128.3, 128.2, 71.8, 71.1, 69.7, 68.5, 68.2, 68.0, 36.5, 35.9, 35.8, 35.6, 35.2, 27.4, 27.1, 26.5, 25.8, 25.5, 22.6, 21.3, 21.1, 20.3, 18.5.

HRMS (ESIpos): m/z calculated for $\text{C}_{25}\text{H}_{30}\text{N}_2\text{NaO}_5$ $[\text{M}+\text{Na}]^+$: 461.2047, found: 461.2045.

HPLC (Chiralcel OD-H, $n\text{Hept}/i\text{PrOH}$ = 90:10, flowrate: 1.0 mL/min, λ = 220 nm):
 $t_{\text{r}(\text{major})}$ = 19.6 min, $t_{\text{r}(\text{minor})}$ = 15.4 min.

Dibenzyl (S)-1-(2-methyl-1-oxo-2,3-dihydro-1H-inden-2-yl)hydrazine-1,2-dicarboxylate (69o)



$[\alpha]_D^{25}$: +2.8 (c 1.0, CH₂Cl₂, 60:40 er).

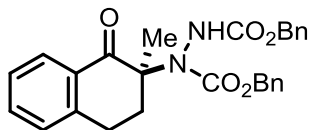
¹H NMR (500 MHz, CDCl₃): δ = 7.91–7.06 (m, 14H), 6.98–6.64 (m, 1H), 5.26–4.88 (m, 4H), 3.92–3.31 (m, 1H), 3.23–2.76 (m, 1H), 1.38–1.20 (m, 3H).

¹³C NMR (125 MHz, CDCl₃): δ = 208.3, 156.8, 154.9, 150.7, 150.2, 135.6, 135.2, 133.4, 128.7, 128.6, 128.5, 128.4, 128.3, 128.1, 128.0, 127.8, 127.6, 127.3, 126.5, 124.8, 68.3, 67.9, 41.5, 22.6.

HRMS (ESIpos): m/z calculated for C₂₆H₂₄N₂NaO₅ [M+Na]⁺: 467.1577, found: 467.1576.

HPLC (Chiralcel OD-3, *n*Hept/*i*PrOH = 90:10, flowrate: 1.0 ml/min, λ = 220 nm):
 $t_{r(\text{major})}$ = 7.8 min, $t_{r(\text{minor})}$ = 5.6 min.

Dibenzyl (S)-1-(2-methyl-1-oxo-1,2,3,4-tetrahydronaphthalen-2-yl)hydrazine-1,2-dicarboxylate (69p)



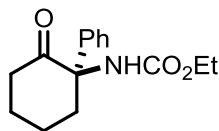
$[\alpha]_D^{25}$: +4.4 (c 1.0, CH₂Cl₂, 66.5:33.5 er).

¹H NMR (500 MHz, CDCl₃): δ = 8.20–6.43 (m, 15H), 5.24–4.93 (m, 4H), 3.21–0.62 (m, 7H).

¹³C NMR (125 MHz, CDCl₃): δ = 196.3, 157.0, 156.5, 154.9, 142.4, 135.7, 135.5, 133.7, 131.2, 128.7, 128.6, 128.5, 128.4, 128.3, 128.1, 128.0, 127.7, 126.9, 68.1, 67.9, 67.8, 67.2, 33.2, 29.7, 26.8, 20.1.

HRMS (ESIpos): m/z calculated for C₂₈H₃₄N₂NaO₅ [M+Na]⁺: 481.1734, found: 481.1736;

HPLC (Chiralcel OD-3, *n*Hept/*i*PrOH = 95:5, flowrate: 1.0 mL/min, λ = 220 nm):
 $t_{r(\text{major})}$ = 13.1 min, $t_{r(\text{minor})}$ = 15.9 min.

Ethyl (R)-(2-oxo-1-phenylcyclohexyl)carbamate (71)

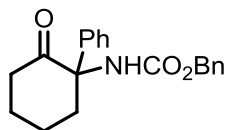
A mixture of **69r** (66.5 mg, 0.19 mmol, 1.0 equiv) and Cs_2CO_3 (373.1 mg, 1.15 mmol, 6.0 equiv) in a flame dried Schlenk-flask was evacuated for 30 min and subsequently put under an atmosphere of argon. MeCN (1.9 mL) and Ethylbromacetate (63.5 μL , 0.57 mmol, 3.0 equiv) were added and the resulting mixture was stirred for 22h at 70°C. The reaction was quenched with sat. aq. NH_4Cl and extracted with EtOAc (3 x 10 mL). The combined organic layers were dried over Na_2SO_4 and concentrated *in vacuo*. The crude product was purified by silica-gel column chromatography (Hex/EtOAc = 10/1) to give **71** (17.8 mg, 35%) as a clear oil.

^1H NMR (500 MHz, CDCl_3): δ = 7.46–7.20 (m, 5H), 6.69–6.48 (s_{br} , 1H), 4.04–3.83 (m, 2H), 3.76–3.39 (m, 1H), 2.43–2.22 (m, 2H), 2.06–1.67 (m, 5H), 1.20–0.90 (m, 3H).

^{13}C NMR (125 MHz, CDCl_3): δ = 208.1, 154.4, 137.6, 128.9, 128.1, 127.6, 66.5, 60.4, 38.7, 36.0, 28.4, 22.6, 14.6.

HRMS (ESIpos): m/z calculated for $\text{C}_{15}\text{H}_{19}\text{N}_1\text{NaO}_3$ $[\text{M}+\text{Na}]^+$: 284.1257, found: 284.1255.

HPLC (Chiralcel OD-3, $n\text{Hept}/i\text{PrOH}$ = 98:2, flowrate: 1.0 mL/min, λ = 220 nm): $t_{\text{r}(\text{major})}$ = 7.4 min, $t_{\text{r}(\text{minor})}$ = 8.6 min.

Benzyl (2-oxo-1-phenylcyclohexyl)carbamate (70)

^1H NMR (500 MHz, CDCl_3): 7.48–7.18 (m, 10H), 6.74 (s, 1H), 5.02 (d, J = 12.3 Hz, 1H), 4.87 (d, J = 12.4 Hz, 1H), 3.75 (dq, J = 14.3, 3.6 Hz, 1H), 2.51–2.26 (m, 2H), 2.02 (ddq, J = 12.0, 5.6, 2.7 Hz, 1H), 1.97–1.82 (m, 3H), 1.75 (ddd, J = 17.7, 10.8, 6.6 Hz, 1H).

7.4 The Direct α -Hydroxylation of Cyclic α -Branched Ketones via Enol Catalysis

7.4.1 General Procedures

General procedure (A) for oxidative cleavage of α -branched ketones: In a headspace GC-vial ketone (0.25 mmol, 1.0 equiv.) and TPP (1.5 mg, 1 mol%) were dissolved in MeCN (0.5 mL). TFA (58 μ L, 0.75 mmol, 3.0 equiv.) was added and the dark green mixture was purged with O₂ for 30 sec. The headspace vial was closed and a balloon of O₂ was connected. After irradiating in the setup depicted Figure 4.2 for 16 h the crude reaction mixture was diluted with CH₂Cl₂ and extracted with sat. Na₂CO₃. Aq. HCl (1 M) was carefully added to the aqueous layer until pH = 1 was reached and then extracted with CH₂Cl₂ (3x). The organic layers were combined and all volatiles were removed under reduced pressure giving the targeted products as clear oils.

General procedure (B) for the direct non-enantioselective hydroxylation of α -branched ketones: In a GC vial the ketone (0.25 mmol, 1.0 equiv.) was dissolved in a solution of trichloroacetic acid (0.75 mmol, 3.0 equiv.) in dry PhMe (2.5 mL) and nitrosobenzene (0.625 mmol, 2.5 equiv.) was added. The vial was closed and the resulting mixture was stirred at room temperature for 16–24h. The crude reaction mixture was directly purified by flash column chromatography (SiO₂, hexanes/EtOAc = 100/0 then 10/1).

Note: Scale up experiments showed, that the removal of trichloroacetic acid required additional work up after purification by column chromatography: A solution of the substrate in CH₂Cl₂ was washed with sat. aq. NaHCO₃ solution, dried over Na₂SO₄ and the solvent removed under reduced pressure. However in reactions on 0.25 mmol scale this was not necessary.

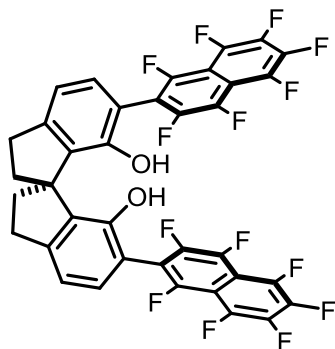
Note: In some cases traces of azoxybenzene, which turned out to be difficult to remove by column chromatography, can be visible in the NMR-spectra.

General procedure (C) for the direct enantioselective hydroxylation of α -branched ketones: **6b** (16.4 mg, 0.02 mmol, 10 mol%) and the corresponding ketone (0.2 mmol, 1.0 equiv.) were placed in a plastic GC vial. After the addition of benzene (0.8 mL) and acetic acid (40 μ L, 0.7

mmol, 3.5 equiv.), nitrosobenzene (21.4 mg, 0.2 mmol, 1.0 equiv.) was added in one portion and the reaction mixture was stirred for 2 h. Then, additional nitrosobenzene (32.1 mg, 0.3 mmol, 1.5 equiv.) was added and stirring was continued for additional 22 h or 46 h. The crude reaction mixture was directly purified by flash column chromatography (hexanes/EtOAc gradient 100/0 to 10/1).

7.4.2 Characterization of Products

(6R,6'S)-6,6'-bis(perfluoronaphthalen-2-yl)-2,2',3,3'-tetrahydro-1,1'-spirobi[indene]-7,7'-diol (86)



General Procedure: In a flame-dried Schlenk, MOM protected SPINOL (1 equiv.) was dissolved in dry THF (0.15 M) and the mixture was cooled down to $-78\text{ }^{\circ}\text{C}$. *n*-BuLi (2.5 M in hexanes, 4.0 equiv.) was added dropwise and the reaction mixture was stirred at $0\text{ }^{\circ}\text{C}$ for 4 h. After cooling to $-78\text{ }^{\circ}\text{C}$, the appropriate fluorinated arene (6 equiv) in THF (0.3 M) was added dropwise. After 2 h of stirring at $-78\text{ }^{\circ}\text{C}$, the initially milky brown solution turned red/purple and was stirred overnight at r.t.. After quenching with sat. aq. NH_4Cl solution, additional CH_2Cl_2 was added, the phases were separated and the aqueous layer was extracted with CH_2Cl_2 three times. The combined organic layers were then washed with brine and dried over Na_2SO_4 . After filtration, the solvents were evaporated under reduced pressure and the resulting crude product was directly redissolved in a 0.1 M solution of a 1:1 mixture of THF/methanolic HCl (1.25 M, 10 eq). In case of solubility issues, more THF was added until a homogeneous solution was observed. The reaction mixture was then refluxed for 2–12 h until TLC analysis showed full conversion of the starting material. The solvents were removed under reduced pressure and the crude product was purified by FCC (hexanes/ Et_2O or hexanes/ CH_2Cl_2).

The title compound was prepared according to the general procedure on 200 mg (0.58 mmol) of (*R*)-MOM-protected 2,2',3,3'-tetrahydro-1,1'-spirobi[indene]-7,7'-diol (MOM-SPINOL) and 960 mg (3.5 mmol) of octafluoronaphthalene. Purification by FCC (hexanes/EtOAc as eluent). Despite extensive attempts, scaling-up of this reaction (>200mg scale) afforded strongly diminished yields.

Appearance: yellowish solid; 224 mg (50%).

The NMR spectra are complicated by the presence of three rotamers.

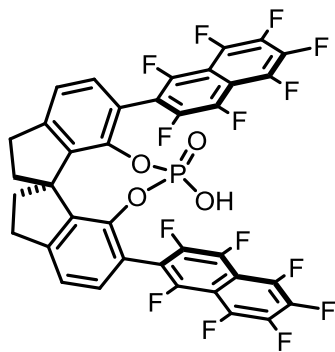
¹H NMR (500 MHz, CDCl₃): δ = 7.28–7.22 (m, 2H), 7.05 (d, *J* = 7.7 Hz, 2H), 4.88–4.83 (m, 2H), 3.24–3.06 (m, 4H), 2.55–2.44 (m, 2H), 2.38–2.27 (m, 2H).

¹³C NMR (¹H, {¹⁹F}, 125 MHz, CDCl₃): δ = 151.0, 149.8, 149.8, 148.2, 148.2, 148.2, 148.1, 146.1, 146.0, 141.8, 141.7, 141.3, 140.7, 139.8, 139.7, 138.7, 138.7, 132.8, 132.8, 130.5, 130.5, 130.4, 130.4, 118.2, 118.2, 116.0, 115.9, 115.8, 115.7, 113.5, 113.5, 111.3, 111.2, 108.1, 108.1, 108.0, 77.4, 77.4, 77.2, 76.9, 58.1, 58.1, 37.7, 37.7, 37.7, 31.5.

¹⁹F NMR (283 MHz, CDCl₃): δ = –117.2 - –117.7 (m), –118.2 - –118.8 (m), –133.9 - –134.2 (m), –134.72 - –134.9 (m), –143.6 - –144.1 (m), –144.1 - –144.4 (m), –146.0 - –146.7 (m), –148.9 - –149.9 (m), –153.7 - –154.1 (m), –155.9 - –156.4 (m).

HRMS (ESI^{neg}) *m/z* calculated for C₃₇H₁₃O₂F₁₄ [M–H][–]: 755.0698, found: 755.0700.

(1*R*,5*aR*,10*S*)-12-hydroxy-1,10-bis(perfluoronaphthalen-2-yl)-4,5,6,7-tetrahydrodiindeno[7,1-de:1',7'-fg][1,3,2]dioxaphosphocine 12-oxide (6b)



General Procedure: In a flame-dried Schlenk, the appropriate 3,3'-substituted SPINOL (1 equiv) was dissolved in dry pyridine (0.2 M) under argon atmosphere. POCl₃ (3 equiv) was added dropwise at 0 °C and the reaction was stirred at 70 °C for 2–12 h. When TLC showed full conversion of the starting material, the mixture was cooled to 0 °C and water was added (~ same amount as pyridine). Then the reaction was stirred at 90 °C for additional 2–4 h. When TLC showed full conversion of the intermediate chloride, the reaction mixture was cooled to r.t. and CH₂Cl₂ was added. The layers were separated and the organic layer was washed with aq. HCl (1 M), dried over Na₂SO₄, filtered and the solvents removed under reduced pressure. The crude product was purified by FCC (CH₂Cl₂/MeOH or CH₂Cl₂/acetone). The isolated compound was dissolved in CH₂Cl₂ and stirred with the same amount of aq. HCl (6 M) for 2 h. Separation of the layers and evaporation of the solvent under reduced pressure afforded the desired phosphoric acid catalyst

The title compound was prepared with 140 mg (0.18 mmol) of **S9** according to the general procedure for phosphoric acid synthesis. Purification by FCC (CH₂Cl₂/MeOH as eluent).

Appearance: yellowish solid; 128 mg (85%).

The NMR spectra are complicated by the presence of three rotamers. Rapid interconversion was detected in CDCl₃, however using DMSO-d₆ interconversion was slow and all three structures could be fully assigned by H,F-HOESY experiments.

$[\alpha]_D^{25}$: +115.0 (c 0.20, CHCl₃).

¹H NMR (500 MHz, DMSO-d₆): δ = 7.44–7.40 (m, 4H), 3.29–3.18 (m, 2H), 3.01–2.89 (m, 2H), 2.47–2.39 (m, 2H), 2.07–1.92 (m, 2H).

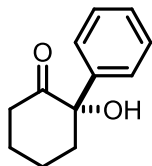
¹³C NMR ({¹H}, {¹⁹F}, 125 MHz, DMSO-d₆): δ = 149.9, 148.6, 148.2, 148.1, 148.1, 148.0, 146.1, 145.1, 144.7, 144.7, 144.6, 144.6, 144.6, 141.0, 140.8, 140.4, 140.4, 140.4, 140.3, 140.3, 140.2, 140.2, 139.8, 139.1, 139.0, 138.1, 138.1, 138.0, 130.7, 130.5, 121.8, 121.8, 121.7, 121.6, 119.8, 119.8, 119.7, 119.7, 116.5, 116.5, 116.4, 116.4, 110.0, 110.0, 107.5, 106.5, 79.2, 79.0, 78.7, 59.2, 59.2, 59.1, 38.6, 38.6, 38.5, 38.5, 30.1.

³¹P NMR (202 MHz, DMSO-d₆): δ = –12.5, –12.6, –12.7.

^{19}F NMR (283 MHz, DMSO-d_6): $\delta = -117.9 - -118.8$ (m), $-113.51 - -135.1$ (m), $-145.1 - -146.0$ (m), $-147.6 - -148.2$ (m), $-151.4 - -152.8$ (m), $-153.6 - -154.1$ (m), $-156.2 - -156.9$ (m).

HRMS (ESI^{neg}) m/z calculated for $\text{C}_{37}\text{H}_{12}\text{O}_4\text{F}_{14}\text{P}$ $[\text{M-H}]^-$: 817.0255, found: 817.0261.

(S)-2-hydroxy-2-phenylcyclohexan-1-one (77a)^[118a]



Appearance: orange oil; 28.7 mg (60%) [Procedure B]; orange oil; 21.5 mg (56%) [Procedure C].

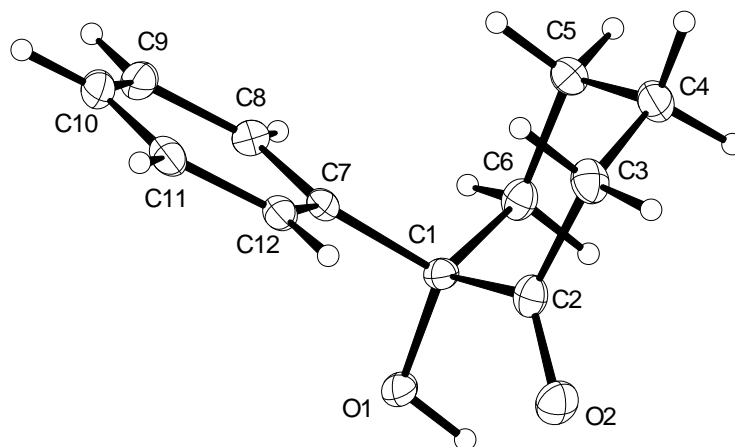
$[\alpha]_{\text{D}}^{25}$: +166.0 (c 0.20, CHCl_3 , 98:2 er).

^1H NMR (500 MHz, C_6D_6): $\delta = 7.18\text{--}7.12$ (m, 2H), $7.11\text{--}7.01$ (m, 3H), 4.61 (s, 1H), 2.73 (dq, $J = 14.3, 3.2$ Hz, 1H), 2.19 (dddd, $J = 13.5, 4.1, 2.7, 1.6$ Hz, 1H), 1.95 (td, $J = 13.5, 6.3$ Hz, 1H), 1.69–1.61 (m, 1H), 1.34 (ddt, $J = 12.5, 6.3, 3.1$ Hz, 1H), 1.29–1.07 (m, 3H).

^{13}C NMR (125 MHz, C_6D_6): $\delta = 211.9, 141.2, 129.1, 126.8, 80.1, 39.2, 38.8, 28.2, 23.1$ (One aromatic signal missing due to overlap with solvent).

HRMS (ESI^{pos}): m/z calculated for $\text{C}_{12}\text{H}_{14}\text{O}_2\text{Na}$ $[\text{M+Na}]^+$: 213.0886; found 213.0885.

HPLC (Chiralpak AD-3, $n\text{Hept/EtOH} = 80:20$, flowrate: 1.0 ml/min, $\lambda = 206$ nm):
 $t_{\text{r}(\text{major})} = 6.88$ min, $t_{\text{r}(\text{minor})} = 9.73$ min.

X-Ray data for **77a**:**Table 1. Crystal data and structure refinement.**

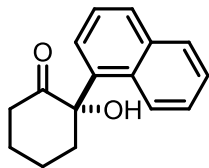
Identification code	10854	
Empirical formula	$\text{C}_{12}\text{H}_{14}\text{O}_2$	
Color	colorless	
Formula weight	190.23 g · mol ⁻¹	
Temperature	100(2) K	
Wavelength	1.54178 Å	
Crystal system	ORTHORHOMBIC	
Space group	P2₁2₁2₁, (no. 19)	
Unit cell dimensions	$a = 6.3053(3)$ Å	$\alpha = 90^\circ$.
	$b = 10.5157(6)$ Å	$\beta = 90^\circ$.
	$c = 14.6033(8)$ Å	$\gamma = 90^\circ$.
Volume	968.27(9) Å ³	
Z	4	
Density (calculated)	1.305 Mg · m ⁻³	

Absorption coefficient	0.701 mm ⁻¹	
F(000)	408 e	
Crystal size	0.304 x 0.113 x 0.070 mm ³	
θ range for data collection	5.183 to 71.909°.	
Index ranges	$-7 \leq h \leq 7$, $-12 \leq k \leq 12$, $-15 \leq l \leq 17$	
Reflections collected	31568	
Independent reflections	1875 [$R_{\text{int}} = 0.0420$]	
Reflections with $I > 2\sigma(I)$	1797	
Completeness to $\theta = 67.679^\circ$	99.0 %	
Absorption correction	Gaussian	
Max. and min. transmission	0.96 and 0.90	
Refinement method	Full-matrix least-squares on F^2	
Data / restraints / parameters	1875 / 0 / 183	
Goodness-of-fit on F^2	1.084	
Final R indices [$I > 2\sigma(I)$]	$R_1 = 0.0297$	$wR^2 = 0.0730$
R indices (all data)	$R_1 = 0.0338$	$wR^2 = 0.0756$
Absolute structure parameter	0.01(6)	
Largest diff. peak and hole	0.2 and -0.2 e · Å ⁻³	

Table 2. Bond lengths [Å] and angles [°].

O(1)-H(1)	0.90(3)	O(1)-C(1)	1.422(2)
O(2)-C(2)	1.220(2)	C(1)-C(2)	1.534(2)
C(1)-C(6)	1.544(3)	C(1)-C(7)	1.530(2)
C(2)-C(3)	1.509(3)	C(3)-H(3A)	1.03(3)
C(3)-H(3B)	1.01(2)	C(3)-C(4)	1.542(3)
C(4)-H(4A)	0.98(2)	C(4)-H(4B)	1.00(2)
C(4)-C(5)	1.522(3)	C(5)-H(5A)	1.00(2)
C(5)-H(5B)	0.99(2)	C(5)-C(6)	1.528(3)
C(6)-H(6A)	0.99(2)	C(6)-H(6B)	0.98(2)
C(7)-C(8)	1.396(3)	C(7)-C(12)	1.394(3)
C(8)-H(8)	0.99(2)	C(8)-C(9)	1.389(3)
C(9)-H(9)	0.97(3)	C(9)-C(10)	1.391(3)
C(10)-H(10)	0.95(3)	C(10)-C(11)	1.386(3)
C(11)-H(11)	0.98(3)	C(11)-C(12)	1.395(3)
C(12)-H(12)	0.96(2)		
C(1)-O(1)-H(1)	108.5(17)	O(1)-C(1)-C(2)	111.18(14)
O(1)-C(1)-C(6)	110.65(14)	O(1)-C(1)-C(7)	105.87(14)
C(2)-C(1)-C(6)	104.93(14)	C(7)-C(1)-C(2)	111.15(14)
C(7)-C(1)-C(6)	113.18(14)	O(2)-C(2)-C(1)	120.18(17)
O(2)-C(2)-C(3)	123.11(18)	C(3)-C(2)-C(1)	116.50(16)
C(2)-C(3)-H(3A)	108.0(14)	C(2)-C(3)-H(3B)	108.2(14)
C(2)-C(3)-C(4)	110.99(17)	H(3A)-C(3)-H(3B)	109.5(19)
C(4)-C(3)-H(3A)	111.6(14)	C(4)-C(3)-H(3B)	108.5(14)
C(3)-C(4)-H(4A)	109.6(14)	C(3)-C(4)-H(4B)	109.3(13)
H(4A)-C(4)-H(4B)	104.7(19)	C(5)-C(4)-C(3)	111.39(16)
C(5)-C(4)-H(4A)	111.1(14)	C(5)-C(4)-H(4B)	110.4(14)
C(4)-C(5)-H(5A)	111.2(13)	C(4)-C(5)-H(5B)	111.1(14)
C(4)-C(5)-C(6)	110.17(16)	H(5A)-C(5)-H(5B)	106.4(18)
C(6)-C(5)-H(5A)	109.0(13)	C(6)-C(5)-H(5B)	108.8(14)
C(1)-C(6)-H(6A)	109.0(14)	C(1)-C(6)-H(6B)	105.9(14)
C(5)-C(6)-C(1)	112.62(15)	C(5)-C(6)-H(6A)	111.4(14)

C(5)-C(6)-H(6B)	110.4(14)	H(6A)-C(6)-H(6B)	107.2(19)
C(8)-C(7)-C(1)	120.55(16)	C(12)-C(7)-C(1)	121.06(16)
C(12)-C(7)-C(8)	118.27(17)	C(7)-C(8)-H(8)	119.4(13)
C(9)-C(8)-C(7)	120.98(18)	C(9)-C(8)-H(8)	119.6(13)
C(8)-C(9)-H(9)	117.9(15)	C(8)-C(9)-C(10)	120.15(19)
C(10)-C(9)-H(9)	121.9(15)	C(9)-C(10)-H(10)	121.6(15)
C(11)-C(10)-C(9)	119.64(19)	C(11)-C(10)-H(10)	118.8(16)
C(10)-C(11)-H(11)	121.1(15)	C(10)-C(11)-C(12)	119.96(19)
C(12)-C(11)-H(11)	118.9(15)	C(7)-C(12)-C(11)	121.01(18)
C(7)-C(12)-H(12)	119.5(13)	C(11)-C(12)-H(12)	119.4(13)

(S)-2-hydroxy-2-(naphthalen-1-yl)cyclohexan-1-one (77b)

Appearance: orange oil; 36.2 mg (60%) [Procedure B]; orange oil; 18.5 mg (38%) [Procedure C].

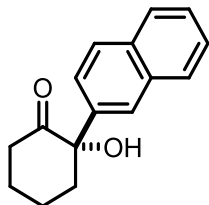
$[\alpha]_D^{25}$: +54.7 (c 0.15, CHCl_3 , 91:9 e.).

$^1\text{H NMR}$ (500 MHz, C_6D_6): δ = 8.34 (d, J = 8.6 Hz, 1H), 7.65–7.57 (m, 2H), 7.43 (d, J = 7.1 Hz, 1H), 7.30–7.01 (m, 3H), 4.62 (s, 1H), 2.98 (dq, J = 14.2, 3.2 Hz, 1H), 2.14 (dtd, J = 11.9, 3.8, 1.7 Hz, 1H), 1.82–1.72 (m, 1H), 1.58 (ddd, J = 14.2, 13.2, 4.0 Hz, 1H), 1.49–1.17 (m, 4H).

$^{13}\text{C NMR}$ (125 MHz, C_6D_6): δ = 215.0, 135.5, 135.3, 132.7, 129.7, 129.3, 126.8, 126.0, 125.8, 125.7, 125.0, 82.0, 43.6, 39.2, 29.9, 23.5.

HRMS (EI): m/z calculated for $\text{C}_{16}\text{H}_{16}\text{O}_2$ $[\text{M}]^+$: 240.1145; found 240.1143.

HPLC (Chiralpak AD-3, $n\text{Hept}/\text{EtOH}$ = 80:20, flowrate: 1.0 ml/min, λ = 224 nm): $t_{\text{r(minor)}}$ = 5.81 min, $t_{\text{r(major)}}$ = 6.64 min.

(S)-2-hydroxy-2-(naphthalen-2-yl)cyclohexan-1-one (77c)

Appearance: orange oil; 34.7 mg (58%) [Procedure B]; orange oil; 27.9 mg (58%) [Procedure C].

$[\alpha]_D^{25}$: +161.8 (c 0.11, CHCl_3 , 97.5:2.5 er).

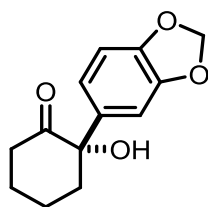
$^1\text{H NMR}$ (500 MHz, C_6D_6): δ = 7.70 (d, J = 1.8 Hz, 1H), 7.63–7.49 (m, 3H), 7.30 (dd, J = 8.6, 1.8 Hz, 1H), 7.28–7.18 (m, 2H), 4.69 (s, 1H), 2.89 (dq, J = 14.3, 3.2 Hz, 1H), 2.39–2.14 (m, 1H), 1.99 (td, J = 13.5, 6.1 Hz, 1H), 1.88–1.60 (m, 1H), 1.50–1.08 (m, 4H).

^{13}C NMR (125 MHz, C_6D_6): δ = 212.0, 138.6, 133.9, 133.4, 129.2, 128.6, 126.7, 126.5, 125.9, 124.9, 80.3, 39.4, 38.9, 28.3, 23.2

HRMS (ESIpos): m/z calculated for $\text{C}_{16}\text{H}_{16}\text{O}_2\text{Na}$ $[\text{M}+\text{Na}]^+$: 263.1042; found 263.1042.

HPLC (Chiralpak AD-3, $n\text{Hept}/\text{EtOH}$ = 80:20, flowrate: 1.0 ml/min, λ = 206 nm): $t_{\text{r}(\text{minor})}$ = 10.22 min, $t_{\text{r}(\text{major})}$ = 14.01 min.

(S)-2-(benzo[d][1,3]dioxol-5-yl)-2-hydroxycyclohexan-1-one (77d)



Appearance: orange oil; 23.4 mg (40%) [Procedure B]; orange solid; 25.0 mg (53%) [Procedure C].

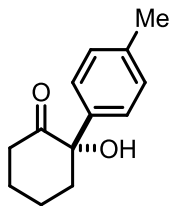
$[\alpha]_{\text{D}}^{25}$: +154.7 (c 0.15, CHCl_3 , 97:3 er).

^1H NMR (500 MHz, CDCl_3): δ = 6.83–6.74 (m, 3H), 5.99–5.95 (m, 2H), 4.43 (s, 1H), 2.94–2.87 (m, 1H), 2.55–2.42 (m, 2H), 2.09–2.02 (m, 1H), 1.89–1.65 (m, 4H).

^{13}C NMR (125 MHz, C_6D_6): δ = 212.7, 148.6, 147.7, 134.1, 120.2, 108.8, 107.1, 101.5, 79.9, 39.2, 38.9, 28.5, 23.2.

HRMS(EI): m/z calculated for $\text{C}_{13}\text{H}_{14}\text{O}_4$ $[\text{M}]^+$: 234.0887; found 234.0886.

HPLC (Chiralpak AD-3, $n\text{Hept}/\text{EtOH}$ = 80:20, flowrate: 1.0 ml/min, λ = 205 nm): $t_{\text{r}(\text{major})}$ = 23.38 min, $t_{\text{r}(\text{minor})}$ = 25.60 min.

(S)-2-hydroxy-2-(p-tolyl)cyclohexan-1-one (77e)

Appearance: orange oil; 29.9 mg (59%) [Procedure B]; orange oil; 22.0 mg (54%) [Procedure C].

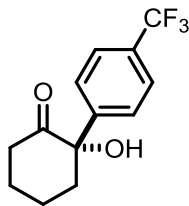
$[\alpha]_{\text{D}}^{25}$: +127.3 (c 0.11, CHCl_3 , 97.5:2.5 er).

$^1\text{H NMR}$ (500 MHz, C_6D_6): δ = 7.12–7.08 (m, 2H), 6.95–6.91 (m, 2H), 4.62 (s, 1H), 2.77 (dq, J = 14.2, 3.2 Hz, 1H), 2.25–2.19 (m, 1H), 2.09–1.98 (m, 4H), 1.71–1.62 (m, 1H), 1.41–1.13 (m, 4H).

$^{13}\text{C NMR}$ (125 MHz, C_6D_6): δ = 212.1, 138.4, 137.7, 129.8, 126.8, 79.9, 39.3, 38.8, 28.3, 23.2, 21.0.

HRMS (ESIpos): m/z calculated for $\text{C}_{13}\text{H}_{16}\text{O}_2\text{Na}$ $[\text{M}+\text{Na}]^+$: 227.1042; found 227.1042.

HPLC (Chiralpak AD-3, $n\text{Hept}/\text{EtOH}$ = 80:20, flowrate: 1.0 ml/min, λ = 204 nm): $t_{\text{r}(\text{major})}$ = 7.92 min, $t_{\text{r}(\text{minor})}$ = 10.90 min.

(S)-2-hydroxy-2-(4-(trifluoromethyl)phenyl)cyclohexan-1-one (77f)

Appearance: orange oil; 36.6 mg (56%) [Procedure B]; orange solid; 15.2 mg (29%) [Procedure C].

$^1\text{H NMR}$ (500 MHz, C_6D_6): δ = 7.28 (d, J = 8.2 Hz, 2H), 6.96 (d, J = 8.2 Hz, 2H), 4.46 (s_{br} , 1H), 2.55–2.49 (m, 1H), 2.19–2.12 (m, 1H), 1.77–1.66 (m, 1H), 1.60–1.52 (m, 1H), 1.37–1.29 (m, 1H), 1.22–0.98 (m, 3H).

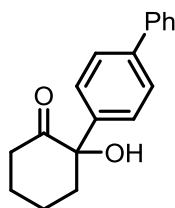
^{13}C NMR (125 MHz, C_6D_6): δ = 210.6, 144.6, 126.9, 125.6 (q, J = 3.8 Hz), 79.2, 38.8, 38.3, 27.7, 22.4 (Signals not visible due to overlap with solvent).

^{19}F NMR (283 MHz, C_6D_6): δ = -62.4.

HRMS (ESIpos): m/z calculated for $\text{C}_{12}\text{H}_{14}\text{O}_2\text{Na}$ $[\text{M}+\text{Na}]^+$: 213.0886; found 213.0885.

HPLC (Chiralpak AD-3, $n\text{Hept}/\text{EtOH}$ = 80:20, flowrate: 1.0 ml/min, λ = 206 nm):
 $t_{\text{r}(\text{major})}$ = 4.43 min, $t_{\text{r}(\text{minor})}$ = 7.05 min.

2-([1,1'-biphenyl]-4-yl)-2-hydroxycyclohexan-1-one (77h)



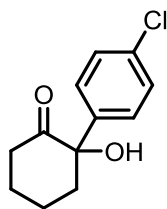
Appearance: orange oil; 31.0 mg (47%) [Procedure B].

^1H NMR (500 MHz, CDCl_3): δ = 7.64–7.55 (m, 4H), 7.48–7.42 (m, 2H), 7.40–7.33 (m, 3H), 4.53 (s_{br}, 1H), 3.08–2.98 (m, 1H), 2.61–2.44 (m, 2H), 2.13–2.05 (m, 1H), 1.95–1.69 (m, 4H).

^{13}C NMR (125 MHz, CDCl_3): δ = 212.8, 141.4, 140.5, 139.1, 129.0, 128.0, 127.7, 127.2, 127.0, 80.0, 39.1, 39.0, 28.5, 23.3.

HRMS (EI): m/z calculated for $\text{C}_{18}\text{H}_{18}\text{O}_2$ $[\text{M}]^+$ 266.1301; found 266.1302.

2-(4-chlorophenyl)-2-hydroxycyclohexan-1-one (77i)



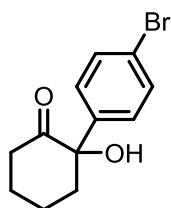
Appearance: orange oil; 29.1 mg (52%) [Procedure B].

^1H NMR (500 MHz, CDCl_3): δ = 7.39–7.35 (m, 2H), 7.27–7.22 (m, 2H), 4.84 (s_{br} , 1H), 3.00–2.92 (m, 1H), 2.59–2.51 (m, 1H), 2.45–2.34 (m, 1H), 2.11–2.02 (m, 1H), 1.92–1.82 (m, 2H), 1.79–1.65 (m, 2H).

^{13}C -NMR (125 MHz, CDCl_3): δ = 212.4, 138.2, 134.6, 129.5, 128.1, 79.9, 39.0, 38.9, 28.4, 23.1.

HRMS (EI): m/z calculated for $\text{C}_{12}\text{H}_{13}\text{O}_2\text{Cl}$ $[\text{M}]^+$ 224.0599; found 224.0596.

2-(4-bromophenyl)-2-hydroxycyclohexan-1-one (77j)



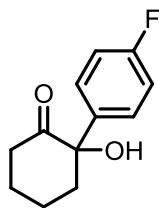
Appearance: orange oil; 30.2 mg (45%) [Procedure B].

^1H NMR (500 MHz, CDCl_3): δ = 7.54–7.50 (m, 2H), 7.21–7.15 (m, 2H), 5.59 (s_{br} , 1H), 2.98–2.90 (m, 1H), 2.59–2.51 (m, 1H), 2.44–2.33 (m, 1H), 2.12–2.02 (m, 1H), 1.92–1.92 (m, 2H), 1.81–1.65 (m, 2H).

^{13}C NMR (125 MHz, CDCl_3): δ = 212.3, 138.8, 132.5, 128.4, 122.8, 122.8, 79.9, 38.9, 28.4, 23.1.

HRMS (EI): m/z calculated for $\text{C}_{12}\text{H}_{13}\text{O}_2\text{Br}$ $[\text{M}]^+$ 268.0094; found 268.0091.

2-(4-fluorophenyl)-2-hydroxycyclohexan-1-one (77k)



Appearance: orange oil; 21.6 mg (41%) [Procedure B].

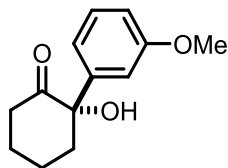
^1H NMR (500 MHz, CDCl_3): δ = 7.32–7.26 (m, 2H), 7.11–7.04 (m, 2H), 4.28 (s_{br}, 1H), 3.00–2.91 (m, 1H), 2.58–2.50 (m, 1H), 2.46–2.34 (m, 1H), 2.13–2.01 (m, 1H), 1.93–1.81 (m, 2H), 1.80–1.66 (m, 2H).

^{13}C NMR (125 MHz, CDCl_3): δ = 212.5, 162.6 (d, J = 247.9 Hz), 135.9, 128.5 (d, J = 8.2 Hz), 116.2 (d, J = 21.4 Hz), 79.7, 39.2, 38.9, 28.5, 23.2.

^{19}F NMR (283 MHz, CDCl_3): δ = –113.4.

HRMS (ESIpos): m/z calculated for $\text{C}_{12}\text{H}_{13}\text{O}_2\text{FNa}$ [$\text{M}+\text{Na}$]⁺ 231.0792; found 231.0793.

(S)-2-hydroxy-2-(3-methoxyphenyl)cyclohexan-1-one (77l)



Appearance: orange oil; 29.7 mg (54%) [Procedure B]; orange oil; 21.5 mg (49%) [Procedure C].

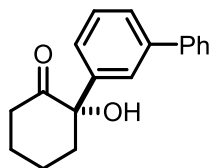
$[\alpha]_{\text{D}}^{25}$: +124.3 (c 0.14, CHCl_3 , 97:3 er).

^1H NMR (500 MHz, C_6D_6): δ = 7.03 (t, J = 8.0 Hz, 1H), 6.96 (t, J = 2.1 Hz, 1H), 6.80 (ddd, J = 8.0, 2.1, 0.9 Hz, 1H), 6.66 (ddd, J = 8.0, 2.1, 0.9 Hz, 1H), 4.61 (s, 1H), 3.25 (s, 3H), 2.74 (dq, J = 14.3, 3.2 Hz, 1H), 2.20 (ddt, J = 13.5, 4.5, 2.2 Hz, 1H), 2.01 (dt, J = 13.5, 6.1 Hz, 1H), 1.69–1.59 (m, 1H), 1.38–1.27 (m, 2H), 1.26–1.08 (m, 2H).

^{13}C NMR (125 MHz, C_6D_6): δ = 211.9, 160.7, 142.8, 130.2, 119.1, 113.6, 112.9, 80.1, 54.8, 39.3, 38.8, 28.2, 23.1.

HRMS (ESIpos): m/z calculated for $\text{C}_{13}\text{H}_{16}\text{O}_3\text{Na}$ [$\text{M}+\text{Na}$]⁺: 243.0992; found 243.0992.

HPLC (Chiralpak AD-3, $n\text{Hept}/\text{EtOH}$ = 80:20, flowrate: 1.0 ml/min, λ = 204 nm): $t_{\text{r}(\text{major})}$ = 14.71 min, $t_{\text{r}(\text{minor})}$ = 17.51 min.

(S)-2-([1,1'-biphenyl]-3-yl)-2-hydroxycyclohexan-1-one (77m)

Appearance: orange oil; 37.6 mg (56%) [Procedure B]; orange solid; 23.2 mg (44%).

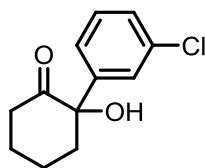
$[\alpha]_D^{25}$: +126.7 (c 0.15, CHCl₃, 97.5:2.5 er).

¹H-NMR (500 MHz, C₆D₆): δ = 7.63–7.61 (m, 1H), 7.50–7.41 (m, 2H), 7.38–7.34 (m, 1H), 7.25–7.07 (m, 5H), 4.67 (s, 1H), 2.81 (dq, J = 14.2, 3.2 Hz, 1H), 2.21 (ddt, J = 13.5, 4.5, 2.3 Hz, 1H), 1.99 (td, J = 13.5, 6.1 Hz, 1H), 1.68 (ddd, J = 14.2, 13.1, 4.5 Hz, 1H), 1.43–1.08 (m, 4H).

¹³C-NMR (125 MHz, C₆D₆): δ = 212.0, 142.6, 141.8, 141.5, 129.7, 129.2, 127.7, 127.6, 127.2, 125.8, 80.2, 39.3, 38.9, 28.3, 23.1 (one signal missing due to overlap with solvent).

HRMS (EI): m/z calculated for C₁₈H₁₈O₂ (M)⁺: 266.1301; found 266.1301.

HPLC (Chiralpak AD-3, *n*Hept/EtOH = 80:20, flowrate: 1.0 ml/min, λ = 207 nm): $t_{r(\text{major})}$ = 7.50 min, $t_{r(\text{minor})}$ = 7.96 min.

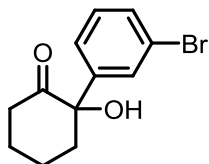
2-(3-chlorophenyl)-2-hydroxycyclohexan-1-one (77n)

Appearance: orange oil; 23.7 mg (42%) [Procedure B].

¹H NMR (500 MHz, CDCl₃): δ = 7.35–7.28 (m, 3H), 7.19–7.15 (m, 1H), 4.51 (s, 1H), 2.97–2.90 (m, 1H), 2.60–2.52 (m, 1H), 2.45–2.35 (m, 1H), 2.13–2.02 (m, 1H), 1.93–1.82 (m, 2H), 1.80–1.67 (m, 2H).

¹³C NMR (125 MHz, CDCl₃): δ = 212.1, 142.2, 135.2, 130.5, 128.7, 126.9, 124.8, 79.8, 39.0, 28.4, 23.2.

HRMS (EI): m/z calculated for C₁₂H₁₃O₂Cl [M]⁺ 224.0599; found 224.0596.

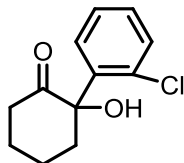
2-(3-bromophenyl)-2-hydroxycyclohexan-1-one (77o)

Appearance: orange oil; 30.1 mg (45%) [Procedure B].

¹H NMR (500 MHz, CDCl₃): δ = 7.49–7.44 (m, 2H), 7.29–7.24 (m, 1H), 7.24–7.20 (m, 1H), 4.51 (s, 1H), 2.98–2.89 (m, 1H), 2.60–2.53 (m, 1H), 2.45–2.35 (m, 1H), 2.14–2.04 (m, 1H), 1.94–1.81 (m, 2H), 1.79–1.68 (m, 2H).

¹³C NMR (125 MHz, CDCl₃): δ = 212.0, 142.5, 131.6, 130.8, 129.8, 125.2, 123.4, 79.8, 39.0, 29.4, 23.2.

HRMS (EI): m/z calculated for C₁₂H₁₃O₂Br [M]⁺ 268.0094; found 268.0092.

2-(2-chlorophenyl)-2-hydroxycyclohexan-1-one (77p)

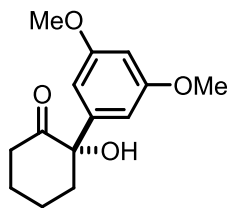
Appearance: orange oil; 35.1 mg (62%) [Procedure B].

¹H NMR (500 MHz, CDCl₃): δ = 7.69 (dd, J = 7.9, 1.6 .

¹³C NMR (125 MHz, CDCl₃): δ = 213.2, 137.3, 134.0, 131.4, 130.0, 128.8, 127.3, 80.8, 41.8, 38.9, 29.5, 22.9.

HRMS (EI): m/z calculated for C₁₂H₁₃O₂Cl [M]⁺: 224.0597; found 224.0599.

(S)-2-(3,5-dimethoxyphenyl)-2-hydroxycyclohexan-1-one (77q)



Appearance: orange oil; 20.3 mg (32%) [Procedure B]; orange oil; 22.8 mg (46%) [Procedure C].

$[\alpha]_D^{25}$: +107.3 (c 0.11, CHCl_3 , 97:3 er).

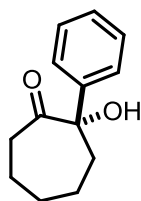
$^1\text{H NMR}$ (500 MHz, C_6D_6): δ = 6.62 (d, J = 2.2 Hz, 2H), 6.45 (t, J = 2.2 Hz, 1H), 4.66 (s, 1H), 3.28 (s, 6H), 2.76 (dq, J = 14.2, 3.2 Hz, 1H), 2.31–2.19 (m, 1H), 2.10 (td, J = 13.5, 6.1 Hz, 1H), 1.66 (td, J = 13.9, 4.0 Hz, 1H), 1.51–1.33 (m, 2H), 1.30–1.10 (m, 2H).

$^{13}\text{C NMR}$ (125 MHz, C_6D_6): δ = 212.0, 162.0, 143.4, 105.2, 100.2, 80.1, 54.9, 39.3, 38.9, 28.1, 23.1.

HRMS (ESIpos): m/z calculated for $\text{C}_{14}\text{H}_{18}\text{O}_4\text{Na}$ $[\text{M}+\text{Na}]^+$: 273.1097; found 273.1098.

HPLC (Chiralpak AD-3, $n\text{Hept}/\text{EtOH}$ = 80:20, flowrate: 1.0 ml/min, λ = 206 nm): $t_{\text{r}(\text{major})}$ = 27.32 min, $t_{\text{r}(\text{minor})}$ = 34.65 min.

(S)-2-hydroxy-2-phenylcycloheptan-1-one (77r)



Appearance: orange oil; 29.9 mg (57%) [Procedure B]; orange oil; 11.4 mg (28%) [Procedure C].

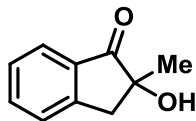
$^1\text{H NMR}$ (500 MHz, CDCl_3): δ = 7.48–7.42 (m, 2H), 7.40–7.34 (m, 2H), 7.33–7.27 (m, 1H), 4.56 (d, J = 1.4 Hz, 1H), 2.88–2.78 (m, 1H), 2.52–2.44 (m, 1H), 2.37–2.24 (m, 2H), 2.06–1.86 (m, 3H), 1.59–1.35 (m, 3H).

$^{13}\text{C NMR}$ (125 MHz, CDCl_3): δ = 213.9, 141.8, 128.9, 128.1, 125.9, 82.6, 39.7, 36.6, 30.7, 28.1, 23.9.

HRMS (ESIpos): m/z calculated for $C_{13}H_{16}O_2Na$ $[M+Na]^+$: 227.1042; found 227.1041.

HPLC (Chiralpak AD-3, n Hept/EtOH = 80:20, flowrate: 1.0 ml/min, λ = 205 nm):
 $t_{r(\text{major})}$ = 5.99 min, $t_{r(\text{minor})}$ = 8.34 min.

2-hydroxy-2-methyl-2,3-dihydro-1H-inden-1-one (77s)



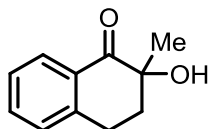
Appearance: orange oil; 26.2 mg (64%) [Procedure B].

1H NMR (500 MHz, $CDCl_3$): δ = 7.79 (d, J = 7.8 Hz, 1H), 7.64 (dt, J = 7.6, 1.2 Hz, 1H), 7.46–7.38 (m, 2H), 3.27 (d, J = 16.8 Hz, 1H), 3.22 (d, J = 16.8 Hz, 1H), 2.34 (s_{br}, 1H), 1.44 (s, 3H).

^{13}C NMR (125 MHz, $CDCl_3$): δ = 208.5, 151.3, 136.0, 133.7, 128.1, 126.9, 125.1, 77.6, 42.3, 25.9.

HRMS (ESIpos): m/z calculated for $C_{10}H_{10}O_2Na$ $[M+Na]^+$: 185.0573; found 185.0574.

2-hydroxy-2-methyl-3,4-dihydronaphthalen-1(2H)-one (77t)

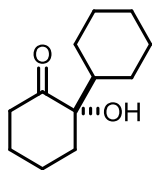


Appearance: orange oil; 26.8 mg (61%) [Procedure B].

1H NMR (500 MHz, $CDCl_3$): δ = 8.03 (dd, J = 7.9, 1.3 Hz, 1H), 7.53 (dt, J = 7.6, 1.4 Hz, 1H), 7.37–7.33 (m, 1H), 7.28–7.25 (m, 1H), 3.89 (s, 1H), 3.15–3.06 (m, 1H), 3.06–2.99 (m, 1H), 2.30–2.18 (m, 2H), 1.40 (s, 3H).

^{13}C NMR (125 MHz, $CDCl_3$): δ = 202.0, 143.6, 134.2, 130.1, 129.2, 128.2, 127.1, 73.7, 36.0, 27.0, 24.1.

HRMS (EI): m/z calculated for $C_{11}H_{12}O_2$ $[M]$: 176.0832; found 176.0832.

(S)-1-hydroxy-[1,1'-bi(cyclohexan)]-2-one (77u)

Appearance: orange oil; 32.2 mg (66%) [Procedure B]; orange oil; 15.8 mg (40%) [Procedure C].

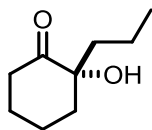
$[\alpha]_D^{25}$: +75.0 (c 0.2, CHCl_3 , 94:6 er).

$^1\text{H NMR}$ (500 MHz, C_6D_6): δ = 4.05 (s, 1H), 2.29–2.22 (m, 1H), 2.20–2.14 (m, 1H), 1.97–1.87 (m, 1H), 1.77–1.68 (m, 2H), 1.63–1.51 (m, 3H), 2.14 (m, 2H), 1.30–0.95 (m, 9H).

$^{13}\text{C NMR}$ (125 MHz, C_6D_6): δ = 214.2, 81.0, 41.0, 38.1, 37.9, 28.2, 26.9, 26.8, 26.5, 26.4, 25.1, 22.1.

HRMS (EI): m/z calculated for $\text{C}_{12}\text{H}_{20}\text{O}_2$ $[\text{M}]^{+}$: 196.1458; found 196.1458.

GC (Astec® ChiralDEX® G-TA, 30.0 m, i.d. 0.25 mm, 0.9 bar H_2 , FID, Injector 230 °C, 110 °C (iso) 50 min, ramp 8 °C/min to 170 °C, 3 min, 350 °C (iso)): $t_{\text{r(minor)}}$ = 40.60 min, $t_{\text{r(major)}}$ = 41.56 min.

(R)-2-hydroxy-2-propylcyclohexan-1-one (77v)

Appearance: orange oil; 20.1 mg (51%) [Procedure B]; orange oil; 10.5 mg (34%) [Procedure C].

$[\alpha]_D^{25}$: +24.0 (c 0.05, CHCl_3 , 85.5:14.5 er).

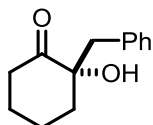
$^1\text{H NMR}$ (500 MHz, CDCl_3): δ = 3.96 (s, 1H), 2.56–2.43 (m, 2H), 2.19 (dq, J = 13.2, 3.0 Hz, 1H), 2.15–2.07 (m, 1H), 1.85 (ddd, J = 13.9, 11.9, 4.7 Hz, 1H), 1.82–1.53 (m, 5H), 1.50–1.37 (m, 1H), 1.09–0.96 (m, 1H), 0.91 (t, J = 7.3 Hz, 3H).

$^{13}\text{C NMR}$ (125 MHz, CDCl_3): δ = 214.7, 79.3, 41.3, 39.7, 38.3, 28.1, 22.9, 16.2, 14.5.

HRMS (ESIpos): m/z calculated for $C_9H_{16}O_2Na$ $[M+Na]^+$: 179.1042; found 179.1043.

GC (BGB-178/BGB-15, 30.0 m, 0.5 bar H_2 , FID, Injector 230 °C, 95 °C (iso) 30 min, ramp 9 °C/min to 220 °C, 3 min, 350 °C (iso)): $t_{r(minor)} = 21.91$ min, $t_{r(major)} = 24.76$ min.

(S)-2-benzyl-2-hydroxycyclohexan-1-one (77w)



Appearance: orange oil; 22.5 mg (44%) [Procedure B]; orange oil; 9.2 mg (23%) [Procedure C].

$[\alpha]_D^{25}$: +177.0 (c 0.2, $CHCl_3$, 92:8 er).

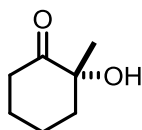
1H NMR (500 MHz, C_6D_6): $\delta = 7.22$ – 7.04 (m, 5H), 3.99 (s, 1H), 2.76 (d, $J = 13.7$ Hz, 1H), 2.68 (d, $J = 13.7$ Hz, 1H), 2.21– 2.13 (m, 1H), 2.07 (td, $J = 13.5, 6.2$ Hz, 1H), 1.95 (dq, $J = 13.5, 3.2$ Hz, 1H), 1.53– 1.37 (m, 2H), 1.32– 1.04 (m, 3H).

^{13}C NMR (125 MHz, C_6D_6): $\delta = 212.2, 136.2, 128.4, 127.1, 79.2, 43.4, 40.6, 38.3, 28.0, 22.7$ (one aromatic signal missing due to overlap with solvent).

HRMS (EI): m/z calculated for $C_{13}H_{16}O_2$ $[M]^+$: 204.1145; found 204.1142.

HPLC (Chiralpak AD-3, n Hept/EtOH = 80:20, flowrate: 1.0 ml/min, $\lambda = 205$ nm): $t_{r(major)} = 6.65$ min, $t_{r(minor)} = 13.71$ min.

(R)-2-hydroxy-2-methylcyclohexan-1-one (77z)



Appearance: n.d.; 87.5:12.5 er [Procedure C].

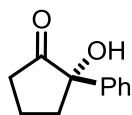
^1H NMR (500 MHz, CDCl_3): δ = 4.82 (s, 1H), 2.60–2.44 (m, 2H), 2.18–2.05 (m, 2H), 1.88–1.79 (m, 1H), 1.78–1.58 (m, 3H), 1.41 (s, 3H).

^{13}C NMR (125 MHz, CDCl_3): δ = 214.5, 76.8, 42.1, 37.9, 28.0, 25.1, 23.2.

HRMS (ESIpos): m/z calculated for $\text{C}_7\text{H}_{12}\text{O}_2\text{Na}$ $[\text{M}+\text{Na}]^+$: 151.0729; found 151.0730.

GC (BGB-177/BGB-15, 30.0 m, 0.5 bar H_2 , FID, Injector 230 $^\circ\text{C}$, 85 $^\circ\text{C}$ (iso) 35 min, ramp 8 $^\circ\text{C}/\text{min}$ to 210 $^\circ\text{C}$, 3 min, 350 $^\circ\text{C}$ (iso)): $t_{\text{r}(\text{minor})}$ = 18.46 min, $t_{\text{r}(\text{major})}$ = 19.30 min.

(S)-2-hydroxy-2-phenylcyclopentan-1-one (77x)



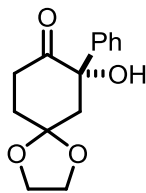
Appearance: orange oil; 5.0 mg (14%); 91.5:8.5 er [Procedure C].

^1H NMR (500 MHz, C_6D_6): δ = 7.38–7.35 (m, 4H), 7.34–7.30 (m, 1H), 2.88 (s, 1H), 2.56–2.40 (m, 3H), 2.23 (ddd, J = 13.3, 9.4, 7.3 Hz, 1H), 2.07 (dtdd, J = 13.6, 7.5, 6.2, 4.4 Hz, 1H), 1.91–1.77 (m, 1H).

HRMS (ESIpos): m/z calculated for $\text{C}_{11}\text{H}_{12}\text{O}_2\text{Na}$ $[\text{M}+\text{Na}]^+$: 199.0729; found 199.0729.

HPLC (Chiralpak AD-3, $n\text{Hept}/\text{EtOH}$ = 80:20, flowrate: 1.0 ml/min, λ = 204 nm): $t_{\text{r}(\text{major})}$ = 5.96 min, $t_{\text{r}(\text{minor})}$ = 9.81 min.

(S)-7-hydroxy-7-phenyl-1,4-dioxaspiro[4.5]decan-8-one (77y)



Appearance: orange oil; 12.4 mg (24%); >98:2 er; [Procedure C].

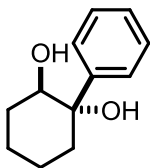
¹H NMR (500 MHz, CDCl₃): δ = 7.42–7.34 (m, 4H), 7.33–7.28 (m, 1H), 4.83 (s, 1H), 4.13–3.78 (m, 4H), 2.98 (ddd, *J* = 14.8, 9.4, 6.2 Hz, 1H), 2.82 (dd, *J* = 14.8, 1.5 Hz, 1H), 2.63 (ddd, *J* = 14.8, 7.0, 5.7 Hz, 1H), 2.26 (dd, *J* = 14.8, 2.3 Hz, 1H), 2.22–2.05 (m, 2H).

¹³C NMR (125 MHz, CDCl₃): δ = 209.1, 140.4, 128.3, 128.0, 126.2, 107.6, 78.5, 64.9, 64.8, 46.3, 35.1, 34.7.

HRMS (ESIpos): *m/z* calculated for C₁₄H₁₆O₄Na [M+Na]⁺: 271.0941; found 271.0943.

HPLC (Chiralpak AD-3, *n*Hept/EtOH = 90:10, flowrate: 1.0 ml/min, λ = 206 nm): *t*_{R(major)} = 24.69 min, *t*_{R(minor)} = 26.14 min.

(1*S*,2*R*)-1-phenylcyclohexane-1,2-diol (79)



Procedure: In a flame-dried Schlenk tube, 2-hydroxy-2-phenylcyclohexan-1-one (50 mg, 0.26 mmol, 1.0 equiv.) was dissolved in dry THF (2.5 mL) under an atmosphere of dry argon. The solution was cooled to −78 °C and K-Selectride[®] (1.0 m in THF, 1.30 mL, 1.31 mmol, 5.0 equiv.) was added dropwise. After addition was completed, the mixture was stirred for 10 min at −78 °C, then warmed up to 0 °C and stirred at this temperature for additional 2 h. The reaction was quenched by dropwise addition of 2 M aq. NaOH (1.5 mL) followed by H₂O₂ (35% in H₂O, 1.5 mL) at 0 °C. The resulting mixture was allowed to warm up to room temperature overnight. Afterwards, H₂O was added and the mixture was extracted with CH₂Cl₂ (3x). The combined organic layers were dried over Na₂SO₄ and the solvent removed under reduced pressure. The

crude product was purified by column chromatography (SiO₂, hexanes/EtOAc = 5/1) to give the title compound as a white solid (46.3 mg, 0.24 mmol, 83%, er = 98:2).

$[\alpha]_D^{25}$: -27.8 (c 0.18, CHCl₃, 98:2 er).

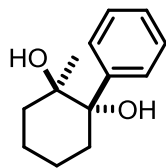
¹H NMR (500 MHz, CDCl₃): δ = 7.61–7.57 (m, 2H), 7.43–7.36 (m, 2H), 7.34–7.29 (m, 1H), 3.83–3.77 (m, 1H), 2.51–2.42 (m, 1H), 2.11–2.01 (m, 1H), 1.84–1.73 (m, 2H), 1.71–1.60 (m, 4H), 1.54–1.47 (m, 1H) 1.29–1.24 (m, 1H).

¹³C NMR (125 MHz, CDCl₃): δ = 146.0, 128.7, 127.9, 126.2, 74.8, 73.4, 31.6, 28.6, 21.3, 19.3.

HRMS (EI): m/z calculated for C₁₂H₁₆O₂ [M]⁺: 192.1145; found 192.1143.

HPLC: Achiral pre-separation: MultoHigh U-Si, *n*Hept/*i*PrOH = 95/5, flowrate: 1.0 min/min, λ = 220 nm, cut after 2.17 min. **Chiral separation:** Chiralpak IA-3, *n*Hept/*i*PrOH = 90/10, flowrate: 1 ml/min, λ = 204 nm): $t_{r(\text{minor})}$ = 8.80 min, $t_{r(\text{major})}$ = 9.66 min.

(1*R*,2*S*)-1-methyl-2-phenylcyclohexane-1,2-diol (80)



Procedure: In a flame-dried Schlenk tube 2-hydroxy-2-phenylcyclohexan-1-one (30 mg, 0.16 mmol, 1.0 equiv.) was dissolved in dry THF (1.5 mL). The solution was cooled down to -78 °C and methylmagnesium chloride (3 M in THF, 0.21 mL, 0.63 mmol, 4 equiv.) was added dropwise. The reaction mixture was allowed to warm up to room temperature and stirred overnight. The reaction was then quenched with sat. aq. NH₄Cl at 0 °C, extracted with CH₂Cl₂ (3x), dried over Na₂SO₄ and the solvent removed under reduced pressure. The crude product was purified by column chromatography (SiO₂, hexanes/EtOAc = 20/1). The desired product was obtained as an inseparable mixture of product and unreacted starting material (25.6 mg, 79%, NMR-ratio ~ 5.8/1, er = 99.5:0.5).

$[\alpha]_D^{25}$: -45.3 (c 0.15, CHCl₃, 99.5:0.5 er).

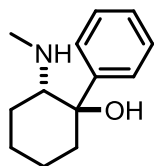
^1H NMR (500 MHz, CDCl_3): δ = 7.63–7.59 (m, 2H), 7.39–7.34 (m, 2H), 7.30–7.26 (m, 1H), 2.69–2.60 (m, 1H), 1.99–1.90 (m, 1H), 1.82–1.46 (m, 7H), 1.15 (s, 1H), 0.98 (s, 3H).

^{13}C NMR (125 MHz, CDCl_3): δ = 144.8, 127.9, 127.2, 127.0, 126.5, 72.7, 35.5, 34.7, 25.6, 21.2, 21.1.

HRMS (EI): m/z calculated for $\text{C}_{13}\text{H}_{18}\text{O}_2$ $[\text{M}]^+$ 206.1301; found 206.1300.

HPLC: (Chiralpak AD-3, $n\text{Hept}/\text{EtOH}$ = 90:10, flowrate: 1.0 ml/min, λ = 220 nm): $t_{\text{r(minor)}}$ = 4.04 min, $t_{\text{r(major)}}$ = 7.28 min.

(*trans*)-2-(methyamino)-1-phenylcyclohexan-1-ol (78)



Procedure: In a flame-dried Schlenk tube titanium isopropoxide (62 μL , 0.21 mmol, 2 equiv.) was given to PhMe (0.5 mL). After the solution was stirred for 10 min 2-hydroxy-2-phenylcyclohexan-1-one (20 mg, 0.11 mmol, 1 equiv.) was added at once. Afterwards methylamine (33% in EtOH, 71 μL , 0.53 mmol, 5 equiv.) was added dropwise and stirred overnight at 80 $^{\circ}\text{C}$. The resulting mixture was then cooled down to 0 $^{\circ}\text{C}$ and MeOH (0.5 mL) and NaBH_4 (20 mg, 0.53 mmol, 5 equiv.) were added and the mixture stirred at this temperature for another hour. After quenching the reaction solution by addition of sat. aq. NaHCO_3 (1.5 mL), the aqueous layer was extracted with CH_2Cl_2 (3x), dried over MgSO_4 and the solvent removed under reduced pressure. The crude product was purified by column chromatography (SiO_2 , hexanes/EtOAc = 1/1 to 0/100) as white solid (17.0 mg, 0.83 mmol, 79%, *trans/cis* = 4:1).

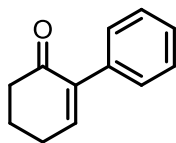
^1H NMR (500 MHz, CDCl_3): δ = 7.58–7.53 (m, 2H, major), 7.52–7.48 (m, 2H, minor), 7.39–7.31 (m, 2H, major/minor), 7.30–7.25 (m, 1H, major), 7.25–7.21 (m, 1H, minor), 2.89–2.84 (m, 1H, minor), 2.71–2.68 (m, 1H, major), 2.48–2.38 (m, 1H, major), 2.15 (s, 3H, major), 2.08 (s, 3H, minor), 1.89–1.32 (m, 7H, major), 1.89–1.32 (m, 8H, minor).

^{13}C NMR (125 MHz, CDCl_3): δ = 148.2 (minor), 146.6 (major), 128.5 (major), 128.3 (minor), 127.5 (major), 126.7 (minor), 126.2 (major), 125.3 (minor), 74.9 (major), 74.5 (minor), 64.8

(major), 63.9 (minor), 39.1, 34.7, 32.8, 27.1, 24.8 (minor), 24.6 (major), 21.7 (major), 21.5 (minor), 19.8.

HRMS (EI): m/z calculated for $C_{13}H_{19}N_1O_1$ $[M]^+$ 205.1461; found 205.1460

4,5-dihydro-[1,1'-biphenyl]-2(3H)-one and 5,6-dihydro-[1,1'-biphenyl]-2(1H)-one (81 and 82)

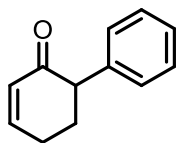


Procedure: In a 1.5 mL vial with cap 2-hydroxy-2-phenylcyclohexan-1-one (50 mg, 0.26 mmol, 1.0 equiv.) and *p*-toluene sulfonic acid (50 mg, 1.0 mmol, 1.0 equiv.) were dissolved in dry PhMe (1.0 mL). The vial was closed and the resulting mixture was stirred overnight at 80 °C. After cooling down to room temperature the crude reaction mixture was directly purified by column chromatography (SiO_2 , hexanes/EtOAc = 100/0 to 100/5) to give the titled product as a clear oil (24.3 mg, 54%). The regioisomer 5,6-dihydro-[1,1'-biphenyl]-2(1H)-one could be obtained as clear oil (7.1 mg, 16%).

1H NMR (500 MHz, $CDCl_3$): δ = 7.40–7.28 (m, 5H), 7.05 (t, J = 4.3 Hz, 1H), 2.65–2.58 (m, 2H), 2.55 (td, J = 6.1, 4.3 Hz, 2H), 2.13 (dq, J = 8.1, 6.1 Hz, 2H).

^{13}C NMR (125 MHz, $CDCl_3$): δ = 198.1, 148.1, 140.6, 136.7, 128.8, 128.1, 127.7, 39.2, 26.8, 23.1.

HRMS (EI): m/z calculated for $C_{12}H_{12}O_1$ $[M]^+$: 172.0883; found 172.0883.

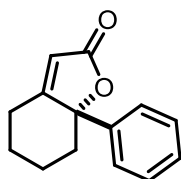


^1H NMR (500 MHz, CDCl_3): δ = 7.38–7.31 (m, 2H), 7.29–7.24 (m, 1H), 7.20–7.14 (m, 2H), 7.04 (ddd, J = 10.1, 4.7, 3.5 Hz, 1H), 6.17 (ddd, J = 10.1, 2.4, 1.7 Hz, 1H), 3.82–3.50 (m, 1H), 2.51–2.45 (m, 2H), 2.34–2.26 (m, 2H).

^{13}C NMR (125 MHz, CDCl_3): δ = 199.6, 150.2, 139.5, 130.4, 128.7, 128.4, 127.1, 53.5, 30.9, 25.7.

HRMS (EI): m/z calculated for $\text{C}_{12}\text{H}_{12}\text{O}_1$ $[\text{M}]^+$: 172.0883; found 172.0883.

(*R*)-7a-phenyl-5,6,7,7a-tetrahydrobenzofuran-2(4H)-one (83)



Procedure: In a flame-dried Schlenk tube, 2-hydroxy-2-phenylcyclohexan-1-one (30 mg, 0.16 mmol, 1.0 equiv.) and (Triphenylphosphoranylidene)ethenone (96 mg, 0.32 mmol, 2.0 equiv.) were dissolved in dry PhMe (1.5 mL) under an atmosphere of dry argon. The resulting mixture was stirred at 100 °C for 3d. The crude product was directly purified by column chromatography (SiO_2 , hexanes/EtOAc = 10/1) to give the title product as a clear oil (23.7 mg, 0.11 mmol, 70%).

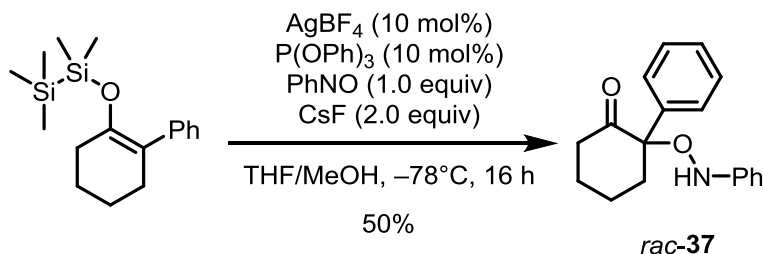
$[\alpha]_{\text{D}}^{25}$: –92.7 (c 0.11, CHCl_3 , 97.5:2.5 er).

^1H NMR (500 MHz, CDCl_3): δ = 7.42–7.31 (m, 5H), 5.96 (d, J = 1.7 Hz, 1H), 3.17–3.10 (m, 1H), 2.92–2.84 (m, 1H), 2.29–2.20 (m, 1H), 2.06–1.99 (m, 1H), 1.89–1.80 (m, 1H), 1.75–1.67 (m, 1H), 1.52–1.37 (m, 2H).

^{13}C NMR (125 MHz, CDCl_3): δ [overlapping signals] = 174.5, 172.6, 136.1, 129.2, 127.0, 114.6, 88.8, 38.0, 28.4, 28.1, 22.6.

HRMS (EI): m/z calculated for $\text{C}_{14}\text{H}_{14}\text{O}_2$ $[\text{M}]^+$ 214.0988; found 214.0986.

HPLC (Chiralpak AD-3, $n\text{Hept}/\text{EtOH}$ = 90:10, flowrate: 1.0 ml/min, λ = 205 nm): $t_{\text{r}(\text{major})}$ = 6.67 min, $t_{\text{r}(\text{minor})}$ = 7.48 min.

2-phenyl-2-((phenylamino)oxy)cyclohexan-1-one (37)

Procedure: In a flame dried Schlenk tube, a mixture of AgBF_4 (9.7 mg, 10 mol%) and P(OPh)_3 (13.1 μL , 10 mol%) were dried under vacuum for 10 min and then purged with dry argon. Anhydrous THF (2 mL) was added and after stirring for 30 min at room temperature the solution was cooled down to -78°C and a solution of nitrosobenzene (53.6 mg, 0.5 mmol, 1 equiv) dissolved in anhydrous THF (1 mL) was added dropwise. After stirring for additional 5 min, the silyl enol ether (152.3 mg, 0.5 mmol, 1.0 equiv) was added dropwise. A solution of CsF (151.9 mg, 1.0 mmol, 2.0 equiv.) in anhydrous MeOH (1 mL) was then slowly added over 16 h at -78°C . After completion of the addition, the reaction mixture was diluted with *n*Hex/EtOAc (3/1) and filtered through a plug of silica. After removing the solvent under reduced pressure the crude product was purified by flash column chromatography on silica gel using *n*Hex/EtOAc as eluent to afford the desired product as a yellow solid (70.6 mg, 50%).

Appearance: yellow solid; 70.6 mg (50%).

^1H NMR (500 MHz, C_6D_6): δ = 7.56–7.49 (m, 2H), 7.46–7.39 (m, 3H), 7.39–7.34 (m, 1H), 7.22–7.12 (m, 2H), 6.94–6.78 (m, 3H), 2.79–2.70 (m, 1H), 2.61–2.50 (m, 2H), 2.40–2.28 (m, 1H), 2.06–1.92 (m, 2H), 1.86–1.72 (m, 2H).

^{13}C NMR (125 MHz, C_6D_6): δ = 209.8, 148.7, 136.5, 129.1, 129.0, 128.9, 128.0, 121.8, 114.7, 90.4, 41.2, 34.2, 27.3, 23.1.

HRMS (ESIpos): m/z calculated for $\text{C}_{18}\text{H}_{19}\text{O}_2\text{Na}$ $[\text{M}+\text{Na}]^+$: 304.1308; found 304.1308.

7.5 α -Oxidation of Cyclic Ketones with 1,4-Benzoquinones *via Enol Catalysis*

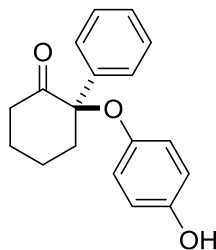
7.5.1 General Procedures

General procedure for the non-enantioselective reaction: In a screw-cap GC-vial diphenyl phosphate (25 mg, 0.1 mmol, 0.5 equiv.), the corresponding ketone (0.2 mmol, 1.0 equiv.) and the corresponding quinone (0.6 mmol, 3.0 equiv.) were dissolved in anhydrous toluene (0.4 mL) and the vial was closed. After stirring the resulting mixture overnight at room temperature the crude product was directly purified by flash column chromatography (SiO₂, hexanes/EtOAc 20/1 \rightarrow 5/1).

General procedure for the enantioselective reaction: A screw-cap GC-vial equipped with the corresponding ketone **68** (0.2 mmol, 1.0 equiv) and quinone **86** (0.6 mmol, 3.0 equiv) in anhydrous benzene (0.4 mL) was placed in a cryostat (0 °C). After stirring the mixture for 10 min, catalyst (*R*)-**1u** (6.3 mg, 0.01 mmol, 5 mol%) was added at once. After stirring the resulting solution at 0 °C for 24 h the crude product was directly purified by flash column chromatography (SiO₂, hexanes/EtOAc 20/1 \rightarrow 5/1).

7.5.2 Characterization of Substrates

(*R*)-2-(4-hydroxyphenoxy)-2-phenylcyclohexan-1-one (**88a**)



Appearance: yellowish solid; 37.9 mg, 67%.

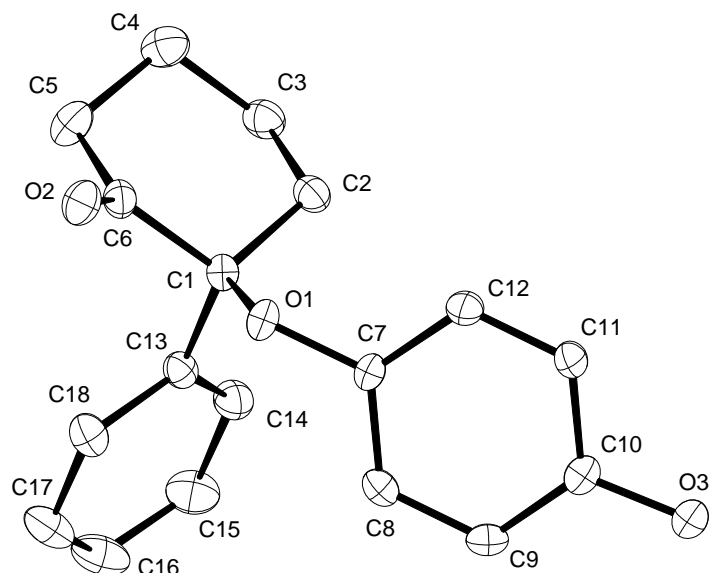
$[\alpha]_D^{25}$: -135.6 (c 0.18, CHCl₃, 96:4 er).

^1H NMR (500 MHz, CDCl_3): δ = 7.40–7.27 (m, 5H), 6.58–6.52 (m, 4H), 4.39 (s, 1H), 2.64 (ddd, J = 12.9, 10.4, 5.5 Hz, 1H), 2.40–2.21 (m, 3H), 2.19–2.08 (m, 1H), 2.05–1.97 (m, 1H), 1.92–1.80 (m, 1H), 1.74–1.65 (m, 1H).

^{13}C NMR (125 MHz, CDCl_3): δ = 209.1, 150.5, 149.1, 138.3, 128.3, 127.9, 127.5, 120.6, 115.7, 87.5, 42.1, 40.7, 28.5, 21.9.

HRMS (ESIpos): m/z calculated for $\text{C}_{18}\text{H}_{18}\text{O}_3\text{Na}$ $[\text{M}+\text{Na}]^+$: 305.1148; found 305.1145.

HPLC: (Chiralcel OJ-3, $n\text{Hept}/i\text{PrOH}$ = 80:20, flowrate: 1.0 ml/min, λ = 204 nm):
 $t_{r(\text{major})}$ = 6.84 min, $t_{r(\text{minor})}$ = 8.11 min

X-Ray Data for (±)-88a:**Table 1. Crystal data and structure refinement.**

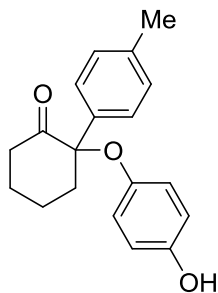
Identification code	10473
Empirical formula	$\text{C}_{18}\text{H}_{18}\text{O}_3$
Color	colorless
Formula weight	282.32 $\text{g} \cdot \text{mol}^{-1}$
Temperature	100(2) K
Wavelength	0.71073 Å
Crystal system	MONOCLINIC
Space group	$P2_1/c$, (no. 14)
Unit cell dimensions	$a = 14.108(10)$ Å $\alpha = 90^\circ$. $b = 8.608(5)$ Å $\beta = 114.75(7)^\circ$. $c = 13.108(9)$ Å $\gamma = 90^\circ$.
Volume	1445.6(18) Å ³
Z	4
Density (calculated)	1.297 $\text{Mg} \cdot \text{m}^{-3}$
Absorption coefficient	0.087 mm^{-1}

F(000)	600 e
Crystal size	0.09 x 0.06 x 0.03 mm ³
θ range for data collection	2.851 to 31.934°.
Index ranges	-20 \leq h \leq 20, -12 \leq k \leq 12, -19 \leq l \leq 19
Reflections collected	25208
Independent reflections	4970 [$R_{\text{int}} = 0.1120$]
Reflections with $I > 2\sigma(I)$	2889
Completeness to $\theta = 25.242^\circ$	99.9 %
Absorption correction	Gaussian
Max. and min. transmission	1.00 and 0.99
Refinement method	Full-matrix least-squares on F^2
Data / restraints / parameters	4970 / 0 / 194
Goodness-of-fit on F^2	1.099
Final R indices [$I > 2\sigma(I)$]	$R_1 = 0.0786$ $wR^2 = 0.1724$
R indices (all data)	$R_1 = 0.1520$ $wR^2 = 0.2180$
Largest diff. peak and hole	0.5 and -0.5 e \cdot Å ⁻³

Table 2. Bond lengths [Å] and angles [°].

O(1)-C(1)	1.447(3)	O(1)-C(7)	1.396(2)
O(2)-C(6)	1.213(3)	O(3)-C(10)	1.364(3)
C(1)-C(2)	1.532(3)	C(1)-C(6)	1.535(3)
C(1)-C(13)	1.525(3)	C(2)-C(3)	1.524(3)
C(3)-C(4)	1.517(3)	C(4)-C(5)	1.534(4)
C(5)-C(6)	1.498(3)	C(7)-C(8)	1.379(3)
C(7)-C(12)	1.384(3)	C(8)-C(9)	1.391(3)
C(9)-C(10)	1.381(3)	C(10)-C(11)	1.382(3)
C(11)-C(12)	1.382(3)	C(13)-C(14)	1.391(3)
C(13)-C(18)	1.388(3)	C(14)-C(15)	1.390(4)
C(15)-C(16)	1.377(4)	C(16)-C(17)	1.377(4)
C(17)-C(18)	1.386(4)		
C(7)-O(1)-C(1)	117.41(16)	O(1)-C(1)-C(2)	111.58(17)
O(1)-C(1)-C(6)	103.73(16)	O(1)-C(1)-C(13)	108.59(17)
C(2)-C(1)-C(6)	108.19(18)	C(13)-C(1)-C(2)	115.27(18)
C(13)-C(1)-C(6)	108.82(18)	C(3)-C(2)-C(1)	113.35(19)
C(4)-C(3)-C(2)	111.15(19)	C(3)-C(4)-C(5)	110.1(2)
C(6)-C(5)-C(4)	110.8(2)	O(2)-C(6)-C(1)	121.2(2)
O(2)-C(6)-C(5)	123.3(2)	C(5)-C(6)-C(1)	115.54(18)
C(8)-C(7)-O(1)	120.8(2)	C(8)-C(7)-C(12)	120.1(2)
C(12)-C(7)-O(1)	118.96(19)	C(7)-C(8)-C(9)	120.0(2)
C(10)-C(9)-C(8)	119.7(2)	O(3)-C(10)-C(9)	123.3(2)
O(3)-C(10)-C(11)	116.5(2)	C(9)-C(10)-C(11)	120.2(2)
C(12)-C(11)-C(10)	120.1(2)	C(11)-C(12)-C(7)	119.9(2)

C(14)-C(13)-C(1)	123.0(2)	C(18)-C(13)-C(1)	118.3(2)
C(18)-C(13)-C(14)	118.6(2)	C(15)-C(14)-C(13)	120.1(2)
C(16)-C(15)-C(14)	120.6(2)	C(17)-C(16)-C(15)	119.8(2)
C(16)-C(17)-C(18)	119.8(2)	C(17)-C(18)-C(13)	121.1(2)

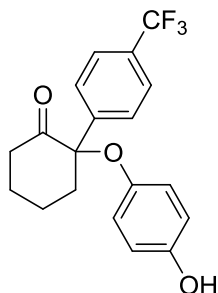
(±)-2-(4-hydroxyphenoxy)-2-(*p*-tolyl)cyclohexan-1-one (88b)

Appearance: red solid; 34.7 mg, 54%.

¹H NMR (500 MHz, CDCl₃): δ = 7.30–7.27 (m, 2H), 7.18 (d, *J* = 8.0 Hz, 1H), 6.63–6.51 (m, 4H), 4.82 (s_{br}, 1H), 2.66 (ddd, *J* = 12.9, 10.0, 5.4 Hz, 1H), 2.40–2.27 (m, 6H), 2.13 (dt, *J* = 13.6, 9.1, 4.1 Hz, 1H), 2.03 (dq, *J* = 18.1, 7.7, 7.0, 3.8 Hz, 1H), 1.89 (dt, *J* = 14.0, 9.5, 4.5 Hz, 1H), 1.72 (ddq, *J* = 13.2, 6.4, 3.3, 2.5 Hz, 1H).

¹³C NMR (125 MHz, CDCl₃): δ = 209.6, 150.7, 149.0, 137.8, 135.2, 129.1, 127.5, 120.8, 115.6, 87.5, 41.6, 40.7, 28.5, 22.0, 21.3.

HRMS (ESIpos): *m/z* calculated for C₁₉H₂₀O₃Na [M+Na]⁺: 319.1305; found 319.1305.

(±)-2-(4-hydroxyphenoxy)-2-(4-(trifluoromethyl)phenyl)cyclohexan-1-one (88c)

Appearance: red viscous oil; 34.7 mg, 53%; inseparable mixture of 1,6/1,4-addition products = 5:1 (by ¹H NMR and ¹⁹F NMR); using (*S*)-**6b**: red viscous oil; 43.6 mg, 62%; inseparable mixture of 1,6/1,4-addition products = 1.4:1 (by ¹H NMR and ¹⁹F NMR); 88:12 er_{1,6}, 81.5:18.5 er_{1,4}.

¹H NMR/mixture (500 MHz, CDCl₃): δ = 7.69 (d, *J* = 8.0 Hz, 2H_{1,4}), 7.60 (d, *J* = 8.3 Hz, 2H_{1,6}), 7.54–7.51 (m, 2H_{1,6}), 7.47 (d, *J* = 8.1 Hz, 2H_{1,4}), 6.79–6.75 (m, 1H_{1,4}), 6.70–6.66 (m, 1H_{1,4}),

6.61–6.57 (m, 2H_{1,6}), 6.56–6.52 (m, 2H_{1,6}), 5.68 (d, $J = 2.5$ Hz, 1H_{1,4}), 4.71 (s, 1H_{1,6}), 2.67 (td, $J = 12.7, 5.9$ Hz, 1H_{1,6}), 2.62–2.54 (m, 1H_{1,4}), 2.42 (dtd, $J = 14.4, 3.7, 2.6$ Hz, 1H_{1,6}), 2.32 (dtd, $J = 12.8, 4.2, 1.3$ Hz, 1H_{1,6}), 2.28–2.17 (m, 1H_{1,6/1,4}), 2.15–2.06 (m, 2H_{1,6/1,4}), 1.92–1.79 (m, 1H_{1,6/1,4}), 1.76–1.67 (m, 1H_{1,6/1,4}).

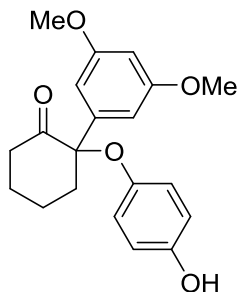
¹³C NMR (125 MHz, CDCl₃): $\delta = 209.1, 150.6, 149.0, 142.9, 137.8, 135.7, 135.6, 130.0, 129.7, 129.0, 127.7, 125.2, 125.1, 125.1, 125.1, 119.1, 116.0, 86.9, 44.0, 40.7, 40.1, 34.3, 28.6, 25.4, 21.8, 21.4$.

¹⁹F NMR (471 MHz, CDCl₃): $\delta = -62.6$ (1,6), -62.8 (1,4).

HPLC: (Chiralcel OJ-3R, H₂O/MeCN = 50:50, flowrate: 1.0 ml/min, $\lambda = 224$ nm): $t_{r-1,6(\text{major})} = 6.59$ min, $t_{r-1,6(\text{minor})} = 8.24$ min; $t_{r-1,4(\text{major})} = 7.14$ min, $t_{r-1,6(\text{minor})} = 7.40$ min

HRMS (ESIpos): m/z calculated for C₁₉H₁₇O₃F₃Na [M+Na]⁺: 373.1022; found 373.1023.

(±)-2-(3,5-dimethoxyphenyl)-2-(4-hydroxyphenoxy)cyclohexan-1-one (88d)

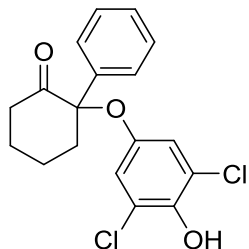


Appearance: colorless solid; 41.2 mg, 60%.

¹H NMR (500 MHz, CDCl₃): $\delta = 6.59$ – 6.52 (m, 6H), 6.42 – 6.39 (m, 1H), 4.68 (s_{br}, 1H), 3.74 (s, 6H), 2.64 (ddd, $J = 12.9, 9.9, 5.5$ Hz, 1H), 2.38 – 2.22 (m, 3H), 2.14 – 2.04 (m, 1H), 2.02 – 1.93 (m, 1H), 1.91 – 1.81 (m, 1H), 1.76 – 1.67 (m, 1H).

¹³C NMR (125 MHz, CDCl₃): $\delta = 208.9, 160.7, 150.7, 148.8, 140.8, 120.8, 115.6, 105.9, 99.9, 87.3, 55.5, 41.2, 40.7, 28.3, 22.0$.

HRMS (ESIpos): m/z calculated for C₂₀H₂₂O₅Na [M+Na]⁺: 365.1359; found 365.1360.

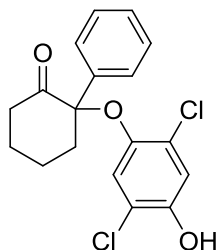
(±)-2-(3,5-dichloro-4-hydroxyphenoxy)-2-phenylcyclohexan-1-one (88f)

Appearance: yellow viscous oil; 45.1 mg, 64% (corresponding hydroquinone as an inseparable impurity).

¹H NMR (500 MHz, CDCl₃): δ = 7.42–7.35 (m, 2H), 7.27–7.19 (m, 3H), 6.81 (s, 1H), 6.60 (s, 2H), 3.05–2.97 (m, 1H), 2.69 (ddd, J = 13.2, 8.5, 4.1 Hz, 1H), 2.63–2.55 (m, 1H), 2.48–2.37 (m, 1H), 2.17–2.07 (m, 1H), 2.01–1.78 (m, 3H).

¹³C NMR (125 MHz, CDCl₃): δ = 209.6, 152.3, 149.2, 142.3, 134.6, 131.4, 129.1, 129.1, 128.1, 121.2, 115.9, 90.9, 40.7, 37.0, 28.3, 22.9.

HRMS (ESIpos): m/z calculated for C₁₈H₁₆O₃Cl₂Na [M+Na]⁺: 373.0369; found 373.0370.

(±)-2-(2,5-dichloro-4-hydroxyphenoxy)-2-phenylcyclohexan-1-one (88g)

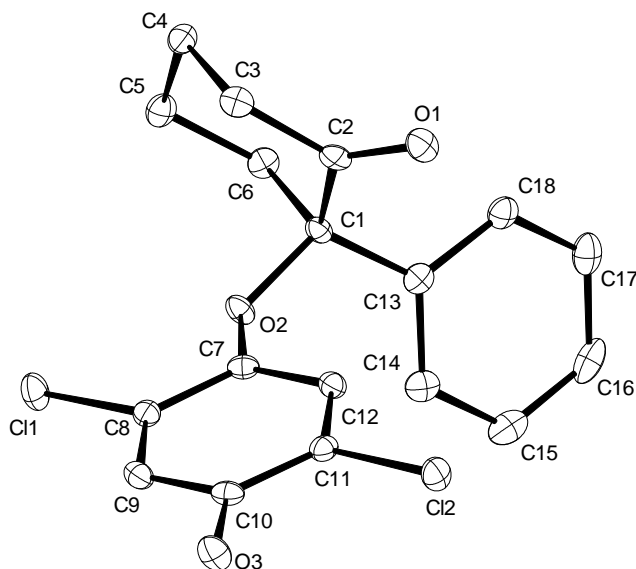
Appearance: yellowish solid; 45.0 mg, 64%. Using (*S*)-**1u**: yellowish solid; 23.2 mg, 33%; 67.5:23.5 er.

¹H NMR (500 MHz, CDCl₃): δ = 7.45–7.30 (m, 5H), 7.04 (s, 1H), 6.50 (s, 1H), 5.18 (s, 1H), 2.72 (ddd, J = 13.2, 10.1, 5.5 Hz, 1H), 2.50 (dddd, J = 14.6, 6.0, 3.8, 1.9 Hz, 1H), 2.42–2.31 (m, 2H), 2.17 (dtt, J = 13.8, 9.8, 4.0 Hz, 1H), 2.09–1.99 (m, 1H), 1.89 (ddq, J = 14.1, 9.7, 4.8 Hz, 1H), 1.77–1.64 (m, 1H).

^{13}C NMR (125 MHz, CDCl_3): δ =208.1, 146.7, 144.8, 137.2, 128.6, 128.5, 127.5, 125.3, 120.3, 117.4, 117.4, 89.5, 41.1, 40.6, 28.2, 21.8.

HPLC: (Chiralcel OJ-3R, $\text{H}_2\text{O}/\text{MeCN}$ = 50:50, flowrate: 1.0 ml/min, λ = 204 nm):
 $t_{r(\text{minor})}$ = 9.64 min, $t_{r(\text{major})}$ = 10.65 min.

HRMS (ESIpos): m/z calculated for $\text{C}_{18}\text{H}_{16}\text{O}_3\text{Cl}_2\text{Na}$ $[\text{M}+\text{Na}]^+$: 373.0369; found 373.0370.

X-Ray Data for (±)-88g:**Table 1. Crystal data and structure refinement.**

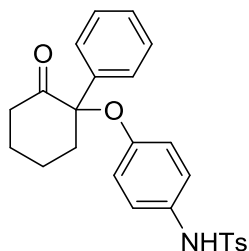
Identification code	11411
Empirical formula	$C_{18}H_{16}Cl_2O_3$
Color	colorless
Formula weight	$351.21 \text{ g} \cdot \text{mol}^{-1}$
Temperature	100(2) K
Wavelength	1.54178 \AA
Crystal system	MONOCLINIC
Space group	$P2_1/c$, (no. 14)
Unit cell dimensions	$a = 11.4609(3) \text{ \AA}$ $\alpha = 90^\circ$. $b = 9.9326(3) \text{ \AA}$ $\beta = 90.2930(10)^\circ$. $c = 13.6207(4) \text{ \AA}$ $\gamma = 90^\circ$.
Volume	$1550.51(8) \text{ \AA}^3$
Z	4
Density (calculated)	$1.505 \text{ Mg} \cdot \text{m}^{-3}$
Absorption coefficient	3.875 mm^{-1}

F(000)	728 e
Crystal size	0.219 x 0.172 x 0.091 mm ³
θ range for data collection	5.512 to 63.542°.
Index ranges	$-13 \leq h \leq 13$, $-11 \leq k \leq 11$, $-15 \leq l \leq 15$
Reflections collected	22268
Independent reflections	2538 [$R_{\text{int}} = 0.0314$]
Reflections with $I > 2\sigma(I)$	2459
Completeness to $\theta = 63.542^\circ$	99.5 %
Absorption correction	Gaussian
Max. and min. transmission	0.8 and 0.6
Refinement method	Full-matrix least-squares on F^2
Data / restraints / parameters	2538 / 0 / 212
Goodness-of-fit on F^2	1.059
Final R indices [$I > 2\sigma(I)$]	$R_1 = 0.0245$ $wR^2 = 0.0642$
R indices (all data)	$R_1 = 0.0253$ $wR^2 = 0.0648$
Largest diff. peak and hole	0.2 and -0.3 e \cdot Å ⁻³

Table 2. Bond lengths [Å] and angles [°].

Cl(1)-C(8)	1.7332(13)	Cl(2)-C(11)	1.7418(13)
O(1)-C(2)	1.2121(17)	O(2)-C(1)	1.4481(16)
O(2)-C(7)	1.3739(16)	O(3)-C(10)	1.3577(17)
C(1)-C(2)	1.5513(18)	C(1)-C(6)	1.5464(18)
C(1)-C(13)	1.5165(19)	C(2)-C(3)	1.504(2)
C(3)-C(4)	1.5362(19)	C(4)-C(5)	1.523(2)
C(5)-C(6)	1.5254(19)	C(7)-C(8)	1.400(2)
C(7)-C(12)	1.3918(19)	C(8)-C(9)	1.380(2)
C(9)-C(10)	1.393(2)	C(10)-C(11)	1.391(2)
C(11)-C(12)	1.3927(19)	C(13)-C(14)	1.393(2)
C(13)-C(18)	1.398(2)	C(14)-C(15)	1.390(2)
C(15)-C(16)	1.386(2)	C(16)-C(17)	1.387(2)
C(17)-C(18)	1.386(2)		
C(7)-O(2)-C(1)	122.46(10)	O(2)-C(1)-C(2)	108.55(10)
O(2)-C(1)-C(6)	103.13(10)	O(2)-C(1)-C(13)	112.10(11)
C(6)-C(1)-C(2)	107.72(10)	C(13)-C(1)-C(2)	115.93(11)
C(13)-C(1)-C(6)	108.55(11)	O(1)-C(2)-C(1)	121.88(12)
O(1)-C(2)-C(3)	123.41(12)	C(3)-C(2)-C(1)	114.69(11)
C(2)-C(3)-C(4)	111.79(11)	C(5)-C(4)-C(3)	110.74(11)
C(4)-C(5)-C(6)	110.94(11)	C(5)-C(6)-C(1)	113.14(11)
O(2)-C(7)-C(8)	115.47(12)	O(2)-C(7)-C(12)	126.18(12)
C(12)-C(7)-C(8)	118.31(12)	C(7)-C(8)-Cl(1)	118.65(10)
C(9)-C(8)-Cl(1)	119.66(11)	C(9)-C(8)-C(7)	121.69(12)
C(8)-C(9)-C(10)	120.33(13)	O(3)-C(10)-C(9)	117.64(12)
O(3)-C(10)-C(11)	124.38(13)	C(11)-C(10)-C(9)	117.98(12)

C(10)-C(11)-Cl(2)	118.28(10)	C(10)-C(11)-C(12)	122.13(13)
C(12)-C(11)-Cl(2)	119.59(11)	C(7)-C(12)-C(11)	119.54(13)
C(14)-C(13)-C(1)	120.73(12)	C(14)-C(13)-C(18)	118.81(13)
C(18)-C(13)-C(1)	119.89(12)	C(15)-C(14)-C(13)	120.71(14)
C(16)-C(15)-C(14)	119.96(14)	C(15)-C(16)-C(17)	119.76(14)
C(18)-C(17)-C(16)	120.38(14)	C(17)-C(18)-C(13)	120.32(14)

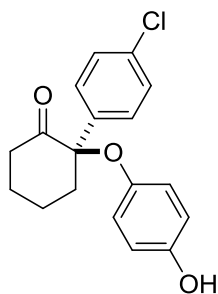
(±)-4-methyl-N-(4-((2-oxo-1-phenylcyclohexyl)oxy)phenyl)benzenesulfonamide (88e)^[201]

Appearance: yellowish solid; 38.7 mg, 44%.

¹H NMR (500 MHz, CDCl₃): δ = 7.52 (d, J = 8.3 Hz, 2H), 7.35–7.28 (m, 5H), 7.17 (d, J = 8.0 Hz, 2H), 6.85–6.70 (m, 2H), 6.61–6.49 (m, 2H), 6.41 (s, 1H), 2.60 (ddd, J = 12.8, 10.9, 5.6 Hz, 1H), 2.44–2.35 (m, 4H), 2.35–2.27 (m, 1H), 2.22 (ddd, J = 14.1, 10.4, 3.7 Hz, 1H), 2.12 (dtt, J = 14.3, 10.4, 3.8 Hz, 1H), 2.03 (dddt, J = 11.4, 5.8, 3.8, 2.0 Hz, 1H), 1.90–1.81 (m, 1H), 1.74–1.65 (m, 1H).

¹³C NMR (125 MHz, CDCl₃): δ = 208.7, 153.6, 143.9, 137.9, 136.1, 130.4, 129.6, 128.3, 128.0, 127.4, 127.3, 124.4, 119.8, 87.7, 42.6, 40.6, 28.5, 21.7 (2x).

HRMS (ESIpos): m/z calculated for C₂₅H₂₅NO₄SNa [M+Na]⁺: 458.1297; found 458.1399.

(R)-2-(4-chlorophenyl)-2-(4-hydroxyphenoxy)cyclohexan-1-one (88h)

Appearance: yellowish solid; 41.8 mg, 66%.

$[\alpha]_D^{25}$: –83.8 (c 0.16, CHCl₃, 94:6 er).

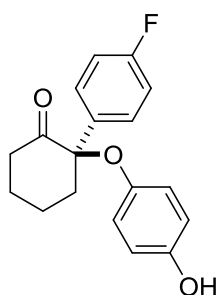
¹H NMR (500 MHz, CDCl₃): δ = 7.37–7.28 (m, 4H), 6.62–6.49 (m, 4H), 4.82 (s_{br}, 1H), 2.66 (td, J = 12.2, 5.7 Hz, 1H), 2.45–2.25 (m, 2H), 2.21–2.01 (m, 3H), 1.90–1.76 (m, 1H), 1.74–1.63 (m, 1H).

^{13}C NMR (125 MHz, CDCl_3): δ = 204.4, 150.6, 148.9, 137.2, 133.8, 128.9, 128.5, 119.8, 115.9, 86.9, 43.1, 40.6, 28.6, 21.6.

HRMS (ESIpos): m/z calculated for $\text{C}_{18}\text{H}_{17}\text{ClO}_3\text{Na}$ $[\text{M}+\text{Na}]^+$: 339.0758; found 339.0760.

HPLC: (Chiralcel OJ-3R, $\text{MeCN}/\text{H}_2\text{O}$ = 50:50, flowrate: 1.0 ml/min, λ = 224 nm):
 $t_{r(\text{minor})}$ = 7.46 min, $t_{r(\text{major})}$ = 8.18 min.

(R)-2-(4-fluorophenyl)-2-(4-hydroxyphenoxy)cyclohexan-1-one (88i)



Appearance: red viscous oil; 44.1 mg, 73%.

$[\alpha]_{\text{D}}^{25}$: -127.3 (c 0.11, CHCl_3 , 93.5:6.5 er).

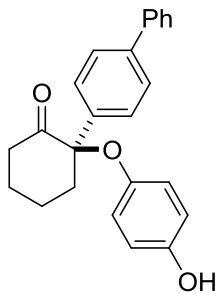
^1H NMR (500 MHz, CDCl_3): δ = 7.38–7.32 (m, 2H), 7.06–7.00 (m, 2H), 6.60–6.50 (m, 4H), 4.63 (sbr, 1H), 2.66 (ddd, J = 12.8, 11.2, 5.6 Hz, 1H), 2.41–2.28 (m, 2H), 2.22–2.10 (m, 2H), 2.09–2.00 (m, 1H), 1.90–1.80 (m, 1H), 1.73–1.64 (m, 1H).

^{13}C NMR (125 MHz, CDCl_3): δ = 209.4, 162.3 (d, J = 247.0 Hz), 150.6, 149.0, 134.3 (d, J = 3.6 Hz), 129.3 (d, J = 8.0 Hz), 120.1, 115.8, 115.2 (d, J = 21.2 Hz), 87.0, 42.8, 40.6, 28.5, 21.7.

^{19}F NMR (471 MHz, CDCl_3): δ = -114.6 .

HRMS (ESIpos): m/z calculated for $\text{C}_{18}\text{H}_{17}\text{O}_3\text{FNa}$ $[\text{M}+\text{Na}]^+$: 323.1054; found 323.1057.

HPLC: (Chiralpak AD-3R, $\text{MeCN}/\text{H}_2\text{O}$ = 50:50, flowrate: 1.0 ml/min, λ = 286 nm):
 $t_{r(\text{majorr})}$ = 10.56 min, $t_{r(\text{minor})}$ = 11.54 min.

(R)-2-([1,1'-biphenyl]-4-yl)-2-(4-hydroxyphenoxy)cyclohexan-1-one (88j)

Appearance: colorless solid; 46.4 mg, 65%.

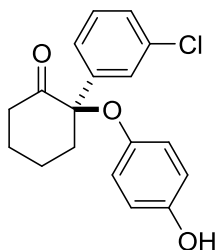
$[\alpha]_D^{25}$: -82.5 (c 0.24, CHCl_3 , 93.5:6.5 er).

^1H NMR (500 MHz, CDCl_3): δ = 7.62–7.55 (m, 4H), 7.47–7.40 (m, 4H), 7.37–7.33 (m, 1H), 6.61–6.51 (m, 4H), 4.80 (s, 1H), 2.71–2.61 (m, 1H), 2.46–2.24 (m, 3H), 2.22–2.11 (m, 1H), 2.10–2.00 (m, 1H), 1.93–1.80 (m, 1H), 1.77–1.65 (m, 1H).

^{13}C NMR (125 MHz, CDCl_3): δ = 209.6, 150.7, 149.1, 140.7, 137.4, 128.9, 127.9, 127.6 (2x), 127.2, 127.0, 120.4, 115.8, 87.4, 42.4, 40.7, 28.5, 21.8.

HRMS (ESIpos): m/z calculated for $\text{C}_{24}\text{H}_{22}\text{O}_3\text{Na}$ $[\text{M}+\text{Na}]^+$: 381.1461; found 381.1461.

HPLC: (Chiralcel OJ-3R, $\text{MeCN}/\text{H}_2\text{O}$ = 50:50, flowrate: 1.0 ml/min, λ = 254 nm):
 $t_{r(\text{minor})}$ = 18.20 min, $t_{r(\text{major})}$ = 23.75 min.

(R)-2-(3-chlorophenyl)-2-(4-hydroxyphenoxy)cyclohexan-1-one (88k)

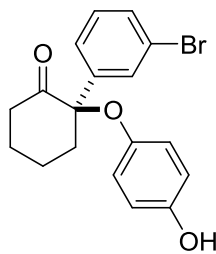
Appearance: red solid; 22.3 mg; 35%; 96:4 er.

^1H NMR (500 MHz, CDCl_3): δ = 7.40 (q, J = 1.4 Hz, 1H), 7.28–7.20 (m, 3H), 6.60–6.50 (m, 4H), 4.75 (s, 1H), 2.64 (ddd, J = 12.9, 11.9, 5.8 Hz, 1H), 2.45–2.35 (m, 1H), 2.34–2.28 (m, 1H), 2.22–2.01 (m, 3H), 1.89–1.77 (m, 1H), 1.68 (dq, J = 13.4, 4.4 Hz, 1H).

^{13}C NMR (125 MHz, CDCl_3): δ = 209.0, 150.6, 148.9, 140.9, 134.2, 129.5, 128.0, 127.6, 125.6, 119.7, 115.9, 86.8, 43.1, 40.7, 28.5, 21.6..

HPLC: (Chiralcel OJ-3R, MeCN/ H_2O = 40:60, flowrate: 1.0 ml/min, λ = 224 nm):
 $t_{r(\text{minor})}$ = 18.39 min, $t_{r(\text{major})}$ = 19.43 min.

(*R*)-2-(3-bromophenyl)-2-(4-hydroxyphenoxy)cyclohexan-1-one (88l)



Appearance: red solid; 34.9 mg, 48%.

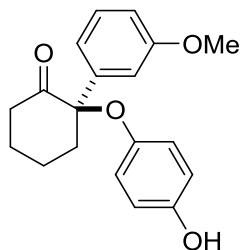
$[\alpha]_{\text{D}}^{25}$: -77.5 (c 0.24, CHCl_3 , 95:5 *er*).

^1H NMR (500 MHz, CDCl_3): δ = 7.56 (t, J = 1.9 Hz, 1H), 7.43 (ddd, J = 7.9, 2.0, 1.0 Hz, 1H), 7.32 (ddd, J = 7.9, 1.7, 1.1 Hz, 1H), 7.21 (t, J = 7.9 Hz, 1H), 6.77–6.19 (m, 4H), 2.65 (ddd, J = 12.8, 11.9, 5.7 Hz, 1H), 2.47–2.36 (m, 1H), 2.36–2.28 (m, 1H), 2.23–1.99 (m, 3H), 1.91–1.78 (m, 1H), 1.70 (dq, J = 13.0, 4.5 Hz, 1H).

^{13}C NMR (125 MHz, CDCl_3): δ = 208.9, 150.6, 148.9, 141.2, 130.9, 130.5, 129.8, 126.0, 122.4, 119.7, 115.9, 86.8, 43.2, 40.7, 28.5, 21.6.

HRMS (ESIpos): m/z calculated for $\text{C}_{18}\text{H}_{17}\text{BrO}_3\text{Na}$ $[\text{M}+\text{Na}]^+$: 385.0253; found 385.0254.

HPLC: (Chiralcel OJ-3R, MeCN/ H_2O = 40:60, flowrate: 1.0 ml/min, λ = 224 nm):
 $t_{r(\text{minor})}$ = 22.04 min, $t_{r(\text{major})}$ = 23.95 min.

(R)-2-(4-hydroxyphenoxy)-2-(3-methoxyphenyl)cyclohexan-1-one (88m)

Appearance: yellowish solid; 29.0 mg, 46%.

$[\alpha]_D^{25}$: -107.6 (c 0.21, CHCl_3 , 95:5 er).

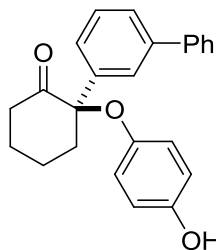
^1H NMR (500 MHz, CDCl_3): δ = 7.34–7.17 (m, 1H), 7.01–6.94 (m, 1H), 6.93 (t, J = 2.1 Hz, 1H), 6.84 (ddd, J = 8.2, 2.6, 0.9 Hz, 1H), 6.58–6.50 (m, 4H), 5.00 (s_{br} , 1H), 3.76 (s, 3H), 2.64 (ddd, J = 13.0, 10.2, 5.5 Hz, 1H), 2.44–2.20 (m, 3H), 2.11 (dt, J = 13.8, 9.8, 4.0 Hz, 1H), 2.03–1.95 (m, 1H), 1.86 (dt, J = 14.3, 9.8, 4.5 Hz, 1H), 1.75–1.65 (m, 1H).

^{13}C NMR (125 MHz, CDCl_3): δ = 209.4, 159.6, 150.8, 148.8, 139.9, 129.4, 120.6, 119.9, 115.7, 113.5, 113.3, 87.3, 55.4, 41.7, 40.7, 28.4, 21.9.

HRMS (ESIpos): m/z calculated for $\text{C}_{19}\text{H}_{20}\text{O}_4\text{Na}$ $[\text{M}+\text{Na}]^+$: 335.1254; found 335.1252.

HPLC: (Chiralcel OJ-3R, $\text{MeCN}/\text{H}_2\text{O}$ = 40:60, flowrate: 1.0 ml/min, λ = 220 nm):

$t_{r(\text{minor})}$ = 9.89 min, $t_{r(\text{major})}$ = 10.71 min.

(R)-2-([1,1'-biphenyl]-3-yl)-2-(4-hydroxyphenoxy)cyclohexan-1-one (88n)

Appearance: colorless solid; 19.6 mg, 55% (0.1 mmol scale).

$[\alpha]_D^{25}$: -105.6 (c 0.18, CHCl_3 , 96.5:3.5 er).

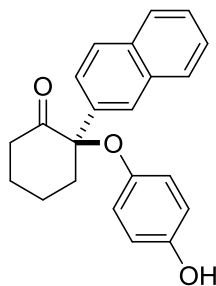
^1H NMR (500 MHz, CDCl_3): δ = 7.59 (t, J = 1.8 Hz, 1H), 7.55–7.51 (m, 3H), 7.45–7.39 (m, 3H), 7.37–7.31 (m, 2H), 4.63 (s_{br}, 1H), 2.67 (ddd, J = 13.0, 10.6, 5.6 Hz, 1H), 2.47–2.26 (m, 3H), 2.17 (dtt, J = 14.0, 10.1, 3.9 Hz, 1H), 2.08–1.99 (m, 1H), 1.93–1.83 (m, 1H), 1.77–1.68 (m, 1H).

^{13}C NMR (125 MHz, CDCl_3): δ = 209.3, 150.6, 149.1, 141.3, 141.1, 138.9, 128.9, 128.7, 127.5, 127.4, 126.8, 126.5, 126.4, 120.5, 115.7, 87.6, 42.4, 40.8, 28.5, 21.9.

HRMS (ESIpos): m/z calculated for $\text{C}_{24}\text{H}_{22}\text{O}_3\text{Na}$ $[\text{M}+\text{Na}]^+$: 381.1461; found 381.1463.

HPLC: (Chiralcel OJ-3R, MeCN/ H_2O = 50:50, flowrate: 1.0 ml/min, λ = 249 nm):
 $t_{r(\text{minor})}$ = 12.64 min, $t_{r(\text{major})}$ = 15.08 min.

(*R*)-2-(4-hydroxyphenoxy)-2-(naphthalen-2-yl)cyclohexan-1-one (88o)



Appearance: yellowish solid; 47.8 mg, 72%.

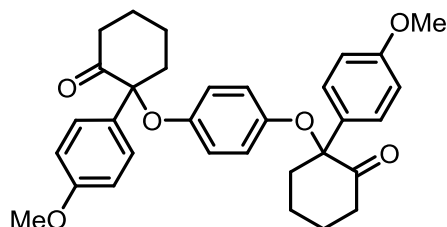
$[\alpha]_D^{25}$: -91.1 (c 0.18, CHCl_3 , 93.5:6.5 er).

^1H NMR (500 MHz, CDCl_3): δ = 7.87 (d, J = 1.8 Hz, 1H), 7.84–7.77 (m, 3H), 7.55–7.43 (m, 3H), 6.62–6.47 (m, 4H), 2.70 (ddd, J = 13.1, 10.5, 5.5 Hz, 1H), 2.48–2.30 (m, 3H), 2.18 (dtt, J = 13.9, 9.9, 4.1 Hz, 1H), 2.08–2.01 (m, 1H), 1.90 (tdt, J = 14.8, 10.6, 4.7 Hz, 1H), 1.76 (dtd, J = 11.8, 6.2, 3.1 Hz, 1H).

^{13}C NMR (125 MHz, CDCl_3): δ = 209.5, 150.7, 148.9, 136.0, 133.1, 132.9, 128.5, 128.0, 127.7, 126.7, 126.5, 126.2, 125.4, 120.6, 115.7, 87.6, 41.8, 40.8, 28.5, 21.9.

HRMS (ESIpos): m/z calculated for $\text{C}_{22}\text{H}_{20}\text{O}_3\text{Na}$ $[\text{M}+\text{Na}]^+$: 355.1305; found 355.1305.

HPLC: (Chiralcel OJ-3R, MeCN/ H_2O = 50:50, flowrate: 1.0 ml/min, λ = 226 nm):
 $t_{r(\text{minor})}$ = 9.53 min, $t_{r(\text{major})}$ = 12.99 min.

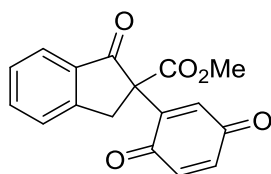
2,2'-(1,4-phenylenebis(oxy))bis(2-(4-methoxyphenyl)cyclohexan-1-one) (90)

Procedure: The product can be obtained using the standard procedure (0.2 mmol scale) as a colorless solid (24.5 mg, 48%, 75:25 er, 1:1 dr). The diastereomeres can only be differentiated by HPLC. Only traces of the targeted monomeric compound were obtained.

¹H NMR (500 MHz, CDCl₃): δ = 7.24–7.19 (m, 4H), 6.87–6.80 (m, 4H), 6.39 (d, J = 2.8 Hz, 4H), 3.80 (s, 6H), 2.59 (ddd, J = 12.8, 9.6, 5.4 Hz, 2H), 2.35–2.18 (m, 6H), 2.09–1.91 (m, 4H), 1.89–1.77 (m, 2H), 1.69–1.61 (m, 2H).

¹³C NMR (125 MHz, CDCl₃): δ = 209.2, 159.2, 150.1, 150.1, 130.1, 130.1, 128.9, 128.8, 120.3, 120.3, 113.7, 87.4, 87.3, 55.3, 41.3, 41.2, 40.5, 28.4, 22.0 (2x).

HRMS (ESIpos): m/z calculated for C₃₂H₃₄O₆Na [M+Na]⁺: 537.2248; found 537.2249.

(±)-methyl 2-(2,5-dihydroxyphenyl)-1-oxo-2,3-dihydro-1H-indene-2-carboxylate (89)

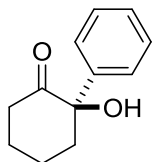
Appearance: red viscous oil; 39.7 mg, 70% (mixture with hydroquinone).

¹H NMR (500 MHz, CDCl₃): δ = 7.84 (dt, J = 7.7, 1.0 Hz, 1H), 7.68 (td, J = 7.5, 1.2 Hz, 1H), 7.49 (dt, J = 7.8, 0.9 Hz, 1H), 7.45 (ddd, J = 8.0, 7.2, 0.9 Hz, 1H), 6.83 (d, J = 10.1 Hz, 1H), 6.80–6.76 (m, 1H), 6.65 (d, J = 2.3 Hz, 1H), 4.30 (d, J = 17.7 Hz, 1H), 3.73 (s, 3H), 3.11 (d, J = 17.7 Hz, 1H).

¹³C NMR (125 MHz, CDCl₃): δ = 198.4, 187.0, 186.4, 168.4, 152.8, 146.7, 136.8, 136.7, 136.7, 136.5, 134.6, 133.1, 128.4, 126.6, 125.3, 62.7, 53.7, 39.8.

HRMS (ESIpos): m/z calculated for $C_{17}H_{12}O_5Na$ $[M+Na]^+$: 319.0577; found 319.0573.

(R)-2-hydroxy-2-phenylcyclohexan-1-one (77a)



Procedure: To a solution of **88a** (50 mg, 0.18 mmol, 1.0 equiv) in MeCN (1 mL) at $-20\text{ }^{\circ}\text{C}$ was added a solution of CAN (388 mg, 0.71 mmol, 4.0 equiv) in MeCN/ H_2O (1/1, 4 mL). The resulting mixture was stirred for an additional hour at $-20\text{ }^{\circ}\text{C}$, then quenched with aqueous Na_2CO_3 solution and diluted with CH_2Cl_2 . The layers were separated and the aqueous layer was washed with CH_2Cl_2 (2x). The combined organic layers were dried over Na_2SO_4 and concentrated under reduced pressure. Purification by flash column chromatography (SiO_2 , hexanes/EtOAc = 10/1) gave the targeted product as a yellow solid (17.3 mg, 51% yield).

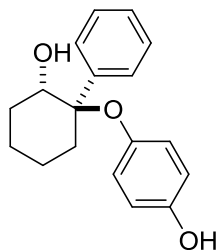
$[\alpha]_D^{25}$: -144.0 (c 0.20, $CHCl_3$, 95:5 er).

1H NMR (500 MHz, $CDCl_3$): δ = 7.42–7.36 (m, 2H), 7.35–7.28 (m, 2H), 4.49 (s_{br} , 1H), 3.04–2.96 (m, 1H), 2.58–2.50 (m, 1H), 2.47–2.40 (m, 1H), 2.11–2.01 (m, 1H), 1.91–1.65 (m, 4H).

^{13}C NMR (125 MHz, $CDCl_3$): δ = 212.9, 140.1, 129.3, 128.5, 126.5, 80.2, 39.0, 39.0, 28.5, 23.2.

HRMS (ESIpos): m/z calculated for $C_{12}H_{14}O_3Na$ $[M+Na]^+$: 213.0886; found 213.0885.

HPLC (Chiralpak AD-3, $nHept/EtOH$ = 80:20, flowrate: 1.0 ml/min, λ = 206 nm):
 $t_{r(minor)}$ = 6.76 min, $t_{r(major)}$ = 9.52 min.

4-(((1*R*,2*S*)-2-hydroxy-1-phenylcyclohexyl)oxy)phenol (91)

Procedure: To a solution of **88a** (56.5 mg, 0.2 mmol, 1.0 equiv) in anhydrous THF (5 mL) was added K-Selectride (1 M in THF, 0.8 mL, 0.4 mmol, 4.0 equiv) at -78°C . The cold bath was removed and the resulting mixture was stirred for 2 h. The reaction was quenched by addition of 1 M NaOH and H_2O_2 (30%) and stirred at room temperature overnight. The layers were separated and the aqueous layer was extracted with CH_2Cl_2 . The combined organic layers were dried over Na_2SO_4 and concentrated under reduced pressure. Purification by flash column chromatography (SiO_2 , hexanes/EtOAc) afforded the targeted product as a colorless solid (49.0 mg, 86%, dr > 20:1).

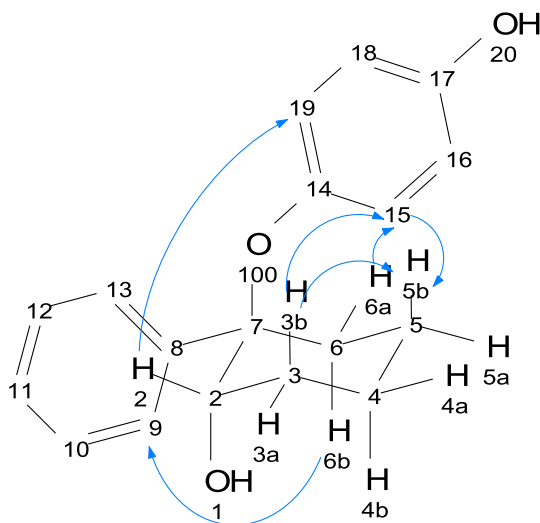
^1H NMR (500 MHz, CDCl_3): δ = 7.55–7.49 (m, 2H, 9, 13), 7.40 (t, J = 8.4, 6.9 Hz, 2H, 10, 12), 7.37–7.29 (m, 1H, 11), 6.54 (d, J = 9.0 Hz, 2H, 16, 18), 6.46 (d, J = 9.0 Hz, 2H, 15, 19), 4.29 (d, J = 1.7 Hz, 1H, 20), 3.96–3.90 (m, 1H, 2), 2.35 (ddd, J = 14.3, 9.9, 7.2 Hz, 1H, 6b), 2.30 (d, J = 13.8 Hz, 1H, 3b), 2.24 (dm, J = 14.3 Hz, 1H, 6a), 1.86 (dq, J = 13.7, 3.0 Hz, 1H, 3a), 1.67 (dt, J = 5.8, 3.1 Hz, 1H, 4b), 1.53–1.45 (m, 3H, 4a, 5a, 5b), 1.23 (dd, J = 2.9, 1.7 Hz, 1H, 1).

^{13}C NMR (125 MHz, CDCl_3): δ = 149.9 (17), 149.2 (14), 144.0 (8), 129.2 (12, 10), 128.2 (11), 127.0 (13, 9), 120.3 (19, 15), 115.8 (18, 16), 82.0 (7), 77.6, 77.4, 77.10, 74.3 (2), 28.5 (3), 24.9 (6), 21.0 (5), 19.3 (4).

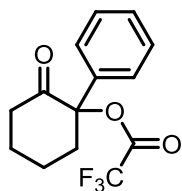
HRMS (ESIpos): m/z calculated for $\text{C}_{18}\text{H}_{20}\text{O}_3\text{Na}$ $[\text{M}+\text{Na}]^+$: 307.1305; found 307.1306.

HPLC (Chiralcel OD-3R, MeCN/ H_2O = 60:40, flowrate: 1.0 ml/min, λ = 220 nm): $t_{r(\text{minor})}$ = 3.66 min, $t_{r(\text{major})}$ = 4.27 min.

The structure was confirmed by 2D-NMR experiments. Obtained NOEs and couplings are depicted below:



2-oxo-1-phenylcyclohexyl 2,2,2-trifluoroacetate (**92**)



Procedure: To a solution of **88a** (30 mg, 0.11 mmol, 1.0 equiv) in CH_2Cl_2 (0.3 mL) was added TFA (81 μL , 1.05 mmol, 10.0 equiv) at room temperature. The solution was stirred for further 6 h and then quenched by slow addition of aq. sat. NaHCO_3 solution. After extraction with CH_2Cl_2 , the combined organic layers were dried over Na_2SO_4 and the solvent was removed under reduced pressure. The crude product was purified by FCC (SiO_2 , hexanes/ EtOAc = 10/1) to give **92** (9.7 mg, 32%) as clear oil.

^1H NMR (500 MHz, CDCl_3): δ = 7.54–7.37 (m, 5H), 2.95 (dq, J = 13.8, 3.5 Hz, 1H), 2.74–2.58 (m, 2H), 2.40 (ddd, J = 14.4, 12.0, 5.7 Hz, 1H), 2.05–1.75 (m, 4H).

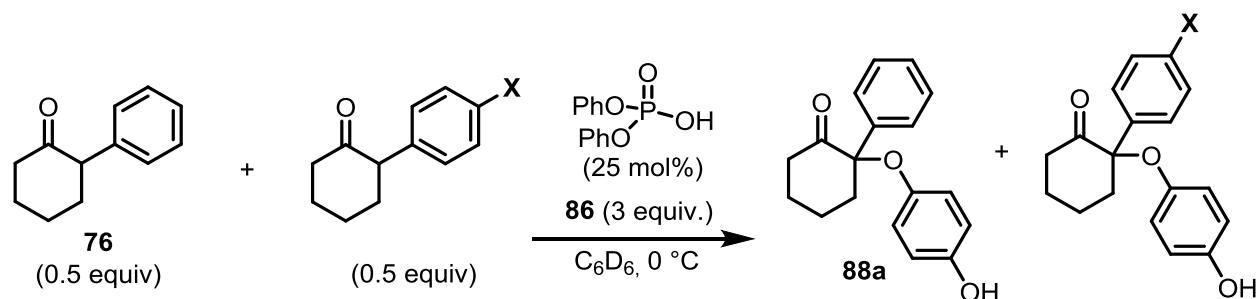
^{13}C NMR (125 MHz, CDCl_3): δ = 202.1, 134.4, 129.8, 129.2, 127.7, 90.9, 40.3, 35.1, 26.6, 23.1 (some signals not visible due to noise).

^{19}F NMR (471 MHz, CDCl_3): δ = –75.34.

HRMS (ESIpos): m/z calculated for $C_{14}H_{13}O_3F_3Na$ $[M+Na]^+$: 307.0709; found 307.0712.

HPLC (Chiralcel OD-3, n Hept/ i PrOH = 98:2, flowrate: 1.0 ml/min, λ = 220 nm): t_{r1} = 3.85 min, t_{r2} = 4.32 min.

7.5.3 Details on Hammett Plot Analysis



Procedure: A screw-cap GC-vial equipped with 2-phenyl cyclohexanone (**76**, 0.05 mmol, 0.5 equiv), the corresponding ketone (0.05 mmol, 0.5 equiv) and 1,4-benzoquinone (**86**, 32.4 mg, 0.3 mmol, 3.0 equiv) in anhydrous C_6D_6 (0.2 mL) was placed in a cryostat ($0\text{ }^{\circ}C$). After stirring the mixture for 10 min, a $0\text{ }^{\circ}C$ cold solution of DPP (12.5 mg, 0.05 mmol, 25 mol%) and triphenylmethane (internal standard, 12.2 mg, 0.05 mmol, 0.25 equiv) in anhydrous C_6D_6 (0.2 mL) was added. Aliquots were taken every 30 min for the next 150 min using a glass pipet and analyzed by 1H -NMR. **Note:** The reaction stops under high dilution.

The kinetic data was analyzed by comparison of product formation to an internal standard, using the aromatic signals of the formed hydroquinone as handle for integration:

X = CF_3 ~6.58 ppm (m, 2H)

X = Me The signal at ~6.30 ppm (overlap of both substrates) was subtracted by twice the integral of the signal at ~6.70 ppm (due to overlap this one equals 1/2 of X = H)

X = Cl ~6.62 ppm (m, 2H)

X = F ~6.25 ppm (m, 1H) compared to 6.29 (X = H, m, 1H)

The determined NMR ratios were used to plot the relative initial rates of the two competing substrates. Using Excel the slope for each pair was determined. Except $X = \text{Me}$ each experiment was performed twice. The $\log(k_X/k_H)$ was calculated from the corresponding slopes.

Using EXCEL, the slope of each relative kinetic profile was determined (when $X = \text{H}$; $k = 0.401$, when $X = \text{CF}_3$; $k = 0.089$) and therefore $\log(k_{\text{Cl}}/k_H) = -0.665$. This procedure was performed on the relative kinetic data with the remaining substrates in comparison to the standard substrate ($X = \text{H}$) to obtain the $\log(k_X/k_H)$ for each substrate. The $\log(k_X/k_H)$ for each substrate was then plotted against the corresponding σ , σ^+ and σ^- values taken from the literature.

8 Bibliography

- [1] a) W. S. Knowles, *Angew. Chem. Int. Ed.* **2002**, *41*, 1998–2007; b) R. Noyori, *Angew. Chem. Int. Ed.* **2002**, *41*, 2008–2022; c) K. B. Sharpless, *Angew. Chem. Int. Ed.* **2002**, *41*, 2024–2032.
- [2] a) B. List, *Angew. Chem. Int. Ed.* **2010**, *49*, 1730–1734; b) G. Bredig, P. S. Fiske, *Biochem. Z.* **1912**, *46*, 7; c) V. Prelog, M. Wilhelm, *Helv. Chim. Acta* **1954**, *37*, 1634–1660; d) H. Pracejus, *Liebigs Ann. Chem.* **1960**, *634*, 9–22.
- [3] B. List, R. A. Lerner, C. F. Barbas, *J. Am. Chem. Soc.* **2000**, *122*, 2395–2396.
- [4] K. A. Ahrendt, C. J. Borths, D. W. C. MacMillan, *J. Am. Chem. Soc.* **2000**, *122*, 4243–4244.
- [5] B. List, *Asymmetric Organocatalysis*, Vol. 291, Springer-Verlag Berlin Heidelberg, **2009**.
- [6] J. Seayad, B. List, *Org. Biomol. Chem.* **2005**, *3*, 719–724.
- [7] M. R. Monaco, G. Pupo, B. List, *Synlett* **2016**, *27*, 1027–1040.
- [8] a) J. N. Brönsted, *Recueil des Travaux Chimiques des Pays-Bas* **1923**, *42*, 718–728; b) T. M. Lowry, *Journal of the Society of Chemical Industry* **1923**, *42*, 43–47.
- [9] D. Parmar, E. Sugiono, S. Raja, M. Rueping, *Chemical Reviews* **2014**, *114*, 9047–9153.
- [10] D. Kampen, C. M. Reisinger, B. List, in *Asymmetric Organocatalysis* (Ed.: B. List), Springer Berlin Heidelberg, Berlin, Heidelberg, **2009**, pp. 1–37.
- [11] M. Fleischmann, D. Drettwan, E. Sugiono, M. Rueping, M. Gschwind Ruth, *Angew. Chem. Int. Ed.* **2011**, *50*, 6364–6369.
- [12] M. S. Sigman, E. N. Jacobsen, *J. Am. Chem. Soc.* **1998**, *120*, 4901–4902.
- [13] Y. Huang, A. K. Unni, A. N. Thadani, V. H. Rawal, *Nature* **2003**, *424*, 146.
- [14] A. G. Doyle, E. N. Jacobsen, *Chem. Rev.* **2007**, *107*, 5713–5743.
- [15] T. Akiyama, J. Itoh, K. Yokota, K. Fuchibe, *Angew. Chem. Int. Ed.* **2004**, *43*, 1566–1568.
- [16] D. Uraguchi, M. Terada, *J. Am. Chem. Soc.* **2004**, *126*, 5356–5357.
- [17] a) M. Hatano, K. Moriyama, T. Maki, K. Ishihara, *Angew. Chem. Int. Ed.* **2010**, *49*, 3823–3826; b) M. Klussmann, L. Ratjen, S. Hoffmann, V. Wakchaure, R. Goddard, B. List, *Synlett* **2010**, *2010*, 2189–2192.
- [18] S. Hoffmann, M. Seayad Abdul, B. List, *Angew. Chem. Int. Ed.* **2005**, *44*, 7424–7427.
- [19] T. Akiyama, Y. Saitoh, H. Morita, K. Fuchibe, *Adv. Synt. Catal.* **2005**, *347*, 1523–1526.
- [20] X.-H. Chen, X.-Y. Xu, H. Liu, L.-F. Cun, L.-Z. Gong, *J. Am. Chem. Soc.* **2006**, *128*, 14802–14803.
- [21] G. B. Rowland, H. Zhang, E. B. Rowland, S. Chennamadhavuni, Y. Wang, J. C. Antilla, *J. Am. Chem. Soc.* **2005**, *127*, 15696–15697.
- [22] K. Mori, K. Ehara, K. Kurihara, T. Akiyama, *J. Am. Chem. Soc.* **2011**, *133*, 6166–6169.
- [23] a) I. Čorić, S. Müller, B. List, *J. Am. Chem. Soc.* **2010**, *132*, 17370–17373; b) F. Xu, D. Huang, C. Han, W. Shen, X. Lin, Y. Wang, *J. Org. Chem.* **2010**, *75*, 8677–8680.
- [24] D. Nakashima, H. Yamamoto, *J. Am. Chem. Soc.* **2006**, *128*, 9626–9627.
- [25] K. Kaupmees, N. Tolstoluzhsky, S. Raja, M. Rueping, I. Leito, *Angew. Chem. Int. Ed.* **2013**, *52*, 11569–11572.
- [26] a) G. Pousse, A. Devineau, V. Dalla, L. Humphreys, M.-C. Lasne, J. Rouden, J. Blanchet, *Tetrahedron* **2009**, *65*, 10617–10622; b) N. D. Shapiro, V. Rauniyar, G. L. Hamilton, J. Wu, F. D. Toste, *Nature* **2011**, *470*, 245.
- [27] a) P. García-García, F. Lay, P. García-García, C. Rabalakos, B. List, *Angew. Chem. Int. Ed.* **2009**, *48*, 4363–4366; b) S. Prévost, N. Dupré, M. Leutzsch, Q. Wang, V. Wakchaure, B. List, *Angew. Chem. Int. Ed.* **2014**, *53*, 8770–8773; c) N. Wakchaure Vijay, S. J. Kaib

- Philip, M. Leutzsch, B. List, *Angew. Chem. Int. Ed.* **2015**, *54*, 11852–11856; d) N. Wakchaure Vijay, B. List, *Angew. Chem. Int. Ed.* **2016**, *55*, 15775–15778.
- [28] a) I. Čorić, B. List, *Nature* **2012**, *483*, 315; b) J. H. Kim, I. Čorić, S. Vellalath, B. List, *Angew. Chem. Int. Ed.* **2013**, *52*, 4474–4477; c) S. Liao, I. Čorić, Q. Wang, B. List, *J. Am. Chem. Soc.* **2012**, *134*, 10765–10768; d) G. Chit Tsui, L. Liu, B. List, *Angew. Chem. Int. Ed.* **2015**, *54*, 7703–7706; e) L. Liu, M. Leutzsch, Y. Zheng, M. W. Alachraf, W. Thiel, B. List, *J. Am. Chem. Soc.* **2015**, *137*, 13268–13271; f) S. Das, L. Liu, Y. Zheng, M. W. Alachraf, W. Thiel, C. K. De, B. List, *J. Am. Chem. Soc.* **2016**, *138*, 9429–9432.
- [29] L. Liu, P. S. J. Kaib, A. Tap, B. List, *J. Am. Chem. Soc.* **2016**, *138*, 10822–10825.
- [30] P. S. J. Kaib, L. Schreyer, S. Lee, R. Properzi, B. List, *Angew. Chem. Int. Ed.* **2016**, *55*, 13200–13203.
- [31] a) L. Liu, H. Kim, Y. Xie, C. Farès, P. S. J. Kaib, R. Goddard, B. List, *J. Am. Chem. Soc.* **2017**, *139*, 13656–13659; b) N. Tsuji, J. L. Kennemur, T. Buyck, S. Lee, S. Prévost, P. S. J. Kaib, D. Bykov, C. Farès, B. List, *Science* **2018**, *359*, 1501.
- [32] I. Fleming, *Molecular Orbitals and Organic Chemical Reactions - Student Edition*, John Wiley & Sons Ltd., **2009**.
- [33] A. Lapworth, *J. Soc. Chem. Trans.* **1904**, *85*, 30–42.
- [34] J. Clayden, N. Greeves, S. Warren, P. Wothers, *Organic Chemistry*, Oxford University Press, New York, **2001**.
- [35] F. G. Bordwell, *Acc. Chem. Res.* **1988**, *21*, 456–463.
- [36] a) E. V. Anslyn, D. A. Dougherty, *Modern Physical Organic Chemistry*, University Science Books, **2006**; b) J. R. Keeffe, A. J. Kresge, N. P. Schepp, *J. Am. Chem. Soc.* **1990**, *112*, 4862–4868.
- [37] H. Hart, *Chem. Rev.* **1979**, *79*, 515–528.
- [38] a) G. S. Hammond, *J. Am. Chem. Soc.* **1955**, *77*, 334–338; b) J. E. Leffler, *Science* **1953**, *117*, 340.
- [39] C. Rappe, W. H. Sachs, *J. Org. Chem.* **1967**, *32*, 3700–3703.
- [40] M. A. Yamada Yoichi, N. Yoshikawa, H. Sasai, M. Shibasaki, *Angew. Chem. Int. Ed.* **1997**, *36*, 1871–1873.
- [41] H. Sasai, T. Suzuki, N. Itoh, K. Tanaka, T. Date, K. Okamura, M. Shibasaki, *J. Am. Chem. Soc.* **1993**, *115*, 10372–10373.
- [42] a) Y. M. A. Yamada, M. Shibasaki, *Tetrahedron Lett.* **1998**, *39*, 5561–5564; b) N. Yoshikawa, Y. M. A. Yamada, J. Das, H. Sasai, M. Shibasaki, *J. Am. Chem. Soc.* **1999**, *121*, 4168–4178.
- [43] a) M. Shibasaki, M. Kanai, S. Matsunaga, N. Kumagai, *Acc. Chem. Res.* **2009**, *42*, 1117–1127; b) H. Gröger, *Eur. J. Org. Chem.* **2016**, *2016*, 4116–4123; c) N. Kumagai, M. Kanai, H. Sasai, *ACS Catal.* **2016**, *6*, 4699–4709.
- [44] N. Kumagai, S. Matsunaga, T. Kinoshita, S. Harada, S. Okada, S. Sakamoto, K. Yamaguchi, M. Shibasaki, *J. Am. Chem. Soc.* **2003**, *125*, 2169–2178.
- [45] a) B. M. Trost, H. Ito, *J. Am. Chem. Soc.* **2000**, *122*, 12003–12004; b) B. M. Trost, H. Ito, E. R. Silcoff, *J. Am. Chem. Soc.* **2001**, *123*, 3367–3368.
- [46] B. M. Trost, M. J. Bartlett, *Acc. Chem. Res.* **2015**, *48*, 688–701.
- [47] a) B. M. Trost, T. Saget, C.-I. Hung, *J. Am. Chem. Soc.* **2016**, *138*, 3659–3662; b) B. M. Trost, J. S. Tracy, T. Saget, *Chem. Sci.* **2018**, *9*, 2975–2980.
- [48] a) H. Inoue, M. Kikuchi, J.-i. Ito, H. Nishiyama, *Tetrahedron* **2008**, *64*, 493–499; b) M. Mizuno, H. Inoue, T. Naito, L. Zhou, H. Nishiyama, *Chem. Eur. J.* **2009**, *15*, 8985–8988.
- [49] R. Mahrwald, B. Ziemer, *Tetrahedron Lett.* **2002**, *43*, 4459–4461.

- [50] W. Li, X. Liu, X. Hao, X. Hu, Y. Chu, W. Cao, S. Qin, C. Hu, L. Lin, X. Feng, *J. Am. Chem. Soc.* **2011**, *133*, 15268–15271.
- [51] a) M. Shang, M. Cao, Q. Wang, M. Wasa, *Angew. Chem. Int. Ed.* **2017**, *56*, 13338–13341; b) M. Shang, X. Wang, S. M. Koo, J. Youn, J. Z. Chan, W. Yao, B. T. Hastings, M. Wasa, *J. Am. Chem. Soc.* **2017**, *139*, 95–98.
- [52] A. Ting, J. M. Goss, N. T. McDougal, S. E. Schaus, in *Asymmetric Organocatalysis* (Ed.: B. List), Springer Berlin Heidelberg, Berlin, Heidelberg, **2009**, pp. 201–232.
- [53] a) T. Takeda, M. Terada, *J. Am. Chem. Soc.* **2013**, *135*, 15306–15309; b) H. Krawczyk, M. Dziegielewska, D. Deredas, A. Albrecht, Ł. Albrecht, *Chem. Eur. J.* **2015**, *21*, 10268–10277.
- [54] a) S. Mukherjee, J. W. Yang, S. Hoffmann, B. List, *Chem. Rev.* **2007**, *107*, 5471–5569; b) P. M. Pihko, I. Majander, A. Erkkilä, in *Asymmetric Organocatalysis* (Ed.: B. List), Springer Berlin Heidelberg, Berlin, Heidelberg, **2009**, pp. 145–200; c) L. Zhang, N. Fu, S. Luo, *Acc. Chem. Res.* **2015**, *48*, 986–997.
- [55] P. Melchiorre, *Angew. Chem. Int. Ed.* **2012**, *51*, 9748–9770.
- [56] a) J. Y. Kang, R. G. Carter, *Org. Lett.* **2012**, *14*, 3178–3181; b) J. Y. Kang, R. C. Johnston, K. M. Snyder, P. H.-Y. Cheong, R. G. Carter, *J. Org. Chem.* **2016**, *81*, 3629–3637.
- [57] X. Yang, R. J. Phipps, F. D. Toste, *J. Am. Chem. Soc.* **2014**, *136*, 5225–5228.
- [58] a) H. Liu, L.-F. Cun, A.-Q. Mi, Y.-Z. Jiang, L.-Z. Gong, *Org. Lett.* **2006**, *8*, 6023–6026; b) M. Rueping, C. Azap, *Angew. Chem. Int. Ed.* **2006**, *45*, 7832–7835.
- [59] Q.-X. Guo, H. Liu, C. Guo, S.-W. Luo, Y. Gu, L.-Z. Gong, *J. Am. Chem. Soc.* **2007**, *129*, 3790–3791.
- [60] K. Mori, T. Katoh, T. Suzuki, T. Noji, M. Yamanaka, T. Akiyama, *Angew. Chem. Int. Ed.* **2009**, *48*, 9652–9654.
- [61] L. Song, Q. X. Guo, X. C. Li, J. Tian, Y. G. Peng, *Angew. Chem. Int. Ed.* **2012**, *124*, 1935–1938.
- [62] G. Pousse, F. L. Cavelier, L. Humphreys, J. Rouden, J. Blanchet, *Org. Lett.* **2010**, *12*, 3582–3585.
- [63] I. Felker, G. Pupo, P. Kraft, B. List, *Angew. Chem. Int. Ed.* **2015**, *54*, 1960–1964.
- [64] a) A. R. Burns, A. G. E. Madec, D. W. Low, I. D. Roy, H. W. Lam, *Chem. Sci.* **2015**, *6*, 3550–3555; b) L.-D. Zhang, L.-R. Zhong, J. Xi, X.-L. Yang, Z.-J. Yao, *J. Org. Chem.* **2016**, *81*, 1899–1904.
- [65] X. Yang, F. D. Toste, *Chem. Sci.* **2016**, *7*, 2653–2656.
- [66] G. Pupo, R. Properzi, B. List, *Angew. Chem. Int. Ed.* **2016**, *55*, 6099–6102.
- [67] a) W. S. Rapson, R. Robinson, *J. Chem. Soc.* **1935**, 1285–1288; b) E. C. du Feu, F. J. McQuillin, R. Robinson, *J. Chem. Soc.* **1937**, 53–60; c) R. E. Gawley, *Synthesis* **1976**, 1976, 777–794.
- [68] C. H. Heathcock, J. E. Ellis, J. E. McMurry, A. Coppolino, *Tetrahedron Lett.* **1971**, *12*, 4995–4996.
- [69] A. J. Frontier, S. Raghavan, S. J. Danishefsky, *J. Am. Chem. Soc.* **2000**, *122*, 6151–6159.
- [70] J. D. White, P. Hrnčiar, F. Stappenbeck, *J. Org. Chem.* **1999**, *64*, 7871–7884.
- [71] B. Shi, N. A. Hawryluk, B. B. Snider, *J. Org. Chem.* **2003**, *68*, 1030–1042.
- [72] American Chemical Society International Historic Chemical Landmarks. The “Marker Degradation” and Creation of the Mexican Steroid Hormone Industry 1938–1945. <http://www.acs.org/content/acs/en/education/whatischemistry/landmarks/progesteronesynthesis.html> (accessed May 8th, 2018).

- [73] C. Djerassi, *Steroids* **1992**, 57, 631–641.
- [74] a) S. Ramachandran, M. S. Newman, *Org. Synth.* **1961**, 41, 38–41; b) S. Swaminathan, M. S. Newman, *Tetrahedron* **1958**, 2, 88–99.
- [75] a) W. Acklin, V. Prelog, A. P. Prieto, *Helv. Chim. Acta* **1958**, 41, 1416–1424; b) Z. G. Hajos, D. R. Parrish, E. P. Oliveto, *Tetrahedron* **1968**, 24, 2039–2046; c) L. Velluz, J. Mathieu, G. Nominé, *Tetrahedron* **1966**, 22, 495–505.
- [76] Z. G. Hajos, D. R. Parrish, German Patent DE 2102623 1971
- [77] Z. G. Hajos, D. R. Parrish, *J. Org. Chem.* **1974**, 39, 1615–1621.
- [78] U. Eder, G. Sauer, R. Wiechert, *Angew. Chem. Int. Ed.* **1971**, 10, 496–497.
- [79] L. Kürti, B. Czako, *Strategic Applications of Named Reactions in Organic Synthesis*, Elsevier Academic Press, **2005**.
- [80] S. Bahmanyar, K. N. Houk, H. J. Martin, B. List, *J. Am. Chem. Soc.* **2003**, 125, 2475–2479.
- [81] a) C. F. Barbas, *Angew. Chem. Int. Ed.* **2008**, 47, 42–47; b) D. W. C. MacMillan, *Nature* **2008**, 455, 304.
- [82] B. W. Katona, N. P. Rath, S. Anant, W. F. Stenson, D. F. Covey, *J. Org. Chem.* **2007**, 72, 9298–9307.
- [83] C. D. Dzierba, K. S. Zandi, T. Möllers, K. J. Shea, *J. Am. Chem. Soc.* **1996**, 118, 4711–4712.
- [84] H. M. Lee, C. Nieto-Oberhuber, M. D. Shair, *J. Am. Chem. Soc.* **2008**, 130, 16864–16866.
- [85] S. P. Waters, Y. Tian, Y.-M. Li, S. J. Danishefsky, *J. Am. Chem. Soc.* **2005**, 127, 13514–13515.
- [86] B. Bradshaw, J. Bonjoch, *Synlett* **2012**, 2012, 337–356.
- [87] T. Akiyama, T. Katoh, K. Mori, *Angew. Chem. Int. Ed.* **2009**, 48, 4226–4228.
- [88] G. Zhong, T. Hoffmann, R. A. Lerner, S. Danishefsky, C. F. Barbas, *J. Am. Chem. Soc.* **1997**, 119, 8131–8132.
- [89] T. Bui, C. F. Barbas, *Tetrahedron Lett.* **2000**, 41, 6951–6954.
- [90] B. Bradshaw, G. Etxebarria-Jardi, J. Bonjoch, F. Vióquez Santiago, G. Guillena, C. Nájera, *Adv. Synt. Catal.* **2009**, 351, 2482–2490.
- [91] C. Xu, L. Zhang, P. Zhou, S. Luo, J.-P. Cheng, *Synthesis* **2013**, 45, 1939–1945.
- [92] a) J. M. Janey, *Angew. Chem. Int. Ed.* **2005**, 44, 4292–4300; b) A. M. R. Smith, K. K. Hii, *Chem. Rev.* **2011**, 111, 1637–1656; c) T. Vilaivan, W. Bhanthumnavin, *Molecules* **2010**, 15, 917; d) D. J. Ager, I. Prakash, D. R. Schaad, *Chem. Rev.* **1996**, 96, 835–876.
- [93] Ketamine is part of the 18th WHO model list of essential medicines. More information can be found on the website of the WHO: <http://www.who.int>
- [94] a) S. Reardon, *Nature* **2015**, 517, 130–131; b) C. J. A. Morgan, H. V. Curran, *Addiction* **2012**, 107, 27–38; c) M. I. Blonk, B. G. Koder, P. M. L. A. Bemt, F. J. P. M. Huygen, *Eur. J. Pain* **2010**, 14, 466–472.
- [95] a) H. A. Adams, C. Werner, *Der Anaesthetist* **1997**, 46, 1026–1042; b) G. Hempelmann, D. F. M. Kuhn, *Der Anaesthetist* **1997**, 46, S3–S7.
- [96] a) G. Li, H. T. Chang, K. B. Sharpless, *Angew. Chem. Int. Ed.* **1996**, 35, 451–454; b) J. A. Bodkin, M. D. McLeod, *J. Chem. Soc., Perkin Trans. 1* **2002**, 2733–2746.
- [97] a) W. Oppolzer, O. Tamura, G. Sundarababu, M. Signer, *J. Am. Chem. Soc.* **1992**, 114, 5900A Modular Strategy for the Direct Catalytic Asymmetric α -Amination of Carbonyl Compounds
- 5902; b) C. Greck, B. Drouillat, C. Thomassigny, *Eur. J. Org. Chem.* **2004**, 2004, 1377–1385.

- [98] a) S. Saaby, M. Bella, K. A. Jørgensen, *J. Am. Chem. Soc.* **2004**, *126*, 8120–8121; b) X. Xu, T. Yabuta, P. Yuan, Y. Takemoto, *Synlett* **2006**, *2006*, 137–140; c) M. Terada, M. Nakano, H. Ube, *J. Am. Chem. Soc.* **2006**, *128*, 16044–16045; d) R. He, X. Wang, T. Hashimoto, K. Maruoka, *Angew. Chem. Int. Ed.* **2008**, *47*, 9466–9468; e) C. Xu, L. Zhang, S. Luo, *Angew. Chem. Int. Ed.* **2014**, *53*, 4149–4153; f) X. Han, F. Zhong, Y. Lu, *Adv. Synt. Catal.* **2010**, *352*, 2778–2782; g) M. Terada, D. Tsushima, M. Nakano, *Adv. Synt. Catal.* **2009**, *351*, 2817–2821; h) C. Xu, L. Zhang, S. Luo, *J. Org. Chem.* **2014**, *79*, 11517–11526; i) F. Zhou, F.-M. Liao, J.-S. Yu, J. Zhou, *Synthesis* **2014**, *46*, 2983–3003; j) H. M. Nelson, J. S. Patel, H. P. Shunatona, F. D. Toste, *Chem. Sci.* **2015**, *6*, 170–173; k) N. Momiyama, H. Yamamoto, *J. Am. Chem. Soc.* **2004**, *126*, 5360–5361; l) K. Ohmatsu, Y. Ando, T. Nakashima, T. Ooi, *Chem* **2016**, *1*, 802–810.
- [99] D. A. Evans, S. G. Nelson, *J. Am. Chem. Soc.* **1997**, *119*, 6452–6453.
- [100] B. List, *J. Am. Chem. Soc.* **2002**, *124*, 5656–5657.
- [101] A. Bøgevig, K. Juhl, N. Kumaragurubaran, W. Zhuang, K. A. Jørgensen, *Angew. Chem. Int. Ed.* **2002**, *41*, 1790–1793.
- [102] A. Bøgevig, H. Sundén, A. Córdova, *Angew. Chem. Int. Ed.* **2004**, *43*, 1109–1112.
- [103] T.-Y. Liu, H.-L. Cui, Y. Zhang, K. Jiang, W. Du, Z.-Q. He, Y.-C. Chen, *Org. Lett.* **2007**, *9*, 3671–3674.
- [104] M. Shang, X. Wang, S. M. Koo, J. Youn, J. Z. Chan, W. Yao, B. T. Hastings, M. Wasa, *J. Am. Chem. Soc.* **2017**, *139*, 95–98.
- [105] a) H. Vogt, S. Vanderheiden, S. Bräse, *Chem. Commun.* **2003**, 2448–2449; b) C. E. Hartmann, T. Baumann, M. Bächle, S. Bräse, *Tetrahedron: Asymmetry* **2010**, *21*, 1341–1349.
- [106] J.-Y. Fu, X.-Y. Xu, Y.-C. Li, Q.-C. Huang, L.-X. Wang, *Org. Biomol. Chem.* **2010**, *8*, 4524–4526.
- [107] a) J.-Y. Fu, Q.-C. Yang, Q.-L. Wang, J.-N. Ming, F.-Y. Wang, X.-Y. Xu, L.-X. Wang, *J. Org. Chem.* **2011**, *76*, 4661–4664; b) C. Liu, Q. Zhu, K.-W. Huang, Y. Lu, *Org. Lett.* **2011**, *13*, 2638–2641.
- [108] a) N. S. Chowdari, C. F. Barbas, *Org. Lett.* **2005**, *7*, 867–870; b) J. T. Suri, D. D. Steiner, C. F. Barbas, *Org. Lett.* **2005**, *7*, 3885–3888.
- [109] Z.-Q. Zhang, T. Chen, F.-M. Zhang, *Org. Lett.* **2017**, *19*, 1124–1127.
- [110] a) M. G. Edwards, M. N. Kenworthy, R. R. A. Kitson, M. S. Scott, R. J. K. Taylor, *Angew. Chem. Int. Ed.* **2008**, *47*, 1935–1937; b) S. Kusumi, H. Nakayama, T. Kobayashi, H. Kuriki, Y. Matsumoto, D. Takahashi, K. Toshima, *Chem. Eur. J.* **2016**, *22*, 18733–18736; c) C. Palomo, M. Oiarbide, J. M. Garcia, *Chem. Soc. Rev.* **2012**, *41*, 4150–4164; d) R. A. Taj, J. R. Green, *J. Org. Chem.* **2010**, *75*, 8258–8270.
- [111] F. A. Davis, B. C. Chen, *Chem. Rev.* **1992**, *92*, 919–934.
- [112] E. Vedejs, D. A. Engler, J. E. Telschow, *J. Org. Chem.* **1978**, *43*, 188–196.
- [113] G. M. Rubottom, M. A. Vazquez, D. R. Pelegriana, *Tetrahedron Lett.* **1974**, *15*, 4319–4322.
- [114] M. Schulz, R. Kluge, L. Sivilai, B. Kamm, *Tetrahedron* **1990**, *46*, 2371–2380.
- [115] T. Chen, R. Peng, W. Hu, F.-M. Zhang, *Org. Biomol. Chem.* **2016**, *14*, 9859–9867.
- [116] G. J. Chuang, W. Wang, E. Lee, T. Ritter, *J. Am. Chem. Soc.* **2011**, *133*, 1760–1762.
- [117] A. S. K. Tsang, A. Kapat, F. Schoenebeck, *J. Am. Chem. Soc.* **2016**, *138*, 518–526.
- [118] a) Y. F. Liang, N. Jiao, *Angew. Chem. Int. Ed.* **2014**, *53*, 548–552; b) M. B. Chaudhari, Y. Sutar, S. Malpathak, A. Hazra, B. Gnanaprakasam, *Org. Lett.* **2017**, *19*, 3628–3631.
- [119] A. Russo, C. De Fusco, A. Lattanzi, *RSC Advances* **2012**, *2*, 385–397.

- [120] a) E. J. Corey, A. Marfat, G. Goto, F. Brion, *J. Am. Chem. Soc.* **1980**, *102*, 7984–7985; b) Y. Hayashi, J. Kanayama, J. Yamaguchi, M. Shoji, *J. Org. Chem.* **2002**, *67*, 9443–9448.
- [121] a) D. Enders, U. Reinhold, *Synlett* **1994**, *1994*, 792–794; b) C. Agami, F. Couty, C. Lequesne, *Tetrahedron Lett.* **1994**, *35*, 3309–3312; c) A. Alexakis, J.-P. Tranchier, N. Lensen, P. Mangeney, *J. Am. Chem. Soc.* **1995**, *117*, 10767–10768.
- [122] a) T. Hashiyama, K. Morikawa, K. B. Sharpless, *J. Org. Chem.* **1992**, *57*, 5067–5068; b) K. Morikawa, J. Park, P. G. Andersson, T. Hashiyama, K. B. Sharpless, *J. Am. Chem. Soc.* **1993**, *115*, 8463–8464; c) M. Lopp, A. Paju, T. Kanger, T. Pehk, *Tetrahedron Lett.* **1997**, *38*, 5051–5054; d) A. Paju, T. Kanger, T. Pehk, M. Lopp, *Tetrahedron* **2002**, *58*, 7321–7326.
- [123] a) W. Zhang, J. L. Loebach, S. R. Wilson, E. N. Jacobsen, *J. Am. Chem. Soc.* **1990**, *112*, 2801–2803; b) T. Fukuda, T. Katsuki, *Tetrahedron Lett.* **1996**, *37*, 4389–4392; c) M. Koprowski, J. Łuczak, E. Krawczyk, *Tetrahedron* **2006**, *62*, 12363–12374.
- [124] a) Y. Zhu, T. Yong, Y. Hongwu, S. Yian, *Tetrahedron Lett.* **1998**, *39*, 7819–7822; b) Y. Zhu, L. Shu, Y. Tu, Y. Shi, *J. Org. Chem.* **2001**, *66*, 1818–1826.
- [125] a) N. Momiyama, H. Yamamoto, *Angew. Chem. Int. Ed.* **2002**, *41*, 2986–2988; b) N. Momiyama, H. Yamamoto, *Org. Lett.* **2002**, *4*, 3579–3582; c) N. Momiyama, H. Yamamoto, *J. Am. Chem. Soc.* **2003**, *125*, 6038–6039; d) M. Kawasaki, P. Li, H. Yamamoto, *Angew. Chem. Int. Ed.* **2008**, *47*, 3795–3797.
- [126] D. A. Dieterich, I. C. Paul, D. Y. Curtin, *J. Am. Chem. Soc.* **1974**, *96*, 6372–6380.
- [127] P. Merino, T. Tejero, I. Delso, R. Matute, *Synthesis* **2016**, *48*, 653–676.
- [128] S. P. Brown, M. P. Brochu, C. J. Sinz, D. W. C. MacMillan, *J. Am. Chem. Soc.* **2003**, *125*, 10808–10809.
- [129] Y. Hayashi, J. Yamaguchi, K. Hibino, M. Shoji, *Tetrahedron Lett.* **2003**, *44*, 8293–8296.
- [130] G. Zhong, *Angew. Chem. Int. Ed.* **2003**, *42*, 4247–4250.
- [131] a) Y. Hayashi, J. Yamaguchi, T. Sumiya, M. Shoji, *Angew. Chem. Int. Ed.* **2004**, *43*, 1112–1115; b) A. Córdova, H. Sundén, A. Bøgevig, M. Johansson, F. Himø, *Chem. Eur. J.* **2004**, *10*, 3673–3684; c) Y. Hayashi, J. Yamaguchi, T. Sumiya, K. Hibino, M. Shoji, *J. Org. Chem.* **2004**, *69*, 5966–5973.
- [132] a) S.-G. Kim, T.-H. Park, *Tetrahedron Lett.* **2006**, *47*, 9067–9071; b) H.-M. Guo, L. Cheng, L.-F. Cun, L.-Z. Gong, A.-Q. Mi, Y.-Z. Jiang, *Chem. Commun.* **2006**, 429–431.
- [133] a) N. Momiyama, H. Yamamoto, *J. Am. Chem. Soc.* **2005**, *127*, 1080–1081; b) C. Palomo, S. Vera, I. Velilla, A. Mielgo, E. Gómez-Bengoa, *Angew. Chem. Int. Ed.* **2007**, *46*, 8054–8056.
- [134] D. B. Ramachary, C. F. Barbas, *Org. Lett.* **2005**, *7*, 1577–1580.
- [135] M. Lu, D. Zhu, Y. Lu, X. Zeng, B. Tan, Z. Xu, G. Zhong, *J. Am. Chem. Soc.* **2009**, *131*, 4562–4563.
- [136] a) M. Masui, A. Ando, T. Shioiri, *Tetrahedron Lett.* **1988**, *29*, 2835–2838; b) E. F. J. de Vries, L. Ploeg, M. Colao, J. Brussee, A. van der Gen, *Tetrahedron: Asymmetry* **1995**, *6*, 1123–1132; c) E. V. Dehmlo, S. Wagner, A. Müller, *Tetrahedron* **1999**, *55*, 6335–6346; d) M. Lian, Z. Li, Y. Cai, Q. Meng, Z. Gao, *Chem. Eur. J.* **2012**, *7*, 2019–2023; e) S.-B. D. Sim, M. Wang, Y. Zhao, *ACS Catalysis* **2015**, *5*, 3609–3612.
- [137] N. Demoulin, O. Lifchits, B. List, *Tetrahedron* **2012**, *68*, 7568–7574.
- [138] M. R. Witten, E. N. Jacobsen, *Org. Lett.* **2015**, *17*, 2772–2775.
- [139] a) B. Schweitzer-Chaput, J. Demaerel, H. Engler, M. Klussmann, *Angew. Chem. Int. Ed.* **2014**, *53*, 8737–8740; b) X. Q. Chu, H. Meng, Y. Zi, X. P. Xu, S. J. Ji, *Chem. Eur. J.* **2014**, *20*, 17198–17206.

- [140] a) M. Schmittel, *Top. Curr. Chem.* **1994**, 183–230; b) A. G. Csaky, J. Plumet, *Chem. Soc. Rev.* **2001**, 30, 313–320; c) M. Schmittel, A. Haeuseler, *J. Organomet. Chem.* **2002**, 661, 169–179; d) P. S. Baran, N. B. Ambhaikar, C. A. Guerrero, B. D. Hafensteiner, D. W. Lin, J. M. Richter, *ARKIVOC* **2006**, vii, 310–325; e) M. Schmittel, M. Lal, R. Lal, M. Röck, A. Langels, Z. Rappoport, A. Basheer, J. Schlirf, H.-J. Deiseroth, U. Flörke, G. Gescheidt, *Tetrahedron* **2009**, 65, 10842–10855.
- [141] a) Y. Kobayashi, T. Taguchi, T. Morikawa, *Tetrahedron Lett.* **1978**, 19, 3555–3556; b) L. A. Paquette, R. A. Snow, J. L. Muthard, T. Cynkowski, *J. Am. Chem. Soc.* **1978**, 100, 1600–1602; c) U. Jahn, P. Hartmann, E. Kaasalainen, *Org. Lett.* **2004**, 6, 257–260.
- [142] a) Y. Ito, T. Konoike, T. Saegusa, *J. Am. Chem. Soc.* **1975**, 97, 2912–2914; b) Y. Ito, T. Konoike, T. Harada, T. Saegusa, *J. Am. Chem. Soc.* **1977**, 99, 1487–1493; c) R. H. Frazier, R. L. Harlow, *J. Org. Chem.* **1980**, 45, 5408–5411; d) L. A. Paquette, E. I. Bzowej, B. M. Branan, K. J. Stanton, *J. Org. Chem.* **1995**, 60, 7277–7283; e) U. Jahn, M. Müller, S. Aussieker, *J. Am. Chem. Soc.* **2000**, 122, 5212–5213; f) J. Ullrich, H. Philip, D. Ina, J. Peter G., *Eur. J. Org. Chem.* **2001**, 2001, 3333–3355; g) J. Ullrich, H. Philip, D. Ina, J. Peter G., *Eur. J. Org. Chem.* **2002**, 2002, 718–735; h) A. A. Gevorgyan, A. S. Arakelyan, S. V. Barsegyan, K. A. Petrosyan, G. A. Panosyan, *Russ. J. Organ. Chem.* **2003**, 39, 1204–1205; i) M. Lal, M. Schmittel, M. Schlosser, H. J. Deiseroth, *Acta Cryst. C* **2004**, 60, o589–o591; j) M. P. DeMartino, K. Chen, P. S. Baran, *J. Am. Chem. Soc.* **2008**, 130, 11546–11560.
- [143] T. Cohen, K. McNamara, M. A. Kuzemko, K. Ramig, J. J. Landi, Y. Dong, *Tetrahedron* **1993**, 49, 7931–7942.
- [144] J. M. Richter, B. W. Whitefield, T. J. Maimone, D. W. Lin, M. P. Castroviejo, P. S. Baran, *J. Am. Chem. Soc.* **2007**, 129, 12857–12869.
- [145] Q. Li, P. Hurley, H. Ding, A. G. Roberts, R. Akella, P. G. Harran, *J. Org. Chem.* **2009**, 74, 5909–5919.
- [146] M. Meciarova, P. Tisovsky, R. Sebesta, *New J. Chem.* **2016**, 40, 4855–4864.
- [147] a) S. Tatsuya, M. Yoshihiro, H. Hiroshi, I. Tamotsu, Y. Kaoru, *Bull. Chem. Soc. Jpn.* **1978**, 51, 2179–2180; b) K. Dietrich, S. Hans, S. Eberhard, *Chem. Ber.* **1974**, 107, 3640–3657; c) Y. N. Ogibin, A. O. Terent'ev, A. I. Ilovaiskii, G. I. Nikishin, *Russ. J. Electrochem.* **2000**, 36, 193–202; d) Y. Okada, R. Akaba, K. Chiba, *Org. Lett.* **2009**, 11, 1033–1035; e) K. D. Moeller, *Synlett* **2009**, 2009, 1208–1218; f) D. A. Frey, S. H. Krishna Reddy, K. D. Moeller, *J. Org. Chem.* **1999**, 64, 2805–2813.
- [148] a) M. Schmittel, M. Kelley, A. Burghart, *J. Chem. Soc., Perkin Trans. 2* **1995**, 2327–2333; b) M. Schmittel, A. Burghart, W. Malisch, J. Reising, R. Söllner, *J. Org. Chem.* **1998**, 63, 396–400; c) M. Schmittel, A. Burghart, H. Werner, M. Laubender, R. Söllner, *J. Org. Chem.* **1999**, 64, 3077–3085; d) Jens O. Bunte, Eike K. Heilmann, B. Hein, J. Mattay, *Eur. J. Org. Chem.* **2004**, 2004, 3535–3550; e) J. B. Sperry, C. R. Whitehead, I. Ghiviriga, R. M. Walczak, D. L. Wright, *J. Org. Chem.* **2004**, 69, 3726–3734; f) K. Uneyama, H. Tanaka, S. Kobayashi, M. Shioyama, H. Amii, *Org. Lett.* **2004**, 6, 2733–2736; g) A. K. Miller, C. C. Hughes, J. J. Kennedy-Smith, S. N. Gradl, D. Trauner, *J. Am. Chem. Soc.* **2006**, 128, 17057–17062; h) M. D. Clift, C. N. Taylor, R. J. Thomson, *Org. Lett.* **2007**, 9, 4667–4669; i) J. Jiao, Y. Zhang, J. J. Devery, L. Xu, J. Deng, R. A. Flowers, *J. Org. Chem.* **2007**, 72, 5486–5492; j) C. T. Avetta, L. C. Konkol, C. N. Taylor, K. C. Dugan, C. L. Stern, R. J. Thomson, *Org. Lett.* **2008**, 10, 5621–5624.
- [149] a) T. Shono, Y. Matsumura, Y. Nakagawa, *J. Am. Chem. Soc.* **1974**, 96, 3532–3536; b) T. Shono, M. Okawa, I. Nishiguchi, *J. Am. Chem. Soc.* **1975**, 97, 6144–6147; c) M.

- Schmittel, J. Heinze, H. Trenkle, *J. Org. Chem.* **1995**, *60*, 2726–2733; d) M. Schmittel, J.-P. Steffen, A. Burghart, *Acta Chem. Scand.* **1999**, *53*, 781–791; e) A. G. Csáký, M. B. Mula, M. Mba, J. n. Plumet, *Tetrahedron: Asymmetry* **2002**, *13*, 753–757.
- [150] a) W. J. Bouma, J. K. MacLeod, L. Radom, *J. Am. Chem. Soc.* **1979**, *101*, 5540–5545; b) J. L. Holmes, F. P. Lossing, *J. Am. Chem. Soc.* **1980**, *102*, 1591–1595; c) J. L. Holmes, F. P. Lossing, *J. Am. Chem. Soc.* **1982**, *104*, 2648–2649; d) N. Heinrich, W. Koch, G. Frenking, H. Schwarz, *J. Am. Chem. Soc.* **1986**, *108*, 593–600; e) M. Czerwińska, A. Sikora, P. Szajerski, J. Adamus, A. Marcinek, J. Gębicki, P. Bednarek, *J. Chem. Phys. A* **2006**, *110*, 7272–7278.
- [151] G. Frenking, N. Heinrich, J. Schmidt, H. Schwarz, *Z. Naturforsch.* **1982**, *37b*, 1597–1601.
- [152] M. Schmittel, U. Baumann, *Angew. Chem. Int. Ed.* **1990**, *29*, 541–543.
- [153] M. Lal, A. Langels, H. J. Deiseroth, J. Schlirf, M. Schmittel, *J. Phys. Org. Chem.* **2003**, *16*, 373–379.
- [154] M.-A. Orliac-Le Moing, G. Le Guillanton, J. Simonet, *Electrochim. Acta* **1982**, *27*, 1775–1779.
- [155] a) J.-i. Yoshida, K. Sakaguchi, S. Isoe, *Tetrahedron Lett.* **1986**, *27*, 6075–6078; b) J. Yoshida, K. Sakaguchi, S. Isoe, *J. Org. Chem.* **1988**, *53*, 2525–2533.
- [156] a) M. Schmittel, M. Röck, *Chem. Ber.* **1992**, *125*, 1611–1620; b) M. Schmittel, A. Abufarag, O. Luche, M. Levis, *Angew. Chem. Int. Ed.* **1990**, *29*, 1144–1146; c) M. Schmittel, G. Gescheidt, M. Röck, *Angew. Chem. Int. Ed.* **1994**, *33*, 1961–1963.
- [157] J. Choi, M. E. Pulling, D. M. Smith, J. R. Norton, *J. Am. Chem. Soc.* **2008**, *130*, 4250–4252.
- [158] D. C. Miller, K. T. Tarantino, R. R. Knowles, *Top. Curr. Chem.* **2016**, *374*, 30.
- [159] F. G. Bordwell, J. P. Cheng, J. A. Harrelson, *J. Am. Chem. Soc.* **1988**, *110*, 1229–1231.
- [160] J. J. Warren, T. A. Tronic, J. M. Mayer, *Chem. Rev.* **2010**, *110*, 6961–7001.
- [161] X. Zhang, J. Ma, S. Li, M.-D. Li, X. Guan, X. Lan, R. Zhu, D. L. Phillips, *J. Org. Chem.* **2016**, *81*, 5330–5336.
- [162] E. C. Gentry, R. R. Knowles, *Acc. Chem. Res.* **2016**, *49*, 1546–1556.
- [163] a) S. Y. Reece, J. M. Hodgkiss, J. Stubbe, D. G. Nocera, *Philos. Trans. Royal Soc. B* **2006**, *361*, 1351; b) S. Hammes-Schiffer, *Acc. Chem. Res.* **2009**, *42*, 1881–1889; c) D. R. Weinberg, C. J. Gagliardi, J. F. Hull, C. F. Murphy, C. A. Kent, B. C. Westlake, A. Paul, D. H. Ess, D. G. McCafferty, T. J. Meyer, *Chem. Rev.* **2012**, *112*, 4016–4093.
- [164] N. Hoffmann, *Eur. J. Org. Chem.* **2017**, *2017*, 1982–1992.
- [165] K. T. Tarantino, P. Liu, R. R. Knowles, *J. Am. Chem. Soc.* **2013**, *135*, 10022–10025.
- [166] a) K. T. Tarantino, D. C. Miller, T. A. Callon, R. R. Knowles, *J. Am. Chem. Soc.* **2015**, *137*, 6440–6443; b) G. J. Choi, R. R. Knowles, *J. Am. Chem. Soc.* **2015**, *137*, 9226–9229; c) D. C. Miller, G. J. Choi, H. S. Orbe, R. R. Knowles, *J. Am. Chem. Soc.* **2015**, *137*, 13492–13495; d) Q. Zhu, D. E. Graff, R. R. Knowles, *J. Am. Chem. Soc.* **2018**, *140*, 741–747.
- [167] H. G. Yayla, H. Wang, K. T. Tarantino, H. S. Orbe, R. R. Knowles, *J. Am. Chem. Soc.* **2016**, *138*, 10794–10797.
- [168] a) K. Qvortrup, D. A. Rankic, D. W. C. MacMillan, *J. Am. Chem. Soc.* **2014**, *136*, 626–629; b) D. Hager, D. W. C. MacMillan, *J. Am. Chem. Soc.* **2014**, *136*, 16986–16989.
- [169] L. J. Rono, H. G. Yayla, D. Y. Wang, M. F. Armstrong, R. R. Knowles, *J. Am. Chem. Soc.* **2013**, *135*, 17735–17738.
- [170] E. C. Gentry, L. J. Rono, M. E. Hale, R. Matsuura, R. R. Knowles, *J. Am. Chem. Soc.* **2018**, *140*, 3394–3402.

- [171] Z. Zhou, Y. Li, B. Han, L. Gong, E. Meggers, *Chem. Sci.* **2017**, 8, 5757–5763.
- [172] G. J. Choi, Q. Zhu, D. C. Miller, C. J. Gu, R. R. Knowles, *Nature* **2016**, 539, 268.
- [173] a) J. C. K. Chu, T. Rovis, *Nature* **2016**, 539, 272; b) W. Yuan, Z. Zhou, L. Gong, E. Meggers, *Chem. Commun.* **2017**, 53, 8964–8967.
- [174] G. Pupo, Universität zu Köln (Köln), **2017**.
- [175] X. Zhang, Y.-H. Chen, B. Tan, *Tetrahedron Lett.* **2018**, 59, 473–486.
- [176] a) J. Breddt, J. Houben, P. Levy, *Ber. Dtsch. Chem. Ges.* **1902**, 35, 1286–1292; b) G. L. Buchanan, *Chem. Soc. Rev.* **1974**, 3, 41–63; c) J. Y. W. Mak, R. H. Pouwer, C. M. Williams, *Angew. Chem. Int. Ed.* **2014**, 53, 13664–13688.
- [177] S. Vellalath, I. Čorić, B. List, *Angew. Chem. Int. Ed.* **2010**, 49, 9749–9752.
- [178] K. Horiguchi, E. Yamamoto, K. Saito, M. Yamanaka, T. Akiyama, *Chem. Eur. J.* **2016**, 22, 8078–8083.
- [179] X. H. Huo, J. H. Xie, Q. S. Wang, Q. L. Zhou, *Adv. Synt. Catal.* **2007**, 349, 2477–2484.
- [180] G. A. Shevchenko, G. Pupo, B. List, *Synlett* **2015**, 26, 1413–1416.
- [181] X. Yang, F. D. Toste, *J. Am. Chem. Soc.* **2015**, 137, 3205–3208.
- [182] M. R. Monaco, R. Properzi, B. List, *Synlett* **2016**, 27, 591–594.
- [183] a) P. Magnus, N. Garizi, K. A. Seibert, A. Ornholt, *Org. Lett.* **2009**, 11, 5646–5648; b) P. Magnus, A. J. Brozell, *Org. Lett.* **2012**, 14, 3952–3954.
- [184] a) A. Córdova, H. Sundén, M. Engqvist, I. Ibrahim, J. Casas, *J. Am. Chem. Soc.* **2004**, 126, 8914–8915; b) H. Sundén, M. Engqvist, J. Casas, I. Ibrahim, A. Córdova, *Angew. Chem. Int. Ed.* **2004**, 43, 6532–6535; c) I. Ibrahim, G.-L. Zhao, H. Sundén, A. Córdova, *Tetrahedron Lett.* **2006**, 47, 4659–4663.
- [185] J. Walaszek Dominika, K. Rybicka-Jasińska, S. Smoleń, M. Karczewski, D. Gryko, *Adv. Synt. Catal.* **2015**, 357, 2061–2070.
- [186] H. J. Bestmann, *Angew. Chem. Int. Ed.* **1977**, 16, 349–364.
- [187] a) J. R. Rocca, J. H. Tumlinson, B. M. Glancey, C. S. Lofgren, *Tetrahedron Lett.* **1983**, 24, 1889–1892; b) G. M. Rubottom, H. D. Juve, *J. Org. Chem.* **1983**, 48, 422–425; c) S. Yao, M. Johannsen, R. G. Hazell, K. A. Jørgensen, *J. Org. Chem.* **1998**, 63, 118–121; d) K. F. Eidman, B. S. MacDougall, *J. Org. Chem.* **2006**, 71, 9513–9516.
- [188] H. Yi, M. Albrecht, A. Valkonen, K. Rissanen, *New J. Chem.* **2015**, 39, 746–749.
- [189] G. Shevchenko, A., B. Oppelaar, B. List, *Angew. Chem. Int. Ed.* **2018**, 0.
- [190] a) A. Bhattacharya, L. M. DiMichele, U. H. Dolling, E. J. J. Grabowski, V. J. Grenda, *J. Org. Chem.* **1989**, 54, 6118–6120; b) S. Fukuzumi, M. Fujita, G.-e. Matsubayashi, J. Otera, *Chem. Lett.* **1993**, 22, 1451–1454; c) X. Guo, H. Mayr, *J. Am. Chem. Soc.* **2013**, 135, 12377–12387.
- [191] E. Kumli, F. Montermini, P. Renaud, *Org. Lett.* **2006**, 8, 5861–5864.
- [192] M. T. Huynh, C. W. Anson, A. C. Cavell, S. S. Stahl, S. Hammes-Schiffer, *J. Am. Chem. Soc.* **2016**, 138, 15903–15910.
- [193] L. Bernardi, G. Bolzoni, M. Fochi, M. Mancinelli, A. Mazzanti, *Eur. J. Org. Chem.* **2016**, 2016, 3208–3216.
- [194] P. G. M. Wuts, T. W. Greene, *Greene's Protective Groups in Organic Synthesis*, 4 ed., John Wiley & Sons, Inc., **2007**.
- [195] C. Hansch, A. Leo, R. W. Taft, *Chem. Rev.* **1991**, 91, 165–195.
- [196] a) N. Vignola, B. List, *J. Am. Chem. Soc.* **2004**, 126, 450–451; b) D. A. Nagib, M. E. Scott, D. W. C. MacMillan, *J. Am. Chem. Soc.* **2009**, 131, 10875–10877; c) B. List, I. Čorić, O. Grygorenko Oleksandr, S. J. Kaib Philip, I. Komarov, A. Lee, M. Leutzsch, S. Chandra Pan, V. Tytmunik Andrey, M. van Gemmeren, *Angew. Chem. Int. Ed.* **2013**, 53,

- 282–285; d) R. Cano, A. Zakarian, P. McGlacken Gerard, *Angew. Chem. Int. Ed.* **2017**, 56, 9278–9290.
- [197] a) Y. Inokoishi, N. Sasakura, K. Nakano, Y. Ichikawa, H. Kotsuki, *Org. Lett.* **2010**, 12, 1616–1619; b) H. Yang, R. G. Carter, *Org. Lett.* **2010**, 12, 3108–3111; c) M. Yoshida, H. Ukigai, K. Shibatomi, S. Hara, *Tetrahedron Lett.* **2015**, 56, 3890–3893.
- [198] Y. Han, S. Breitler, S.-L. Zheng, E. J. Corey, *Org. Lett.* **2016**, 18, 6172–6175.
- [199] R. Pedrosa, J. M. Andrés, R. Manzano, C. Pérez-López, *Tetrahedron Lett.* **2013**, 54, 3101–3104.
- [200] C. Beattie, M. North, P. Villuendas, *Molecules* **2011**, 16, 3420–3432.
- [201] L. Liao, C. Shu, M. Zhang, Y. Liao, X. Hu, Y. Zhang, Z. Wu, W. Yuan, X. Zhang, *Angew. Chem. Int. Ed.* **2014**, 53, 10471–10475.

9 Appendix

9.1 Erklärung

„Ich versichere, dass ich die von mir vorgelegte Dissertation selbständig angefertigt, die benutzten Quellen und Hilfsmittel vollständig angegeben und die Stellen der Arbeit - einschließlich Tabellen, Karten und Abbildungen -, die anderen Werken im Wortlaut oder dem Sinn nach entnommen sind, in jedem Einzelfall als Entlehnung kenntlich gemacht habe; dass diese Dissertation noch keiner anderen Fakultät oder Universität zur Prüfung vorgelegen hat; dass sie - abgesehen von unten angegebenen Teilpublikationen - noch nicht veröffentlicht worden ist sowie, dass ich eine solche Veröffentlichung vor Abschluss des Promotionsverfahrens nicht vornehmen werde. Die Bestimmungen dieser Promotionsordnung sind mir bekannt. Die von mir vorgelegte Dissertation ist von Prof. Dr. Benjamin List betreut worden.“

(Grigory André Shevchenko)

Mülheim an Ruhr, Mai 2018

Bisher sind folgende Teilpublikationen veröffentlicht worden:

„Catalytic Asymmetric α -Amination of α -Branched Ketones *via* Enol Catalysis”, G. A. Shevchenko, G. Pupo, B. List, *Synlett* **2015**, 26, 1413–1416.

“An Unexpected α -Oxidation of Cyclic Ketones with 1,4-Benzoquinone *via* Enol Catalysis”, G. A. Shevchenko, B. Oppelaar, B. List. *Angew. Chem. Int. Ed.* **2018**, 10.1002/anie.201804445; *Angew. Chem.* **2018**, 10.1002/ange.201804445.

9.2 Lebenslauf

Grigory André Shevchenko

Geboren am 01. September 1989 in Leningrad/Russland

Staatsangehörigkeit: Deutsch

Akademischer Werdegang

02.2014–07.2018 Promotion am Max-Planck-Institut für Kohlenforschung, Mülheim an der Ruhr unter der Leitung von Prof. B. List zum Thema

Enol Catalysis – Enantioselective Transformations via Bifunctional Brønsted Acid Promoted Enolization

10.2011–10.2013 Studium der Chemie an der Georg-August-Universität Göttingen

Abschluss: **Master of Science**

Masterarbeit unter der Leitung von Prof. L. Ackermann zum Thema

Cobalt-Catalyzed C–H Bond Functionalizations with Secondary Alkylchlorides

10.2008–10.2011 Studium der Chemie an der Georg-August-Universität Göttingen

Abschluss: **Bachelor of Science**

Bachelorarbeit unter der Leitung von Dr. D. B. Werz zum Thema

Stereoselektive Synthese einer trisaccharidischen Untereinheit eines Heptasaccharids aus Providencia rustigianii

Schulausbildung

09.2001–07.2008 Martin-Andersen-Nexö Gymnasium Dresden (vertieft mathematisch-naturwissenschaftliches Profil)

Abschluss: **Abitur**